VNIVERSITAT ID VALÈNCIA

Facultat de Química

TOWARDS PORTABILITY IN ANALYTICAL CHEMISTRY: NEW TOOLS

Thesis presented to obtain the PhD degree under the "Doctorado en Química (R.D. 99/2011)"

Adrià Martínez Aviñó

Supervisors:
Profa. Dra. Pilar Campíns Falcó
Profa. Dra. Carmen Molins Legua

Valencia, October 2022

Vniver̩sitat ᴅᴇ València [ð̯ ⁎] Facultat ᴅᴇ Química

Departament de Química Analítica

Pilar Campíns Falcó y Carmen Molins Legua, ambas Catedráticas del Departamento de Química Analítica de la Universidad de Valencia,

CERTIFICAN

Que la presente memoria, titulada "*Towards portability in analytical chemsitry: new tools*", constituye la Tesis Doctoral de Adrià Martínez Aviñó para optar al grado de Doctor en Química, y que ha sido realizada en los laboratorios del Departamento de Química Analítica de la Universidad de Valencia, bajo su dirección y supervisión.

Y para que así conste a los efectos oportunos, firman el presente certificado en

Valencia, a 20 de Octubre de 2022.

Fdo. Dra. Pilar Campíns Falcó Fdo. Dra. Carmen Molins Legua
Directora de Tesis Codirectora de Tesis

"No se puede enseñar nada a un hombre,
sólo se le puede ayudar a descubrirse a sí mismo"

Galileo Galilei

AGRAÏMENTS

Diuen que l'important no és la meta, sinó el camí recorregut... I ara que he tingut la sort d'aplegar al final d'aquesta bonica etapa, no puc més que agrair a totes aquelles persones que m'han ajudat a recórrer aquest llarg viatge. Unes persones sense les quals no haguera aplegat tan lluny i que sempre portaré amb mi.

En primer lloc, vull agrair a Pilar per la confiança depositada, per donar-me l'oportunitat de poder fer aquest doctorat i per treballar en un grup d'investigació com aquest. Un grup que m'ha fet sentir com a casa i on gràcies a la família que hi ha formada sempre ha sigut un plaer treballar. Gràcies Pilar per ser sempre un exemple, per ajudar-me en tot moment i per ensenyar-me que els objectius només depenen de cadascú.

Gràcies Carmen, per ser com una segona mare i per escoltar-me sempre amb un somriure. Gràcies pels teus consells i per estar sempre per a tot el que he necessitat. Gràcies per confiar i haver tret el millor de mi, amb la teua ajuda tots els reptes que he afrontat al llarg d'aquests anys han sigut més fàcils. Tan tu com Pilar heu sigut unes tutores immillorables i sempre estaré agraït a vosaltres.

Gràcies a Yolanda i Rosa, vosaltres també sou part fonamental de que haja aconseguit superar aquest repte. Gràcies per estar dispostes a ajudar-me en tot moment i per tindre sempre unes paraules de suport. Les quatre juntes formeu un grup del que és un plaer formar part.

No volia oblidar-me de Rob, per acollir-me sempre allà on ha estat i per donar-me l'oportunitat de realitzar la meua estància doctoral a la Universitat de Dublín. Gràcies per fer-me veure que jo era vàlid per a fer un doctorat i per donar-me l'oportunitat de continuar aquesta aventura. Gràcies també al "Johnson's Group" per la vostra amistat i per rebrem de la millor manera.

El més reconfortant a l'acabar una etapa és mirar cap arrere i veure totes les amistats que s'han fet pel camí, per això volia donar gràcies als meus companys de laboratori, Maria, Anabel, Pascu, Neus, Rodrigo, Henry, Sara, Ana, Lusine, Lorenzo, Sergio, Camila, Rocío, Héctor, Ivan, Aarón, Carlos, Belén, Pepe,

RESUMEN

Desde principios de siglo los cambios en la sociedad, la investigación de nuevos (nano)materiales y la aparición de internet y de nuevas tecnologías han sido tres pilares fundamentales en los que se ha basado el desarrollo de la química analítica. Gracias a los recientes avances tecnológicos se ha generado un gran impulso hacia la creación de nuevas herramientas y dispositivos. Esto, junto con la evolución en la informática ha conllevado a la automatización y miniaturización de los sistemas analíticos, reduciendo los tiempos de análisis y mejorando los resultados obtenidos.

Una de las exigencias a tener en cuenta dentro de la química actual es aproximarla a los calificativos sostenible y verde. El concepto "sostenible" apareció por primera vez en los años 70, basándose en la unión del desarrollo económico y la preservación de los ecosistemas naturales. Se planteó con la intención de concienciar sobre las consecuencias negativas en el medio ambiente derivadas de la globalización, la industrialización y del crecimiento de la población. En concreto, la química sostenible, tiene en cuenta los posibles efectos producidos por el procesado de materiales, la obtención de recursos energéticos y el impacto social y económico. Al mismo tiempo, la química sostenible también se centra en el control del consumo de recursos y de energía, de manera que se puedan regenerar de forma natural y que la generación de residuos vaya a un ritmo más lento que la gestión de estos. Más tarde, debido a la preocupación por la contaminación ambiental producida por la industria química, apareció en la década de los 90 el termino química verde. Fueron Anastas y Warner quienes en 1998 plasmaron estas preocupaciones en una lista de 12 principios como guía para realizar buenas prácticas en química. Así, la química verde puede ser entendida como el diseño, el desarrollo y la puesta en práctica de procesos químicos o de productos para reducir o incluso eliminar el uso y la generación de sustancias tóxicas y peligrosas. En el campo de la química analítica, siguiendo los pasos de la química verde, apareció la necesidad de crear protocolos y dispositivos para evitar el uso de reactivos peligrosos y para facilitar el análisis in-situ, la miniaturización de procedimientos y de instrumentación y la reducción de costes, de residuos y de consumo de energía, entre otros. Así pues, Gałuszka propuso doce principios para ayudar a la creación de laboratorios analíticos más verdes. Teniendo en cuenta estos principios, es importante encontrar el equilibrio entre rendimiento, coste, complejidad,

fiabilidad y sostenibilidad en el momento de elegir la mejor opción para abordar cualquier cuestión que se plantee.

Siguiendo las ideas expuestas anteriormente y en consonancia con los problemas de la sociedad actual, se ha observado la necesidad de desarrollar nuevos dispositivos que sean capaces de resolver problemas de la vida diaria en el mismo sitio donde aparecen. Estas necesidades, junto con las recientes evoluciones en las tecnologías de microsensores, ha conducido al desarrollo de instrumentación portátil como una posible alternativa para la solución de estos problemas.

Estas herramientas se caracterizan por tener un tamaño y peso reducido, bajo consumo de energía, relación calidad precio muy satisfactoria, trabajar con interfaces de usuario sencillas, ser capaces de trabajar en diferentes ambientes y tener la capacidad de procesar y comunicar los datos obtenidos con facilidad. Cabe destacar también su facilidad para ser utilizados por personal no especializado, además de presentar una gran versatilidad, lo que les permite ser utilizados en diferentes campos de aplicación.

En esta Tesis se ha descrito el concepto de instrumentación portátil tal como se entiende en la actualidad y se ha evaluado el posible uso de varios de estos dispositivos como instrumentos de medidas para realizar análisis in situ con diferentes técnicas y en diferentes campos. En los últimos 10 años, la mayoría de dispositivos portátiles desarrollados se han centrado en métodos de análisis espectroscópicos, seguidos de métodos cromatográficos, electroquímicos y de espectrometría de masas. Las principales características de las técnicas analíticas mencionadas han sido comparadas con instrumentación de laboratorio, estableciendo sus principales puntos fuertes y débiles. Concretamente, en esta tesis se ha evaluado la portabilidad en la química analítica desde tres estrategias distintas:

1- Sensores ópticos y medidas con instrumentación portátil.
2- Cromatografía de capa fina de alto rendimiento miniaturizada y medidas con dispositivos portátiles.
3- Sensores electroquímicos y voltamperometría cíclica portátil.

Un (bio)sensor óptico consiste en un elemento de reconocimiento que interacciona con el compuesto de interés produciendo un cambio de color. Este

color es proporcional a la concentración del analito objeto de estudio y puede ser fácilmente detectado por el ojo humano, aunque para obtener un análisis cuantitativo es necesario el uso de instrumentación. Diversos estudios se han realizado de manera satisfactoria utilizando estos tipos de sensores combinados con instrumentación portátil. Además, más recientemente también se ha visto como su combinación junto con el uso de teléfonos móviles puede dar lugar a aplicaciones sostenibles en diversos campos como la salud, la seguridad alimenticia y la protección medioambiental.

Existen diversos tipos de dispositivos sensores ópticos, como los sensores de liberación de reactivos, sensores sólidos, kits de pruebas, tiras reactivas, plataformas microfluídicas, tubos colorimétricos, matrices colorimétricas y sensores plasmónicos. Además, estos dispositivos pueden estar producidos con diferentes materiales, en consecuencia, la investigación de nuevos polímeros capaces de presentar alternativas más sostenibles y la investigación de nanomateriales es una de las principales corrientes de estudio en el desarrollo de (bio)sensores.

Los nanomateriales presentan una gran superficie específica que tiene un papel clave en la inmovilización de (bio)moléculas, además, muestran propiedades fisicoquímicas únicas difíciles de encontrar en las moléculas pequeñas. En consecuencia, una gran variedad de nanomateriales se ha utilizado para mejorar numerosas técnicas de desarrollo de (bio)sensores. Celulosa, zeína proteína que se extrae del maíz, polidimetilsiloxano (PDMS), nylon, vidrio o tetraetilortosilicato (TEOS) son algunos de los materiales utilizados en los últimos años. En esta Tesis se ha prestado especial atención al PDMS, Nylon y celulosa como soportes para diferentes sensores colorimétricos. Además, también se ha estudiado el TEOS como modificador hidrofílico y utilizado el vidrio para inmovilizar la enzima ureasa.

Tradicionalmente, los sensores ópticos se han medido con instrumentación convencional; sin embargo, las medidas espectroscópicas también pueden realizarse con instrumentación portátil y con teléfonos móviles. Existen espectrómetros miniaturizados que pueden acoplarse a la cámara del smartphone para realizar el análisis espectral. Además, el espectrómetro puede equiparse con sondas de fibra óptica con el fin de obtener mediciones más exactas y precisas. Así pues, debido a su pequeño tamaño, su versatilidad y su fácil portabilidad, los

espectrómetros para teléfonos móviles son una buena alternativa que puede ser utilizada en diferentes aplicaciones.

Los teléfonos móviles también ofrecen la posibilidad de capturar imágenes con sus cámaras para su posterior análisis de imagen. Recientemente se han lanzado al mercado smartphones con mejores cámaras que presentan ajustes más complejos. Estas nuevas configuraciones permiten a los clientes ajustar parámetros de la cámara como la sensibilidad a la luz (ISO), el balance de blancos, el tiempo de exposición o la temperatura del color, reduciendo los errores sistemáticos al realizar el análisis del color. Para llevar a cabo el análisis del color, los colores de una imagen digitalizada se convierten en parámetros o valores numéricos, que dependen del modelo de color seleccionado, utilizando un software de edición de imágenes, los cuales permiten también procesar las imágenes para obtener mejores resultados. Los parámetros de color obtenidos dependen del modelo de color elegido, como las coordenadas rojo-verde-azul (RGB), cian-magenta-amarillo-negro (CMYK), tono-saturación-valor (HSV) o los parámetros CIELAB. Además, hoy en día, debido a su uso generalizado en todo el mundo, existe un amplio tipo de Apps comerciales para Android y para iOS que dan también la posibilidad de obtener parámetros de color al instante, así como aplicaciones diseñadas que analizan los datos obtenidos al instante para obtener resultados directos.

En las últimas décadas se ha producido un importante crecimiento en el interés y la popularidad de la cromatografía hasta convertirse en una técnica líder en la química analítica motivado por la necesidad de separar analitos para el estudio de matrices complejas. La cromatografía de capa fina de alto rendimiento (HPTLC) es una técnica que permite realizar mediciones in situ con una detección rápida y un análisis de bajo coste. Para obtener un análisis cualitativo y cuantitativo adecuado, el desarrollo del método es uno de los pasos más críticos y puede dividirse en los siguientes pasos: selección de la fase estacionaria, selección y optimización de la fase móvil, aplicación de la muestra, desarrollo cromatográfico y detección. La HPTLC puede combinarse con diferentes metodologías de detección proporcionando separaciones eficientes y buenas sensibilidades. Además, también ofrece la posibilidad de realizar análisis cuantitativos utilizando instrumentación más moderna como los smartphones, lo que ha llevado a un rápido crecimiento con importantes implicaciones en el marco de la química analítica. En esta Tesis se ha estudiado la combinación de HPTLC con smartphones, para la determinación de lactosa y gluten en diferentes matrices.

La electroquímica ofrece una perspectiva prometedora para la miniaturización de los sistemas analíticos, con características que incluyen una alta sensibilidad, bajo coste, bajos requisitos de energía y alta compatibilidad con tecnologías avanzadas. En consecuencia, las metodologías portátiles para el análisis electroquímico se han utilizado para la detección de analitos importantes (proteínas, ácidos nucleicos, proteínas, contaminantes, metabolitos o metales) en muchas áreas diferentes de la química analítica como, por ejemplo, la salud, el análisis clínico, la calidad de los alimentos y del agua, y la seguridad del medio ambiente.

En este sentido, el desarrollo de sensores electroquímicos ha sido un tema de gran interés dentro de la química analítica. Se basa en tres componentes esenciales: la muestra, donde se encuentra el analito de interés, el elemento de reconocimiento, donde se produce una interacción biológica o química con la especie objeto de estudio y el transductor, un elemento físico-químico que convierte esta interacción en una respuesta electroquímica. Existen diferentes tipos de transductores que pueden utilizarse para construir biosensores. Los más utilizados son el oro (Au), el platino (Pt), el mercurio (Hg) y los materiales basados en el carbono como los electrodos de carbono serigrafiados (SPCE), diamante dopado con boro (BDD) y carbono vítreo (GC). Además, Los sensores electroquímicos pueden mostrar una alta selectividad y sensibilidad debido a la posibilidad de adaptar la interacción específica de los compuestos mediante la inmovilización, en la superficie del transductor, de elementos de reconocimiento químico o biológico que tengan una afinidad de unión específica con la molécula objetivo. Este proceso se conoce como modificación de la superficie y puede realizarse mediante diferentes estrategias. En la actualidad, existen diferentes métodos conocidos para la modificación de superficies, como la salinización y la fosfatación de superficies oxidadas, el autoensamblaje de tioles en oro y otros metales y la reacción electroquímica conocida como electrografting. En esta tesis se ha estudiado la modificación superficial de electrodos GC y BDD, prestando especial atención al electrografting por reducción de sales de diazonio para su posterior funcionalización. La modificación de los electrodos y la medida de su respuesta se han realizado mediante voltamperometría cíclica utilizando un potenciostato portátil.

El objetivo general de esta Tesis es la evaluación de la instrumentación portátil y el estudio de varias estrategias para su combinación con diferentes

metodologías analíticas con el fin de demostrar que no sólo pueden ser una alternativa adecuada a la instrumentación convencional, sino que, además, pueden aportar soluciones óptimas para el análisis in situ. En concreto, los objetivos específicos son:

1- Evaluar y optimizar instrumentación portátil, incluyendo smartphones. Estudio de diferentes estrategias de control de las condiciones experimentales y de la influencia de la luz. Realización de análisis con la instrumentación portátil propuesta para las mediciones de sensores ópticos in situ.

2- Desarrollar métodos analíticos basados en la combinación de HPTLC con medidas utilizando instrumentación portátil para la detección y cuantificación in situ de alérgenos alimenticios en diferentes muestras reales.

3- Modificar la superficie de electrodos de GC y BDD mediante electrografting de sales de diazonio para la fabricación de biosensores, y su posterior medida con voltametría cíclica utilizando instrumentación portátil.

Se ha establecido la información proporcionada por varios instrumentos desde un punto de vista analítico, verde y sostenible, para evaluar la instrumentación portátil. Uno de los aspectos más importantes relacionados con la medida con smartphones es el control de las condiciones experimentales y de medida. Para ello, se estudió la influencia de condiciones, como el modelo de teléfono móvil y el tamaño y la posición de la muestra, y se han establecido reglas utilizando una paleta de 45 colores como conjunto de validación. Se obtuvieron buenos resultados en términos de intensidades de absorbancia, forma del espectro y en términos de precisión (RSD < 2.5%) en comparación con la instrumentación de laboratorio y otros equipos portátiles. Además, mediante la huella de carbono se observó que los teléfonos inteligentes son una alternativa adecuada y más sostenible para el análisis in situ.

Otro aspecto clave a la hora de trabajar con smartphones es controlar la influencia de la luz. Es por esto, que se estudió su influencia, evaluando varias fuentes de luz, como la halógena, la LED y la luz diurna, con el fin de estudiar su

influencia en los resultados analíticos. El análisis espectral y del color de la imagen se llevó a cabo utilizando una caja portátil de luz, para controlar la luz incidente, y un conjunto de 45 colores y una paleta de corrección del color como conjunto de validación. La paleta de corrección del color también se utilizó para el diseño de una metodología de procesado de imagen para la aproximación a colores reales. Los resultados obtenidos para el análisis espectral fueron mejores cuando se utilizó una lámpara halógena, sin embargo, para el análisis de las coordenadas RGB se obtuvieron mejores resultados con luz LED. También se estudió la elección de una determinada coordenada de color RGB observando que los mejores resultados se obtenían cuando el parámetro RGB seleccionado era el más cercano al color complementario del tono de color del sensor analizado.

Otro de los enfoques estudiados en esta Tesis es el desarrollo de dispositivos colorimétricos para el análisis in situ y su posterior medición mediante las estrategias validadas. En este sentido, se ha propuesto un sensor colorimétrico basado en la inmovilización de NQS como reactivo derivatizante en un composite de PDMS/TEOS/SiO_2NPs como sensor de amoníaco para cuantificar NH_4^+ y urea en muestras de agua y orina humana. El sensor mostró una buena precisión (RSD < 8%), una estabilidad satisfactoria y una versatilidad prometedora al analizar diferentes muestras de aguas residuales y diferentes orinas humanas. La respuesta colorimétrica obtenida se registró mediante reflectancia difusa con un instrumento de laboratorio como referencia y medidas con smartphone para el análisis cuantitativo. En ambos casos, se obtuvieron resultados satisfactorios y mostraron una buena concordancia. También se analizó su respuesta a urea sin y con la hidrólisis de la urea en presencia de la enzima ureasa en solución e inmovilizada en un soporte de vidrio. Los resultados obtenidos indican que el sensor propuesto también puede aplicarse para analizar grupos amino presentes en matrices biológicas, como la orina, además de matrices acuosas, demostrando también la idoneidad de los dispositivos móviles para realizar análisis colorimétrico de sensores sólidos.

Las estrategias desarrolladas también se ensayaron analizando sensores de múltiples colores, cubriendo diferentes rangos espectrales. En este sentido, se han propuesto como casos de estudio un sensor plasmónico soportado en nylon para la evaluación de sulfuro de hidrógeno en muestras de aliento, un sensor basado en papel para determinar sulfuro de hidrógeno en matrices de agua y un sensor de PDMS que dispensa el reactivo de Griess para medir la presencia de nitritos en

disolución. Se estableció el uso de la fibra óptica como la mejor opción cuando se trabaja con el espectrómetro portátil unido al teléfono móvil utilizando una fuente de luz halógena. Por otro lado, para el análisis de imágenes, se demostró que el uso de luz LED seguido del procesamiento de imágenes proporcionaba los mejores resultados. Los resultados obtenidos han demostrado que los teléfonos inteligentes son una herramienta satisfactoria para el análisis in situ.

Se ha propuesto la combinación de la cromatografía en capa fina de alto rendimiento con una reacción de derivatización y detección colorimétrica basada en las medidas con un smartphone. Se han realizado dos estudios diferentes. Por un lado, se llevó a cabo una separación de carbohidratos para la detección de lactosa y por otro lado, también se realizó una separación cromatográfica de proteínas para el aislamiento del gluten. El objetivo de este estudio era la detección selectiva de ambos alérgenos en muestras reales. Se obtuvieron resultados satisfactorios alcanzando LOD a nivel de trazas y se demostró la potencial aplicación del método determinando lactosa en muestras de leche y en muestras de leche sin lactosa. Se obtuvieron buenos resultados en términos de precisión y exactitud con valores de RSD inferiores al 9% y una recuperación media del 102 %. También se ensayaron muestras de superficies de puntos críticos de industrias alimentarias y muestras de aguas efluentes de industrias lácteas obteniendo buenos resultados.

También se ha desarrollado un método de separación de proteínas que combina la HPTLC con la detección colorimétrica con un smartphone para el análisis in situ del gluten. Se obtuvieron parámetros analíticos satisfactorios como la linealidad, LODs, LOQs y RSD. Además, se propuso un método de cribado que proporciona una respuesta sí/no utilizando el LOD como valor de corte para determinar gluten en las industrias alimentarias. Se analizaron muestras de superficies de puntos críticos de industrias alimenticias utilizando el método propuesto obteniendo resultados prometedores.

También se ha evaluado el uso de instrumentación portátil en electroquímica. Se ha demostrado que la modificación de la superficie de los electrodos de trabajo puede ser una herramienta importante para obtener una mayor selectividad y sensibilidad. En este sentido, se ha estudiado el desarrollo de dos sensores electroquímicos y el uso de diferentes estrategias para su fabricación. En primer lugar, se evaluó un sensor electroquímico basado en la inmovilización de un compuesto redox activo como molécula sonda como la antraquinona en dos

electrodos de trabajo diferentes con el fin de elaborar mejores biosensores. Por otro lado, también se estudió la determinación de 2,6-DNT por voltamperometría cíclica modificando un electrodo de carbono vitrificado mediante la reducción de una sal de diazonio y su posterior funcionalización con 2,6-DNT.

Así pues, se ha propuesto una ruta fiable y consistente para la modificación superficial de electrodos de GC y BDD a través de la reducción de una sal de diazonio seguido de una inmovilización cruzada de antraquinona. La modificación de la superficie y la inmovilización de la antraquinona en los sensores electroquímicos se confirmó mediante voltamperometría cíclica utilizando un potenciostato portátil. Además, se demostró que la antraquinona inmovilizada en interfaces de GC y BDD mediante procedimientos idénticos tiene diferentes densidades superficiales, valores aparentes de pK_{a1} y cinética de transferencia de electrones. Los resultados obtenidos pusieron de manifiesto que las propiedades químicas y electroquímicas fundamentales de las moléculas adheridas dependen en gran medida del sustrato, lo que proporciona pautas para un mejor desarrollo de biosensores.

También se ha estudiado la inmovilización de 2,6-DNT en la superficie de un electrodo de GC, tanto para superficies no modificadas como para superficies modificadas. Ambos electrodos mostraron buenas linealidades, sin embargo, se logró una mayor sensibilidad cuando se utilizaron electrodos modificados. Además, se han estudiado dos comportamientos diferentes que tienen lugar en función de la concentración de 2,6-DNT mediante el estudio de la densidad superficial, los eventos de transferencia de electrones acoplados y la cinética de transferencia. Todos los procesos de preparación del sensor y el análisis cuantitativo se realizaron mediante voltamperometría cíclica utilizando un potenciostato portátil. Se ha desarrollado un dispositivo novedoso, portátil, rápido, ultrasensible y de coste efectivo para la determinación in situ de 2,6-DNT a nivel de trazas.

ABSTRACT

Currently, society is demanding new devices for monitoring real applications to solve in place problems. This, along with the recent evolution in new technologies, have contributed to the development of portable instrumentation. In this sense, the use of portable instrumentation has significantly increased over the last years in a wide range of scientific areas.

The present Thesis is focused on the evaluation of several portable devices from different techniques and the development of new strategies in order to enhance the portability and sustainability in analytical chemistry. The proposed methodologies have been based on the control of experimental and measurement conditions in order to perform more accurate in situ analysis following the trends of sustainable and green analytical chemistry.

Therefore, the analytical information given by several instruments has been compared from an analytical and a sustainable point of view in order to evaluate portable instrumentation. The control of experimental and measurement conditions has been optimized, and some rules have been stablished for working with smartphones. Another key aspect when working with smartphones is to control of the influence of light. In this sense, several light sources and different measurement strategies have been evaluated in order to improve the results provided.

Another approach studied in this Thesis is the development of colorimetric devices for in situ analysis and their following measurement using the validated strategies. Accordingly, a NQS-doped PDMS-based sensor was evaluated as a potential application to determine NH_4^+ and urea in water and urea samples respectively. The developed strategies were also tested analyzing sensors of multiple colors, covering different spectral ranges, and supported in different materials. In this regard, a nylon-supported plasmonic sensor for the evaluation of hydrogen sulfide in breath samples, a paper-based sensor to determine hydrogen sulfide in water matrices and a PDMS delivery sensor to measure the presence of nitrites in solution have been proposed as study cases.

HPTLC is a very useful technique that can be used to separate analytes in complex matrices. Two different studies have been performed with the aim of studying the selective detection of food allergens in real samples. To this end, the combination of high-performance thin layer chromatography with a derivatization reaction and colorimetric detection based on smartphone measurements has been proposed. On the one hand, a carbohydrate separation was carried out for the detection of lactose and on the other hand, a protein chromatographic separation was also performed for the isolation of gluten.

The use of portable instrumentation in electrochemistry has also been evaluated. In this sense, the development of two electrochemical sensors and the use of different strategies for their fabrication have been studied. First, an electrochemical sensor based on the immobilization of a redox active compound as a probe molecule such as anthraquinone on two different working electrodes was evaluated in order to elaborate better biosensors. On the other hand, the determination of 2,6-DNT by cyclic voltammetry was also studied by modifying a glassy carbon electrode through the reduction of a diazonium salt and its subsequent functionalization with 2,6-DNT. The immobilization of studied molecules was confirmed by cyclic voltammetry using a portable potentiostat demonstrating that, although portable instrumentation is usually selected for field analysis, it can also be used for laboratory measurements.

Therefore, in this Thesis the suitability of portable devices, including smartphones, for performing in situ analysis have been widely demonstrated being satisfactorily combined with different methodologies such as colorimetric sensors, HPTLC and electrochemical procedures.

INDEX

CHAPTER 1. INTRODUCTION

1.1. THE CONTEXT: RECENT TRENDS IN ANALYTICAL CHEMISTRY

Since the beginning of the century, the produced social changes, the investigation in new (nano)materials and the implementation of internet and new technologies, are some pillars on which the development of Analytical Chemistry have been based[1]. Thanks to technological breakthroughs, new tools and equipment have emerged. This, together with the evolution in computer sciences have led to the automation and miniaturization of analytical systems, reducing the time of analysis and improving the results obtained from analytical methods.

In the context of current chemistry, the requirements of sustainable and green chemistry have also to be considered. The concept "sustainable" first appeared in the 70`s, it is connected to the idea of liaising the economic development with the preservation of natural ecosystems[2]. The term sustainability was reached in 1987 from the Brundtland report in the World Commission on Environment and Development: Our Common Future[3]. This report warned about the negative impacts and consequences of economic development and globalization in the environment, suggesting alternatives to solve the problems derived from industrialization and population growth. Sustainable chemistry also considers the effects of processing, materials, energy, social and economic impacts[4].

Later on, green chemistry emerged from the concern about environmental contamination caused by pollution from chemical industry in 1990s. These interests were expressed by Anastas and Warner in 1998, who established a list of 12 principles as a guide for a good practice in green chemistry[5]. In this sense, green chemistry can be understood as the design, development and implementation of chemical processes or products to reduce or eliminate the use and generation of hazardous and toxic substances[6]. In parallel, sustainable chemistry is also focused on the consumption of resources, including energy, in a rate which they can be naturally replaced and their waste generation is slower than their management solution. In this context, there is an intersection zone between the mentioned subjects, greenness and sustainability, both included into the wider concept of suitable chemistry[4].

In the field of analytical chemistry, sustainable and green chemistry leads to the necessity of developing protocols and devices for in situ analysis, the use of non-harmful reagents, recycling and minimization of wastes, miniaturization of procedures and instrumentation and reduction of power costs, among others. Gałuszka et al.[7] proposed a set of twelve principles in order to help making greener analytical laboratories.

1. Application of direct analysis techniques to avoid sample treatment.
2. Integration of analytical processes and operations to save energy and reduce the consumption of reagents.
3. Minimization of the use of energy.
4. Reduction and proper management of generated waste.
5. Minimization of the size and number of samples
6. Selection of automated and miniaturized methods.
7. Preference for reagents obtained from renewable sources.
8. Increase of the safety for operators.
9. Performance of in situ measurements.
10. Derivatization should be avoided.
11. Toxic reagents should be eliminated or replaced.
12. Multi-analyte or multi-parameter methods are preferred versus methods using one analyte at a time

As input in this field, MINTOTA has introduced a quantitative tool, named HEXAGON for testing and classifying analytical methods in terms of greenness and sustainability and bearing in mind a given use case[8–10]. The analytical methods can be classified into three categories: in-line, on-line, and off-line based on the way in which the analytical process is carried out. A balance between performance, equipment cost, complexity, and reliability is required for selecting the best option for a given problem and, considering the factors involved in the development of the current and future devices indicated in the first paragraph of this section.

Currently, society is demanding new devices for monitoring real applications to solve in place problems, what means the capability to solve problems where the target compound is present. This, along with the recent evolution in microsensors technologies, have contributed to the development of portable instrumentation[11].

According to Eren portable instrumentation is characterized by finely tuned design features[12] as:

- Limited size and weight.
- Limited sized batteries.
- Low power consumption.
- Trade-off between the instrument cost and its performance.
- User friendly interface options.
- Operation in diverse environmental conditions.
- Data processing and data communication

Following these characteristics, portable instrumentation can be defined as devices, which have been designed to be light and small enough to be easily carried or moved[13]. Portable equipment has become an extensive and growing topic that led to potential benefits including more cost-effectiveness and less carbon footprint. It is also remarkable that, due to the easy-to-use of the user interfaces, non-specialized personnel can perform analysis. Besides, versatility and potential applications in different fields make portable devices a promising alternative to traditional laboratory equipment.

In this sense, the use of portable instrumentation has significantly increased over the last years in a wide range of scientific areas. This is reflected in the increasing number of articles related to this topic during the last twenty years in the web of science (WOS) database. Currently, more than 24,000 results can be obtained from searching "portable instrumentation", being 14% related to the chemistry field. The first article about these two topics was published by With in 1957, who used a portable source of wood light for porphyrin analysis, proving that the seek for portable instrumentation is a matter of interest for many years[14]. Figure 1 shows the evolution of the number of publications over the last 20 years related to portable instrumentation.
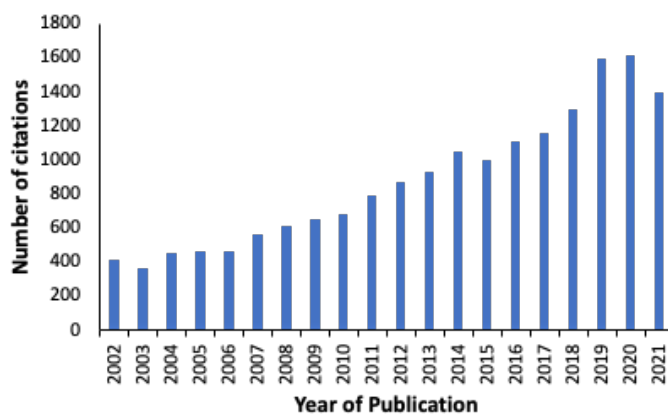
Figure 1. Number of publications in the Web of Science database from 2002 to 2021 with the topic "portable instrumentation", consulted in August 2022.

Nowadays, portable instrumentation is a valuable tool in different fields of analytical chemistry such as environmental[15], health[16] and food or drinks industries[17]. Figure 2 shows the different percentages of the most common areas for portable instrumentation. It is remarkable its use in health and environment fields.
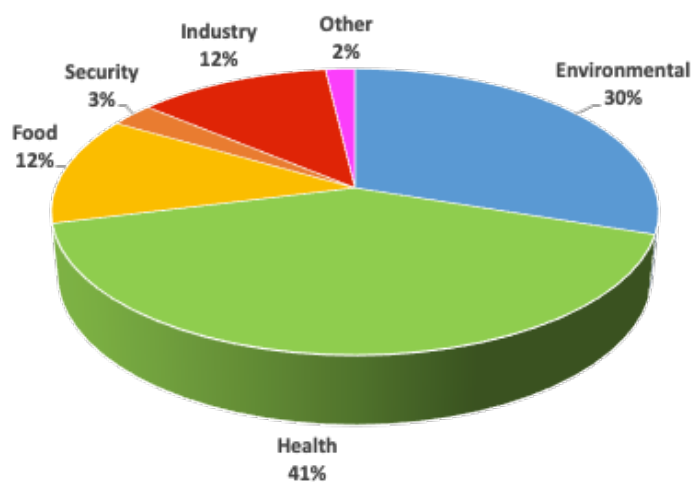
Figure 2. Percentage of different applications for portable instrumentation. Source: Web of Science, consulted in August 2022.

Portable instrumentation can be applied to different techniques within analytical chemistry. Currently, portable spectroscopy is the most common

6

technique gathering the 57% of the publications according to the WOS database. Nevertheless, chromatography (≈18%), electrochemistry (≈13%) and mass spectrometry (8%) are also techniques with a growing interest in portable instrumentation over the last 10 years. Figure 3 shows the number of publications per year of the four different techniques from 2011 to 2021.
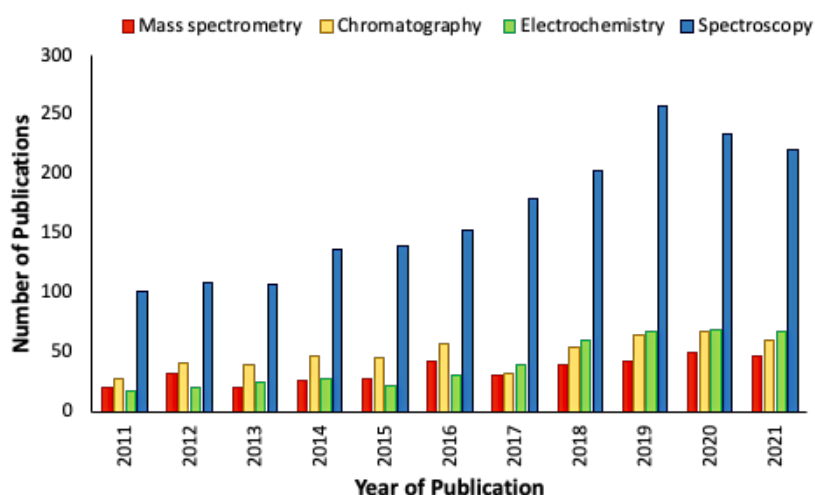
Figure 3. Number of publications from Web of Science Database from 2011-2021 with the keywords "Portable instrumentation" refined with "Mass spectrometry", "Chromatography", "Electrochemistry" and "Spectroscopy" respectively, consulted in August 2022.

Table 1 compiles the main characteristics of the aforementioned analytical techniques mentioning their principal strengths and weaknesses when using portable instrumentation. The features considered in the table are the need for specialized operators, their cost, the requirement of a power supply and the possibility to perform measurements using a smartphone. Some portable devices need to be connected to an energy source in order to carry out their measurements. Whereas devices working with batteries or coupled to smartphones can work wireless, so, a power supply is not needed.

Table 1 Comparison of the main characteristics and advantages and disadvantages of different analytical techniques

Analytical techniques	Main features	Advantages and disadvantages	
Chromatography[18]	• Operator: High specialized • Cost: High/Moderate cost • Power Supply: Wireless • Smartphone connection: Not possible	√ Accuracy √ Precision √ High selectivity	× Moderate sensitivity × Destructive analysis
Spectroscopy[13]	• Operator: Low specialized • Cost: Low cost • Power Supply: Wireless • Smartphone connection: Possible	√ Accuracy √ Precision √ High/moderate sensitivity √ Non-destructive analysis	× Moderate selectivity
Electrochemistry[19]	• Operator:Moderate specialized • Cost: Low cost • Power Supply: Wireless • Smartphone connection: Possible	√ High sensitivity √ Accuracy √ High-moderate selectivity √ Non-destructive analysis	× Moderate precision
Mass Spectrometry[20]	• Operator: High specialized • Calibration: High cost • Power Supply: Wired • Smartphone connection: Not possible	√ High sensitivity √ Accuracy √ Precision √ High Selectivity	× Destructive analysis

The main advantages and drawbacks of each technique when using portable instrumentation have been also described, being accuracy, precision, selectivity, sensitivity and the possibility to carry out non-destructive analysis the characteristics considered in Table 1.

In light of the information described in Table 1, this thesis pays special attention to the development of in situ methodologies for spectroscopic, chromatographic and electrochemical techniques. These methodologies have been combined with portable instrumentation and smartphones in order to perform in place measurements because of their interesting features, such as moderate/low cost, portability and versatility.

Portable spectroscopic techniques allow the performance of accurate, precise and sensitive analysis[13]. It must be highlighted that the number of articles related to this issue in the WOS database has increased significantly in the last 10 years to more than 9,000 being almost a 52% from the chemistry field. Figure 4 shows the evolution of the number of publications over the last 10 years related to portable spectroscopy.
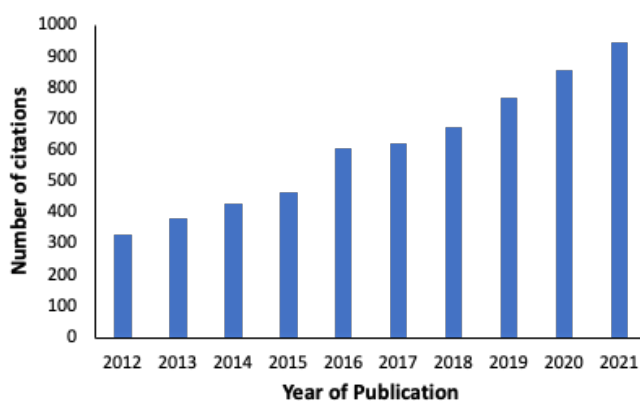
Figure 4 Number of publications in the Web of Science database from 2012 to 2021 with the topic "Portable spectroscopy" consulted in August 2022.

Among the different analytical techniques within portable spectroscopy, colorimetric methods have become one of the most well-known. These methods are generally based on a chemical reaction between a chromophore and a target compound that produces a color change that can be easily detected. The obtained

color intensity is related to the analyte concentration allowing not only qualitative analysis but also quantitative ones. Traditionally, color is measured by the naked eye for qualitative or semiquantitative analysis [21] or by a noninvasive technique such as absorbance or diffuse reflectance (DR) spectroscopy for a quantitative analysis [22,23]. However, there is the possibility of setting more economic portable instruments using handheld components and optical fibers (Figure 5). Nowadays several studies have been reported using portable devices coupled to fiber optic probes to perform color measurements including reflection probes.
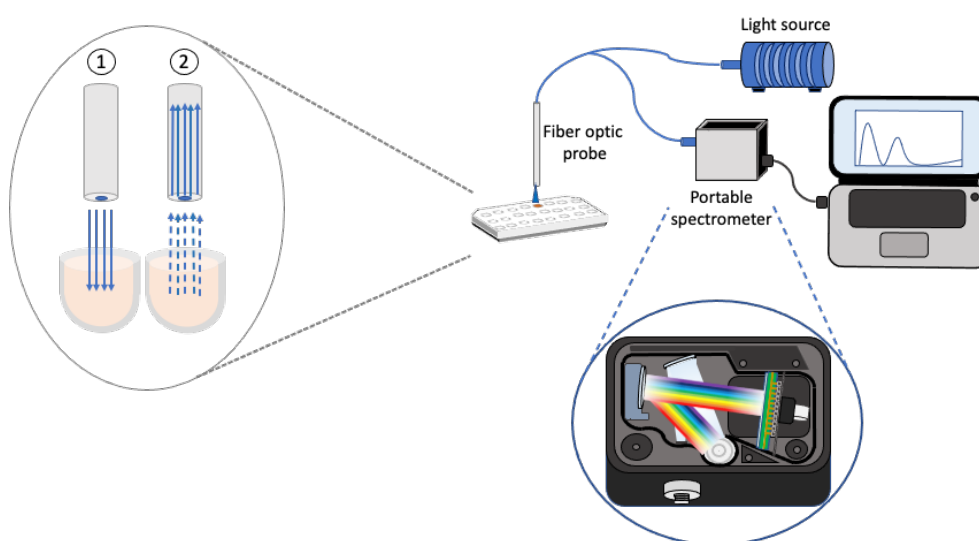
Figure 5. Schematic representation of measurements configuration using a portable spectrometer and a fiber optic probe*.*

According to the new guidelines marked by the implementation of sustainable and green analytical chemistry, in the last decade, there has been also a growing interest in the development of new rapid and cost-effective alternatives to perform in situ electrochemical measurements. This, together with the electronical revolution witnessed in the last years, has led to a remarkable progress towards portability in electrochemistry[24].

In this sense, more than 1,500 publications have been reported in this topic according to the WOS, being almost 1,000 published in the last 5 years, showing a remarkable increase in this period of time as can be seen in Figure 6.
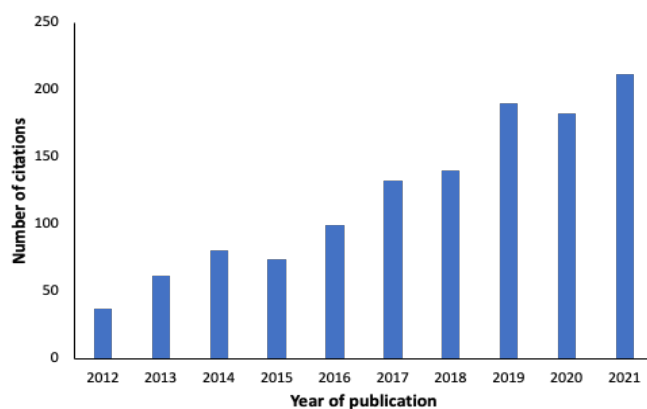
Figure 6 Number of publications in the Web of Science database from 2012 to 2021 with the topics "electrochemical measurements" and "portable" September 2022.

On the other hand, smartphones have become currently an indispensable tool in peoples day-to-day because of their capability to read documents, their fast online connectivity and the recent advances in their integrated cameras.

In this sense, there is a growing trend in smartphone-based applications for science. Accordingly, more than 55,000 articles have been published related to this topic as the WOS shows in the last 10 years, of which, only 7.3% are related to chemistry. However, present trends in technologies and the demands of real time measurements have made smartphones an emerging alternative for quantitative purposes. Hence, they have become a valuable tool within the framework of in situ analysis. Figure 7 reveals the growing interest of the scientific community for the use of smartphones as analysis instruments in the last decade.

According to this, there are several studies in literature that show that smartphone-based analyzers can be successfully implemented to different analytical techniques. Guo utilized a smartphone-powered medical dongle as a miniaturized electrochemical analyzer for blood β-ketone monitoring[25], Fu et al. presented a palm-sized uric acid test powered by a smartphone for proactive gout management using a photochemical dongle[26] and, a nano-SERS chip combined with a smartphone-based Raman detector was reported by Mu et al. for the identification of pesticide residues[27].
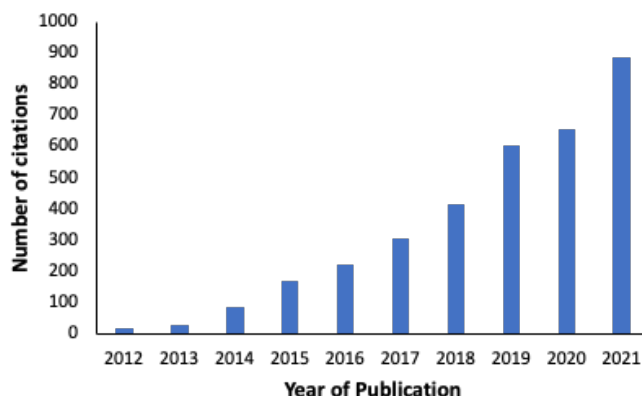
Figure 7 Number of publications in the Web of Science database from 2012 to 2021 with the topics "smartphone" and "chemistry" consulted in August 2022.

In the last years, new instruments for color analysis have become available at more affordable prices thanks to the development of digital cameras and smartphones[28,29]. For this reason, many studies have reported the use of smartphone-based spectrophotometers when using colorimetric detection. It has been studied in bibliography before that spectral analysis can be performed coupling a portable spectrometer to a smartphone camera[30]. Smartphones also give the opportunity to capture images with their integrated cameras, to perform further color analysis[31], making them a key tool for in situ analysis. To sum up smartphones have proved to be a versatile option for colorimetric analysis that provides not only spectral results but also image analysis in a fast and cost-effective way.

Although smartphone-based studies have come up as a powerful alternative to conventional instrumentation, monitoring a set of experimental conditions related to image are essential to carry out appropriate color analysis. In this sense, controlling the sample and smartphone position, smartphone type or the incident light are required. Also, when performing spectral analysis, a calibration of the instrument is commonly needed to minimize the uncertainty in reproducibility across smartphone devices[32]. Nevertheless, the main drawback of using smartphones as analytical instruments is that color analysis presents a strong dependence on lightning conditions due to light affecting the color response of the samples[33]. The quality of image may be subject to non-uniformity and non-reproducibility when light conditions are not controlled, affecting negatively to the

accuracy of the measurements. Thus, monitoring the incident light in all measurements can be relevant.

In order to prevent interferences from ambient light, several settings have been proposed in the literature such as the use of the phone flash light[34], incorporating the smartphone in boxes with light[35] or taking references areas to normalize[36]. Besides, each type of light provides not only a different information in certain wavelength regions, but also an alternative color temperature. Accordingly, it is important to select the most suitable light source depending on the wavelength region of interest when performing spectral analysis. Furthermore, prior to perform image analysis, the correct color temperature must be selected from the camera settings relying upon the type of light employed. It has been studied that different characteristics of incident light such as light intensity or color temperature can be monitored with a tool for light characterization[37]. All these aspects must be taken into consideration for getting the most representative results.

In this thesis, a comparative study has been carried out for different types of instruments, giving special attention to measurements performed using smartphones. Some rules and strategies have been stablished for a variety of use cases.

1.2 OPTICAL SENSORS AND PORTABLE MEASUREMENT

1.2.1 In-situ optical sensors

More than 29,000 publications have been reported from the WOS database with the topics "optical sensors" and "spectroscopy". According to this, there are several studies in literature that show that optical sensors with portable devices can be successfully implemented for different applications[38–42]. Recently, some studies have been also carried out using optical sensors and smartphone-based applications with low carbon footprint[43] in important fields of analytical chemistry such as health[44], food control[45] and environmental protection[46].

A colorimetric sensor consists of a recognition element, which interacts with a target compound producing a change of color. This color change is proportional to the analyte concentration and can be easily detected by the naked

eye, although a spectroscopic instrument is required in order to perform a more accurate quantitative analysis.
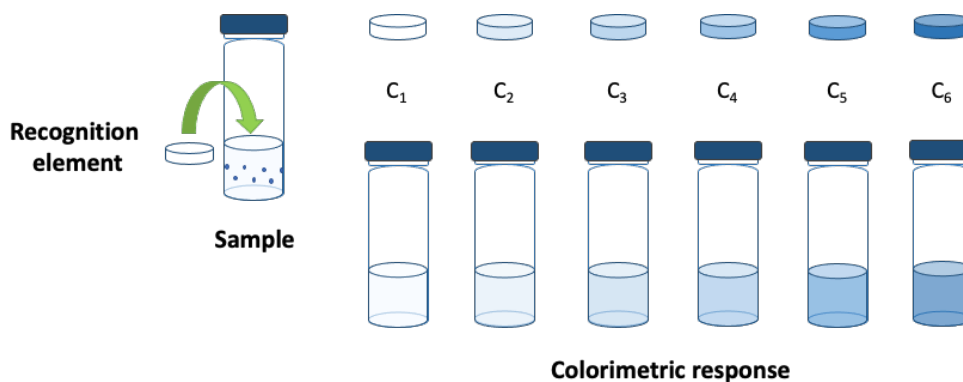
Figure 8 Schematic illustration of the colorimetric response for several analyte concentrations of an optical sensor reacting: in a solid support and in solution from a delivery reagent device.

Figure 8 as an example, shows several forms to carry out a colorimetric reaction. Different types of devices have been developed and recently reported in the literature:

- o Devices for delivery reagents: The immobilization of the derivatizing reagents takes place into a solid support such as polymers or paper. The optical device is immersed into the sample and the reagent diffuses from the support to the solution, where the target molecule is, giving rise to the derivatization reaction[22,23].

- o Solid sensors: In these devices, the chromophore reagent is also immobilized in a solid support. Once immersed the optical device into the sample solution, the analyte diffuses into the sensor where the derivatization reaction takes place[22,31,47,48].

- o Test kit: They are developed by mixing the reagents with the sample solution producing a color change in presence of the target analyte. These kits are commonly used to monitor the levels of chlorines in swimming pools or as pH detectors. Additionally, they are very helpful in forensic analysis and drug determination[49].

o Test strips: These tests consist in the immobilization of chromophores on a solid support, mainly paper. They give the possibility of detecting several analytes in one measurement performing rapid specific and low-cost analysis. Test strips are regarded as a simple method with different applications in the fields of environmental sciences, food and biomedicine[50,51]. However, just qualitative and semiquantitative analysis can be carried out with test strips[52].

o Microfluidic platforms: They are miniaturized devices in which the derivatization reagents are embedded on a support, mainly cellulose. The samples flows by capillarity along a channel, derivatization reaction is produced when the target analytes reaches the area where the reagent are deposited giving rise to a color change[53,54].

o Colorimetric tubes: They consist of a tube packed with porous material impregnated with the derivatization reagent. The colorimetric reaction takes place when generally a gas containing the target analyte passes through it manually or assisted by an automatic pump[55,56].

o Colorimetric arrays: Consist of multiple color dyes adsorbed onto a support whose color change is produced by its interaction with different analytes. Pattern recognition relies on the combined response of several sensors. Colorimetric arrays give the possibility to analyze and determine numerous compounds such as explosives[57–59], polysaccharides[60], environmental pollutants[61] and volatile organic compounds[62].

o Plasmonic sensors: The development of plasmonic sensors is increasing in recent years as metallic nanoparticles (MNPs) are emerging as an alternative to colorimetric reagents. MNPs such as silver nanoparticles (AgNPs) and gold nanoparticles (AuNPs) show a localized surface plasmon resonance in the visible region which exhibits a different color when aggregated in presence of the analyte[63], being this the most employed option. The optical changes can be quantified performing absorbance measurements or by diffuse reflectance. Many studies have been reported recently for several applications like health[64,65], food[66,67] and environmental analysis[68].

In conclusion, colorimetric analysis can be performed using different optical devices, where color changes can be mainly produced in solution or on a solid support. Traditionally, a broad range of different materials have been used as colorimetric supports, however, in order to reduce the use of conventional polymers derived from petroleum, an increasing concern in studying new polymers has emerged[69]. In this sense, the investigation of new nanomaterials is a current trend in analytical chemistry, because of their significance in the development of (bio)sensors.

Nanomaterials present a large specific surface area which has a key role in the immobilization of (bio)molecules, besides, they show unique physicochemical properties difficult to find in small molecules. Accordingly, a wide variety of nanomaterials have been used in literature to improve numerous (bio)sensors development techniques. Paper is one of the most commonly used because of its availability, its low cost and its ease to be handled. In this context, several publications related to paper-based sensors have been reported for different applications[70–72]. Zein is a protein from corn, it is an inexpensive and biodegradable material, obtained as a waste from bioethanol manufacturing, with excellent properties to form films because of its chemical structure. In this sense, a biokit based on a zein film for alkaline phosphatase and substrates delivery has been reported by Jornet-Martinez et al.[73]. Also a zein sensor for delivering enzymes, organic and inorganic compounds has been published by Bocanegra-Rodríguez et al.[74]. Moreover, Alqahtani et al. studied the use of zein for oral drug delivery[75]. On the other hand, polydimethylsiloxane (PDMS) is a silicon-based material with a non-toxic nature and great versatility that can be used in several fields. It is widely employed as support material for the immobilization of chromogenic reagents, nanoparticles and quantum dots[76–78]. Nylon is a synthetic polymer that can form highly porous membranes, it also presents a high homogeneity and surface/volume ratio, which makes it a good option as a support material. In this context, its capacity as a support membrane has been tested in a plasmonic assay based on the aggregation of AgNps[63]. A flexible and breathable strain sensor based on a nylon support have also been proposed by Yuan et al.[79]. Glass has also been reported in literature as a support material[80]. Tetraethylortosilicate (TEOS) has been used as a sol-gel support because of its highly porosity, allowing a large diffusion. Accordingly, a sol-gel based device composed by TEOS/Dodecyl-TEOS has been tested as a colorimetric pH sensor[81].

From all the aforementioned materials, in this Thesis, special attention has been given to PDMS, Nylon and Paper as based supports for colorimetric sensors. However, TEOS has also been studied as a hydrophilic modifier and glass was used for immobilizing an enzyme.

Paper-based sensors: Paper is one of the cheapest and most widely used flexible substrate in peoples day-to-day. It is also environmentally friendly as it is made of renewable raw materials and it is recyclable. Although paper have been traditionally used for packaging and for displaying and storing information, recently, it has also emerged as a potential substrate for solid supports[82]. The use of paper as a material support have undergone a rapid growth with significant implications under the umbrella of analytical chemistry. In this sense, almost 5,000 publications have been reported in this topic according to the WOS, showing a notable increase in the last decade as can be seen in Figure 9.
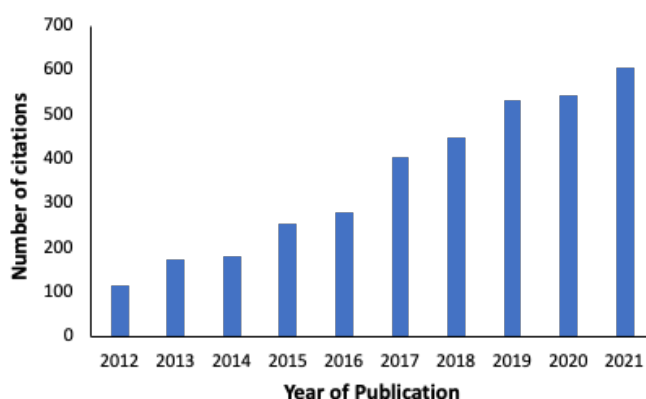
Figure 9 Number of publications in the Web of Science database from 2012 to 2021 with the topic "paper-based sensor" consulted in August 2022.

This increase, can be explained as a direct consequence of its unique and intrinsic characteristics such as, porosity, chemical structure and availability in a broad range of thickness[83]. Besides, depending on the type of paper substrate, it can present interesting properties like gas permeability and high mechanical flexibility. Furthermore, it can offer the possibility to be impregnated through capillarity, to hold and retain liquids, allowing them to be colored and chemically functionalized[82]. As a result, numerous studies of colorimetric paper-based sensors

have been published in different fields of analytical chemistry such as health[84,85], food control[86], and environmental analysis[87,88] , between them .

Additionally, they can be measured using portable instrumentation, including smartphones, being an interesting combination in order to perform in place analysis. Pla-Tolós et al. have reported a paper-based support for in-situ determination of hydrogen sulfide in waters and atmospheres using a smartphone to perform image analysis[31].

PDMS composites: PDMS is a silicon-based homopolymer known for its covalent bonds of multiple units of [-Si(CH$_3$)$_2$O-]n groups (Figure 10). PDMS usually forms long chains where molecules can rotate around the covalent bonds providing a high flexibility[89].
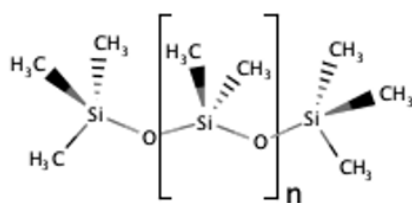
Figure 10. Chemical structure of PDMS.

It is one of the most used polymers in several fields due to its chemical inertness, biocompatibility, thermal stability, low cost, non-toxicity and easy processing[90]. In this sense, more than 35,000 publications have been reported to date regarding the topic "PDMS" in the WOS database.

PDMS is a hydrophobic material permeable to gas and organic solvents with low polarity, in this sense, PDMS composites can be utilized for analyte extraction from aqueous media. Thus, the covalent immobilization of reagents inside PDMS devices is commonly used for analysis and quantification of non-polar analytes[91]. However, its hydrophobicity can sometimes be a limitation, thus, several physical and chemical modifications have been proposed. In this sense, polyvinyl alcohol (PVA)[92], polyethylene glycol (PEG)[93], TEOS[94] and 1-methyl-3-octylimidazolium hexafluorophosphate (ionic liquid)[95] have been studied as chemical treatments in order to obtain more hydrophilic and more sensitive PDMS composites. Some of these polymeric mixtures can crack when the composite is gelled, in this sense, the addition of silica nanoparticles (SiO$_2$NPs) has been proposed by Li et al. It has been

demonstrated in this study that the addition of SiO$_2$NPs cause an increment of the pore size, preventing the cracking[96].

Additionally, PDMS is optically transparent, allowing to carry out colorimetric measurements without producing color interferences, thus, several colorimetric PDMS-based solid sensors have been reported in bibliography [23,97]. As an example, Argente-Garcia et al. proposed a PDMS-based sensor doped with 1,2-napthoquinone-4-sulfonate (NQS), using a sol-gel process, for the determination of amphetamines [48]. PDMS membranes can also be used as devices for delivery reagents, accordingly, a Fast Blue B functionalized PDMS composite for the evaluation of 3,5-dihydroxyhydrocinnamic acid (3,5-DHCA) as biomarker for gluten intake was studied by Hakobyan et al.[98]. Moreover, PDMS composites present several advantages such as simplicity, versatility, being low cost and providing rapid and reliable responses. They also give the possibility to carry out colorimetric analysis with portable instrumentation and smartphones, reporting promising results[99].

Nylon membranes: Nylon is a synthetic polymer containing an amide group based on chains of multiple units of [C$_6$H$_{11}$NO]$_n$. Depending on the degree of polymerization, different types of nylon can be achieved such as nylon 6, nylon 6.6 or nylon 12 among others. Due to the excellent combination of its remarkable mechanical properties such as a high thermal stability and a great tensile strength[79,100] and its easy processability, nylon is used in a wide range of applications[101]. Moreover, it is significantly applied in clinical studies because of its non-toxicity and chemical inertness[102]. In this context, according to the WOS database, more than 80,000 studies have been published to date related to nylon.

Nylon is a hydrophilic material and its membranes are chemically resistant to alkaline solutions and organic solvents, thus, it is broadly used for particle removing filtration in both aqueous and organic media. Besides, nylon membranes are composed by structures with a high porosity that can provide a large specific surface area, being a suitable material for biomolecules immobilization[103]. Similarly, plasmonic sensors can be developed supporting MNPs on nylon membranes[63]. Jornet-Martinez et al. have proposed a nylon-supported plasmonic assay based on the aggregation of AgNPs to monitor H$_2$S in breath samples, reporting satisfactory results when implementing smartphones to perform image analysis [63](Figure 11). Moreover, derivatization reagents can also be incorporated

into nylon supported sensors giving the possibility to perform colorimetric analysis[104].
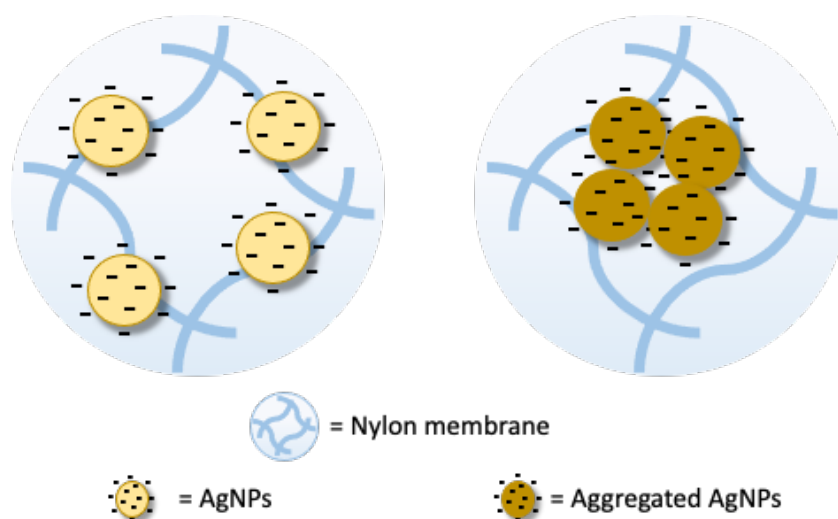
Figure 11. Schematic representation of the color change due to the aggregation of AgNPs in presence of the target analyte.

1.2.2 Response measurement

Traditionally, optical solid sensors have been measured using conventional instrumentation, however, spectroscopic measurements can also be performed using smartphones. To carry out spectral analysis, a miniaturized spectrophotometer can be assembled combining the integration of complementary metal-oxide semiconductors (CMOS) camera image sensors with an optical grating and a spectrum processing technique. Different designs have been explored in bibliography based on the smartphone spectrophotometer assembling using transmission and reflective diffraction gratings [105–107]. All the spectrophotometer elements can be integrated into a compact device that can be coupled to the smartphone camera to perform spectral analysis. Also, depending on whether the analyzed sample material is opaque or transparent (or translucent) it can measure in reflectance mode where the light is reflected off the sample or in transmittance mode where the light travels through the sample. Besides, fiber optic probes can also be adapted to the smartphone spectrometer, when measuring in reflectance mode, with the aim of obtaining more accurate and precise

measurements. In terms of software, the data acquisition and the processing capacity of the phone play an important role [108,109]. Data is usually gathered by a commercial app when performing spectral analysis and it is exported to external computer programs for being processed. However, there is also the possibility of using a designed app for direct calculation, which can provide several advantages such as storing the analyzed data or getting real time results and transferring them via Wi-Fi. Accordingly, it has already been seen that a miniaturized spectrometer can be coupled to a smartphone in order to perform colorimetric biosensing obtaining encouraging results[110]. Therefore, because of the small size, its versatility and easy portability, smartphone spectrometers are a suitable alternative to conventional optical spectroscopic techniques and can be used in many different applications[111].

A main feature of smartphones is that they also give the chance of capturing images with their cameras, which can be digitalized (JPEJ format) for further image analysis. Traditionally control over smartphone camera parameters was mostly limited, in this sense, image parameters were applied automatically obtaining modified images that varied significantly from the reality. Recently smartphones with upgraded cameras have been launched with more complex settings. These new settings allow customers to adjust camera parameters such as the sensitivity to light (ISO), white balance, the exposure time or the color temperature, reducing the systematic errors when performing color analysis[29].

In order to carry out color analysis, the colors of a picture firstly digitalized are converted into parameters or numerical values, which depend on the selected color model, by using an image editing software like Adobe®Photoshop, GNU Image Manipulation Program (GIMP), MATLAB or ImageJ. Some of these softwares allow also the possibility to process images. It has been seen previously in literature that images can be processed to improve the results obtained, achieving higher linearities and sensitivities[30]. As pointed out above, the obtained color parameters are dependent on the chosen color model such as red-green-blue (RGB) coordinates, cyan-magenta-yellow-black (CMYK), hue-saturation-value (HSV) or CIELAB parameters[112]. Recently, several works have been published in analytical chemistry reporting the use of these color parameters as analytical signals for calibration[28,113] being the RGB color model the most commonly used [114,115].

In RGB model, colors are obtained from different mixtures of the primary colors red, green and blue. Their numerical values can go in a range from 0 to 255 depending on their intensities, where a pure black color is obtained for (0,0,0) and a pure white color is obtained for (255,255,255). Nowadays, because of their generalized use around the world, there is a wide type of commercial Apps for Android and for iOS that give also the possibility to obtain color parameters instantly. These data can be analyzed for prediction by using multivariate methods[116], or by the correlation of the target analyte concentration with one component[117] or with the ratio between two components[118]. In addition, designed apps that analyzes the obtained data instantly can also be utilized in order to obtain direct results. Some examples of colorimetric detection applying different strategies when using smartphones are given in Table 2 covering a variety of areas.

Table 2 Summary of selected detection methods using smartphones in the literature between 2018 and 2022

Type of Colorimetric Analysis	Matrix	Analyte	Colorimetric reagent	LODs
Spectroscopic analysis Transmission[119]	Aqueous samples	Ascorbic acid	Methylene blue	5 µg·mL^{-1}
Spectroscopic analysis Transmission and Reflection[120]	Tablets	Ibuprofen	Phenolphthalein	4 µg·mL^{-1}
Image analysis RGB-Designed App[121]	Serum	Glucose	Methylene blue	1.5 µM
Image analysis RGB -Designed App[122]	Milk	Alkaline phosphatase (ALP)	5-Bromo-4-Chloro-3-Indolyl Phosphate (BCIP)	0.87 U·mL^{-1}
Image analysis RGB – External Software[123]	Serum	Osteopontin (OPN)	Bradford reagent	5 ng·mL^{-1}
Image analysis RGB - Commercial App[124]	Beverages	Ethanol	Ceric ammonium nitrate and Nitric acid	0.19 % (v/v)
Image analysis RGB-Commercial App[125]	Beverages	Cu^{2+}	1-(4-(dimethylamine) benzaldehyde) thiocarbazone	0.18 mg·L^{-1}
Image analysis HSV-Designed App[126]	Food	Alternariol monomethyl ether (AME)	Gold nanoparticle (AuNps)	0.2 ng·mL^{-1}

1.3 MINIATURIZED HPTLC AND PORTABLE MEASUREMENTS

Over the last decades there has been a significant growth of interest and popularity in Chromatography to become a leading technique in instrumental analytical chemistry. This has been motivated by the need of separating analytes for the study of complex matrices as shown in Figure 12. *Particularly, in this thesis High Performance Thin Layer Chromatography (HPTLC) has been studied.*
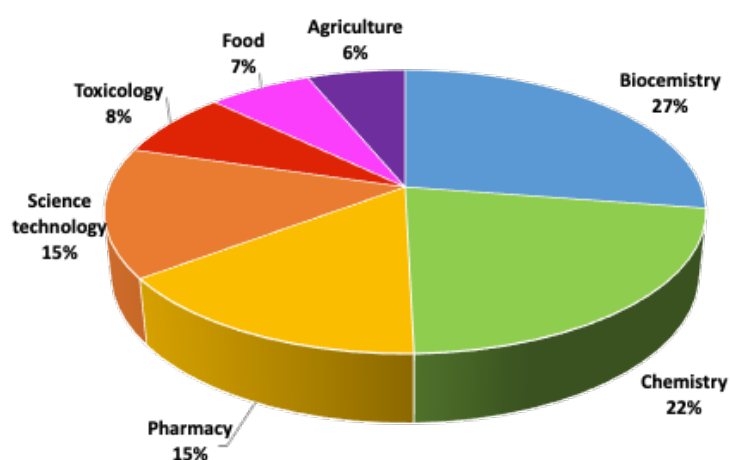
Figure 12 Percentage of different applications in Chromatography. *Source: Web of Science, consulted in August 2022.*

HPTLC is a chromatographic technique that allows the performance of in situ measurements with a rapid detection and low-cost analysis. Besides, it can be combined with different detection methodologies providing efficient separations and suitable sensitivities[127].

The general procedure to perform TLC has remained unchanged over the last decades. It involves the use of a thin support (aluminum glass or plastic) in which a sorbent, known as stationary phase, has been applied. The sample is dissolved using an appropriate solvent prior to its application onto the stationary phase. A single solvent or a mixture of solvents, as mobile phase, migrates by capillary action from one edge of the stationary phase to the opposite eluting the different compounds from the sample. In this sense, components with a stronger

interaction with the stationary phase are more retained, while components that have a higher preference for the mobile phase are easier eluted. As a consequence, compound separation is achieved[128] as it is shown in Figure 13.
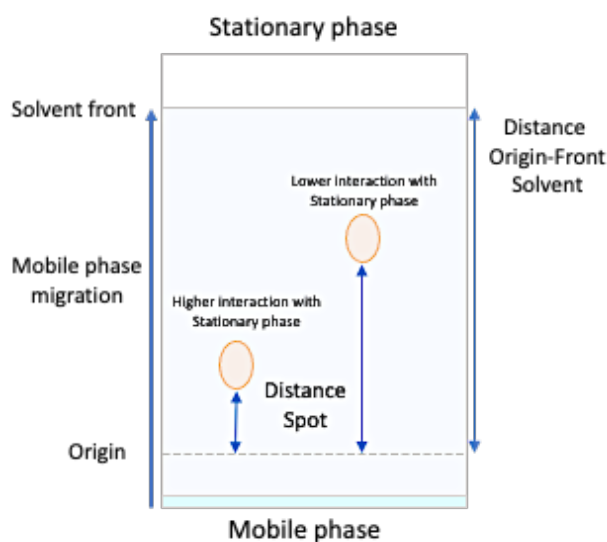
Figure 13 Schematic representation of a TLC development.

The migration distance of each compound can be quantified using a parameter known as retention factor (Rf) and it is determined by the ratio between the spot migration distance and the distance from the origin to the solvent front (Equation 1)[128].

$$Rf = \frac{Distance_{spot}}{Distance_{solvent}}$$ *(Equation 1)*

As the components from a sample migrate along the chromatographic plate, they separate from each other. The difference between the middle point of the spot of one component and the spot middle-point of another component is known as the center-to-center distance (Δx). The resolution (R_s) in a chromatographic separation is defined as the ratio between the center-to-center distance and the width of a spot (w) (Equation 2)[128].

$$R_s = \frac{\Delta x}{w}$$ *(Equation 2)*

The most straightforward and commonly used criteria in TLC stablishes that a suitable resolution has been achieved when R_s is equal or greater than the unity ($R_s \geq 1$).

HPTLC presents several improvements with respect to TLC in order to enhance the separation of different compounds and increase their resolution. HPTLC materials are characterized by smaller average particle size and a narrower size distribution than those employed in TLC[129]. Moreover, there is the possibility to use chromatographic chambers, reducing the time of analysis and the volume of mobile phase needed. The main advantages of HPTLC compared to traditional TLC have been highlighted in Table 3.

Table 3 Comparison between TLC and HPTLC extracted from [130].

Feature	TLC	HPTLC
Plates	Lab made / Pre-coated	Pre-coated
Plate height	30 μm	12 μm
Sorbent layer	250 μm	100 μm
Stationary phase	Silica gel, Alumina	Nano silica gel and C_{18}
Analysis time	20-200 min	1-5 min
Mean particle size	10-12 μm	5-6 μm
Resolution	Low	High
Sample tracks per plate	≤ 10	≤ 32
Development chamber	High volume	Reduced volume
Connectivity to equipment	No	Yes
Quantitative analysis	No	Yes

Another advantage of HPTLC is the availability of automated instruments for sample application providing improved precision and accuracy. HPTLC also gives the possibility to perform quantitative analysis using traditional instrumentation such as densitometers and video scanners[131] or combining HPTLC with modern instrumentation like smartphones[132]. Accordingly, it has proved to be a simple, cost-effective, flexible and high-throughput separation technique. This together,

with its increased accuracy, reproducibility and sensitivity, have made HPTLC a promising tool, especially for in place analysis.

In this sense, the use of this technique has undergone a rapid growth with significant implications under the framework of analytical chemistry. Thus, more than 7,000 publications have been reported in this topic according to the WOS, showing a notable increase in the last twenty years as can be seen in Figure 14.
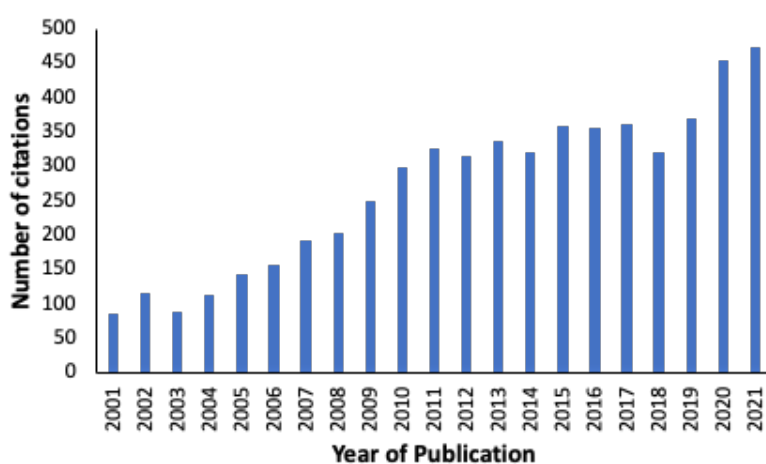
Figure 14 Number of publications in the Web of Science database from 2002 to 2021 with the topic "HPTLC".

This increase can be explained as a direct consequence of the different fields in which HPTLC can be applied, being one of the most used analytical techniques in pharmaceutical industries, clinical and forensic chemistry, food and drug analysis, biochemistry, cosmetics and environmental analysis, among others.

In order to get suitable qualitative and quantitative analysis, method development is one of the most critical steps in thin layer chromatography[133]. According to Shewiyo et al. method development can be divided in the following steps: selection of the stationary phase, mobile phase selection and optimization, sample application, chromatographic development and detection[134]. There are numerous methods to develop the separation in HPTLC, including ascending, descending, two-dimensional chromatography, gradual and multiple developments, radial, centripetal and forced flow planar chromatography.

However, in order to get an improved resolution ascending chromatography is the mainly used in the literature.

1.3.1 Stationary phases

Selection of stationary phase should rely on the properties of the compounds to be separated. In planar chromatography separations can be performed on unmodified, modified and on impregnated-stationary phases. The most suitable stationary phase should be selected depending on the different chemical properties between the substances in the sample and the adsorbent material[133]. In this sense, the following types of stationary phases for HPTLC have been developed and described in the bibliography[135].

- o Nanosilica gel: Silica gel is a white porous material which structure is based on bonded siloxane groups. Most of the absorptive properties of silica gel are provided by the residual hydroxyl groups on the surface, giving raise to unique separation characteristics. The synthetic nature of silica gel allows the control of pore size, pore volume and particle size, which directly affects the efficiency. Pore size also affects the selectivity altering the migration rates and hence the resolution of sample components. In this sense, Nanosilica (NanoSiO$_2$) gel plates of 5-6 μm are commonly used in HPTLC. Nanosilica gel plates are extremely versatile being used in a wide range of applications. Solvent mixtures of polar and non-polar solvents can be used and also acid and base modifiers are well tolerated for satisfactory separations[136–138].

- o Reversed phase: Reversed phases are obtained bonding chemically organosilanes of different chain lengths to Nanosilica gel plate. Chains of 2, 8 and 18 carbons bonded to the siloxane matrix are the most commonly produced by commercial manufacturers. The hydrophobicity of the layer increases with the degree of surface modification, getting highly hydrophobic plates when the alkyl chains are larger. In this sense, only low proportions of water are allowed in the developing solvent mixture. It is commonly used for samples with polar substances, in applications where separation

28

must be carried out according to lipophilic properties and chain lengths, steroids[139] or in amino acid separations among others[140].

- o Amino modified phase: Amino modified nano silica gel layers are prepared linking amino propyl groups to nano silica gel plates through siloxane bonds. The resulting plate is quite versatile, stable and hydrophilic. Because of the hydrophobic properties of the propyl group, it can be used for reverse-phase separation using aqueous based eluents. Moreover, since the (-NH) group is polar, normal-phase is also possible using organic eluents with low polarity. The main applications of amino modified phases are the resolution of steroids, nucleotides, alkaloids, sulfonic acids, purines, pyrimidines and phenols[141–143]. It is also important to remember that these plates are chemically reactive since they amine group is a primary amine.

- o Cyano modified phase: These phases are prepared by bonding chemically a cyanopropyl group to a nanosilica gel plate. The bonding to the silica matrix is carried out via a siloxane, using the same procedure as in the amino bonding phases. The cyano phase shows properties between reversed and normal-phase materials, hence, with an appropriate choice of mobile phase both separations can be achieved. Cyano modified layers have already been utilized in a broad range of applications, such as, derivatives of benzodiazepine, antibiotics, pesticides, phenols and alkaloids[144–146].

- o Diol bonded phase: Diol modified phases are bonded to the silica gel surface via an alkyl ether spacer group. These layers present a hydrophilic nature, and its behavior is usually very similar to the silica gel unmodified phases. However, sample components use to migrate further on the diol phase when using the same mobile phase. It commonly used as normal-phase, thus the retention factor of samples analytes can be controlled. Diol modified HPTLC layers have proved to perform suitable separations including phenols, steroids, glycosides, aromatic amines and dihydroxybenzoic acids[147,148].

o   Chiral separation phases: These plates are prepared coating an amino-acid derivative of hydroxyproline in the presence of a copper salt on to a reversed-phase plate, creating a ligand exchange surface. The mechanism of enantiomer separation consists in the formation of complexes between the diastereomer and the copper ion. The retention on the stationary phase of each enantiomer will vary depending on the stability of the formed complex allowing to achieve suitable resolutions. These ligand-exchange plates have proved to provide adequate resolution of different amino-acids, polyphenols among others[149–151].

o   Cellulose phases: Cellulose is a natural sorbent with a polymeric structure, that present a myriad of hydroxyl groups available for hydrogen bonding. HPTLC cellulose plates are based on microcrystalline cellulose, resulting in a highly reduced diffusion. In this sense, adsorbed water or alcohols can be easily retained by cellulose layers, providing ideal separation of hydrophilic substances like, amino-acids, carbohydrates, phosphates, antibiotics, petroleum derivatives and nucleic acids[152–155].

o   Polyamide phases: Polyamide layers can be produced from nylon 6, nylon 11 or nylon 66. The separation of compounds present in sample rely on the capability of their amide and carbonyl group to form hydrogen bonds. The retention strength of the compounds depends on the eluting solvent and its capability to dissociate these bonds. The suitable resolution of several mixtures using polyamide layers as stationary phase has been reported before in literature[156–158].

1.3.2 Mobile phases

Other of the key points in separation techniques is the choice of the mobile phase. Simplifying as much as possible the components of the mobile phase should be the principal aim of solvent optimization. Traditionally the selection of the mobile phase has been based on the analyst experience, on similar separation

procedures reported in literature or on trial-and-error experiences[159]. Additionally, several procedures have been proposed for systematic mobile phase selection and optimization like the selectivity triangle of Snyder[160] or the PRISMA model proposed by Nyiredy et al [133]. A more recent model has been suggested from CAMAG laboratory as a four level technique for mobile phase selection and optimization[161].

First level consists in the use of different pure solvents in order to find which solvents can provide an average suitable separation for the desired components. Subsequently, the solvents are classified depending on the obtained retention factor (Rf) values. If the solvent provides a suitable Rf value (0.2<Rf<0.8) it will be classified as group A. Group B contains solvents that produce an Rf higher than 0.8 and Group C those solvents that produce an Rf lower than 0.2.

Second level consist in the addition of water or hexane in order to increase or to decrease the eluent strength as required. Eluent strength of Group B solvents can be reduced by adding a weak solvent like hexane, heptane or cyclohexane in different proportions depending on the previous separation obtained. For solvents in group C a strong solvent like acid (Formic acid, acetic acid) or base (diethyl amine, ammonia) is added to increase the solvent strength. Water may also be suitable for this purpose if the solvent is miscible.

Third level involves the use of mixtures composed of solvents selected in the two previous levels which can be improved by the further use of modifiers like bases or acids. It is recommended to start using 1:1 mixtures as a first trial and if improved resolution is obtained, try different proportions. If the analytical problem is yet not solved an alternative option can be tried directly combining solvent from group B and C from level one. Depending on the obtained eluent strength the most adequate solvent proportion should be stablished.

Level four involves minor refinements of eluent strength, which can be carried out using modifiers to improve the shape, and hence the resolution, of the separated zones. Acid and bases with varying strength can be used as modifiers. If a suitable separation is not achieved at the end of level four, the whole four levels should be repeated using an alternative stationary phase.

In order to substitute conventional organic solvents for greener and more sustainable ones, Byrne et al. classified most of the existing solvents using some

tools and guides stablished by known pharmaceutical companies [162]. In this sense, following the trends of analytical chemistry, it is very important to use solvents as sustainable as possible and reduced volumes to generate the minimum waste.

1.3.3 Sample application and derivatization

Sample application onto the stationary phase can be carried out manually, with conventional simple equipment, or automated using more sophisticated instrumentation. Generally, both, accurate control of the position of the sample and the volume applied allow the achievement of more reliable chromatographic results. The selection of a sample application technique relies on the type of the matrix sample, the separation layer and the sample volumes to be applied[163,164].

Manual application can be performed with several application methods such as capillary dispensing systems, microsyringes or band applicators. When using capillaries and syringes, samples must be applied precisely with the correct angle, also, a controlled flow rate must be achieved when administrating the sample for quantitative separation. On the other hand, one of the major problems when using band applicators is the damage of plate surfaces by capillaries. In this sense, it is important to use procedures where contact between the capillary and the sorbent can be avoided as much as possible. A good straight-line application can be obtained using applicators with a small tank for sample solution, however, it is very difficult to administrate uniform concentrations over the spots in the whole band length.

Automatic or at least semi-automatic equipment can be used to administrate the sample improving significantly the quality of sample application. When using semi-automated spot application systems, sample can be administrated precisely positioned onto the layer surface, minimizing or avoiding plate damage and in a controlled dosage of the desired volume. Automated equipment is based on fully robotic systems that can be controlled using a personal computer. Sample solutions can be loaded as spots or bands resulting in high reproducible and reliable quantitative analysis.

Another relevant advantage of HPTLC is that derivatization can be performed to enhance the detectability of the separated compounds. Derivatization reactions can be carried out in situ either before or after the

chromatographic separation, being post-chromatographic derivatization the most famous and commonly used. The derivative reagents can be applied by spraying or by immersing or dipping the developed HPTLC layer. Numerous types of more sophisticated devices for spray and dipping derivatization are commercially available. These devices allow a higher control in the derivative reagent's application, providing more reproducible quantitative analysis and less reagent consumption. In some reactions migrated spots appear colored immediately in contact with the derivative reagent, however, it is more common that drying or heating the plate is needed. Table 4 shows a list of some of the more common derivative reagents and their possible applications.

Table 4. List of common derivatization reagents for HPTLC derivatization.

Derivatization reagent	Compounds of interest	Detection techniques
Iodine (Vapor/Solution)[165]	Alkaloids, Opiates, Lipids, Carotenoids, Conjugated double bonds	UV/Visible light, Fluorescence quenching
Dragendorff reagent[166]	Alkaloids, Heterocyclic nitrogen compounds	UV/Visible light
Ninhydrin[167]	Amino acids, Biogenic amines, Peptides	Visible light
Phenol/H_2SO_4[168]	Carbohydrates, Sugars, Glycosides	Visible light
Fast Blue B[169]	Phenolic compounds, tannins, cannabinoids	UV/Visible light
Vanillin/Anisaldehyde acid reaction[170]	Steroids, Alkaloids, Flavonoids, Essential oil compounds, Phenols, Glycosides	UV light, Fluorescence
Aniline-diphenylamine-phosphoric acid[171]	Sugars, Glycosides	Visible light
Phosphomolybdic acid[172]	Fatty oils, phospholipids, steroids, essential oils compounds, morphine	UV/Visible light
Natural products reagent /polyethylenglycol[173]	Flavonoids, carbohydrates, plant acids	UV light, Fluorescence

As can be seen in Table 5 separated species that usually do not respond to UV/ Visible, can be derivatized into UV/Visible absorbing compounds in order to improve their detectability. In this sense, derivatization reactions are an important HPTLC detection alternative that permits in situ visualization of the chromatographic results. Furthermore, it facilitates the combination of HPTLC with spectroscopic portable instrumentation in order to perform in situ analysis.

1.3.4 Response measurement

In order to perform suitable quantitative analysis, the combination of HPTLC with adequate determination techniques is required.

Traditionally response measurements have been performed by scanning plates using a densitometer. The first study reporting the use of a densitometer was published in 1966 by Huber et al. [174]. In densitometry quantitative information can be obtained from the zones where samples have been retained after the chromatographic development. In order to measure the separated samples, layers are scanned with a light beam that can be adjusted in length and width as required. The diffuse reflected light from the separation plate is detected by the photosensor of the densitometer displaying a chromatogram with suitable resolution peaks where the samples are completely separated[163]. It can be programmed to scan at different wavelengths in order to automatically scan all the developed tracks on the chromatographic layer. Densitometric measurements can also be carried out by fluorescence, reaching higher sensitivities. Because of the outbreak of digital cameras, video densitometry emerged as an alternative to classic densitometric measurements[175]. It is a very profitable tool especially for rapid quantification and for documentation purposes, since it allows to register and to analyse the chromatograms of all the tracks on a separation plate in one file. It also provides a high versatility as results can be storage in a wide variety of file formats being compatible with computer softwares for data analysis. However, it was not till recent progresses in digital imaging that video densitometry provided results with enhanced reproducibility and accuracy. In this sense, the combined utilisation of video densitometry and classical scanning densitometry, to take advantages of both types of densitometry, have been usually reported in bibliography[176]. Currently, densitometry is widely used for many applications and as a consequence many publications have been recently reported[177–179].

In the last years, the combination of HPTLC with conventional laboratory techniques have also been reported in bibliography. The aim of combining these techniques is to maximize the analytical information that can be gathered from the chromatographic plates after being developed. In this context, different options have been successfully coupled to HPTLC like mass spectrometry (MS), image analysis and several spectroscopic techniques[180].

HPTLC coupled to MS have been used in numerous studies, it has proved during many years that it is one of the most valuable combination techniques. Different methodologies have been described in bibliography for obtaining mass spectrometry analysis from developed layer spots. Originally, the analyte would be eluted from the sorbent and inserted into the ion source of the spectrometer. This procedure, although efficient, is time consuming. Alternatively, molecules can be desorbed from the top layers of the chromatographic plate by particle beam sputtering or laser ablation techniques. The most commonly used methodologies included secondary-ion mass spectrometry (SIMS), fast atom bombardment (FAB) and more recently, matrix-assisted laser desorption/ionization (MALDI)[181] and desorption electrospray ionization (DESI)[182,183]. Currently, the coupling of HPTLC with MS is broadly stablished resulting in successful analysis. Especially, the combination of chromatographic plates with MALDI-MS have shown significant advantages, in this sense, high resolution separation and remarkable detection sensitivities have been reported for many different applications[184–186].

HPTLC have been also combined successfully with different spectroscopic laboratory equipment. The combination of HPTLC with Fourier transform infrared (FTIR) spectroscopy is useful for the identification of complex matrices[163]. It can be especially helpful for the quantification of substances that cannot be suitably detected by UV light and are not susceptible to undergo derivatization. Prior to the measurement, all solvents must be removed carefully and a background correction must also be applied to obtain adequate spectra[180]. HPTLC has been linked to FTIR in many studies reported in bibliography, it has been especially utilised for the analysis of biocomponents present in plants[187–189].

The combination of HPTLC with Raman spectroscopy has also been evaluated. Raman spectroscopy is especially interesting because of the weak signal produced by HPTLC sorbents, giving raise to low background interfaces. Surface enhanced raman spectroscopy (SERS) is one of the most used options due to its

remarkable sensitivities, being able to detect compounds at very low concentrations. In this sense, Koglin developed a method for activating SERS surfaces, depositing colloidal silver spheres on HPTLC plates, achieving limits of detection at the picogram level[190]. Recently, HPTLC-SERS have been widely used in analytical chemistry for numerous applications including the identification of dyes[191], food[192] and drug analysis[193] and the determination of some herbal compounds in plants[194].

Another possibility that have been explored in bibliography is the combination of HPTLC with conventional UV/Vis spectrometers. In this sense, a study has been carried out by Ţebrencu et al. where both densitometry and conventional UV/Vis spectrophotometry were used successfully for the evaluation of 1,8-dihydroxyanthraquinones derivatives in buckthorn[195]. Additionally, an analysis of phenolic compounds from fruits was performed by Ferreira et al.[196]. Recently, Morlock et al. have also developed a quantitative HPTLC/UV-Vis method for the detection of sweeteners in food products[197].

Data analysis in HPTLC can also be conducted by analyzing digital images of the chromatographic plates. Image analysis present several advantages including fast data acquisition, wide compatibility and availability of external softwares for image evaluation, rapid and simple image processing and the possibility to store images for further analysis[198]. Different strategies have been evaluated for image processing. In this sense, a system to automatically eliminate the noise using morphological operators was developed by Báez et al.[199]. Ristivojevic et al. also proposed a method for image processing using the techniques know as warping for data acquisition of different propolis extracts[200]. The combination of HPTLC with Image analysis can also be a valuable tool for fingerprinting analysis. The decomposition of color in different parameters give rise to multiple variables that can be helpful to differentiate compounds together with chemometric techniques[201–204]. Regarding quantitative analysis it has been proved that an improved accuracy and sensitivity can be achieved using HPTLC coupled to image analysis. Accordingly, Ibrahim et al. compared different softwares to carry out image analysis using scanners and digital cameras coupled to HPTLC for pursuing polyphenolic and antioxidant profiles during alfalfa sprouting achieving for all cases enhanced detection for the digitalized pictures[131].

Some of the advantages own by HPTLC are that it is fast, low cost, and presents an easy portability. For many years, development of chromatographic plates has been performed in laboratories using conventional equipment for quantitative purposes. However, due to the recent progresses in portable instrumentation and the implementation of smartphones as analytical devices, HPTLC has emerged as a valuable tool to perform in situ analysis. Currently, there is the possibility of setting more economic portable instruments using handheld components that allow to perform on site measurements.

Different strategies have been reported in literature combining HPTLC with portable devices. One of the most studied combinations is the use of portable raman spectrometers to perform SERS in thin layer chromatography plates. In order to active the surface of the plates metal colloids, like silver or gold, are usually added to the sorbent layer after the chromatographic development[190]. Numerous studies have been conducted achieving high sensitivities for detecting analytes in different fields of analytical chemistry, such as, botanical, food and environmental analysis [205–208]. In this sense, HPTLC-SERS have proved to be a cost-effective simple and sensitive strategy for mixture sensing that has been extensively used for targeting molecules in complex samples[209].

The combination of smartphones with HPTLC is an interesting alternative for quantitative purposes as target molecules from complex matrices can be detected via derivatization of previously separated compounds, followed by colorimetric analysis. As previously explained in Section 1.2, when using smartphone, two different strategies have been established to perform colorimetric measurements. On the one hand, image analysis can be carried out utilizing the high-resolution camera to capture images from the developed HPTLC plate. Data acquisition can be achieved with a smartphone application (Commercial or designed) or by image processing using an external software (ImageJ, MATLAB, GIMP or Adobe® Photoshop). On the other hand, a miniaturized spectrometer can also be coupled to the smartphone camera to perform spectral analysis of the derivatized spots.

Accordingly, several studies have been previously reported where smartphones are used as digital cameras for on-site measurements achieving suitable determinations in different applications. As an example, Yu et al. proposed the determination of histamine in fish by image analysis using a diazotized

visualization reagent[210]. A quantitative analysis for the determination of medroxyprogesterone acetate in pharmaceutical injectables using a smartphone and an open-source software has been recently reported by Sowers et al.[211]. Whilst, Ibrahim et al proposed a portable detector using a smartphone with a commercial application for the chromatographic determination of some gastrointestinal tract drugs[212].

Although, the use smartphone-based spectrometers for colorimetric analysis has been previously seen in literature, no studies have been performed combining these devices with HPTLC for the best of our knowledge.

In this Thesis, the combination of HPTLC with smartphones, including spectral analysis, have been studied for the determination of several analytes in different matrices. The chromatographic development has been optimized and comparative analysis, using different strategies for smartphone-based detection, has also been performed for quantitative purposes.

1.4 ELECTROCHEMICAL SENSING AND PORTABLE VOLTAMMETRY

Electroanalysis offers remarkable promise for scaling down analytical systems, with features that include high sensitivity, inherent miniaturization, low-cost, low-power requirements, and high compatibility with advanced micromachining and microfabrication technologies[213]. Accordingly, portable methodologies for electrochemical analysis has been used for detecting important analytes (proteins, nucleic acids, proteins, pollutants, metabolites or metals) in many different areas of analytical chemistry such as, personal and public health, clinical analysis, food and water quality, and environmental monitoring[214].

1.4.1 Electrochemical biosensors

Electrochemical sensors have covered numerous topics in literature, more than 3,000 reviews have been published in the last 5 years according to the WOS database (Searching "electrochemical" and "sensors" in September 2022). Electrochemical sensors have been widely used in many different fields such as, environmental[215–217] and food[218–220] analysis, agricultural[221] and pharmaceutical[222] applications or biomedical monitoring[223–225].

In particular, an electrochemical biosensor is based on three essential components: the sample, the recognition element and the transducer (Figure 15). The sample is where the target analyte is located. The recognition element or (bio)recognition site utilizes a biological interaction with the species of interest and the transducer is a physico-chemical element that turns this binding interaction into an electrochemical response.
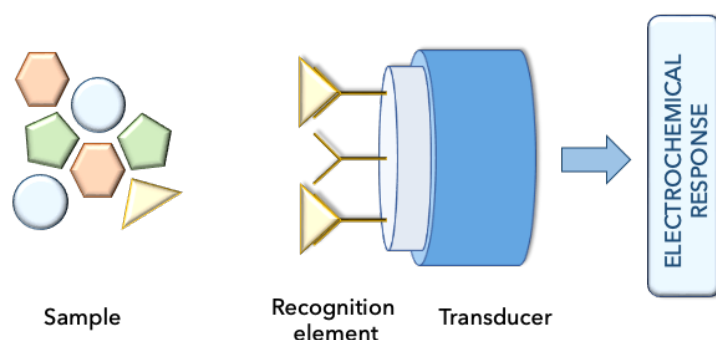
Figure 15. Schematic representation of an electrochemical biosensor

Since reactions are generally detected only in a close proximity to the electrode (transducer + recognition site), the electrodes themselves play a vital role in the performance of electrochemical biosensing[226]. The selectivity and the sensitivity of the sensors is commonly attributed to the recognition element, whilst accuracy is mainly correlated to the transducer and the electrochemical technique used. However, good stability and high sensitivity have also been linked to the transducer. Thus, a good selection of both, recognition site and transducer is key to develop analyte-specific, accurate and sensitive electrochemical sensors[227].

There are different types of transducers that can be used to build biosensors. The most commonly used are gold (Au), platinum (Pt), mercury (Hg) and carbon-based materials like screen printed carbon electrodes (SPCE), boron doped diamond (BDD) and glassy carbon (GC). Traditionally, Au was the most popular electrode material for fabricating biosensors due to its ability to form self-assembled monolayers (SAMs) with thiols, forming strong bonds with the gold atoms on the surface[228]. One limitation of Au electrodes is their poor anodic window, due to oxidative desorption[229]. Pt electrodes demonstrate suitable electrochemical inertness and ease of fabrication into many forms; however, it has some disadvantages. If there are small amounts of water or acid present in the electrolyte, it will lead to the reduction of the hydrogen ion to form hydrogen gas

at moderately negative potentials overlapping any useful analytical signal[229]. Besides, both Au and Pt electrodes can also be quite expensive. Mercury displays an excellent cathodic potential window; however, it is extremely susceptible to oxidation at low negative potentials and it has limited use in modern times due to its toxicity[229].

In the last years, carbon-based electrodes have become very popular in the field of electrochemistry. Recently, SPCE have been used as biosensors due to the reduced sample volume required, allowing the miniaturization of the sensing devices[230]. One of their main drawbacks is that organic solvents can be responsible for the dissolution of insulate inks, what can affect to their sensitivity. They have also showed low electron transfer rates, hence high interferences can be observed caused by electroactive species present in samples[230]. GC electrode is a gas-impermeable electrically conductive material highly resistant to chemical attack[231]. The increase in popularity of GC electrodes can be attributed to its ease of production, cost-effectiveness, wide electrochemical potential window, good biocompatibility and chemical stability and inertness [232,233]. One practical limitation of GC, as an electrode, is its inability to be easily machined into pre-defined geometries[234]. Therefore, difficult surface modification is commonly required[235,236]. BDD has all the existing benefits of glassy carbon, but also exhibits several other specials properties like a lower background current and a higher resistance to fouling [237].

Electrochemical sensors can show high selectivity and sensitivity due to the possibility to tailor the specific interaction of compounds by immobilizing, onto the transducer surface, chemical or biological recognition elements that have a specific binding affinity to the target molecule[238]. This process is known as surface modification and can be performed using different strategies. Currently, there are different well-known methods for surface modification such as salinization and phosphonatation of oxidized surfaces, thiols self-assembly on gold and some other metals and the electrochemical reaction known as electrografting. However, most of the mentioned methods have shown several drawbacks, being electrografting the most currently utilized surface modification strategy.

Electrografting is commonly defined as the electrochemical reaction that permits organic layers to be attached to a solid conducting material. This method can be performed by oxidative or either reductive electrochemical reaction and

have been broadly studied in order to build chemical sensors and biosensors and for several industrial applications. *However, in this thesis special focus has been given to the use of electrografting for sensing purposes.*

Oxidative electrografting can only be performed on non-oxidative substrates, thus, it has only been successfully applied to surfaces like GC, Au, and Pt. Accordingly, the oxidative electrografting of amines and alcohols have been studied with analytical purposes. In this sense the detection of H_2O_2, NO_2, acetaminophen or dopamine as chemical sensors[239–242], and the immobilization of DNA and proteins as biosensors[243–245] with several applications have been reported in literature.

More broad studies have been performed in reductive electrografting. Special interest has been given to the electrografting of vinylic compounds and diazonium salts due to their potential implementation in building sensors. Vinylic electrografting is carried out formatting an electrochemically induced bond between the transducer and the polymer. One of the main advantages of the polymeric bonding is that polymers can suffer further functionalization with other molecules. As an example, the detection of biotin and immunoglobulin G antigen has been reported[246]. However, the main drawback of using vinylic compounds for surface modification is the necessity to use anhydrous conditions.

Diazonium salts reduction on transducers surfaces is one of the most used and studied methods for surface modification. These compounds attach to the surface through an electrochemically induced loss of a nitrogen molecule (N_2) and the formation of an aryl radical[247]. These salts are stable in aqueous acid solutions, they suffer a decrease in stability at pH above 2-3[248]. A large variety of materials can be derivatized by reduction of diazonium salts, special interest has been shown in carbon-based transducers as they can be utilised for building stable electrochemical sensors. In this sense, GC have proved to form layers that present a high stability in time[249]. Another advantage showed by these compounds is the possible post-functionalization as, once the phenyl groups are attached to the surface, a wide variety of organic reactions can be carried out for the modification of these substituents.
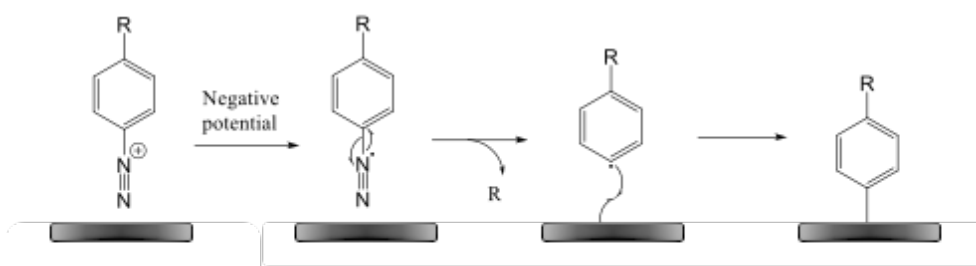
Figure 16 Schematic representation of the electrographting of a diazonium salt

Accordingly, a large number of chemical sensors have been reported in literature. As an example, the detection of several ions[250–254] and molecules of pharmaceutical[255] and environmental[256] interest have been studied. Furthermore, these species can also be used for the development of biosensors attaching DNA and proteins to different substrates like carbon, diamond and silicon[257–259].

In this Thesis the surface modification of GC and BDD electrodes have been studied. Specially attention has been given to the reductive electrografting of diazonium salts for further functionalization on both type of substrates.

1.4.2 Response measurement

In electrochemical sensing a response is generated due to the electrical changes produced by the target compound when attaching the recognition site. Traditionally the reaction under investigation would either generate a measurable current (amperometric), a measurable potential (potentiometric) or a measurable alteration in the conductive properties of a medium (conductimetric) between electrodes[238]. Recently, other type of electrochemical techniques has been studied like impedimetric, which measures impedance, and field-effect, which measures the current of a potentiometric effect using transistor technologies[260,261].

Because of the outcome of the advances in new technologies at the beginning of the century, there was an increased interest on minimizing the dimensions of conventional electrochemical equipment in order to perform in-field and in-situ analysis. Accordingly, a wide variety of reduced potentiostats was developed increasing the portability and versatility of these instruments without compromising the accuracy and the sensitivity of the response obtained from their measurements. These devices usually allow the utilization of most of the well-

known electrochemical techniques. In this sense potentiometric[262–264], conductometric[265,266] and amperometric techniques [267] have been proposed in bibliography using these type of devices.

Cyclic Voltammetry (CV) is one of the most widely used techniques applied for electrochemical sensing. It is very useful for obtaining information about the redox species present in the analyte solution. Additionally, it has been proved to provide reliable, accurate and sensitive results in different situations. In this sense, several cyclic voltammetry methodologies have been proposed by Huang et al. for the development of molecularly imprinted biosensors to determine dopamine and bilirubin, respectively using portable potentiostats[268,269]. In the field of environmental analysis, a low-cost inject-printed paper-based potentiostat for monitoring the quality of water was developed by Bezuidenhout et al[270]. Numerous different studies have been also performed in the field of food safety, in this context, a pc software-based portable system for the determination of E. coli was developed by Xu et al[271], in the same vein, Nagabooshanam et al. proposed a micro analytical device interfaced with a portable potentiostat to determine organophosphate pesticides in the food chain[272].

The more recent developments in nanotechnology have offered new possibilities of miniaturizing and optimizing existing microscale devices to the nanoscale level. The higher surface-to volume ratio of nano-objects makes their electrical properties increasingly susceptible to external influences resulting in higher sensitivity measurements[273]. In this sense, especial attention has been given to these devices for the monitoring of samples in different fields of analytical chemistry, such as, environmental analysis[274,275], medical biosensing[276,277], and DNA detection[278,279]. Furthermore, some of the studies in bibliography have reported miniaturized potentiostats that offer wireless connection. These devices can be monitored using a smartphone enabling the possibility of in place analysis and decision making in real time. Accordingly, numerous studies have been reported for different applications, such as, environmental and food analysis[280–282], biomedical monitoring[283,284] and detection of DNA related diseases[285].

In this thesis different studies have been performed using surface modified electrodes with cyclic voltammetry. In addition, this technique has been evaluated for the determination of 2,6-DNT using a portable potentiostat.

1.5 STUDIED ANALYTES AND PORTABLE MEASUREMENT OPTIONS

The different analytical methodologies developed within the framework of this Thesis have been employed for the determination of compounds related to a wide variety of fields, such as, health, food safety or environmental control and security. The main characteristics related to these compounds as well as the need for their determination have been exposed in detail. Additionally, a bibliographic review regarding the different methods reported for their analysis is included.

1.5.1 Ammonium, and nitrate in water samples

One of the main reasons that have caused the decrease of the quality of water in the last years is the rising levels of nitrogen in it[286]. Nitrogen is a good quality indicator; it can be found in natural water as dissolved organic nitrogen (DON) and as dissolved inorganic nitrogen (DIN). DON is composed of peptides, amino sugars, free amino acids and nucleic acids in water produced by the metabolic activities of microorganisms, plants and animals[287,288]. However, most of the total dissolved nitrogen (TDN) in water correspond to DIN, which play a key role in water quality. Ammonium, nitrite and nitrate are the main species of DIN, which come from agricultural activities, alimentary and cosmetic factories, domestic sewage discharge and atmospheric deposition[289,290].

Eutrophication is produced by increase of some nutrients in water like nitrogen and phosphoric compounds, although it also depends on parameters like the pH, the temperature, salinity or sunlight. Furthermore, nitrogen concentrations have been enhanced by the increasing human impact derived from the recent population growth, the industrialization and the intensified agricultural activities[291,292]. Besides, the growing concern for climate change has focused its attention on emissions and discharges of these compounds[293]. In this sense, the development of methods for real-time and in-situ measurements to monitor these contaminants has become mandatory to facilitate the decision-making process[294].

The quantification of nitrate, nitrite and ammonium in water samples is usually performed measuring each compound separately. In addition, most of the methods reported in bibliography does not allow in situ measurements. In this context, Table 5 summarizes different methodologies reported in literature for the in-situ quantification of the aforementioned compounds. In this table several

aspects like the type of sample, the time of analysis, the limits of detection and the techniques to perform the analysis have been taken in consideration. All the methodologies proposed in the table are considered portable or at least portability could be implemented.

Table 5. Comparison of different methods for in situ determination of nitrate, nitrite and ammonium.

Sensing element	Technique	Analyte	LOD	Analysis time	Sample
PVC membrane[295]	UV-Vis spectroscopy	NO_3^-	26 µM	5 min	Fresh Water
DTP sensor[297]	Dispersion turning points	NO_3^-	2.74 µM	-	Seawater
Deep-UV LED detector[298]	UV spectroscopy	NO_3^- / NO_2^-	0.64/ 0.1 µM	< 3 min	Tank, waste and fresh water
PDMS membranes[299]	UV-Vis spectroscopy	NO_3^- / NO_2^-	0.5/0.1 mg·L^{-1}	< 10 min	Tap and river water
AgNps and Azodyes[300]	SERS	NO_2^-	$9 \cdot 10^{-3}$ µM	-	Tap and sea water
Diazocompound[301]	Smartphone-based Image analysis	NO_2^-	0.187 µM	-	Tap, spring and river water
PDMS-thymol composite[23,302]	UV-Vis spectroscopy	NH_4^+	0.4 / 0.03 mg·L^{-1}	10 / 5 min	Environmental water
3D microfluidic paper-based device[303]	Digital image/ Reflectance	NH_4^+	0.41 / 0.6 mg·L^{-1}	5 min	Freshwater
Ion-selective electrode[304]	Potentiometry	NH_4^+	0.22 mg·L^{-1}	5 min	Tap water
LDR molybdenum blue sensor[296]	Diffuse Reflectance	NH_4^+	14.9 µM	1 min	Freshwater

1.5.2 Urea in urine samples

Urea is a nitrogen-containing compound that is also present in the environment, coming from agricultural processes (soil)[305,306] and water[307]. Typically, urea is employed as fertilizer that can be indirectly determined as ammonia after urea hydrolysis reaction. In addition to environmental pollution, urea detection is relevant in medical diagnosis, since urea is one of the main waste products of protein and amino acid metabolism and is eliminated from the body through urine[308]. Urine ammonium compounds excreted by the human body can be considered as remarkable biomarkers for indicating diseases or pathophysiological conditions[309–311]. At a physiological pH (7.3), urea is neutral, with an expected concentration in the range of 155–388 mM (9.3–23.3 g L^{-1}) in humans [312].

In the literature, several analytical methods for the determination of urea use enzymatic hydrolysis, which is carried out in the presence of the urease enzyme in the working medium[313–316]. There are also several immobilization strategies[317] on different supports[311,313,315,318]. The development of in situ methodologies for the detection of urea is a matter of concern among the scientific community. In this sense, selected methodologies for the determination of this compound, which were proposed or could be adapted for in situ analysis, are summarized in Table 6.

Table 6 Comparison of different methodologies for in situ determination of Urea in samples

Option	Technique	Reagents	LOD (mg·L^{-1})	Sample
Biosensor	Potentiometry	Urease-modified nanomaterial	2.4	Urine
Biosensor	Amperometry	Urease, poly(3-aminopropyl-pyrrole-co-pyrrole) support, electrochemical deposition on indium-tin-oxide-coated glass	1.2	Human serum
pH sensor	Potentiometry	Iridium oxide films, silicon-based thin-film platinum microelectrode	4.7	Urine
Enzyme-based field effect transitions	Potentiometry	Urease, layered double hydroxide (LDH) clay matrix, glutaraldehyde cross-linker	0.21	Urine, blood
Enzymatic optical biosensor	Optical	Urease, FITC-dextran sensing probe entrapped in TMOS	0.15	River water, serum

1.5.3 Hydrogen Sulfide in waters and atmospheres

Hydrogen sulfide (H_2S), is a corrosive, colorless, flammable, and highly toxic gas with a "rotten egg" odor[319]. This gas can be produced by naturally (because of some volcanic activities or by bacteria) o by means related to industrial activities, such as, oil drilling, natural gas production, coal mining or paper manufacturing[320–322]. Hydrogen sulfide is particularly hazardous for people who work in oil drilling and refinery plants, wastewater treatment plants and dumps, as well as for farmers who work close to manure wells[323].

This compound is especially dangerous because it inhibits the cellular respiration, however, this substance can also be harmful for people's health damaging the olfactory nerves, the eyes and the brain[324]. As a consequence of its toxicity and the risks related to the exposure to this gas in certain work places, the detection of hydrogen sulfide has become increasingly important in the framework of analytical chemistry[325]. The limit of detection of the human sense of smell for this compound can be close to $10 \; \mu L/m^3$ (depending of the person and the exposure time), however, there is a maximum sensitivity value around $100 \; mL/m^3$, that if it is exceeded the perception of this gas disappears due to neurotoxic effects that inhibits the olfactory nerve. Accordingly, the Directive 2019/161/EU established a list of Indicative Occupational Exposure Limit Values in which the reference values of hydrogen sulfide for a daily (8 hours) or for a 15 minutes exposure at work are 5 and $10 \; mL/m^3$, respectively.

Due to the aforementioned reasons, the development of in situ methodologies for the detection of hydrogen sulfide has attracted the attention of the scientific community. In this sense, several methods proposed in literature for the determination of this compound in the last five years are summarized in Table 7 in which portable instrumentation has been or can be implemented.

Table 7 Comparison of different methodologies for in situ determination of H_2S in samples using portable instrumentation.

Sensing element	Technique	LOD	Analysis time	Sample
Functionalized paper strip[326]	Smartphone image analysis	0.14 mg·L^{-1}	5 min	Waste water
3D printed portable platform[327]	Smartphone image analysis	0.02 μM	20 min	Waste and lake water
Fluorescent paper strip sensor[328]	Smartphone image analysis	0.2 μM	2 min	Waste water
Paper based sensor[329]	Smartphone image analysis	1.8 ppm / 0.6 ppm	30 / 0.5 min	Air / Water waste samples
Nylon supported plasmonic assay[63]	Image analysis	150 ppb	10 min	Air samples
Capacitive sensor[330]	Capacitance	50 ppb	4 min	Fish atmospheres

1.5.4 Allergens in food

Food allergy, an adverse immune response to food components has become an emerging major public health problem worldwide[331]. Most of the common foods which account for 90% of all reported food allergies are peanuts, soy beans, crustacea, fish, milk, eggs, nuts and wheat[332]. Especial attention has been given to gluten (wheat) and to lactose (milk) in the last years.

1.5.4.1 Lactose

Lactose is one of the principal sugars present in milk, on average cow milk is composed of 87% water, 4-5% lactose, 3% proteins, 3-4% fat, 0.8% minerals and 0.1% vitamins[333]. Lactose is a disaccharide that must be hydrolyzed by lactase, which is an enzyme produced in the mucosa of the intestine that catalyzes the breakdown of lactose into its constituents monosaccharides, glucose and galactose[334]. Approximately 75% of the world's population has intolerance to this sugar, due to the total absence or deficiency of lactase, which is the inability of the intestine to digest it and transform it[335].

The EU dairy industries represents 4% from the whole world food industry[336]. Milk is the most important European Union agricultural product in terms of value, accounting for around 22% of the EU's agricultural output[337]. An estimated 145.7 million metric tons of cow milk were produced in the European Union in 2021, which is the main dairy product followed by cheese, yogurt and other fermented milks and powder.

Due to the problems associated with lactose intolerance, many lactose-free food products are being manufactured by the food industry[338,339]. In light of this, there is the need to avoid the presence of residual lactose in manufacturing processes to avoid cross-contamination[340]. In this sense, the quantification of lactose is a significant challenge in many areas of economic interest that have led to the development of several methodologies to detect lactose at very low concentration levels. Table 8 summarizes some of the most recent methodologies reported in literature in the last years for the in-situ determination of lactose implementing or giving the possibility to implement portable devices.

Table 8. Comparison of different methodologies for in situ determination of lactose

Sensing element	Technique	LOD	Analysis time	Sample
Portable 3D printing biosensor[341]	Smartphone Image analysis	56 ppb	25 min	Milk and Lactose-free milk samples
HPTLC-Densitometer[342]	UV-Vis spectroscopy	2.5 ppb	45 min	Milk samples
Two-enzyme biosensor[343]	Cyclic Voltammetry	4.8 ppb	20 min	Whole milk samples
Electrochemical Gold biosensor[344]	Amperometry	0.16 ppb	10 min	Dairy products
Enzymatic test kit[345]	UV-Vis spectroscopy	0.5 ppb	83 min	Low-lactose and lactose-free samples

1.5.4.2 Gluten

Gluten is a mixture of proteins mostly composed of gliadins and glutenins present in wheat, barley, rye oats and related grains. The consumption of this compound is associated with celiac disease, a chronic autoimmune disorder that induces an inflammatory response resulting in different symptomatic manifestations such as gastrointestinal problems, nutrient deficiencies, anemia, reduced bone density, dermatitis and liver and biliary disease, among others[346]. Celiac disease affects a percentage of 0.6 to 1% of the world population, however, these values could be higher taking into account the underdiagnose of the disease[347].

Despite the high prevalence of celiac disease, the only treatment consists of a gluten-free diet to ensure the symptoms minimization, antibodies control and recovery of the normal intestinal activity. With this aim, gluten content is crucial in food labelling for individual protection. Indeed, Codex Standard established a maximum of 20 mg Kg^{-1} for food labelled as "gluten-free". However, food cross-contamination can accidentally occur as a consequence of inadequate procedures in food processing industry[348]. Transport of gluten through food companies and inadequate cleaning of the shared production lines before producing gluten-free products can result in the inadvertent presence of this allergen[349,350].

In this sense, there has been an increasing demand for the development of new methodologies that allow the in-place identification of gluten to avoid cross-contamination in food industries. Hence, there is a need for rapid response in real time, cost-effective and easy-handling devices to asses an efficient decision-making process. Table 9 summarizes some of the most recent studies regarding portable methods for the determination of gluten.

Table 9. Comparison of different methodologies for in situ determination of gluten or its constituents

Sensing element	Technique	Analyte	LOD	Analysis time	Sample
Handheld portable sensor[351]	Optical	Gliadin	20 ppm	4 min	Food samples
Immunochip[352]	Electrochemical impedance spectroscopy	Gliadin	0.2 ppm	60 min	Beer and flour samples
Optical sensor[353]	UV-Vis spectroscopy	Gluten	12.14 $\mu g \cdot mL^{-1}$	1 min	Gluten-free samples
Lateral flow strip[354]	Optical	Gluten	2.5 / 5 ppm	5 min	Surfaces/ Food samples
Portable chemical sensor[355]	Potentiometry	Gliadin	0.1 ppm	< 10 min	Food samples
Immunosensor[356]	Differential pulse voltammetry	Gliadin	8 ppb	< 5 min	Gluten-free samples

1.5.5 2,6-Dinitrotoluene

The nitro aromatic compounds 2,6-dinitrotoluene (2,6-DNT), along with 2,4-dinitrotoluene (2,4-DNT), are the most common isomers produced in the synthesis of TNT (trinitrotoluene), which is a highly explosive compound used in various explosives for military and industrial applications[357,358]. 2.6-DNT is a yellow-red solid at room temperature and is one of the longer-lived species present in explosives and their residues[359]. It can also be detrimental to public health as the compound is highly toxic and exposure to it via ingestion, inhalation, or dermal contact, can attribute to a number of adverse health effects, such as mild irritation of respiratory passages, sneezing, epistaxis, rhinitis, as well as irritation of the skin, which can produce erythema and popular eruptions[359,360]. It can also cause anemia, cataract, and abnormal liver function in humans and animals[361].

Nitro-aromatic energetic materials are persistent pollutants of soil and groundwater at sites where these materials are stored and produced. DNT is not a naturally occurring compound and mostly arises from military activities and

explosives[361]. It is commonly deposited through live-fire and blow-in-place detonations at military ranges. Additionally, it can be found in waste streams and soil near munitions manufacturing and processing facilities[362]. Due to the low volatility of the compounds, they do not usually form a vapor from water or soil. Instead, they are released into the environment in the form of dust or aerosols from these manufacturing plants or adsorbed onto various different suspended particles in the air[363]. Furthermore, as a results of the recent escalating threats of terrorist activities and growing environmental concerns there are urgent security needs around the world for the rapid and sensitive detection of such explosives[364–367]. However, most of the methods currently proposed in literature do not allow to perform in situ analysis or the implementation of portable devices.

In this context, the aforementioned challenges have generated the demand for the development of novel and innovative devices capable of performing a sensitive, rapid, straightforward and reliable detection for on-site and in-situ analysis. Several studies have been reported using different electrochemical techniques for the determination of 2,6-DNT and other nitroaromatic species present in military explosives and in environmental samples. A disposable carbon screen-printed sensor using cyclic voltammetry for quantitative analysis was developed by Caygill et al.[368]. Additionally, Banga et al. proposed a chronoamperometric method using a room-temperature ionic liquid modified interdigitated electrode[369], whilst, a film-modified glassy carbon electrode sensor was reported by Sağlam et al using square wave voltammetry[361]. A solid phase micro extraction-ion mobility spectrometry system has been also developed for the detection of explosives residues in quart sized cans in military areas[370]. Selected electrochemical methodologies for the determination of DNT, which were proposed or could be adapted for in situ analysis, are summarized in Table 10.

Table 10 Comparison of different methodologies proposed or that could be adapted for in situ determination of DNT.

Sensing element	Electrode material	Technique	LOD	Linear Range
AuNPs/Poly(carbazole-aniline)[361]	Glassy carbon	Square wave voltammetry	30 ppb	100-1000 ppb
Screen printed carbon sensor[368]	Carbon	Cyclic voltammetry	0.7μM	1-200 μM
[EMIM][BF$_4$][369]	Glassy carbon	Square wave voltammetry	1 ppm	1-100 ppm
Mesoporous SiO$_2$ modified electrode[371]	Glassy Carbon	Voltammetry	0.6 ppb	-
Reduced graphene oxide[372]	Glassy carbon	Stripping voltammetry	42 nM	0.55-11μM
Perovskite (SrTiO$_3$) and reduced graphene oxide[373]	Glassy carbon	Cyclic voltammetry	128 nM	0.5-0.8 μM

CHAPTER 2. OBJECTIVES

The technological revolution, the rapid changes undergone in society and the investigation in new materials and nanoscience, are main bases of the research progresses in analytical chemistry. In this context, miniaturized equipment and new tools like smartphones, have emerged as possible alternatives to traditional instrumentation. This, together with the need for a more sustainable and greener chemistry has led to the development of new methodologies towards portability in analytical chemistry.

In this context, the use of portable instrumentation and devices has increase over the last years in scientific areas such as environmental, health, food safety, security and industrial applications.

For this reason, the general objective of this Thesis is the evaluation of portable instrumentation and the study of several strategies to combine them with different analytical methodologies in order to demonstrate that not only they can be a suitable alternative to conventional instrumentation but also, they can provide numerous advantages in Analytical Chemistry. Specifically, this Thesis is focused on the implementation of portable devices, combined with spectroscopic including smartphones, chromatographic, and electrochemical techniques. The three specific objectives in which this Thesis have been based can be summarized in the following headings.

1. Evaluation and optimization of different portable instrumentation, including a smartphone and its coupling to a mini-spectrometer, for spectral measurements and image analysis. Comparative study of portable instrumentation and laboratory equipment from an analytical and environmental point of view. Study of different strategies to control experimental conditions and the influence of light and establishment of a protocol guide to perform suitable measurements. Set up of some rules for selecting the most suitable light source depending on the required information. Performance of analysis using the proposed portable instrumentation for measurements of in-situ optical sensors. Determination of NH_4^+ and Urea with a PDMS-based membrane, determination of nitrites with a PDMS-based delivery sensor, and determination of H_2S using a paper-based solid sensor and a plasmonic nylon-based sensor.

2. Development of a new eco-friendly analytical method based on HPTLC methodology for the in-place detection and quantification of carbohydrates in different real samples. Measurement of the derivative products using optimized smartphone-based instrumentation. Comparative studies of the results obtained for spectral measurements and image analysis. Lactose quantification in milk samples and lactose-free milk samples at the level of traces. Lactose determination in effluent samples from dairy industries and in critical points of some food processing companies. Development of a colorimetric analysis platform based on HPTLC and bicinconinic acid for the screening of gluten cross contamination in critical points of a food processing industry. Study and IR characterization of gluten and its constituents solubilized with different commercial solvents. Detection of gluten using of a smartphone to perform spectral measurements and image analysis.

3. Surface modification of glassy carbon and boron doped diamond electrodes by the reductive electrografting of aryl diazonium salts. Functionalization of both electrodes with the redox active molecule Anthraquinone for studying the electrochemical and chemical properties of this molecule on both substrates. Comparative investigation of the electron transfer kinetics, surface coverage and pKa with the two materials. Development of a glassy carbon surface modified sensor for the determination of 2,6- DNT in aqueous media using a portable potentiostat for cyclic voltammetry measurements. Comparative study of the quantification capacities of surface modified and unmodified glassy carbon electrodes. Study of the surface density, the proton-coupled electron transfer events and the electrons transfer kinetics of 2,6-DNT modified glassy carbon electrodes.

The aims presented in this Thesis have become possible thanks to the following projects of MINTOTA-UV research group, due to several research contracts:

> o AVI-INNVAL 10/18/040 - Prueba de concepto basada en el desarrollo de un prototipo (SMART-SENS-H2S) y los estudios de validación y transferencia a escala real, financed by Agencia Valenciana de la Innovación. UV

o TOLERA (CPI-19-152) - Investigación industrial de nuevos ingredientes, alimentos, tecnologías y seguridad en el ámbito de alergias e intolerancias alimentarias, financed by CDTI. UV y Betelgeux SA

o COV-CRISPIS (CPI-20-77) – Diagnóstico rápido, ultraespecífico y portátil de SARS-COV-2 basado en CRISPR CAS y tiras comerciales de ensayos inmunocromatográficos, financed by CRUE-Santander. CSIC-UV

o VLC-BIOMED (AK-GLUTEN-DETECT) - Desarrollo de un sistema de análisis in-situ para la estimación de alquilresorcinoles como biomarcadores de la ingesta de gluten, financed by Universitat de València in collaboration with Instituto sanitario La Fe .

o RNA-PLUSPLUS (CPI-22-197) - Programmable ribonucleoproteins that regulate translation for circuit sequence-to-function design in biotechnology, financed by Generalitat Valenciana. CSIC-UV

In addition, this Thesis is part of the following other projects granted to MINTOTA research group.

o Project PROMETEO2016/109, granted by Generalitat Valenciana – Prometeo program for excellent research groups; Development of new strategies for the design of in situ analysis devices: nano and biomaterials (4 years).

o Project CTQ2017-90082-P, granted by Spanish Ministry of Science and Innovation, and EU-FEDER; In-tube solid phase microextraction coupled online to liquid nanochromatography: new opportunities for/from the nanoscale and chromatography (4 years).

o PDC2021-121604-100, granted by Spanish Ministry of Science and Innovation, and EU-FEDER; Resilient ammonia solid chemosensors for controlling atmospheres of poultry farms - NH3ControlFarm (2 years).

During the development of this PhD Thesis four scientific papers have been published. Moreover, there is one paper already submitted, and another two drafted and waiting for sending. Each of them is detailed below:

1. **Martínez-Aviño, A**; Molins-Legua, C; Campíns-Falcó, P; Scaling the Analytical Information Given by Several Types of Colorimetric and Spectroscopic Instruments Including Smartphones: Rules for Their Use and Establishing Figures of Merit of Solid Chemosensors. Anal Chem, 2021, 93, 6043-6052. Doi: 10.1021/acs.analchem.0c03994

2. **Adrià Martínez-Aviñó**, Lusine Hakobyan, Ana Ballester-Caudet, Yolanda Moliner-Martínez, Carmen Molins-Legua and Pilar Campíns-Falcó; NQS-Doped PDMS Solid Sensor: From Water Matrix to Urine Enzymatic Application. Biosensors 2021, 11, 186. Doi: 10.3390/bios11060186

3. **Martínez-Aviñó A**, Molins-Legua C, Campíns-Falcó P. Combining high performance thin layer chromatography with minispectrometer-fiber optic probe-coupled to smartphone for in place analysis: Lactose quantification in several matrices. J Chromatogr A. 2022, 1661:462694. Doi: 10.1016/j.chroma.2021.462694.

4. **Martínez-Aviñó A**, De Diego-Llorente-Luque M, Molins-Legua C, Campíns-Falcó P. Advances in the measurement of polymeric colorimetric sensors using portable instrumentation: Testing the light influence. Polymers 2022, 14,4285. Doi: 10.3390/polym14204285

5. **Martínez-Aviñó A**, Moliner-Martínez Y, Molins-Legua C, Campíns-Falcó P. Colorimetric analysis platform based on thin layer chromatography for monitoring gluten cross-contamination in food industries. Draft

6. Shane P. O Neill, **Adria Martinez**, Charlie Keane, Sammi Hassan, Catriona Houston, Shekemi Denuga, Emer Farrell, Guzman G. Ramirez, Robert P. Johnson; Comparative Proton Coupled Electron Transfer at Glassy Carbon and Boron-Doped Diamond Electrodes. Draft

7. **Martínez-Aviñó A**, O Neill SP, Grealish R, Johnson R.P. Surface modification of glassy carbon electrode for ultrasensitive 2,6-DNT detection. Draft

The works carried out during this Thesis have been presented in the following National and International Congresses

- o **A. Martínez-Aviñó**, C. Molins-Legua, P. Campíns-Falcó, From visual observation to complex spectrometers: Portable instruments for in situ analysis or smartphone as colorimetric devices. XXII Reunión de la Sociedad Española de Química Analítica (SEQA). Valladolid, Spain. July 2019. National congress. Poster contribution.

- o **A. Martínez-Aviñó**, C. Molins-Legua, P. Campíns-Falcó, Combining HPTLC with fiber optic probe coupled to smartphone for in situ analysis: lactose quantification in several matrices. 23rd International Symposium on Advances in Extraction Technologies (ExTech). Online Event. June-July 2021. International congress. Poster contribution.

- o Shane P. O Neill, **Adria Martinez**, Catriona Houston, Robert P. Johnson, Comparison of proton coupled electron transfer of Anthraquinone at glassy carbon and boron-doped diamond electrodes. Electrochem 2022 Edinburgh, UK, September 2022. International congress. Poster contribution.

- o **A. Martínez-Aviñó**, R. Marquez-Costa, G. Rodrigo, P.Campíns-Falcó, Rapid and ultraspecific SARS-CoV-2 diagnostics based on CRISPR-Cas12 technologies and commercial immunochromatographic assay strips. RNAct Final Conference, Valencia, Spain 2022. International congress. Poster contribution

CHAPTER 3. METHODOLOGY

3.1 CHEMICALS AND REAGENTS

The chemicals and reagents employed in this Thesis are listed in Table 11. The commercial suppliers and the hazard pictograms according to the Regulation R (CE) nº 1272/2008 of the Parliament and Council about classification, labelling and packing of substances and mixtures (January 20th, 2009) are also included.

Table 11 Summary of reagents used in this Thesis, with their hazard pictograms, where = Flammable (GHS02); = Corrosive (GHS05); = Toxic (GHS06); =Harmful (GHS07); =Health hazard (GHS08); = Environmental hazard (GHS09).

Reagent	Supplier	🔥	💣	☣	☠	!	⬥	🌿
1-methyl-3-octylimidazolium hexafluorophosphate	Sigma						x	
2-propanol	VWR Chemicals	x					x	
2,6-dinitrotoluene	SIgma				x		x	
4-(N-Boc-aminomethyl) aniline	Sigma						x	
Acetic acid	VWR Chemicals	x		x				
Acetonitrile	VWR Chemicals	x					x	
AgNPs (20 nm)	Sigma							x
Albumin from chicken white egg	Sigma							
Ammonium Chloride	Probus					x		
amino propyl trimethoxy silane	Sigma							
Bicinchoninic acid	Sigma						x	
Casein	Sigma							
Citric acid monohydrate	VWR Chemicals					x		
Copper sulphate pentahydrate	Merck					x		x
D(-) fructose	Scharlau							

Reagent	Supplier	Flammable (GHS02)	Oxidising (GHS03)	Corrosive (GHS05)	Toxic (GHS06)	Harmful/Irritant (GHS07)	Health hazard (GHS08)	Environmental (GHS09)
D(+) galactose	Sigma							
D(+) glucose monohydrate	Panreac							
D(+) sucrose	Scharlau							
Di-Sodium hydrogen phosphate anhydrous	Panreac			x		x		
Dioxane in 4.0M HCl	Fluorochem	x		x		x	x	
Ethanol	Scharlau	x						
Ferrocenemethanol	Fluorochem					x		
Gliadin	Sigma							
Gluten from wheat	Sigma							
Glycerol	Sigma					x		
Hydrochloric acid	Scharlau			x		x		
Hydrogen Peroxide	VWR Chemicals			x				
Iron (III) Chloride	Probus			x		x		
Lactose monohydrate	Guinama							
N-(1-Naphthyl)ethylenediamine dihydrochloride	Fluka					x		
N-(3-dimethylaminopropyl)-N'-ethylcarbodiimide hydrochloride	Fluorochem			x	x	x	x	x
N-hydroxysuccinimide	Sigma					x		
N,N-Dimethyl-p-phenylendiamine	Sigma				x			
N,N-Dimethylformamide	Sigma	x				x	x	
Orthophosphoric acid	Scharlau			x				
Polydimethylsiloxane Sylgard	Dow Corning							
Potassium chloride	Fischer Scientific							
Potassium dihydrogen phosphate	VWR Chemicals					x		
Potassium hydrogen phosphate	VWR Chemicals					x		

Reagent	Supplier	🔥	💨	🧪	☠	❗	⚕	🌿
Potassium hydroxide	Honeywell			x		x		
Potassium nitrite	Merck		x		x			x
SiO$_2$ NPs	Sigma					x		
Sodium 1,2-Naphtoquinone-4-sulfonate	Sigma					x		
Sodium acetate	Sigma							
Sodium anthraquinone-2-sulfonate	Sigma					x		
Sodium bicarbonate	Sigma							
Sodium carbonate	Sigma							
Sodium dihydrogen phosphate monohydrate	Merck							
Sodium hydroxide	VWR Chemicals			x		x		
Sodium hypochlorite	Probus			x				
Sodium nitrate	Sigma		x			x		
Sodium Nitroprusside	Probus				x			
Sodium sulfide hydrate	Scharlau			x	x			x
Sodium tartrate	VWR Chemicals					x		
Sulfanilamide	Guinama							
Sulfuric acid	Merck			x				
Tetrabutylammonium tetrafluoroborate	Fluorochem			x		x		
Tetraethylorthosilicate	Sigma	x				x		
Thymol	Riedel-de Haen			x		x		x
Trichloroacetic acid	Merck			x		x		x
Urea	VWR Chemicals							
Urease	Sigma							

3.2 INSTRUMENTATION

The different experimental procedures described in this Thesis have been performed using the following instruments and materials:

- Magnetic stirrer (450W) (Stuart Scientific, UK)
- Crison micropH 2000 pH-meter (Crison Instruments, Spain)
- Nanopure II water system (Barnstead, UK)
- ZX3 vortex mixter (VELP Scientifica, Italy)
- Nylon membranes (0.2 μm) (Sartorious Stedim, Germany)
- Grade 41 whatman filter paper (Sigma, USA)
- NanoSiO$_2$ gel plates (Macherey-Nagel, Germany)
- CN modified NanoSiO$_2$ gel plates (Macherey-Nagel, Germany)
- Hettich zentrifuge EBA 20 (Merck Germany)
- Ultrasonic bath Sonitech (Terratech, Spain)
- White box with LED illumination (20x20x20cm)(PULUZ, China)
- Spider Checker ColorV2 corrector palette (Datacolor, Switzerland)
- Plastic well plates (Sigma, USA)
- 96-well plates (Sigma, USA)
- CarbiMet silicon carbide abrasive paper (Buehler, USA)

The analytical techniques used along the development of this Thesis can be classified into two different groups: spectroscopic and electrochemical. The sensor fabrication and the chromatographic techniques will be described separately.

3.2.1 Spectroscopic techniques

3.2.1.1 UV-Vis spectrophotometry

Portable spectrophotometric measurements were carried out using a Samsung Galaxy A70 (Samsung electronics, South Korea) coupled to a miniaturized spectrophotometer GoSpectro (Alphanov, France). This device was fitted with a fiber optic probe (Alphanov, France) (Figure 17). Data was recorded and processed using an android-based GoSpectro App (Alphanov, France). In order to characterize the incident light when performing measurements using smartphone-based spectrometer, a WaveGo handheld spectrometer (Ocean optics, USA) was utilized.
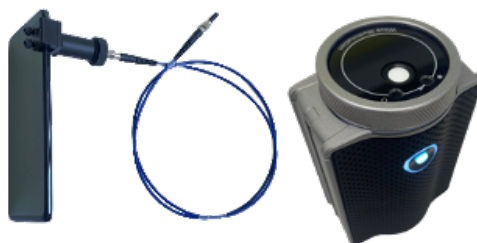
Figure 17 GoSpectro miniaturized spectrophotometer coupled to a Samsung Galaxy A70 smartphone fitted with a fiber optic probe and WaveGo hand held spectrometer.

In situ spectrophotometric measurements were performed using a portable spectrophotometer Flame (Ocean Optics, USA). This spectrophotometer is fitted with an integrating sphere ISP-80-8-RGT (Ocean Optics, USA) (Figure 18).

Figure 18 Flame portable spectrophotometer fitted with the ISP-80-8-RGT Integration Sphere.

Cary 60 Fiber Optic UV-Vis spectrophotometer (Agilent Technologies, USA) was to carry out reference spectrophotometric measurements. This spectrophotometer is fitted with a fiber optic accessory from Harrick Scientific Products (Pleasantville, USA) for measuring diffuse reflectance (Figure 19). Measurements were performed in a spectral range from 200 to 900 nm. Data was gathered and processed using the Cary WinUV software (Agilent Technologies Products, Australia).

Figure 19. Cary 60 Fiber Optic UV-VIS spectrophotometer and remote diffuse reflectance accessory.

3.2.1.2 Infrared spectroscopy

Fourier transform infrared-attenuated total reflectance (FTIR-ATR) measurements were carried out using an Agilent Cary 630 FTIR spectrophotometer fitted with a diamond ATR accessory (Agilent Technologies, Germany) (Figure 20). Spectra was registered in a range from 4000 to 600 cm^{-1} at a resolution of 4 cm^{-1}. A background scan was made against the air, and 8 scans were averaged for each measurement. For data gathering and processing, MicroLab FTIR and ResolutionPro software (Agilent Technologies) were used respectively.

Figure 20 Cary 630 FTIR-ATR spectrophotometer.

3.2.2 Microscopic techniques

3.2.2.1 Optical microscopy

A Nikon microscope Eclipse E200LED MV Series (Nikon Corporation, Japan) was used to take microscopic images. The instrument was equipped with three objective lenses (10x, 50x, 100x) (Figure 21). A Nis-Elements Software was used for acquiring and processing the image.

Figure 21 Nikon microscope Eclipse E200LED MV Series.

3.2.2.2 Scanning electron microscope (SEM)

The study of the PDMS-based sensor morphology was performed with a Hitachi S-4800 scanning electron microscope. System operated at a 20 keV voltage. In order to enable electron conduction, sensors were coated with a mixture of gold and palladium (Figure 22).

Figure 22 Scanning electron microscope (SEM) Hitachi S-4100.

3.2.3 Electrochemical techniques

3.2.3.1 Cyclic Voltammetry

Portable electrochemical measurements were performed on a EmStat^3 potentiostat (PalmSens BV, Netherlands) data collection and processing was carried out using the software PS Trace 5.7 (PalmSens BV, Netherlands). Reference measurements were carried out on a BioLogic SP-300 potentiostat (BioLogic, France) data was gathered and processed with the EC-lab software (BioLogic, France). A standard three-electrode configuration was set-up for all the measurements, comprising a glassy carbon electrode ($\varnothing$ = 3mm) (IJ Cambria, UK) or a boron doped diamond electrode (BioLogic, France) as working electrodes, a saturated calomel reference electrode (SCE) (Ag/AgCl) (IJ Cambria, UK) and platinum wire counter electrode ($\varnothing$ = 0.5 mm) (Alfa aesar, USA).
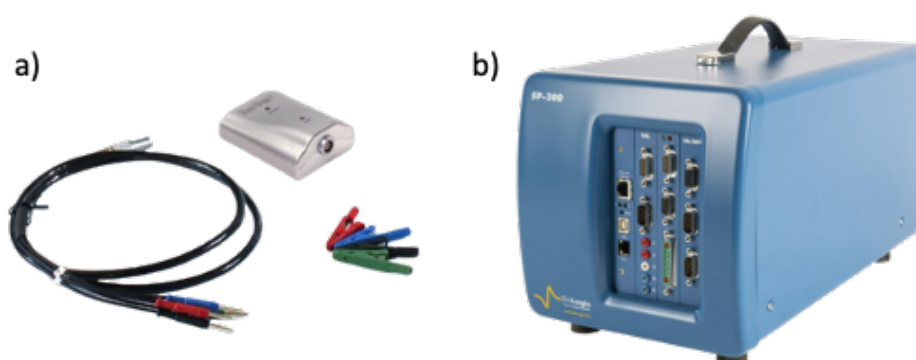

*Figure 23* a) EmStat^3 portable potentiostat b) BioLogic SP-300 potentiostat.

3.3 SYNTHESIS OF SENSORS

During the development of this Thesis, different sensors have been studied. The respective procedures for their preparation are described above.

3.3.1 PDMS based sensors

3.3.1.1 PDMS/TEOS-NQS-SiO$_2$ NPs Sensing Membrane for ammonium and urea determination
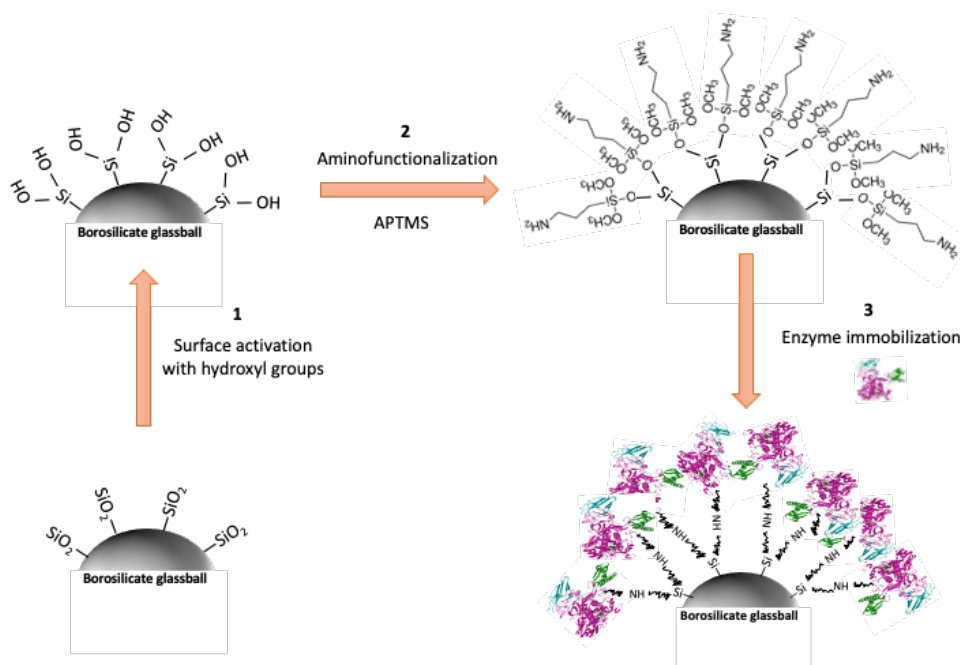
The fabrication of the PDMS/TEOS-SiO$_2$ NPs composite using NQS as derivatization reagent was performed following the procedure previously established by our group MINTOTA[94]. The schematic representation of the experimental procedure is described in Figure 24. First, the derivatizing NQS (0.35%) was mixed with TEOS (59%) and ultrasonicated for 10 min. Then SiO$_2$ NPs (0.41%) were added to the NQS-TEOS suspension, and the mixture was ultrasonicated for 1 minute to dissolve the NPs completely. The PDMS elastomer base (36.5%) was added to the resulting NQS-TEOS- SiO$_2$ NPs mixture under vigorous stirring for 15 minutes. Drops of PDMS curing agent (3.65%) were then added. Finally, 200 μL of the homogeneous mixture were deposited on plastic molds (∅ = 15 mm) for gelation. The sensors were cured at 40°C for 24 hours.
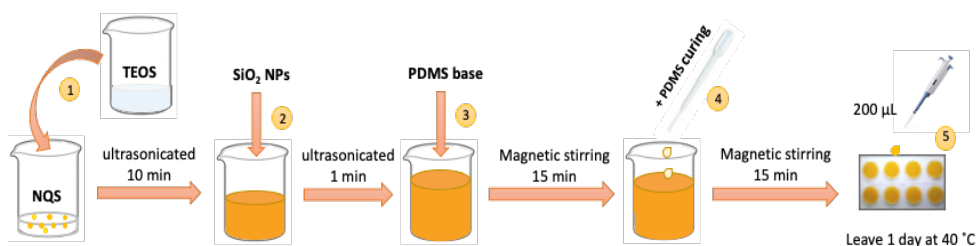
Figure 24 Steps of the procedure for the PDMS/TEOS-NQS-SiO$_2$ NPs sensors preparation for the determination of Ammonium and Urea.

For the determination of urea, the enzyme urease was immobilized on borosilicate glass balls supports (∅ = 5 mm) following a combination of experimental procedures found in literature for silicate-based materials[374–376] The strategy for urease immobilization was based on three steps, depicted in Figure 25. First, glass balls were treated with a mixture of H$_2$O:HCl (37%):H$_2$O$_2$ (30%) (5:1:1) and stirred for 2h to eliminate contaminants and activate the glass surface with

hydroxyl groups, then ,the balls were washed with deionized water and air-dried. On the other hand, an urease solution was prepared by dissolving 9 mg of the enzyme in 1 mL of phosphate buffer (pH=7) and stored at 4°C in the dark. Meanwhile, a solution composed of 1 mL of aminopropyltrimethoxysilane (APTMS), 5mL of 0.1M acetic acid and 5mL of isopropanol was prepared in a plastic beaker and stirred for 2h. Then, adding 89 mL of isopropanol was added to the mixture, which was poured on the activated glass surface to aminofunctionalize them and left at 60°C until dry. Finally, the enzyme was covalently bonded to the APTMS immersing the glass balls in 300 µL of urease solution and stirring for 1 h.


Figure 25 Schematic diagramo of covalent immobilisation on a borosilicate glass Surface involving Surface functionalisation with APTMS.

3.3.1.2 PDMS/SiO2NPs-SA-NEDD-OMIM PF$_6$ for nitrite determination

The fabrication of the PDMS/SiO2NPs-SA-NEDD-OMIM PF$_6$ composites was carried out following the procedure proposed by Jornet-Martinez et al.[377] with some modifications[299]. First, the reagents that form the azo compound, such as sulfanilamide (SA) (4.18%) and N-1-Naphthyl ethylenediamine dihydrochloride (NEDD) (1.14%), with the 1-methyl-3-octylimidazolium hexafluorophosphate (OMIM PF$_6$) (7%) were mixed and stirred for 10 min. Secondly, the elastomer base

(84.04%) was added to the previous mixture and the resulting combination was stirred during 10 min more to get a homogeneous dispersion. Then, SiO_2NPs (0.11%) were added to the mixture and stirred vigorously to obtain a homogenous mixture. Finally, the curing agent (4.98%) was added to the previous solution leaving 5 min under stirring. The final solution was added to a 96-multiwell plate, dropping 20 μL in each well. The gelation procedure was carried out at 30°C for 8 h.
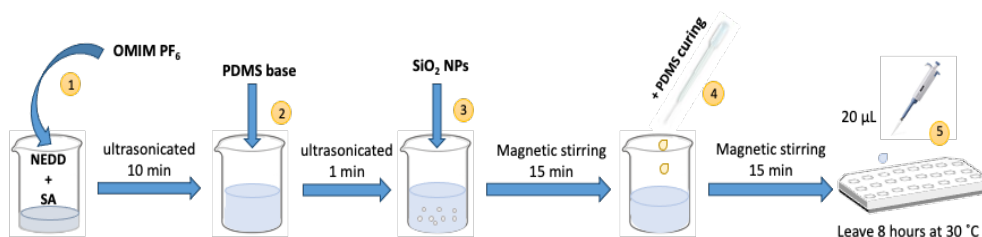
Figure 26 Steps of the procedure for the PDMS/SiO2NPs-SA-NEDD-OMIM PF$_6$ sensors preparation.

3.3.2 Paper-based N,N-Dimethyl-p-phenylenediamine/ FeCl₃ sensor

Following the procedure proposed by Pla-Tolós et al. the immobilization of the reagents was performed on grade 41 Whatman filter papers (∅ = 13 mm)[31]. A solution of 0.25 M of $FeCl_3$ and 0.28 M of N,N-Dimethyl-p-phenylenediamine was prepared using HCl 6 M as a solvent. Then, glycerol was added to the mixture in a ratio 1:1:0.1 and stirred till complete homogenization. Each filter paper was impregnated with 50 μL of the previous mixture and, finally, vacuum dried for 15 min.

3.3.3 AgNPs nylon supported plasmonic sensors

The plasmonic sensors were prepared following the experimental procedure proposed by MINTOTA[63]. Sensors were synthetized on a rectangular nylon membrane sheet (110 mm x 75 mm). A 96-hole surface plate was used as a mold to obtain numerous sensors in one time (∅ = 7 mm). The nylon membrane was placed between the mold and a 96-whole surface pumping system. By means of a multichannel micropipette the current amount of AgNPs was added to each hole and the AgNPs solution was vacuumed through the nylon sheet. Thus, the nanoparticles were retained on the membrane without surface functionalization, avoiding chemical reagents and solvents. Nylon plates with different number of

75

sensors and amounts of silver nanoparticles were synthetized as needed filling the remaining holes with nanopure water (Figure 27).
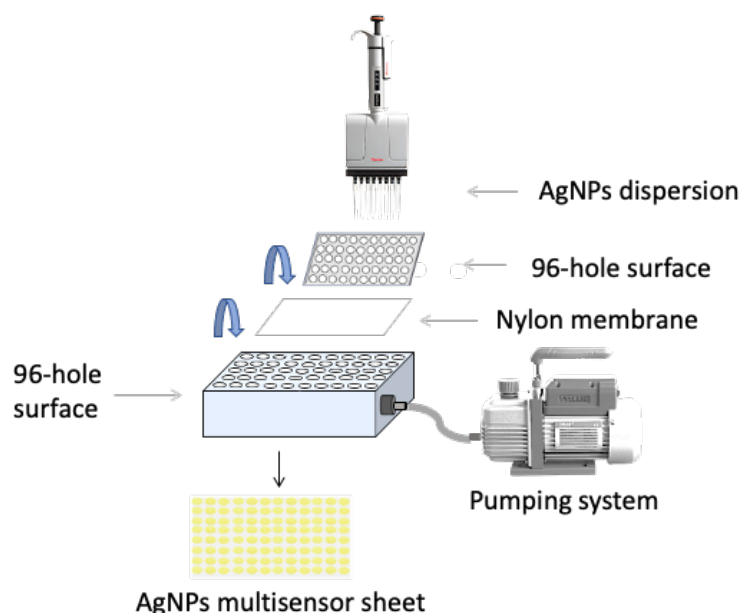

Figure 27 Preparation scheme of the AgNPs multisensor sheet

3.3.4 Anthraquinone modified electrochemical sensor

Glassy carbon and boron doped diamond surface electrodes were modified through the electrografting of a diazonium salt and following functionalization. The followed procedure included different steps. Prior to surface modification, the working electrodes were mechanically cleaned using CarbiMet S silicon carbide abrasive paper P1200. The GC electrodes then underwent a second wet polish with 1.0 μm alumina powder. The electrodes were rinsed well with deionized H_2O, before undergoing an electrochemical clean with sulfuric acid solution by varying the potential between 0 V and 1.5 V vs. SCE for 20 cycles at 0.1 V s-1. Finally, the electrodes were rinsed with deionized water before use. On the other hand, 4-[(N-BOC-aminomethyl) benzene] diazonium tetrafluoroborate was synthesized following previously described procedures[378]. Briefly, 0.0075 M 4-([N-BOC]-aminomethyl) aniline and 0.0075 M tetrafluoroboric acid (40%) were dissolved in water. Sodium nitrate 0.008 M was also dissolved in water and this solution was added dropwise to the original solution under an inert N_2 atmosphere while

stirring. The reaction mixture was stirred for one hour and cooled on ice prior to filtration. This was then washed with diethyl ether and dried under vacuum. Then, the BOC-protected amino benzene species were electrografted onto the surface via a reduction of the diazonium, as previously described by Bartlett et al.[379] Briefly, the potential was swept between 0.6 V and -1.0 V versus SCE for five scan cycles at a scan rate of 0.05 V s-1 in a solution of 0.01 M of the synthesized linker and 0.1 M tetrabutylammonium tetrafluoroborate dissolved in acetonitrile. The surface modified electrodes were then suspended in 4.0 M HCl in dioxane for 4 hours to remove the BOC-protecting group. Finally, the electrodes were suspended in a solution of 0.1 M anthraquinone-2-carboxylic acid (AQ), 0.1 M N-(-3-dimethylaminopropyl)-N'-ethylcarbodiimide hydrochloride (EDAC) and 0.06 M N-hydroxysuccinimide (NHS) dissolved in dimethylformamide for 16 hours (Figure 28).
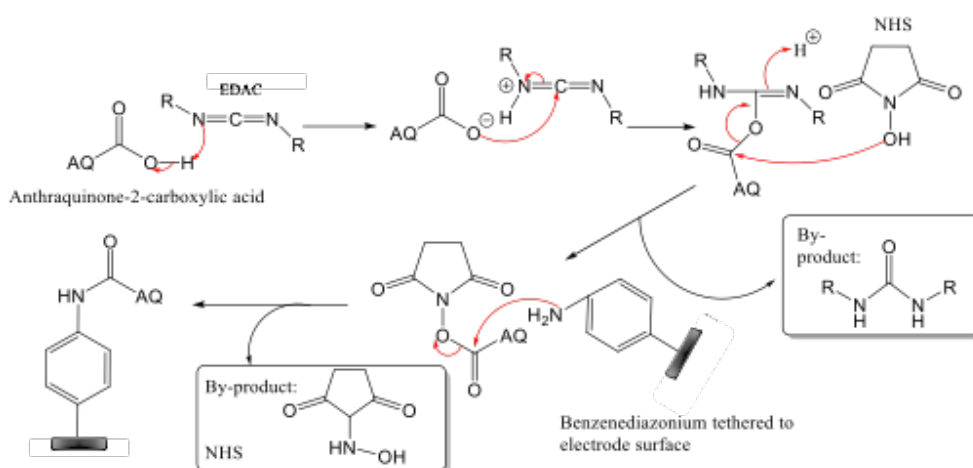
Figure 28 Diagram showing the mechanism of amide bond formation between the immobilized diazonium salt and Anthraquinone carboxylic acid.

3.3.5 Modified electrochemical sensor for 2,6-DNT determination

Glassy carbon electrodes were modified through the electrographting of a diazonium salt and further functionalization. The procedure was the same as described in section 3.3.4 with some modifications. After the N-Boc deprotection, the electrodes were suspended in a 2,6-DNT aqueous solution for 16 hours.

3.4 HPTLC development

Two different HPTLC methodologies have been developed during this Thesis. The procedures for their respective chromatographic separation are described in the following.

3.4.1 Separation of sugars present in food

Standard and reaction solutions of glucose, galactose, lactose, sucrose and fructose were deposited with a Camag 10 μL Syringe (Hamilton, Switzerland) on 3 x 5 cm HPTLC plates using nanoparticle silica gel as stationary phase. A volume of 1 μL of each standard solution was placed in a plate and dried using a hairdryer for 45 seconds. Separation of different sugars was performed using a 70:26:4 Acetonitrile: H_2O: Acetic Acid solution as the mobile phase. The plate was developed in the chamber with 5 mL developing solvent by ascending chromatography over 4.5 cm at ambient temperature.
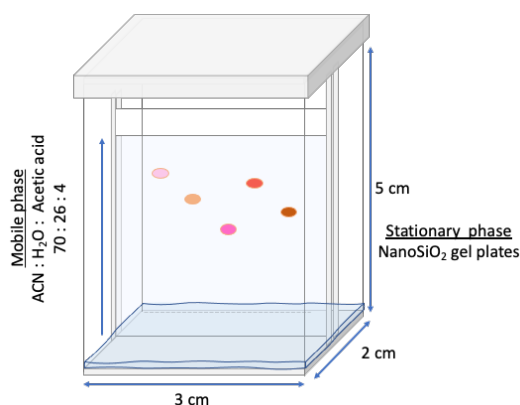
Figure 29 Representation of the HPTLC separation of different sugars in the development chamber.

3.4.2 Separation of proteins present in food

Standard and samples solutions of gluten, gliadin, albumin and casein were deposited with a Camag 10 μL Syringe (Hamilton, Switzerland) on 3 x 5 cm HPTLC plates using CN modified silica gel as stationary phase. A volume of 1 μL of each standard solution was placed in a plate and dried using a hairdryer for 45 seconds. Application process was repeated 10 times in order to increase signal response. Separation of different proteins was performed using a 30:70 Acetonitrile: H_2O

solution as the mobile phase. The plate was developed in the chamber with 5 mL developing solvent by ascending chromatography over 4.5 cm at ambient temperature.

3.5 PROCEDURES AND EXPERIMENTAL CONDITIONS

3.5.1 Reactions involved and experimental conditions of the in situ optical sensors

The experimental conditions for obtaining response of the polymeric sensors studied in this Thesis are summarized in Table 12. The table includes, information about the support material, the reagents utilized to obtain the response, the sample matrix in which the sensor applicability has been evaluated and the detection analytical techniques.

Table 12 Experimental conditions for the polymeric sensors used in this Thesis

Sensor	Reagent	Analyte	Sample matrix	Reaction time	Detection	Section
PDMS-TEOS-SiO$_2$NPS	NQS	Ammonium and Urea	Waste water, urine	10 min	Absorbance λ=590 nm	4.2.1
Paper - glycerol	Methylene blue	Hydrogen sulfide	Waste water	30 sec	Absorbance λ=650 nm	4.2.2.1
Nylon	AgNPs	Hydrogen sulfide	Breath	10 min	Absorbance λ=500 nm	4.2.2.3
PDMS-SiO$_2$NPS-OMIM-PF$_6$	SA-NEDD	Nitrite/ Nitrate	Waters	8 min	Absorbance λ=540 nm	4.2.2.4

3.5.1.1 PDMS sensor for ammonium and urea determinations

The ammonium and urea content, detected as ammonia by the chemical sensor, was determined by spectroscopic techniques. Colorimetric detection occurs when the target analyte diffuses along the porous PDMS/TEOS membrane and reacts with the colorimetric probe, NQS, embedded inside the sensing membrane, yielding a colorimetric signal that changes from a yellowish orange to a brownish color.

Sodium 1,2–Naphtoquinone–4–sulfonate
(Yellowish/ Orange color)

4–amino–1,2–Naphtoquinone
(Brownish color)
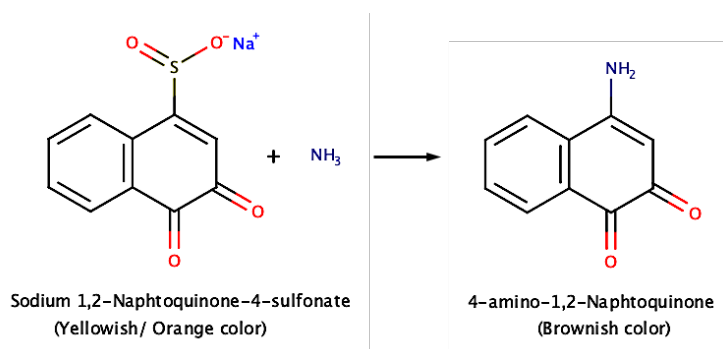
Figure 30 Scheme of the colorimetric reaction of the NQS in the presence of ammonia.

In order to hydrolyze urea from urine samples 1:10 dilution step with deionized water was performed. Urease solution was prepared by dissolving 9 mg of the enzyme in 1 mL phosphate buffer (pH=7) and stored at 4 °C in the dark until use. Then, 100 µL of the diluted urine solution was mixed with 1 mL of phosphate buffer (pH =7.4) in an Eppendorf tube, and 20 µL of urease solution was added. The resulting solution was heated at 37 °C for 5 min in a water bath. The measurement of NH_4^+ in aqueous matrices and urea in urine samples was performed by introducing the sensing membrane into a vial containing 1 mL of the sample solution and 1 mL of carbonate buffer (pH = 11). The solution was then heated at 100 °C for 10 minutes. Finally, the sensing device was removed from the solution and the color change was measured by absorbance and by digital image.

3.5.1.2 Paper-based sensor for hydrogen sulfide determination

Hydrogen sulfide in water samples was determined by the colorimetric analysis of the derivatized sensors. Sensors were prepared impregnating paper filters with 50 µL of a mixture containing N,N-Dimethyl-p-phenylenediamine, $FeCl_3$ and glycerol. Hydrogen sulfide reacts with N,N-Dimethyl-p-phenylenediamine in presence of $FeCl_3$ to produce the methylene blue, which has a characteristic blue color that allow the monitoring of the reaction (Figure 31).
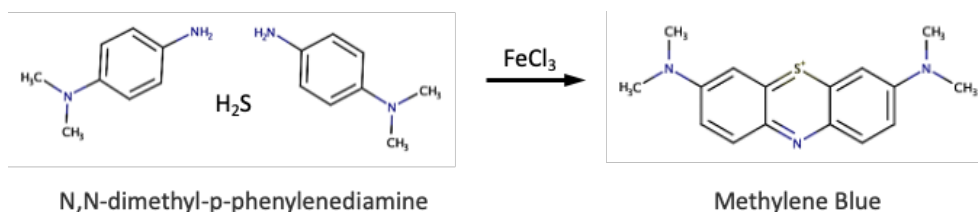
Figure 31 Scheme of the methylene blue formation in presence of H_2S

The sensor was submerged into 1 mL of sample and was left to react for 30s. After that, it was washed with 5 mL of water to remove the excess of reagent. Finally, the sensors were dried and color measurements were performed.

3.5.1.3 Nylon supported plasmonic sensor for hydrogen sulfide determination

The content of hydrogen sulfide in breath samples was also evaluated by colorimetric analysis. It is well known that sulfur groups have strong interactions with noble metals[380]. In this sense, AgNPs were retained on a nylon-support to study the interactions between the noble nanoparticles and the hydrogen sulfide. It was observed that, in presence of volatile H_2S, membranes suffered a color change from yellow to an orange/brownish color indicating the aggregation of the AgNPs. Moreover, the characteristic plasmon band of AgNPs at around 400 nm decreased and shifted to higher wavelengths ($\approx$480 nm).

Human oral breath samples of 10 volunteers were collected by exhaling a mixture of mouth and alveolar air into plastic bags of 250 mL. Prior to collecting the sample, the membrane was put into the empty bag and the bag was heat-sealed. After 10 min of sampling, the sensor was removed from the bag and the response was registered.

3.5.1.4 PDMS sensor for nitrite determination

The nitrite content in samples was determined by colorimetric analysis. In order to evaluate the response of PDMS sensors to the NO_2^- concentration both reagents involved in Griess reaction were entrapped in a PDMS membranes. Taking into account the ratio and the number of reagents used in solution, these reagent proportions were maintained in the fabrication of the sensor. It was observed that when a sensor is introduced into the sample, the reagents (SA and NEDD) release from the membrane to the solution and reacts with the analyte (Figure 32). The

reaction between the Griess reagents and NO_2^- can be followed by the color change that switches from the clear color samples to a strong pink color.
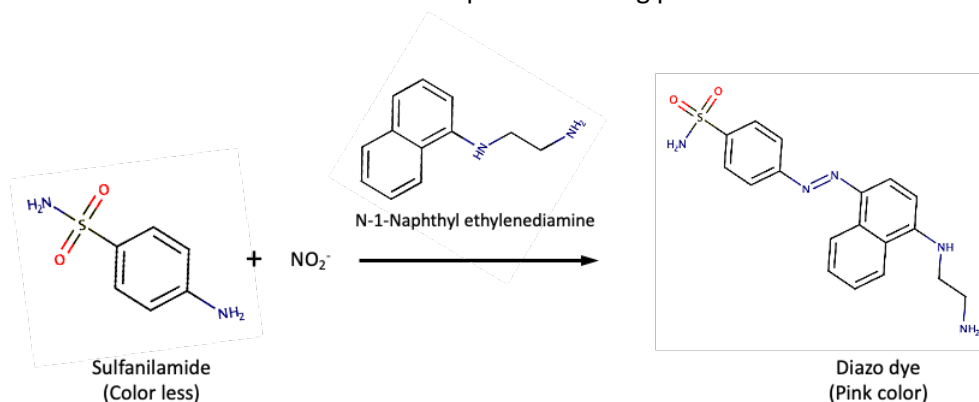
*Figure 32* Scheme of the Griess reaction in the presence of nitrites.

The measurement of nitrite by using the synthesized composite was performed by introducing the PDMS-membranes in a 96-well microplate. The composite was placed in the bottom of the well and 150 µL of citrate buffer (330 mM) and 150 µL of standard or sample were added. Finally, the color was measured in the solution.

3.5.2 Reactions involved and experimental conditions of the HPTLC plates

3.5.2.1 Carbohydrates determination

In order to determine the content of lactose, colorimetric detection was performed on the chromatographic plates after the sugar separation. Derivatization of the chromatography layer was achieved using a thymol-sulfuric acid solution. The reaction solution was prepared dissolving 0.25 g of thymol in a 50 mL EtOH solution containing 2.5 mL of concentrated H_2SO_4. The addition of sulfuric acid to the carbohydrates spots causes the dehydration of the sugars. In this reaction the compound 5-hydroxymethylfurfural (HMF) is produced by the dehydration of the hexoses. In presence of thymol, HMF facilitates the formation of complexes that allow the coloration of carbohydrates spots and thus, the quantification of lactose.
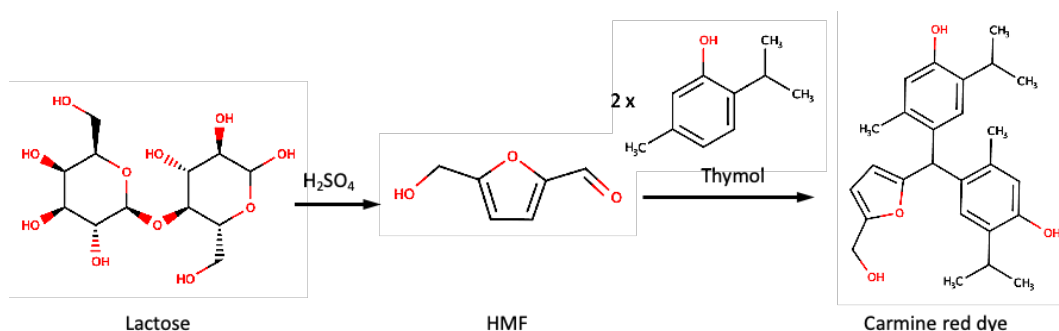
Figure 33 Scheme of the thymol/ sulfuric acid reaction in presence of Lactose

For the chromatographic layer derivatization, the plate was sopped with 750 µL of the Thymol-sulfuric acid reaction solution for 90 s. Then the plate was dried for 45 seconds and placed into an oven for 3 min at 90°C. Finally, color analysis was performed measuring the color derivatives formed on the plate surface.

3.5.2.2 Gluten determination

The content of gluten present in samples from critical points of food industries was determined by colorimetric analysis of the chromatographic plates. After protein separation, a derivatization process was carried out using a reaction solution composed of bicinchoninic acid and copper (II) sulfate. First, 0.013g of bicinchoninic acid was dissolved in 5mL of carbonate buffer solution pH≈11 and separately, 0.11g of $CuSO_4 \cdot 5H_2O$ in 1 mL of water. The reaction solution was prepared adding 100 µL of the copper (II) sulfate solution into the bicinchoninic acid solution. In this reaction, the Cu^{2+} ions from the $CuSO_4$ solution are reduced to Cu^+ by the peptide bonds in protein. Next, two molecules of bicinchoninic acid chelate with each Cu^+ ion, forming a purple-colored complex that can be monitored by colorimetric analysis (Figure 34).
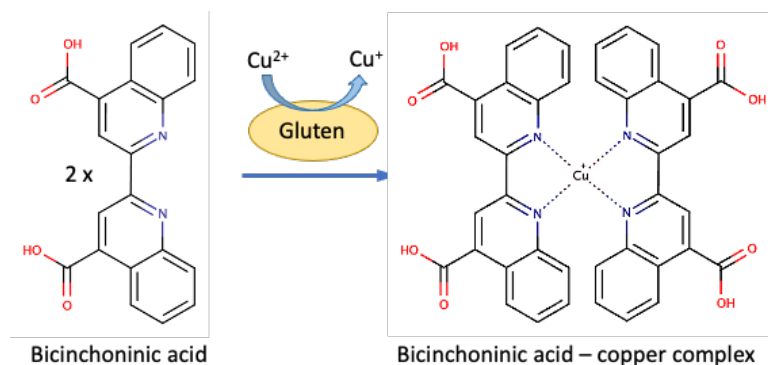
Figure 34 Scheme of the bicinchoninic acid- copper reaction in presence of gluten.

For the colorimetric derivatization, the plate was sprayed with 5 mL of the reaction solution and left at room temperature for 15 minutes. Then, plates were dried for 1 minute and finally, colorimetric analysis was performed.

3.5.3 Reactions involved and experimental conditions of electrochemical sensors

3.5.3.1 Anthraquinone modified sensors

Glassy carbon and boron doped diamond electrodes were used to provide a reliable route for the modification of carbon-based electrodes to produce a stable, immobilized layer of surface bound anthraquinone. The method is based on a diazonium salt reduction and subsequent anthraquinone functionalization. The successful immobilization of anthraquinone was confirmed observing the characteristic oxidation peaks between -0.45V and -0.55V by cyclic voltammetry measurements. Cyclic voltammetry was performed varying the potential between 0.6 V and -1.5 V in a pH=7 phosphate buffer solution. Data was collected for different scan rates from 0.05 V·s^{-1} to 0.5 V·s^{-1}.
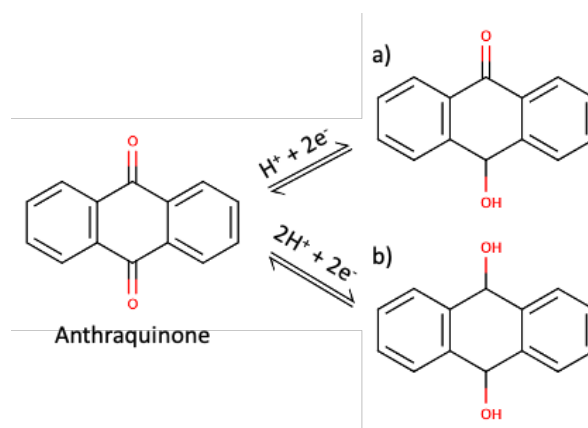
Figure 35 Proton-coupled electron-transfer scheme from anthraquinone to the formation of a) semiquinone b) and hydroxyquinone.

The electron transfer kinetics, surface coverage and pK_a of the immobilized anthraquinone was investigated and compared for both electrodes. For the pK_a analysis, cyclic voltammetry measurements were carried out at 0.05 V·s^{-1} varying from pH= 3 to pH=11.

3.5.3.2 Determination of 2,6-DNT

Glassy carbon electrodes were used to develop an ultra-sensitive electrochemical sensor to determine 2,6-DNT in aqueous matrices. The detection method is based on the irreversible reduction of the nitro groups (NO_2) of the 2,6-DNT to nitroso groups (NO) and subsequent reversible reduction of the nitroso groups to hydroxylamine (NHOH) (Figure 36).
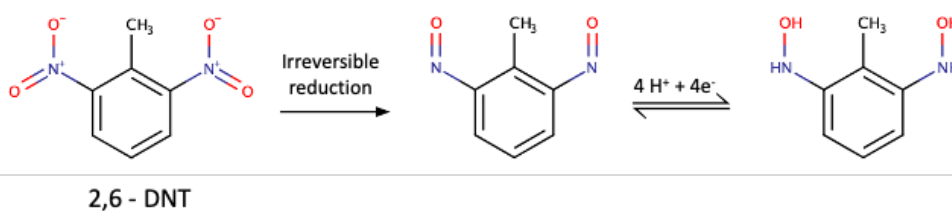
*Figure 36* Scheme of the irreversible reduction of the nitro groups on 2,6-DNT to the nitroso groups and subsequent 4H+ and 4e- reversible redox reaction to the hydroxylamine groups

The successful immobilization of 2,6-DNT was confirmed observing the characteristic oxidation peaks between -0.1 and -0.2 V by cyclic voltammetry measurements. Cyclic voltammetry was performed varying the potential between

0.6 V and -1.2 V in a pH=7 phosphate buffer solution. Data was collected for different scan rates from 0.05 $V \cdot s^{-1}$ to 0.5 $V \cdot s^{-1}$. The electron transfer kinetics, surface coverage and pK_a of the immobilized 2,6-DNT was investigated. For the pK_a analysis, cyclic voltammetry measurements were carried out at 0.05 $V \cdot s^{-1}$ varying from pH= 3 to pH=11.

3.5.4 Colorimetric measurements

Different color measurements were carried out in this Thesis. In order to evaluate the colorimetric measurements performed by portable instrumentation, a set of 45 colors, which covered the visible color range, and a corrector palette of 24 color (Spyder checker Color V2) were selected as the validation set (Figure 37). The different colors were registered by absorbance and diffuse reflectance and RGB parameters were obtained by digital image analysis.
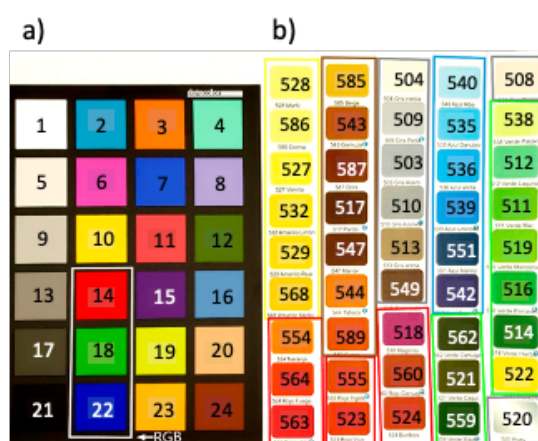
Figure 37 Validation set composed of a) Color correction palette of 24 colors b) Set of 45 colors of different spectral ranges

A smartphone coupled to a miniaturized GoSpectro spectrometer, that uses the camera of the phone, was used for measuring the colors. To carry out color measurements the mobile phone was placed on a support at 5 cm of the surface and the color sample was placed at 0.5 cm of the GoSpectro device (Figure 38).
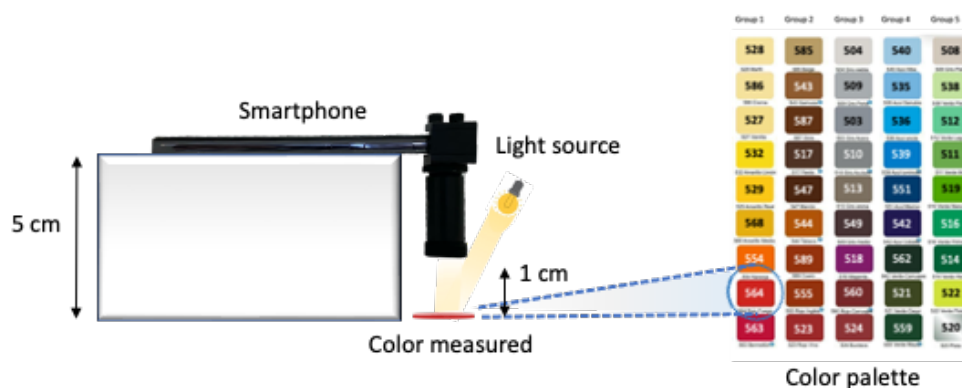
Figure 38 Scheme of the spectrometer coupled to a smartphone to measure colors from a color palette.

Besides, the color change of optical solid sensors was obtained by reflectance and by transmission mode (Figure 39). In order to perform the measurements in the transmission mode a homemade sample holder was made. It consisted on a cylindrical plastic piece with a small hole that will be fitted at the extreme of the spectrometer. The sample was introduced at the base of the cylindrical piece and it was placed in between of both pieces (the plastic piece and spectrometer) (Figure 39).
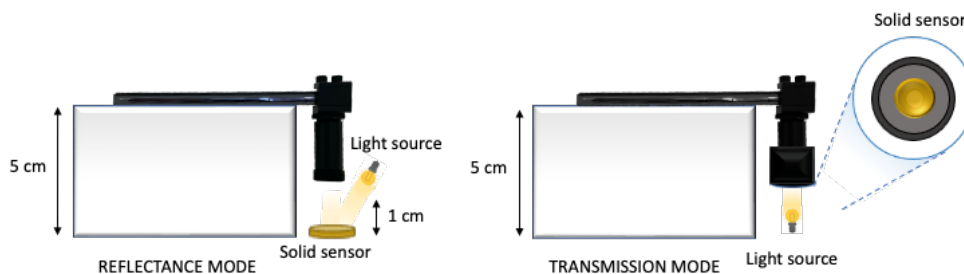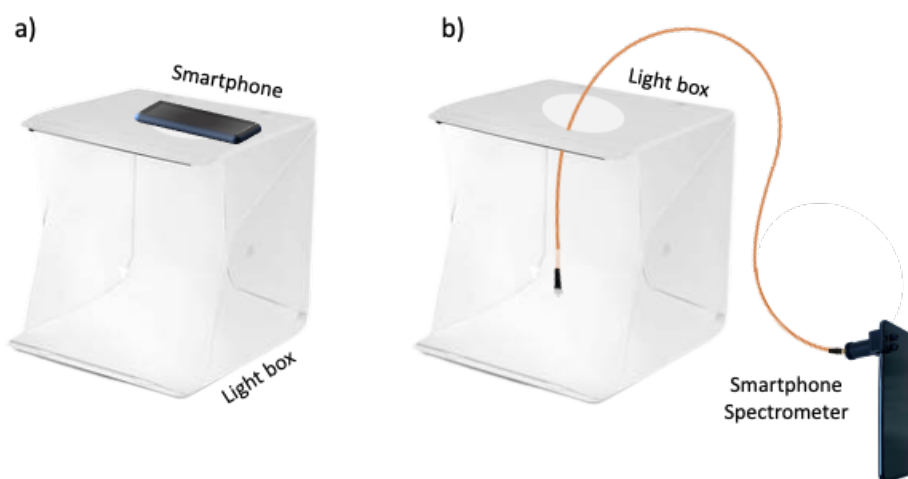

Figure 39. Schematic representation of the spectrometer adapted to a smartphone for both reflectance and transmission mode and the handmade sample holder prototype for the transmission mode option.

This device can also be fitted with a fiber optic probe in order to obtain a higher accuracy. Prior to measurements the device was calibrated against a white paper using a fluorescent light source. The smartphone was placed into a white box illuminated by a halogen lamp in order to control the influence of light (Figure 40b). A background scan was performed against a white reference standard. Finally, the sample was placed at 1 cm of the device and color intensity was measured. In order to get absorbance, the negative logarithm of the ratio between the sample measurement (I) and the background scan (I_o) was calculated (Equation 3).

$$Absorbance = -log\frac{I}{I_o} \qquad\qquad (\textit{Equation 3})$$

A smartphone was also used to perform color analysis by digital image. All the measurements were performed using a white light box in order to control illuminations conditions (Figure 40a). The WaveGo portable spectrometer was used to characterize the light. When photos were taken, the camera settings were fixed in autofocus, ISO at 100, and brightness at 1.3. The color temperature was fixed depending on the light source used. The smartphone was situated on the top of the box, at 5 cm of sensor or the image to be photographed. The acquired images were processed by using GIMP program and RGB values were obtained.

Figure 40 .Schematic representation of the two proposed strategies using a white box and LED light for a) Digital image analysis b) Smartphone spectrometer measurements.

Colorimetric response was also measured using a portable spectrometer for comparative studies. It consisted of a modular device constituted by a halogen light source, a detector, fiber optic connections, an integrating sphere and a laptop (Figure 41). In first place, a background scan was performed against a white standard and a blank was also measured, then, the sample was placed under the integrating sphere which was connected to the lamp and color absorbance was measured.

Figure 41 Schematic representation of the set-up using the portable spectrometer fitted with an integration sphere.

Diffuse reflectance measurements were carried out using the lab Cary 60 UV-Vis spectrophotometer and were used as a reference for the validation of results obtained with portable instrumentation. The followed procedure was similar to the one employed for the portable spectrometer. First, a background scan was made against a white diffuse reflectance standard and a blank was also measured, then, the derivatized samples were placed under the diffuse reflectance accessory and absorbance measurements were registered.

3.5.5 Electrochemical measurements

Electrochemical measurements were carried out in a 0.01 M KCl, 0.1 M phosphate buffer (pH=7) solution, at room temperature and with the absence of oxygen. Oxygen was removed by purging the solution with a N_2 current for 20 minutes. A gentle nitrogen flow was maintained over the liquid surface to prevent the oxygen to come into the solution during the measurements. A standard three-electrode cell was set up using the modified working electrodes, a silver-silver chloride reference electrode (Ag/AgCl saturated KCl) and a platinum wire counter electrode. Cyclic voltammetry was performed using a EmStat[3] potentiostat operated with a PS Trace 5.7 software. Reference measurements were also carried out using a Biologic SP-300 potentiostat coupled to an ultra-low current probe monitored with an EC-Lab software. Data was recorded swiping voltage between 0.6 V to -1.5V.

3.6 SAMPLES

Different types of samples have been studied in this Thesis. Table 13 summarizes the analytes studied in each sample as well as the section in which the results of these samples are discussed.

Table 13 Analyte studied per sample and method used for its detection.

Sample	Analyte	Method	Section
Waste water	Ammonium	PDMS colorimetric sensor	4.2.1
Urine	Urea	PDMS colorimetric sensor	4.2.1
Effluent water	Lactose	HPTLC combined with color analysis	4.3.1
Samples from critical points of food industries	Gluten, Lactose, Glucose,Galactose	HPTLC combined with color analysis	4.3.1 4.3.2
Milk samples	Lactose	HPTLC combined with color analysis	4.3.1
Lactose-free milk samples	Lactose traces level	HPTLC combined with color analysis	4.3.1

3.6.1 Water samples

In this thesis two different types of water samples were analyzed. On the one hand, ammonium was monitored in water samples coming from two different water treatment plants (Valencia). The sensing membrane was introduced in a vial containing 1 mL of sample and 1 mL of carbonate buffer (pH=11). Previously, the samples were diluted if necessary. The response was obtained following the procedure described in section 3.5.4.1. In addition to these water samples, waste waters subjected to oxic and anoxic treatment processes were also studied. Samples were collected from the input and from the output of both reactors.

On the other hand, effluent samples gathered from dairy companies producing mainly cheese were also evaluated. Samples were collected at different stages of a Clean-in-place (CIP) process used to clean the pasteurizer, tanks and pipes. Cleaning is accomplished by circulating hot water and solutions of chemicals

through the equipment or pipe work in contact with the products. The cleaning system contains four stages: rinse with warm water, rinse with highly alkaline and acidic solutions and chemical disinfection. Three samples of the first two steps of the cleaning process, and two samples of the last two steps were collected. After the arrival to the laboratory, the samples were stored at 4°C until analysis. Before the analysis each sample was vigorously shaken by hand for 30 s. Samples were analyzed in triplicate and at room temperature.

3.6.2 Urine samples

Urine samples were obtained from healthy volunteers. Protein precipitation was performed by adding 5 mL of 15% trichloroacetic acid to a 10 mL urine sample, and the mixture was left to stand for 5 min. The mixture was then centrifuged for 10 min at 3500 rpm and the precipitate-free liquid was taken and stored at 4°C under dark conditions until the moment of the analysis. A quantity of 100 μL of urea standards or urine samples was introduced into a vial containing 1 mL of carbonate buffer (pH 11). A fourth part of the sensor was placed inside the vial and the mixture was heated at 100°C for 10 min. Finally, the sensor was removed from the solution and its response was quantitatively measured by diffuse reflectance using a conventional laboratory spectrometer as reference and by absorbance using a smartphone-based spectrometer.

3.6.3 Industrial samples

Samples from critical points of different food companies were analyzed. Sample collection was carried out using sterilized cotton swabs (Deltalab, Spain). 21 samples were supplied by Betelgeux S.L (Gandia, Spain). The presence of gluten was studied for all samples while lactose quantification and glucose and galactose detection were performed just in 8 samples. Extraction of both types of analytes was carried out sequentially following a simple two-step process (Figure 42).
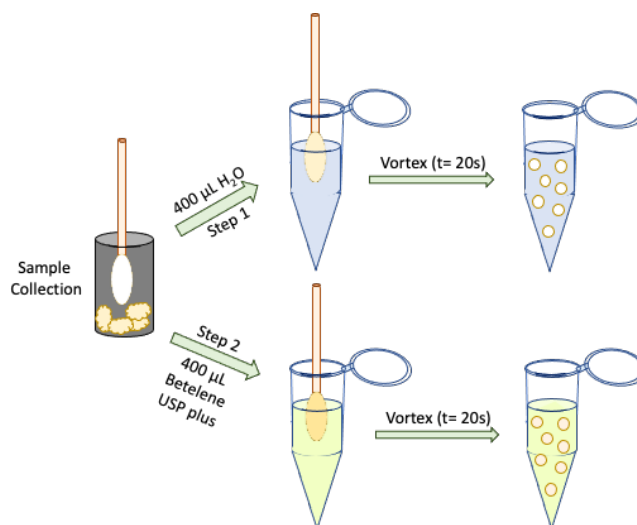
Figure 42 Scheme of the extraction process of lactose (step 1) and gluten (step 2) from samples of critical points of a food company,

First, sugars were extracted placing each cotton swab into an eppendorf tube containing 400 μL of water, the eppendorf was vortexed for 20 seconds and the cotton swab was removed. Lactose, and sugars in general, are soluble in water, when vortexed they are extracted from the cotton swab and diffuses to the solution while possible content of gluten remains in the cotton swab because of their hydrophobicity. Same procedure was repeated with an eppendorf tube containing 400 μL Betelene USP Plus, a surfactant supplied by Betelgeux S.L to extract the gluten. Proteins are soluble in this surfactant; thus, gluten is extracted from the cotton swab when vortexed. For lactose and gluten analysis procedures described in sections 3.4.1 and 3.4.2 were followed, respectively.

3.6.4 Milk samples

Five samples of well-known milk brands of whole, semi-skimmed and skimmed milk from different supermarkets were analyzed. Two lactose-free milk samples were also studied in order to determine lactose at the level of traces. For samples containing lactose, 10 μL were diluted with water to 1 mL before the analysis. For the recovery study samples were spiked with known concentration of lactose standard. Lactose-free samples were also spiked with known concentrations of lactose standard to evaluate the treatment with the enzyme lactase.

CHAPTER 4. RESULTS AND DISCUSSION

4.1 STABLISHING RULES FOR THE USE OF COLORIMETRIC AND SPECTROSCOPIC PORTABLE DEVICES.

In this Thesis the applicability of portable instrumentation to carry out colorimetric in situ analysis have been evaluated. Several portable devices have been proposed as an alternative to conventional laboratory equipment. In this sense, a comparative study has been performed between a laboratory diffuse reflectance spectrophotometer, a portable modular spectrometer and the use of smartphones for both, spectroscopic with the aid of a coupled mini-spectrometer and digital image analysis. Moreover, a study has been done to evaluate the influence of light in smartphone-based measurements. As a result, some rules have been stablished for selecting the most suitable instrumentation and experimental conditions according to the desired information and the in-situ device to measure.

4.1.1 Scaling the analytical information given by several colorimetric and spectroscopic instruments

In this section, the analytical information given by different types of instruments was scaled in order to stablish properly the figures of merit of a given methodology based on the color measurement. Different lab and portable instruments, including smartphone with and without a miniaturized spectrometer accessory, have been tested. In order to obtain broad information and using objective criteria, these instruments have been compared from two different perspectives:

1. The analytical point of view, considering mainly, selectivity, accuracy and intra and inter day precision, size, components and costs.
2. Environmental point of view, based on their footprint as kg of CO_2.

Four different instruments were used for the comparative study, Cary 60 UV-Vis Diffuse Reflectance Spectrometer, UV-Vis Portable Reflectance Spectrometer fitted with an integrating sphere, a Xiaomi mi 8 lite smartphone for color analysis and the smartphone coupled to a GoSpectro miniaturized spectrometer for spectral analysis.

Table 14 shows the characteristics evaluated for the aforementioned equipment; portability related with size, weight and autonomy; cost and sustainability measured as carbon footprint according to Plà-Tolós et al.[381]

Table 14 Main analytical properties of the different types of instrumentation used

Specifications	Smartphone (Digital image)	Smartphone-miniaturized spectrometer	Portable reflectance Spectrometer	Laboratory reflectance spectrometer
Analysis type	Image analysis	Spectral analysis	Spectral analysis	Spectral analysis
Spectral Resolution	---	1.5nm	0.5nm	0.3-1.5 nm
Spectral Range	---	380-750 nm	190-1100 nm	190-1100 nm
Light Source	LED or halogen lamp	LED or halogen lamp	Halogen, Vis-NIR	Xenon Flash Lamp (80 Hz)
Run time	5 s	2 s	20 s	30 s
CV (%)	< 1,5	< 1,5	< 1	< 1
Light Source Power	10W	10W	20W	9-18W
Operating System	Android or iOS	Android or iOS	-	-
Size	---	50 x 20 x 20 mm	89 x 63.3 x 32 mm	550 x 420 x 270 mm
Weight	---	30 g (just device)	265 g (just spectrometer)	20 kg
Cost	Very low	Low	Moderate	High
Sustainability (Carbon Footprint)	0.0014 kg CO_2	0.0014 kg CO_2	0.024 kg CO_2	0.17 kg CO_2

To evaluate analytical parameters, a 45-color palette covering the whole spectral range was selected as the validation set. A three-digits number was given to each color according to the pantone matching system (PMS) in order to facilitate the identification of each color.

Quantitative analytical parameters were calculated such as the signal to noise ratio (S/N) (Calculated as 5 × Standard deviation/Δsignal) and the intraday and interday precision calculated as the %RSD from spectra registered in the same

working session and in different ones (n=3). Parameters obtained by different spectroscopic instrument for 4 colors covering the whole spectral range can be seen in Table 15.

*Table 15* %RSD inter- and Intraday and signal to noise ratio for different colors.

Equipment	Lab reflectance spectrometer	Portable reflectance spectrometer	Smartphone-spectrometer[1]
#529 (460 nm) Interday/Intraday (%RSD)	0.70/0.9	0.1/0.5	1.5/1.6
#564 (495 nm) Interday/Intraday (%RSD)	0.2/1.4	0.1/0.5	0.4/2.2
#539 (590 nm) Interday/Intraday (%RSD)	0.2/0.4	0.05/0.3	0.8/1.2
#519 (710 nm) Interday/Intraday (%RSD)	1.6/2.0	0.05/0.2	0.3/1.6
S/N	34	47	18

[1] Smartphone spectrometer working in reflectance mode

4.1.1.1 Response using a laboratory diffuse reflectance equipment as reference

The characteristics evaluated for the lab equipment can be seen in Table 14. It has a versatile spectral resolution enabling measurements of 0.3 nm and a wide range of wavelengths from 190 to 1100 nm. The drawbacks of this instrument are lack of portability, its cost and its high carbon footprint.

To obtain quantitative analytical parameters the spectra of the panel of 45 colors (Figure 43) were registered, considering colors divided into five groups of nine components each one. As an example, Figure 43 shows the spectra obtained by the lab instrument when the different colors of the red range were measured.
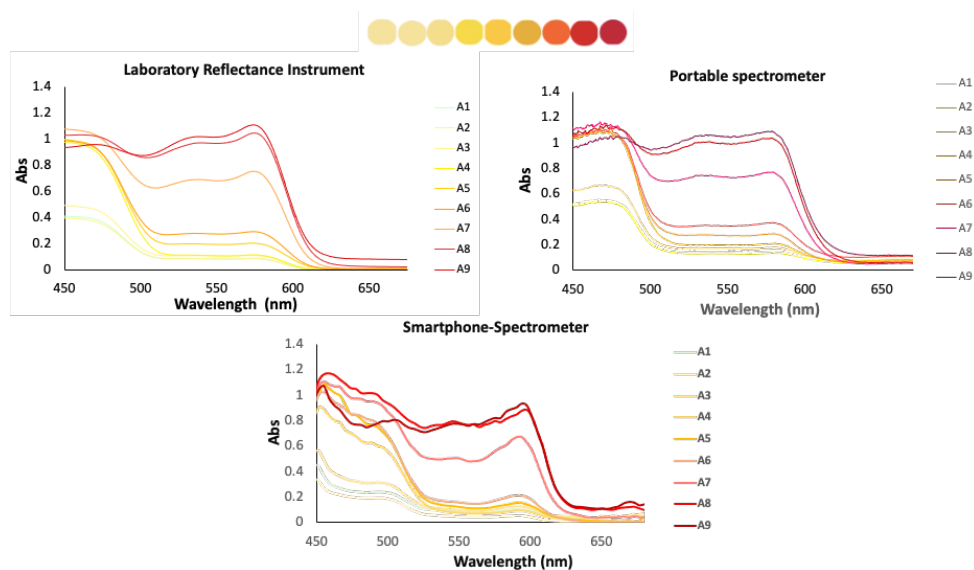
Figure 43 Reflectance spectra corresponding to colors from the red range (Group 1) obtained using the different instruments used.

A high signal to noise ratio of 34 was obtained as indicated in Table 15. This table also shows the % RSD obtained from n=3 spectra registered in the same working session and in different ones. As can be seen, the precisions inter and intraday were lower than 2% for this instrument. Accordingly, measurements performed with the laboratory spectrophotometer were used as reference to validate the results obtained using portable instrumentation.

4.1.1.2 Response using a portable diffuse reflectance UV-Vis spectrometer

The instrument used in this work consisted of a modular device constituted by a lamp, a portable spectrometer, fiber optic connections and an integrating sphere ($\varnothing$ = 8mm) . As can be seen in Table 14 from the instrumental point of view this instrument presents very good resolution (<0,5 nm). Because of its relative reduced weight, around 1 kg, all the components can be set on a suitcase and easily transported. The price is lower than the conventional lab instrument with the diffuse reflectance accessory. Regarding to the sustainability, the carbon footprint is much lower than traditional equipment. As well as the conventional laboratory instrument, the measuring methodology is very well stablished, and the measuring conditions usually are not affected by environmental conditions.

Concerning to measurements performed on the color palette control, the spectra obtained by using this instrument are similar to those obtained by using the lab instrument (see Figure 43). The highest precision was obtained by using the integrating sphere, it has showed to provide reliable results with lower values of % RSD. Concerning to the ratio S/N a very good value of 47 was obtained too (Table 15).

4.1.1.3 Responses with a smartphone fitted with a miniaturized spectrometer

A smartphone coupled to a minispectrometer that uses the camera of the phone, was employed. The GoSpectro spectrometer has an app for Android and iOS licensed by Alphanov, that allows light calibration and spectra registration. The instrumental characteristics of this device are shown in Table 14. It has a resolution of 1.5 nm and an optical entrance of 0.6 mm; this parameter will determine the size of the sample to be measured and the position of the device regarding the sample. It can measure in the reflectance or transmittance mode (if the material is transparent or translucent), depending if the collected light is reflected off the sample or if the light travels through the sample. Besides, it can be connected to a fiber optic probe to enhance the precision of its measurements. Concerning its design, it presents a reduced size and weight, thus, it can be held on one hand being a suitable option for in situ analysis. Furthermore, as it is battery-operated it can be transported without power supplies. Therefore, as can be seen in Table 14, the carbon footprint is smaller than the other compared instruments. The cost of this device is also one of its main advantages as it presents a low price. The appropriate data acquisition with minispectrometer-smartphone devices requires controlling the parameters regarding to the own instrument (calibration) and other external parameters, such as light, sample position or type of mobile phone employed. The calibration of the spectrometer can be easily done using the smartphone application in a simple step process; however, the calibration step needs to be done prior to start each set of measurements. One of the main drawbacks of this device is that experimental conditions, such as light, instrument position and the distance to the sample, need to be controlled carefully. This is a common problem in all these types of instruments, due to high influence of light in color responses[382].

Regarding to the position of the instrument, it was concluded that the better way to obtain precise results was to fix the instrument (spectrometer) 90º respects to the horizontal surface, while the smartphone was placed horizontally

lying on a support. This position guarantees that the distance between the sample and the spectrometer device is the same all over the sample. The distance to the sample was dependent on the sample size. It was observed that the smaller the area of the sample, the closer the spectrometer device should be placed. For round samples of $\varnothing$= 10 mm, the optimum distance of the spectrometer end to the sample was 1 cm, while the distance from the smartphone to the surface was 5 cm approximately.

The environmental light should be controlled to perform the measurement too. Thus, the sample spectra were registered using different lights; environmental lights like sunlight and fluorescent tubes (50 W) as natural and artificial source respectively, and incident lights from LED (5 W) and from halogen bulb (10 W) were evaluated (Figure 44a). As can be observed, the sunlight spectrum is more uniformly distributed and more sensitive; however, the signal precision was poor due to its dependence on the time of the day or the weather. The use of fluorescent tube was not recommended because of its poor intensity and less lighting wavelengths. Although LED bulb provided good results and large range of wavelength, the use of halogen light was proposed because it provides a higher sensitivity (Figure 44b). Further studies about this matter have been performed in this Thesis. In this sense, the influence of light when using smartphone instrumentation will be more extensively discussed in following sections (section 4.1.2).
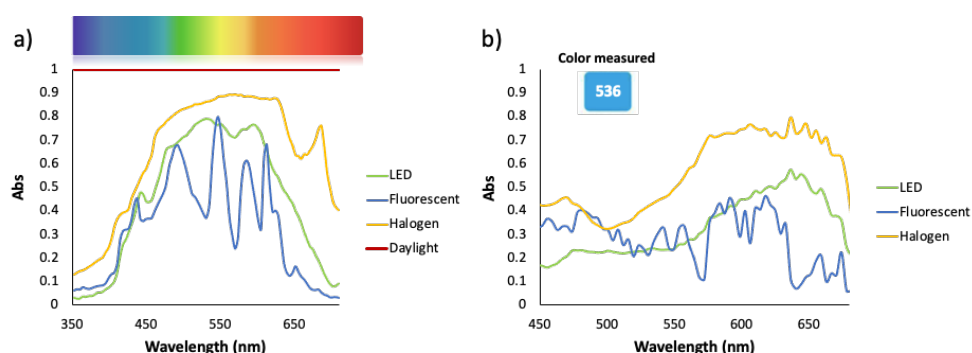
Figure 44 a) Recorded spectrum of light emitted by different light sources b) Reflectance spectra corresponding to the blue color by using different light sources.

Another problem of using a smartphone as analytical instrument is the uncertain reproducibility across smartphone devices[32]. The effect on the signals

when using different smartphones was tested. The results obtained with three different smartphones (iPhone SE, iPhone 6 Plus, iPhone 5S) from the same brand was compared by registering the spectra of four paper colors yellow (#529) red (#564), blue (#536) and green (#519). As an example, Figure 45 shows the obtained spectra corresponding to the blue color using the three mentioned smartphones.
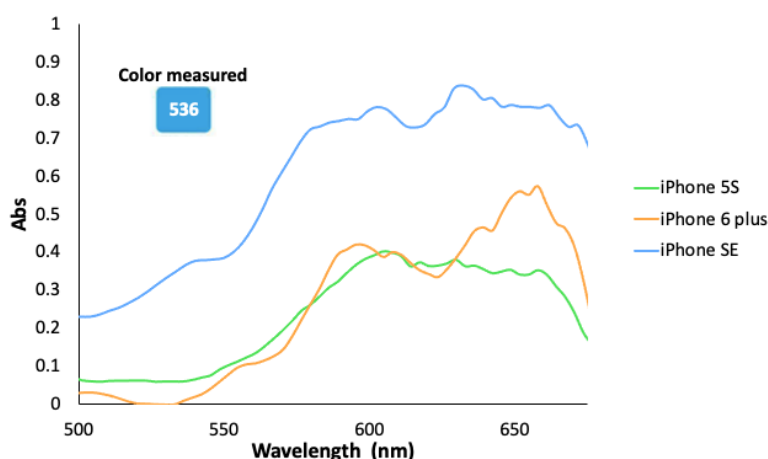

Figure 45 Reflectance spectra corresponding to the blue color by using different smartphones from the same brand.

It was observed that the spectra shape obtained in all cases were quite similar to each other; however, the absorbance value was dependent on the model phone. Based on these results, it was concluded that smartphone calibration and sample measurements should be done with the same smartphone device to obtain reproducible signals under controlled light conditions, position and size of the sample.

By working at the optimal experimental conditions, the reflectance spectra of the pallet of 45 color were registered. As can be seen (Figure 43), the analytical signals obtained with the smartphone spectrometer were similar to the ones obtained by the reflectance instruments, however, the absorbance values were slightly lower. A minor shift in the maximum of absorption can also be observed when using the smartphone-base miniaturized spectrometer. This displacement can be explained taking into account the differences in spectral resolution of the different employed instruments. Although the values of intra-day precision were higher than those given by the other instruments, these results were appropriated

(<5%) (Table 15). As it was expected the ratio S/N was also lower than the obtained with other compared instruments. However, these results were considered as satisfactory.

By using this instrument, the raw data obtained corresponds to the light intensity. These data can be converted in absorbance. Therefore, the blank signal (blank material) is needed to be registered in order to obtain the *Io* and the *I* of the different samples. These data are processed in order to obtain the absorbance from the transmittance using Lambert Beer law (Figure 46).
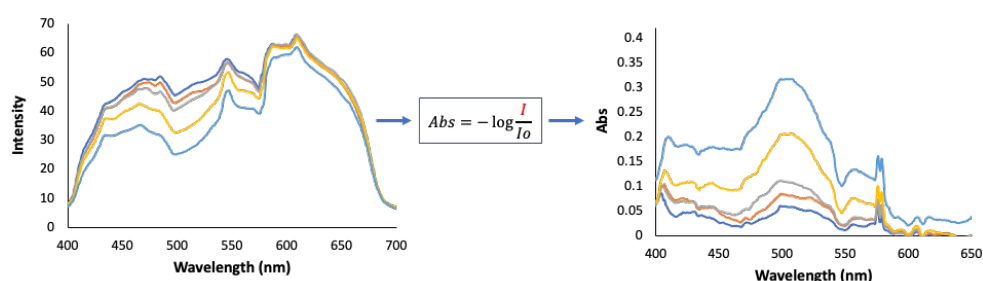
Figure 46 Schematic representation of the data conversion from intensity to absorbance values.

From the analytical point of view there is the need to calculate the concentration using standards and their absorbance. In this case, there are two different ways to calculate it when using this prototype i) by exporting and processing the raw spectral data to external programs such excel or ii) by using an app designed for direct calculation. The app for spectrometer-smartphone software has many advantages such as it is quicker, and the data can be stored and easily transferred via Wi-Fi. In this sense a calculation option was included in the GoSpectro app from MINTOTA research group. By clicking the calculation button, the concentration of the sample will be calculated by using the data spectra of the blank, two standard of known concentration and the sample. Thus, user will only need to perform the four mentioned measurements. A calibration of one point will be used as a calibration model for each standard, in which a *K* constant will be calculated (Equation 4) and used to calculate the concentration of the sample (Equation 5). Figure 47 shows the app results.

Calculation of the K constant:

$$K = \frac{Conc.\ Standard}{(Abs\ Standard - Abs\ Blank)}$$ *(Equation 4)*

Calculation of the sample concentration:

$$Conc.Sample = \frac{(Abs\ Sample - Abs\ Blank)}{K}$$ *(Equation 5)*

This calculation will be done for both standards, thus two concentrations, each one related to one specific standard, will be facilitated by the app. The app also has the option to select up to five wavelengths, allowing the concentration to be calculated for each one of them.
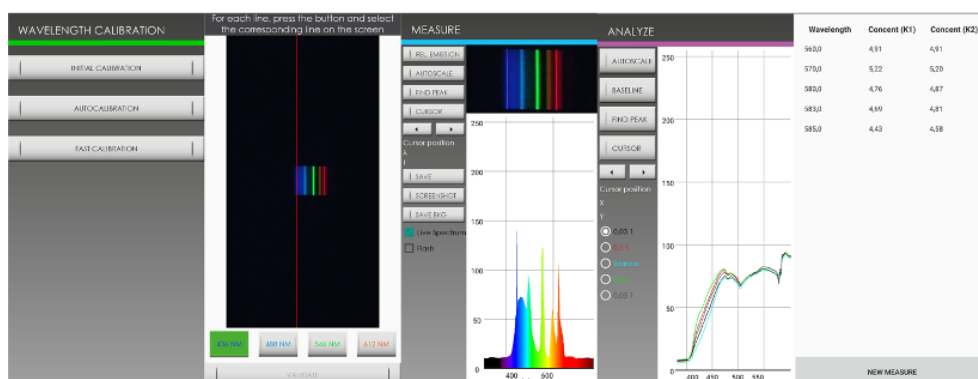

Figure 47. Designed App for calculating the concentration of a sample using the spectra

Multivariate methods were used to analyze the information provided by using the spectra data of the color palette. Accordingly, a principal component analysis (PCA) was performed for the absorbance values obtained at different wavelengths (ranged from 400 to 650 nm) using the smartphone spectrometer results (Figure 48). Supervised soft independent modeling of class analogy (SIMCA) models were also employed.

PC1 and PC2, explained almost all the variance, being PC1 70% and PC2 25%. Several clusters can be observed, distributed depending on the color. The primary colors, green (Grey), blue (Pink) and red (Red) were clearly distrusted forming clusters. The mixtures colors (yellow, grey, or brown) were located between the primary colors employed.
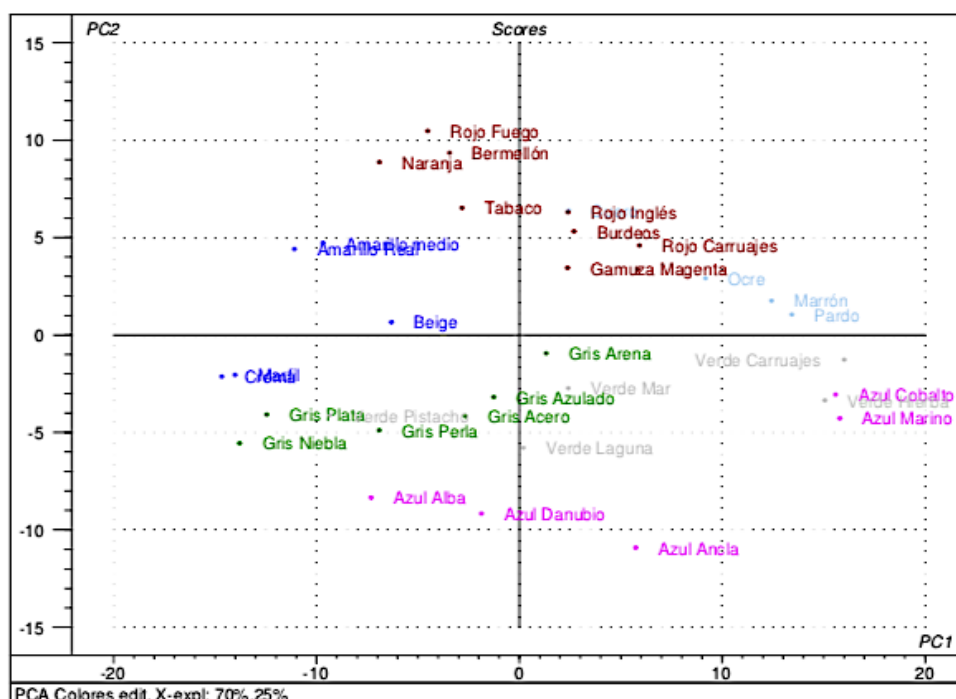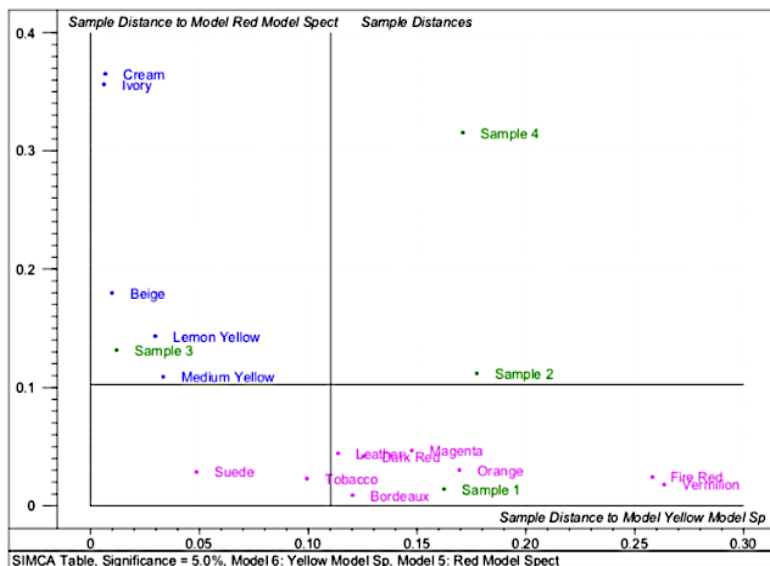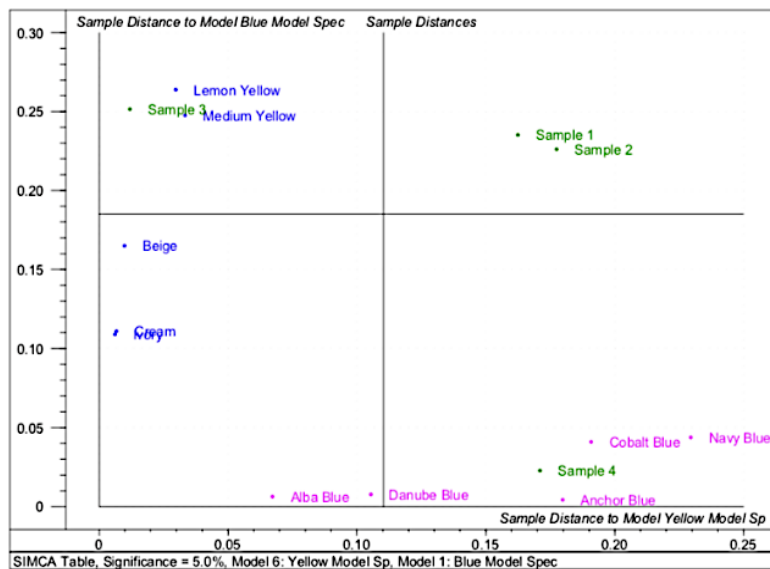
Figure 48 PCA plot for the analytical data obtained using the smartphone spectrometer

The SIMCA class models were constructed based on 38 colors from the color palette, classified using 6 category variables, Blue, Green, Red, Brown, Grey and Yellow. Four colors were used as a prediction set for model validation. When SIMCA was applied as classification model satisfactory results were obtained. In order to obtain more information from the classificatory supervised models, Cooman's plots were represented. Cooman's plots show class distances for two classes against each other in a scatter plot. Successfully classification was obtained when using spectra data, as the samples laid well beyond the 95% confidence level in their respective areas.
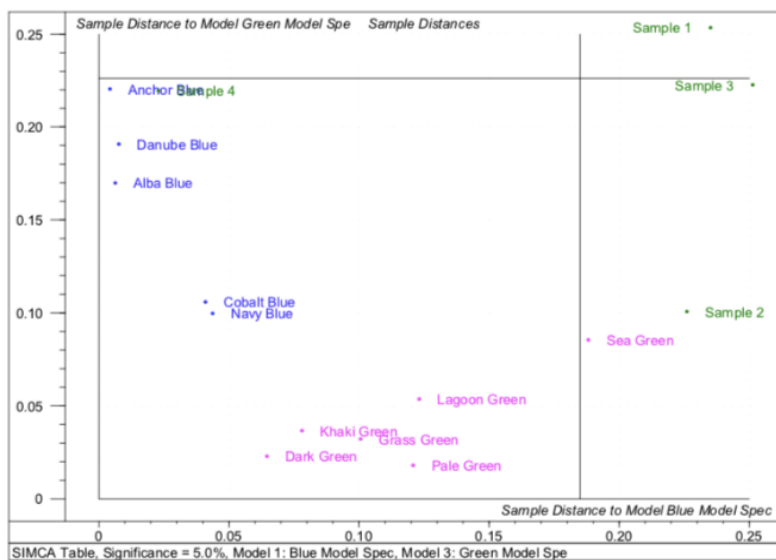
a)

b)

c)

SIMCA Table, Significance = 5.0%, Model 1: Blue Model Spec, Model 5: Red Model Spect

d)

SIMCA Table, Significance = 5.0%, Model 6: Yellow Model Sp, Model 3: Green Model Spe
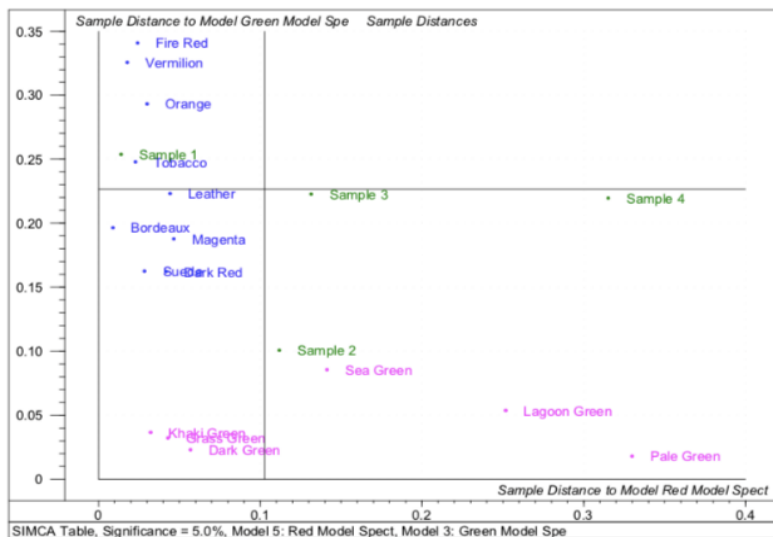
e)

f)

Figure 49 Cooman's Plot obtained with data from the spectra analysis of a) Yellow model vs Red model b) Yellow model vs Blue model c) Blue model vs Red model d) Yellow model vs Green model e) Blue model vs Green model and f) Red model vs Green model

4.1.1.4 Response with smartphone and RGB color coordinates

A smartphone can also be used to obtain digital images in order to obtain color coordinates. These values can be correlated with the analyte concentrations. However, the obtained color parameters are dependent on the chosen color model. RGB is one of the most commonly used color models in image processing, although, color can be converted to other models such as CMYK, hue, saturation, and value (HSV); hue, saturation, and lightness (HSL); hue, saturation, and intensity (HSI); and lightness, green-red, and blue-yellow (L*a*b*). The smartphone cameras have mostly limited control of camera parameters by default (ex. exposure time, shutter speed, ISO, and color balance, and no access to raw image data) and the image processing are applied automatically and vary significantly across smartphones. These methods disturb the linearity of the pixel intensity values, which causes loss of information. In this sense, in further sections of this Thesis is discussed the suitability of using the professional mode of more recent smartphone cameras. This allows to change the camera settings in order to get more realistic images.

On the other hand, ambient light conditions are hard to control during imaging in uncontrolled environments. In this sense, the mobile phone can be set in the same conditions described previously for reflectance mode or using the protocol developed by Pla-Tolós et al.[31], which used a box and artificial light for controlling de light conditions. The digitalized images obtained (JPEJ format) can be processed by external programs such as GIMP, imageJ or MATLAB in order to obtain the color components. Besides that, commercial apps, such as Color Grab* for android and color Assist for iOS, allows easily to obtain the color coordinates. These data can be analyzed for prediction by using multivariate methods[116], or by the correlation of the target analyte concentration with one component[117] or with the ratio between two components[118].

Taking all these into consideration, the RGB components of the pallet of 45 colors were gathered. In order to obtain reproducible signals, conditions such as light source, mobile and sample position, and smartphone used, need to be stablished. Thus, all images were taken using the measurements conditions previously described (Section 4.1.1.3) and RGB parameters were obtained using the free color treatment program ImageJ. The precision obtained were 4.0/3.9 for intra e inter-day (n=3), respectively for a blue color as an example. Here in an app, that

allows calculating the concentration from the RGB of the image, has been also developed. In order to get the concentration in a sample, the user will need photos of the blank signal, a standard with known concentration and the sample with unknown concentration, obtained at the same time. By using the calibration of one point as a calibration model, the app can calculate the sample concentration. By performing the assay in these conditions, we will guarantee that the environmental measurement conditions are equal for all the point measured. The app will obtain the values of RGB for the blank, the standard and the sample, and the concentration obtained for the sample by using the three RGB components (see Figure 50).
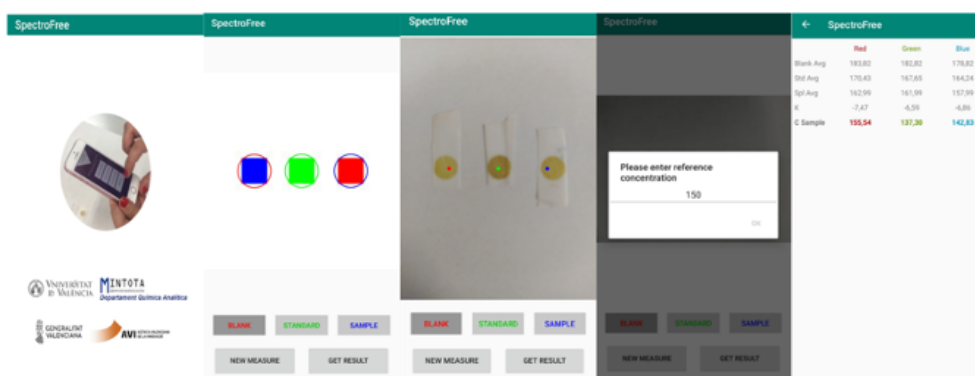
Figure 50 Designed App for calculating the concentration of a sample using the RGB components.

To evaluate the information that RGB parameters can provide using the values obtained with a smartphone, multivariate methods were also used. Accordingly, a principal component analysis was performed for the intensity, brightness and RGB values obtained by using a smartphone and the ImageJ program (Figure 51). Supervised SIMCA models were also employed.
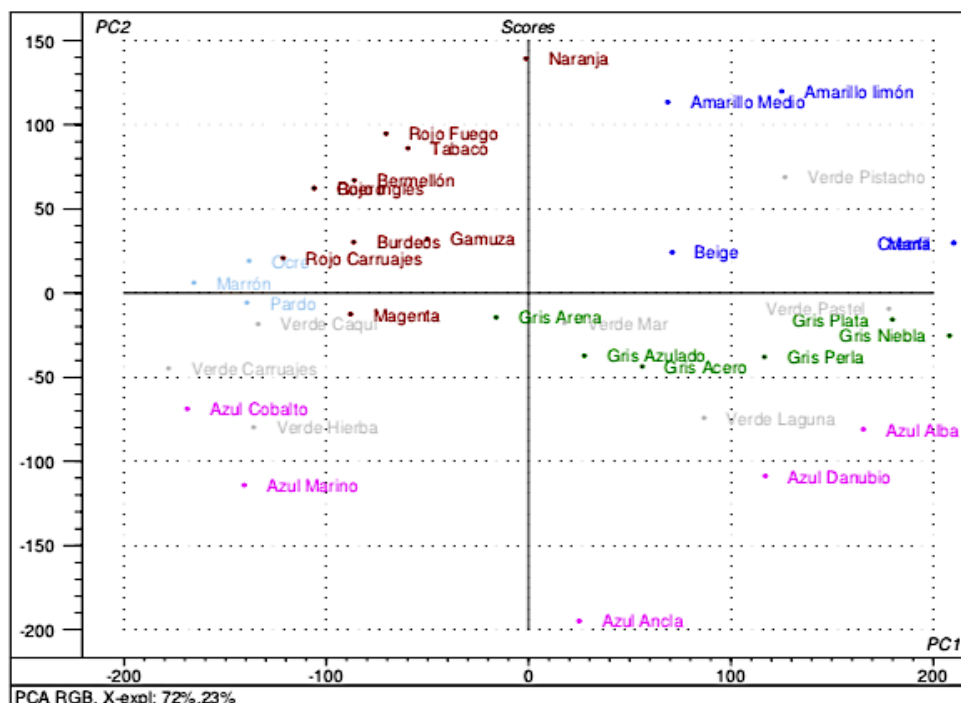
Figure 51 PCA plot for the analytical data obtained using image analysis with a smartphone

For this model, PC1 and PC2, explained almost all the variance, being PC1 PC1 72% and PC2 23%. Several clusters could also be observed, distributed depending on the color. As previously noticed for data gathered from the spectral analysis, the primary colors, green, blue and red were clearly distrusted forming clusters. The mixtures colors (yellow, grey, or brown) were located between the primary colors employed. Although a poorer distribution was observed when using image analysis data.

When SIMCA was applied as classification model (Figure 52), the results obtained by using the data from images were similar to that obtained by using the spectral data. These models were used to predict four colors, the use of RGB components provided less accuracy in the prediction models showing some limitation for distinguishing similar colors when the color coordinates are used. Cooman's plots show that when RGB data is used, a less accurate classification is performed as one of the samples fits well in all the models. This lack in prediction accuracy can be caused by the quantity of information provided in each data set.

While the spectra model gives rise to 1200 variables, yielding a more accurate classification, the information in RGB model is given by only 5 variables.
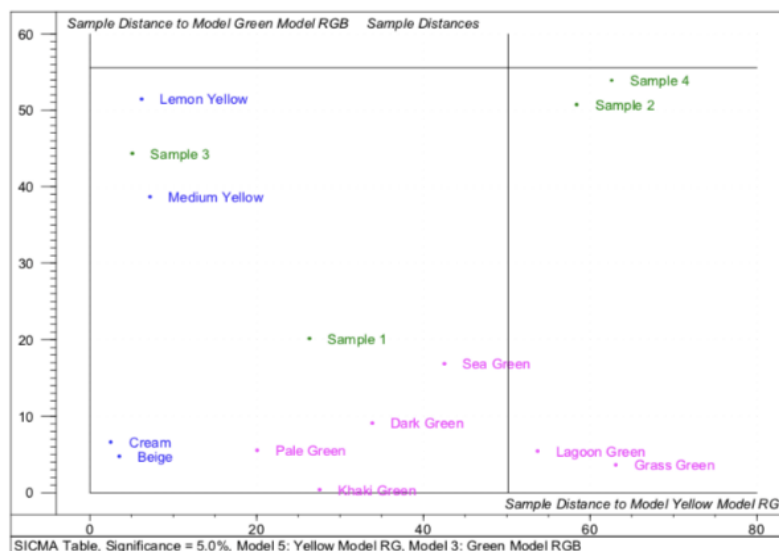
a)
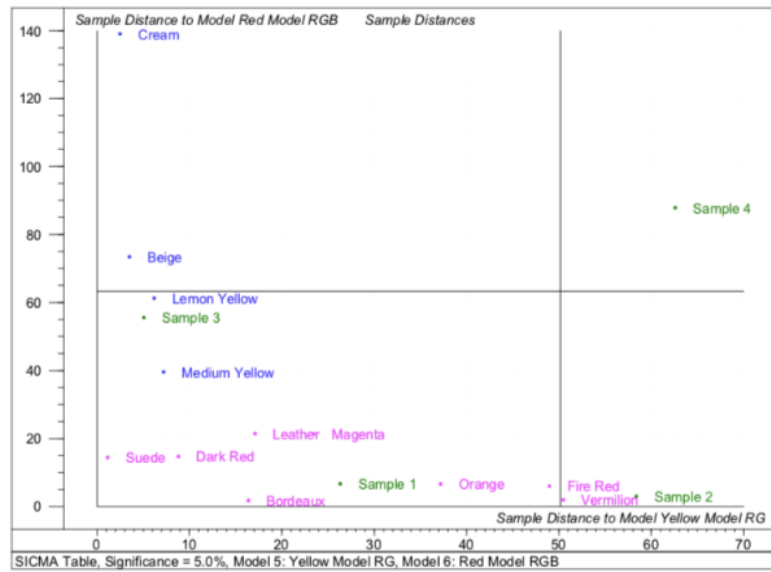
b)
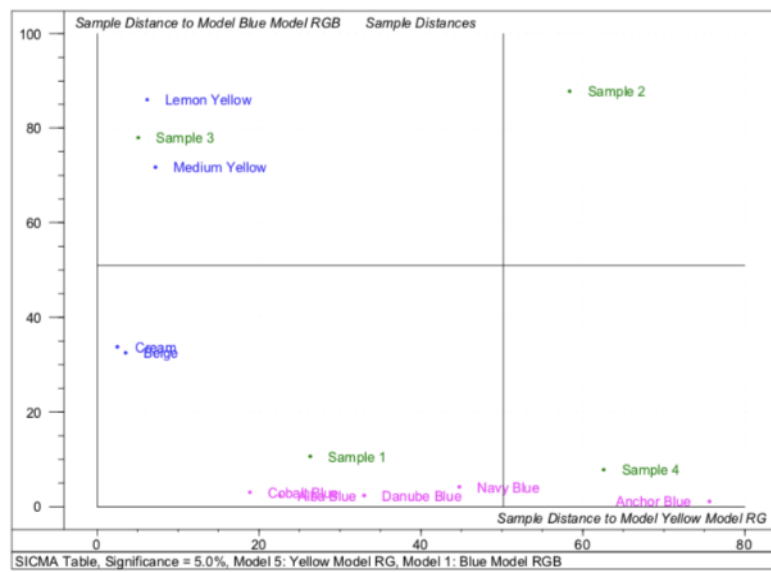
c)

d)

e)

f)

Figure 52 Cooman's plot obtained with data from the image analysis for a) Yellow model vs Red model b) Yellow model vs Blue model c) Blue model vs Red model d) Yellow model vs Green model e) Blue model vs Green model and f) Red model vs Green model.

Finally, from a sustainable point of view, as can be seen in Table 14, smartphone for colorimetric digital image analysis is one of the simpler devices. Thus, it is an economic option as nowadays everybody has a smartphone and the cost to download the app is very low. Furthermore, it is the most sustainable choice within the compared instruments in this study. However, from an analytical point of view, the RBG univariate models presents a lack of selectivity and these models are not selectivity enough to stablish differences between very similar colors. Small color changes cannot be detected in an analysis as the red, green, and blue (RGB) intensity values may not be sufficient. These aforementioned concerns make smartphones limited for fully applicability to quantitative analysis. In this sense, further investigations have been performed in this thesis to obtain enhanced results when using smartphone to carry out colorimetric analysis.

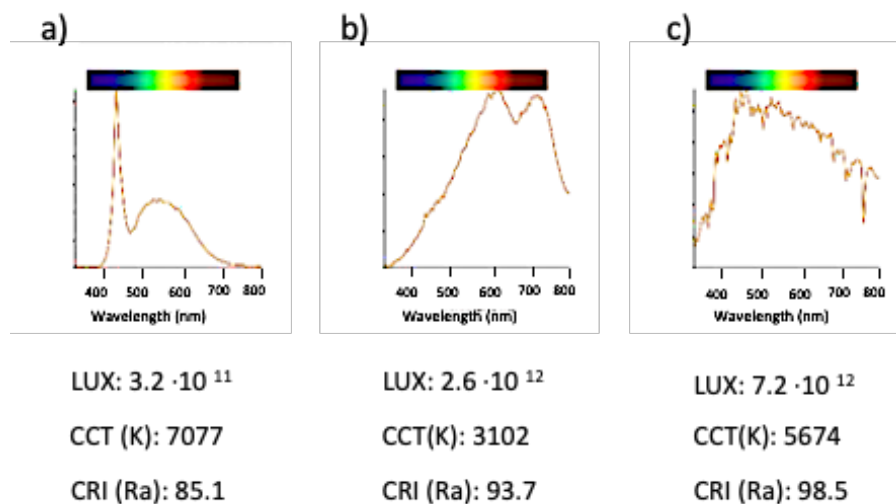### *4.1.2 Testing the influence of light in smartphone measurements*

In this section different analytical strategies are proposed to optimize colorimetric measurements when using smartphones. Measurements have been performed using a smartphone combined to a minispectrometer coupled or not to a fiber optic probe for spectra analysis and a smartphone with a digital camera in order to obtain RGB parameters. With the aim of improving the results previously obtained when using the RGB coordinates for colorimetric analysis, digitalized images were processed using external programs. A protocol guide to perform suitable measurements using a smartphone has been stablished employing a color correction palette of 24 colors, and a testing set of 45 colors. Three different lights, LED, halogen and daylight, have been characterized and further applied as incident light. In order to minimize the influence of external environmental light, a white light box have been utilized. All results have been validated by comparison with a laboratory spectrometer.

4.1.2.1 Characterizing of incident lights

A portable spectrometer (WaveGo) was used to analyze different parameters of incident light such as color temperature CCT (K), Color Rendering Index (CRI), and intensity (LUX). CCT (K) is the temperature of an ideal black body radiator that radiates light of a color comparable to that of the light source and it is characteristic of visible light. LUX refers to the strength or amount of light produced by a specific lamp source. This measures the wavelength-weighted power

emitted by a light source. Illumination intensity is a physical term that refers to the luminous flux of visible light received per unit area. Referred to it as illuminance, the unit is Lux or lx. It is used to indicate the intensity of the light and the amount of the surface area of the object being illuminated. The CRI value, is the measurement of how colors look under a light source when compared with sunlight, this parameter indicates how accurately a color is represented in the measured light versus an ideal light source. Figure 53 shows the spectra and light parameters obtained for the three light sources studied in this work. The lights used had differences in lux, temperature and the absolute spectra irradiance.

LUX: $3.2 \cdot 10^{11}$ LUX: $2.6 \cdot 10^{12}$ LUX: $7.2 \cdot 10^{12}$

CCT (K): 7077   CCT(K): 3102   CCT(K): 5674

CRI (Ra): 85.1   CRI (Ra): 93.7   CRI (Ra): 98.5

Figure 53 . Light spectra and parameters of light intensity and light temperature for different incident light sources: a) LED light b) Halogen light c) Daylight, using a spectrometer (WaveGo).

4.1.2.2 Measuring of the spectra

A first set of experiences consisted of registering the Vis spectra of the color correction palette of 24 colors, and a set of 45 colors by using the different light sources in order to evaluate the light influence.

Color correction palette

First, spectra of the colors from the corrector palette were registered, using the miniaturized spectrometer at different light conditions. Focus was kept most specially in the three primary colors, red (#14), green (#18) and blue (#22). Similar

spectra were obtained for all lights, nevertheless, there were differences in absorbance intensities as it can be observed in Figure 54. These differences can be related with the CRI parameter and the light intensity (Figure 53), as, the higher the lux value the more absorbance intensity observed. The spectra obtained by using the portable spectrometer were comparable to those obtained by using the laboratory instrument (Figure 54).
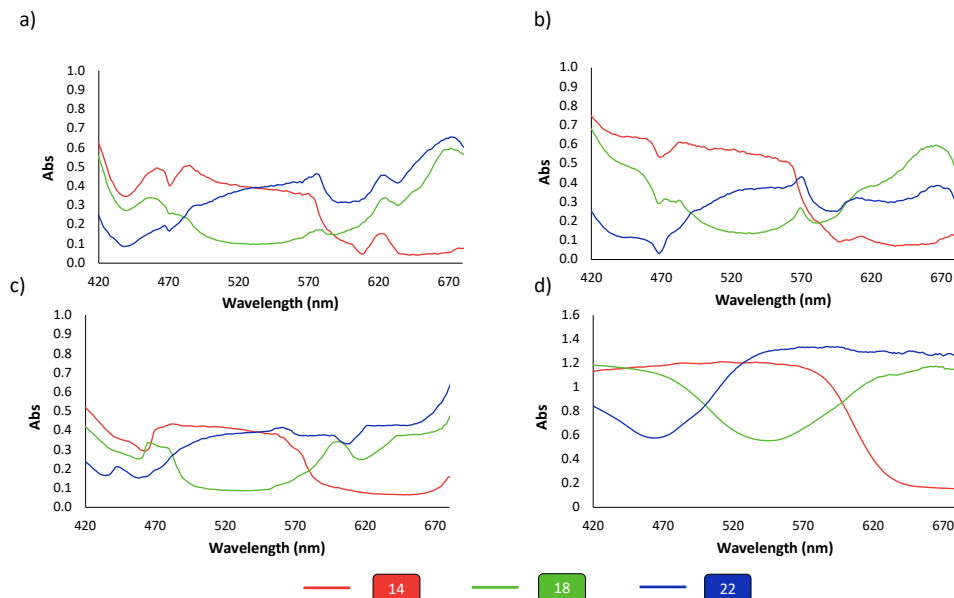

Figure 54 Vis-Spectra at different wavelengths of the three primary colors Red, Green and Blue by using different lights and the mini-spectrometer. a) Led; b) Halogen; c) Daylight; d) Laboratory spectrometer.

Set of 45 colors

The spectra of the set of 45 colors were also registered. Colors were clustered into six groups depending on their color tone (Yellow, red, brown, grey, blue and green). Halogen, LED and indirect daylight were used as light sources) in order to test the influence of incident light. Measurements were performed coupling a fiber optic probed to the smartphone-spectrometer. Registered spectra were also compared with the results obtained using a reference laboratory spectrometer. Figure 55 shows the obtained spectra of the brown color group when the previously commented incident lights were applied.

It was observed that satisfactory spectra were obtained in terms of absorbance when daylight was used as light source, however slightly poor results were observed regarding reproducibility (Table 16). On the other hand, registered spectra using a light box with LED illumination showed suitable signals in terms of absorbance and reproducibility. On its behalf, halogen lamp presented spectra with higher absorbance signals, allowing colors from the same group to be differentiated more efficiently.
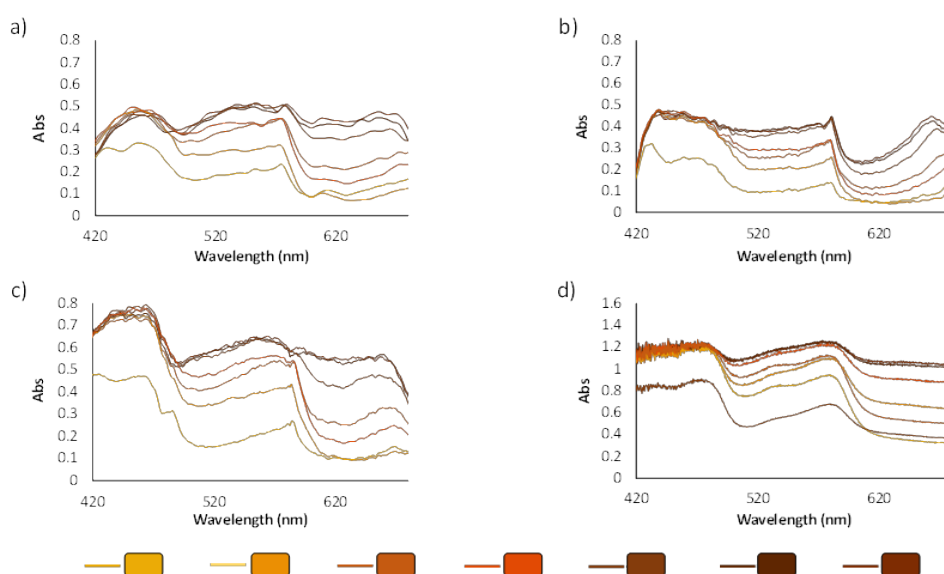
Figure 55 Spectra of the brown color group by using different lights a) Halogen lamp b) LED   light c) Daylight compared to d) Laboratory spectrometer.

It was observed that satisfactory spectra were obtained in terms of absorbance when daylight was used as the light source. Registered spectra using a white box with LED illumination showed a suitable absorbance signal and halogen lamp presented spectra with a higher absorbance signal, allowing colors from the same group to be differentiated more efficiently. Good precision was achieved, as can be observed from the results in Table 16, although daylight provided higher percentage RSD values, which can be explained due to the changes that sunlight can suffer throughout intra-day and inter-day analysis. For Spectra obtained for red and blue color groups for all light sources the same remarks can be made.

Table 16 RSD Values (%) of four colors 511, 529, 536 and 575 using a smartphone spec-trometer with different light sources and a laboratory spectrometer.

Light source	RSD (%) of 511 (λ=475 nm)	RSD (%) of 529 (λ=475 nm)	RSD (%) of 536 (λ=660 nm)	RSD(%) of 555 (λ=580nm)
Smartphone-Spectrometer				
LED	2.35	1.87	1.36	0.57
Halogen	1.75	2.31	1.79	0.9
Daylight	4.31	3.04	1.6	2.71
Laboratory spectrometer				
UV-Vis	0.05	0.08	0.05	0.08

The spectra obtained using a conventional reflectance diffuse instrument was similar to those achieved using the mini-spectrometer (GoSpectro) independently of the light source used. GoSpectro only works in the 420–680 nm range of the wave-lengths. Better spectra shapes were obtained using halogen or daylight instead of LED light in reference to those provided by the lab benchtop equipment. Halogen light was selected as the best option to measure the spectra.

4.1.2.3 Image analysis and RGB color coordinates registration

To perform the image analysis, pictures were taken with a smartphone. Most of the smartphone models have, by default, limited control of camera settings. Thus, values of parameters such as white balance, exposure time, sensitivity to light (ISO) and contrast to brightness ratio are automatically preestablished, causing large variations with illumination conditions. In this sense, images were taken using the professional mode of the camera and parameters were set up in order to obtain images as close as possible to reality. According to this, the parameters were set to 1-1.3 brightness contrast, ISO 100, autofocus mode and color temperature according to the light used.

Going on the study, the next experiments were focused specially in the three primary colors from the color correction palette, red (#14), green (#18) and blue (#22). A lineal correction method was applied to rescale the RGB values of the tested colors adjusting the contrast and brightness values of the image. The main objective of these modifications was to obtain the RGB parameters of the black and white references as close as possible to pure black (0,0,0) and to pure white (255,255,255) respectively. It was observed that almost pure primary colors were

obtained for processed images (255, 0, 0) for Red, (0, 255, 0) for green and (0, 0, 255) for blue. In any case, independently of the light used, the processing treatment improved the responses of the RGB parameters, and a better approximation to the real RGB components was reached (Figure 56).
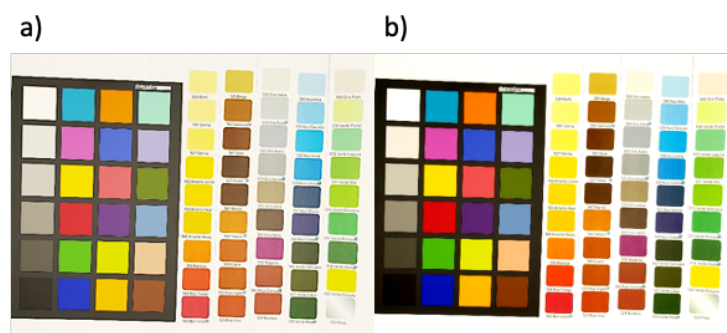
Figure 56 Comparative of a) Original image b) Processed imaged using LED light.

A comparative study of the obtained RGB parameters for both original and processed image was carried out for the three primary colors using the three different sources. It was observed that when using LED light, image processing removes G component from red and blue colors and B component from red and green colors, obtaining more purified primary colors than when using halogen lamp. On the other hand, when halogen light is used, image processing removes R component from blue and green color, and intensifies it for red. This is explained more graphically in Figure 57.

The range of maximum and minim values of RGB parameters for original and processed images was determined for each primary color using different light sources. It was observed that the RGB coordinate that allows a completely differentiation between colors is the R parameter as its ranges for the different primary colors were clearly defined. In addition, a better ratio separation for each primary color was observed when images were processed, within ranges of R_{Red} [224-255], R_{Green}[17-74] and R_{Blue} [0-6]. By processing the image, when using LED light, almost the pure color is obtained, intensifying each corresponding RGB coordinate and decreasing the values of the other two parameters. In this sense, it was concluded that image processing is a valuable tool in order to improve color separation and thus color analysis.
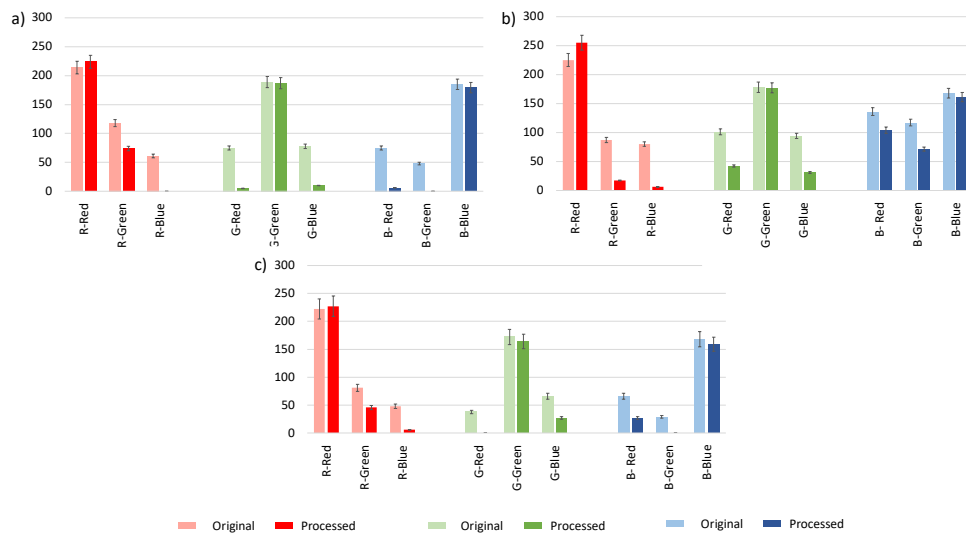
Figure 57 Comparative of the obtained RGB coordinates with original and processed images from the three primary colors Red, Green and Blue using different light sources: a) Halogen b) LED c) Daylight.

The same study was applied for the panel of 45 colors. As previously discussed, colors were clustered into the six aforementioned groups depending on their color tone. It was observed that, for the color ranges composed of warm colors, such as yel-low, red and brown, halogen and LED light sources provided more information for all the RGB coordinates. Conversely, for the color ranges composed of cold colors like green and blue, only the LED light source achieved good separation in terms of RGB values for colors with similar tonalities. The grey group of colors remained significantly unchanged in regards to light conditions as they are colors in the scale between white and black. Additionally, image processing allowed for a better differentiation between colors in the same group, which meant a higher sensitivity for color analysis. A common trend observed for all color groups was that LED light reported the most useful details for color evaluation. Additionally, this set up caused a lower loss of in-formation when processing images. Depending on the analyzed color, the best results were observed with different RGB coordinates, as its suitability hinges on the color tone. In this sense, the yellow group showed a better differentiation in the B parameter, while red and brown color groups showed that the G component provided more useful information, and for green and blue colors, the R coordinate was the most suita-ble to perform the color analysis.

Depending on the analyzed group of colors best differentiations were observed using a different RGB coordinate, as its suitability hinges on the color tone. In this sense, yellow group showed a better differentiation in the B parameter, while, red and brown groups showed that G component provided more useful information, on the other hand, it was observed that for green and blue colors the R coordinate was the most suitable to perform color analysis. It was concluded that best results were obtained were the RGB parameter was the closer to the complementary color of the tone of the analyzed color.

4.1.2.4 Conclusions

In this study, several approaches have been proposed to measure the color covering the full range of colors. The influence of light in portable instrumentation was evaluated. Several light sources using two different measurement methodologies were scaled. In order to characterize the color behavior, response of the smartphone spectrometer coupled to a fiber optic probe was studied using LED light, halogen light and daylight for a corrector color palette and a set of 45 colors with different color groups. RGB color coordinates were also obtained for the different incident lights, image processing was evaluated as an alternative to obtain more realistic colors in order to improve color analysis and study optimized conditions were set for both measurement methods. The results obtained for spectra analysis were slightly better when performing the measurements using a halogen lamp, however better results were obtained with LED light when RGB coordinates analysis was carried out. Daylight results were suitable in terms of sensitivity, but not in terms of precision as its light intensity varies from day to day. In this sense, it has been demonstrated that controlling the measurement conditions is of vital importance to perform suitable analysis using portable instrumentation. The choice of a specific RGB color co-ordinate was also studied in this work. It was observed that best results were obtained were the RGB parameter was the closer to the complementary color of the tone of the analyzed color. The achieved results indicate that halogen and LED light can be suitable options to perform in situ analysis, and their adequacy would be evaluated depending on the demanding information. Furthermore, image processing has also been proved to be a remarkable tool to enhance the performance of color analysis.

4.2 DEVELOPMENT OF SENSORS AND MEASUREMENT WITH PORTABLE INSTRUMENTATION

In this section a colorimetric sensor is proposed based on the NQS embedding as derivatizing reagent into a PDMS/TEOS/SiO$_2$NPs composite as an ammonia sensor to detect NH$_4^+$ and urea in water and human urine samples respectively. NQS is a reagent typically used to determine amines, as mentioned before, it is a yellow-orange reagent that in presence of primary and secondary amino groups forms a brownish color derivative allowing the colorimetric determination to be performed. The NQS-based colorimetric sensing device proposed in this work offers a sustainable alternative that possesses advantages such as versatility, simplicity, rapidity, satisfactory robustness, cost-effectiveness, energy-efficiency and reliable response. To verify the applicability of smartphones in real cases and to evaluate the different strategies studied in previous sections of this Thesis, the colorimetric analysis of the proposed sensor has been performed using portable instrumentation including smartphones. Furthermore, these strategies have been also tested using sensors supported in different materials. In this sense, a nylon-supported plasmonic sensor for the evaluation of hydrogen sulfide in breath samples, a paper-based sensor to determine hydrogen sulfide in water matrices and a PDMS delivery sensor to measure the presence of nitrites in solution have been proposed as cases of study. In addition, analytical parameters as linear range, sensitivity and precision were estimated for all the proposed sensors and compared bearing in mind the different instrumentation used.

4.2.1 Development of a PDMS-based sensor containing NQS for the determination of ammonium and urea

Colorimetric detection occurs when the target analyte diffuses along the porous PDMS/TEOS based membrane and reacts with the colorimetric probe NQS, embedded inside the sensing membrane. In this sense, several parameters were studied and optimized in order to carry out the sensor fabrication and to stablish the reaction conditions to get suitable responses.

4.2.1.1 Optimization of the NQS-PDMS/TEOS-SiO$_2$ NPs sensing membranes.

For quantification purposes, initial studies were carried out in aqueous standards (NH$_4^+$ = 50 mg L^{-1}) using the sensing membrane at room temperature and pH= 7 during sufficient reaction time to allow the colorimetric signal to evolve.

Figure 58a shows the variation of the analytical response as a function of the content of the colorimetric dye measured with the lab benchtop UV-Vis spectrophotometer with a reflectance diffuse accessory. Experimentally, it was observed that a colorimetric dye content equal or higher than 0.34% favored the diffusion of the derivatizing analyte toward the solution. In addition to this, no significant enhancement of the sensitivity was observed for the highest dye content during a 24 h reaction time, as can be seen in Figure 58a. Thus, 0.34% NQS content was selected as the optimal composition for the sensor.
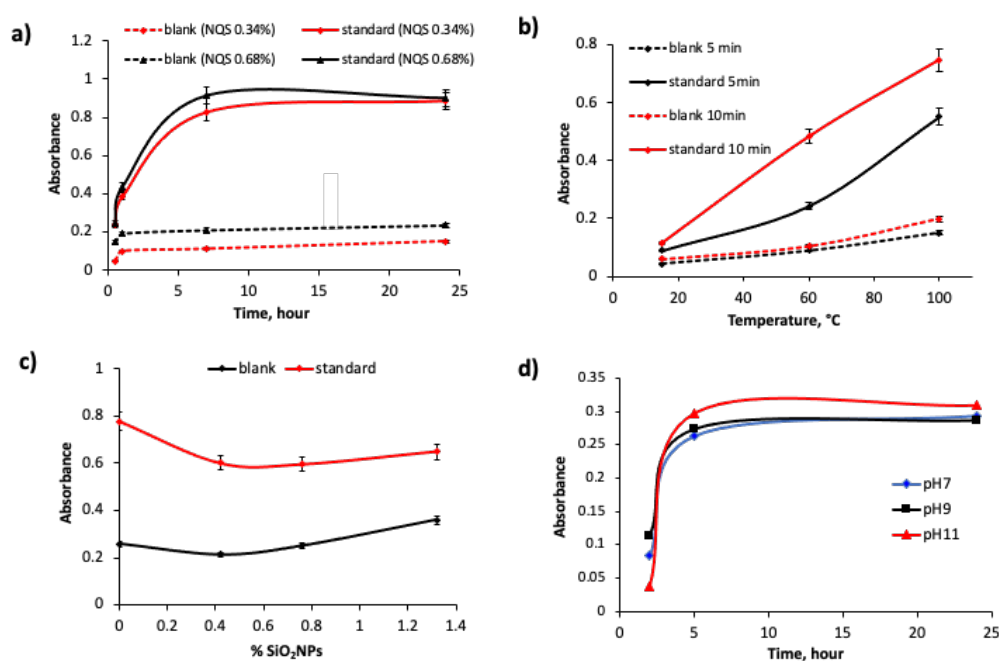
Figure 58 NH$_4^+$ (50 mg L−1) standard solutions: (a) Variation of the colorimetric signal as a function of the NQS content and exposure time at room temperature. (b) Variation of the analytical signal as a function of the temperature for 5 and 10 min reaction time. (c) Variation of sensor response depending on the SiO$_2$ NPs composition tested. (d) Analytical response as a function of the pH and exposure time.

On the other hand, it was found that more than 5 h were required for the colorimetric signal to reach an adequate sensitivity level. In an attempt to reduce the reaction time and improve the sensitivity, a thermal treatment was evaluated, since changes in the reaction temperature can change the adsorption behavior and thereby affect the sensitivity. To this end, three different temperatures (15, 60, and 100 ◦C) at two reaction times (5 and 10 min) were studied, as shown in Figure 58b. The results suggested that an increased temperature drastically reduced the

reaction time to achieve a given sensitivity, and therefore would be advantageous for practical application. However, the thermal treatment also induced a loss of physical robustness of the sensing membrane. With the aim of improving the thermal stability of the membrane, SiO_2 NPs were tested as dopants. The results indicated in Figure 58c confirmed that the presence of SiO_2 NPs enhanced the stability of the sensors during the thermal treatment, as the sensing membrane deformation was completely avoided using a percentage of 0.4%. Moreover, the presence of SiO_2 NPs also helped to prevent the leaching of the colorimetric dye to the solution at high temperatures, most likely because the NPs acted as additional adsorption sites. Additionally, the sensing device performance was examined under different pH conditions (pH 7, 9, and 11) in order to determine the extent to which the membranes respond to these changes and find the optimal working conditions. As depicted in Figure 58d, the sensor response increased as a function of pH, as the NQS reaction is favored at higher pH[383]. Therefore, pH 11 was chosen as the best working condition.

Interday and intraday precision of the proposed sensor were evaluated by the relative standard deviation (%RSD) values. Satisfactory interday (7.25%) and intraday (7.83%) RSD values were obtained. Regarding batch-to-batch precision, intraday RSD values were lower than 8%, and the interday RSD value was 6%, which are satisfactory precision RSD values. Additionally, it should be noted that the sensing membrane was stable as the sol-gel methodology guarantees the stability of the guest molecules as well as the reaction products. The stiffness of the silica matrix prevented the polymeric matrix of agglomerations and guest molecule leaching. These results bear evidence to the fact that the proposed sensing membrane is a reliable and reproducible device to achieve an estimation of NH_3/NH_4^+ in an aqueous medium.

4.2.1.2 Characterization of the sensing membranes.

Scanning electron microscopy (SEM) was employed for the characterization of the proposed sensing membrane. Taking into account the optimal synthetic procedure as well as performance conditions of the PDMS sensor, SEM images of the reference sensor (blank) were obtained. The morphology of the PDMS polymeric matrix exhibited noticeable porosity, as shown in Figure 59a. In addition, the presence of SiO_2 NPs confers the stability of the sensor in the thermal treatment, enhancing its mechanical properties (see Figure 59b).
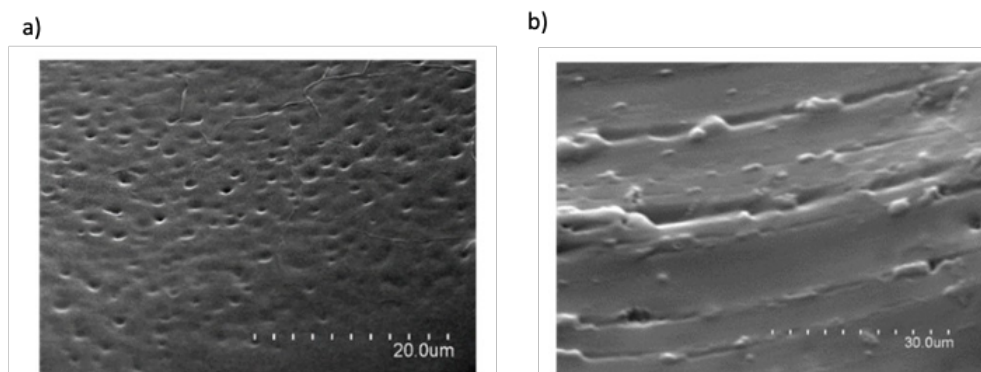
Figure 59 SEM images of synthesized NQS-PDMS sensing membrane, scale: a)20 µm and b) 30 µm.

The PDMS membrane was also characterized by optical microscopy. The colorimetric reaction was followed and the differences in the membrane after and before the derivatization can be clearly observed in Figure 60.
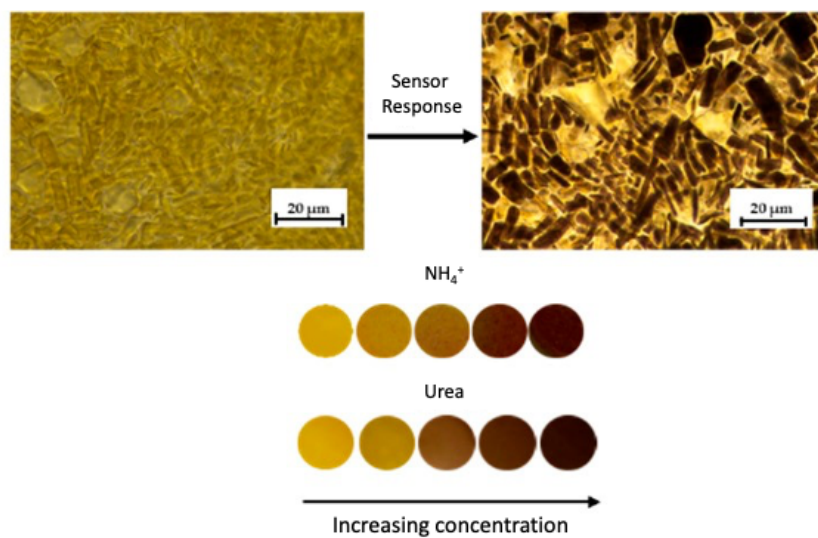
Figure 60 Top: Optical microscopy images of the PDMS membrane before (left) and after (right) the colorimetric reaction, scale bar: 20 µm. Bottom: Evolution of the sensor color as a function of ammonium or urea concentration in solution.

4.2.1.3 Response of solid support to ammonium and urea

4.2.1.3.1 Sensitivity for ammonium and urea standard solutions

The performance of the NQS colorimetric probe encapsulated within the PDMS matrix was investigated in the presence of NH_4^+ (expressed as NH_3) and amine groups of urea standards, $CO(NH_2)_2$ in an aqueous solution. Diffuse reflectance measurements using the conventional spectrophotometer were registered as a reference. A smartphone-based spectrometer was also used to register absorption spectra. A maximum absorption was found at 590 nm for ammonium and urea standards when representing the difference in UV–visible spectra with respect to the blank standard (see Figure 61c). Moreover, RGB parameters were also obtained using a smartphone to perform colorimetric analysis. The experimental settings applied for the smartphone devices measurements where the used in section 4.1.1.

Table 17 Calibration curves obtained for ammonium and urea determination.

Analyte	Instrumentation	Linearity (y= a+ bx)		
		Intercept (a±s_a)	Slope (b±s_b)	R^2
Ammonium	Diffuse reflectance	0.007 ± 0.010	0.035 ± 0.002	0.990
Ammonium	Smartphone spectrometer	0.006 ± 0.010	0.032 ± 0.002	0.999
Ammonium	Smartphone Digital Image RGB (G)	0.003 ± 0.004	0.024 ± 0.001	0.996
Urea	Diffuse reflectance	0.003 ± 0.010	0.153 ± 0.008	0.995
Urea	Smartphone spectrometer	-0.004 ± 0.009	0.149 ± 0.005	0.995

Calibration curves obtained for both analytes, listed in Table 17, indicated satisfactory sensitivity and good linearity of the proposed NQS-based sensor. These results suggest that the NQS-doped PDMS sensor can be a potential candidate for monitoring ammonium and urea in water and urine samples, respectively. Besides, it also proves that, when using a colorimetric sensor as a case of study, results obtained with smartphone instrumentation are comparable to those obtained with the laboratory reference equipment.

4.1.2.3.2 Sensor device performance for hydrolyzed urea: Urease in solution vs immobilized borosilicate glass balls

We further explored the applicability of the sensing device for monitoring ammonia generated in situ in the working medium when enzymatic catalysis of urea takes place in the presence of urease[316]. This enzyme hydrolyzes urea into ammonium, and the catalytic reaction typically occurs in solution. The optimal reaction conditions employed were 37 °C and a 5 min reaction time. Regarding urease solution, several urease volumes were assayed in order to determine the optimal urease quantity for hydrolyzing 5.3 mg L^{-1} of urea. As listed in Table 18, a 20 μL volume was found to be the most appropriate to perform the analysis as the sensor response was not significantly enhanced for higher urease volumes. In these conditions, the urease enzyme was capable of hydrolyzing an amount of urea equivalent to 6.2 mg L^{-1} of ammonia in solution. Satisfactory accuracy values near 100% were obtained.

Table 18 Assayed volumes from urease solution, with absorbance at 590nm, and equivalence to ammonia concentration

V_{urease} (μL)	Abs 590 nm	[NH$_3$] (mg L^{-1})	Recovery (%)
0	0.2050	-	-
10	0.3820	5	95
20	0.4806, 0.4782	6.2, 6.1	117, 116
40	0.4984,0.4911	6.7, 6.5	127, 123

By fixing the previous reaction conditions, urea hydrolysis was studied. The calibration curve obtained for hydrolyzed urea in solution was obtained in a conventional spectrophotometer and with the smartphone spectrometer and is indicated in Table 17. A similar slope was found for both ammonia and hydrolyzed urea determinations, which broadens the applicability of the ammonia sensor for detecting both ammonium and hydrolyzed urea. Moreover, the catalytic reaction was investigated in the presence of urease enzyme when it was immobilized on a glass support[317]. Borosilicate glass balls were selected as a solid support on which urease covalently bonded by following the experimental procedure given in section 3.3.1.1. The sensor performance was investigated in the presence of either urease in solution or immobilized on a glass surface. Diffuse reflectance measurements were performed for hydrolyzed urea standards, and calibration slopes were

compared. As shown in Figure 61, the calibration slope of urease in solution was 0.0333 ± 0.0015 L mg^{-1}, and 0.033 ± 0.0004 L mg^{-1} was obtained for immobilized urease. This result implies that urea hydrolysis is equally effective for both types of experiments. Hence, it is worth mentioning that the immobilization process accounts for an interesting alternative when urease stability and reusability are considered. Additionally, spiked urine samples (n = 2) were analyzed, and similar slopes were obtained for the samples and both urea hydrolysis strategies, as plotted in Figure 61. This implies that no matrix effects were present for hydrolyzed urea determination, making the proposed sensing device a potential candidate for in situ detection.
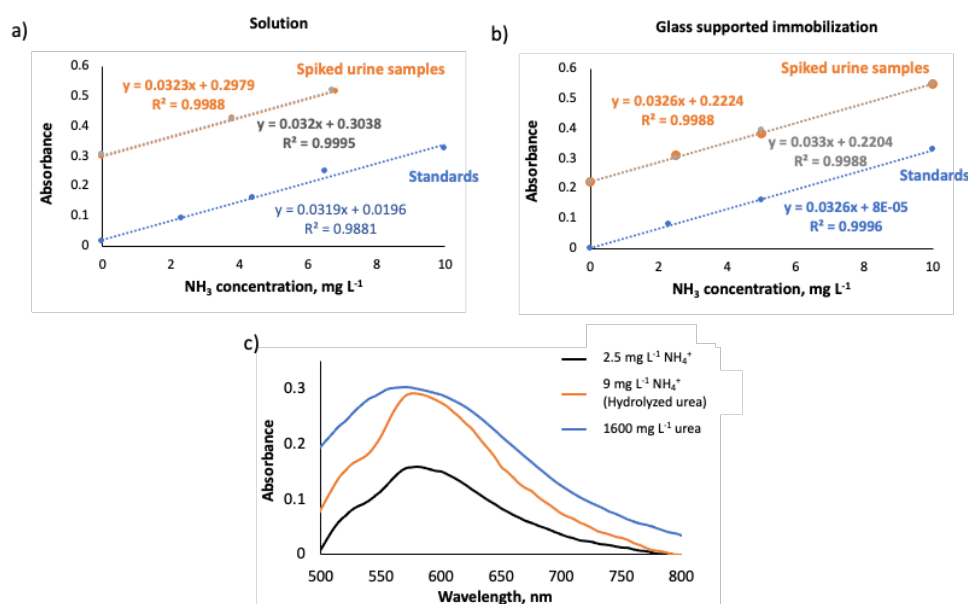
Figure 61 Calibration curves for hydrolyzed urea standards (blue) and spiked urine samples (n=2, orange and grey) for urea catalysis by means of a) Urease enzyme in solution, b) Glass-supported urease immobilization and c) Difference in UV-Vis spectra between standards of 2.5 mg/L of ammonium (black line), 9 mg/L of ammonium coming from hydrolyzed urea (orange line), and 1600 mg/L of urea (blue line) and the blank standard

4.1.2.4 Analysis of real samples

In order to verify the suitability of these sensors for determining ammonium and urea, samples in different matrices were evaluated. Water samples and human urine samples were used to determine ammonium and urea respectively.

Ammonium determination in water matrices

Ammonium was monitored in water samples coming from two different water treatment plants (region of Valencia). In the case of water treatment plant 1, the found concentrations and colorimetric response for the entrance, decantation, and exit stages are given in Table 19.

The colorimetric sensor response and absorbance signals were in agreement with the expected results, that is, the lowest ammonium concentration was found at the exit stage of the treatment plant. In addition to these water samples, wastewaters subjected to oxic and anoxic treatment processes were also studied with the proposed sensing device. The found concentrations calculated for samples S1 and S2 (anoxic treatment reactor input and output, respectively) and samples S3 and S4 (oxic treatment reactor input and output, respectively) were in agreement with the treatments undergone by the samples in the different reactors. In fact, the main difference between the oxic and anoxic processes is the employment of oxygen during water treatment. Typically, anoxic treatment processes are used for the treatment of waste that has a high concentration of biodegradable organic material. Additionally, a recovery study was carried out by analyzing spiked samples with NH_4^+ 1.5 mg L^{-1}. As listed in Table 19, these values were also satisfactory, involving no significant matrix effects in ammonium determination.

Table 19 Colorimetric sensor response and found concentration from different stages of water treatment plants and sensor images for each respective stage of PLANT 1.

PLANT 1	Concentration after dilution $\pm$ s (mg L^{-1})	Real Concentration $\pm$ s (mg L^{-1})
Entrance	6.15 ± 0.16	123.0 ± 3.2
Decantation	6.99 ± 0.11	139.8 ± 2.2
Exit	2.42 ± 0.09	4.82 ± 0.18
PLANT 2	**Found Concentration (mg L^{-1}) (n=3)**	**Recovery (%) (n=3)**
Anoxic reactor	18.0 ± 0.7[1]	95 ± 5
	4.8 ± 0.2[2]	90 ± 7
Oxic reactor	2.5 ± 0.2[1]	87 ± 7
	< LOD[2]	100 ± 4

[1] Water samples from the entrance of the treatment plant. [2] Water samples from the exit of the treatment plant.

Urea determination in urine samples

Direct urea analysis was assayed considering the possible interferences of the nitrogen- based contribution provided by proteins in urine. For the sake of comparison, different urine samples with and without protein precipitation pre-treatment were analyzed. As shown in Table 20, absorbance values for untreated urine and for deproteinized urine samples, suggest that the presence of proteins in urine samples interfered with direct urea detection, giving rise to an overestimation of the nitrogen-based content. Hence, protein precipitation was considered an essential pre-treatment step for eliminating protein interference. The sensor response was analyzed, and urea concentration was quantitatively determined, as listed in Table 20. The results obtained fall in the upper part of the expected human urea range[312]. Thus, the proposed sensor proved its suitability to carry out in-situ analysis for the determination of urea in real samples.

Table 20 Absorbance values for untreated and deproteinized urine samples and found urea concentrations

Urine	Absorbance 590 nm		Urea Concentration (g·L^{-1})
	Untreated	**Deproteinized**	
Sample 1	0.6615	0.3869	27.7
Sample 2	0.5654	0.2895	20.7

Sensor performance was also assessed when urease-catalyzed hydrolysis of urea took place in urine samples. In this case, the sample pre-treatment step consisted of diluting the urine without the protein precipitation procedure. In fact, the blank sensor response (0.2273) was similar to sample responses (0.2169 and 0.1974), which implied the absence of protein interference. Therefore, different pretreatment steps are required depending on the target analyte, that is, urea or hydrolyzed urea. The quantitative analysis yielded the urea concentrations indicated in Table 21. Similar urea concentrations were found for both types of enzymatic catalysis, that is, urease in solution or urease immobilized on a glass support. These results imply that the proposed sensor is reliable and independent of the conditions of the catalytic process, giving rise to a robust in situ analytical method.

Table 21 Urea concentration found in hydrolyzed urine simples.

Urine	Urea Concentration (g L^{-1})	
	Hydrolysis in solution	Glass supported hydrolysis
Sample 1	12.3	11.8
Sample2	12.7	11.8
Average	12.5 ± 0.3	12 ± 0

4.1.2.5 Conclusion

This work demonstrated the potential application of NQS-doped PDMS-based sensors to determine both NH_4^+ in water samples and urea in urine samples. The sensing device showed good precision (RSD < 8%), satisfactory stability, and promising versatility when analyzing different wastewater samples and different human urines. The colorimetric response obtained was registered by conventional diffuse reflectance measurements and smartphone-supported spectrometric measurements for quantitative analysis. In both cases, satisfactory results were obtained and showed good concordance. The response was also analyzed by image analysis using the RGB parameters of the images taken with a smartphone. In this sense, the suitability of smartphone devices for performing colorimetric analysis of solid sensors have been demonstrated. Moreover, semi- quantitative analysis is available by visual inspection of the sensor color, making it a user-friendly device for in situ analysis purposes. In addition to ammonia, direct urea detection was also assessed by the proposed sensing device. Urea hydrolysis was also analyzed in the

presence of urease enzyme in solution and immobilized on a glass support. Both hydrolysis reactions were demonstrated to be quantitative, which increases the feasibility of the proposed sensors as a promising sensing device. Hence, the results obtained broaden the application of the NQS-based sensor to analyze amino groups present in biological matrices, such as urine, in addition to water matrices.

4.2.2 Evaluating the utilization of portable devices to analyze the response of different colorimetric chemosensors

Different light sources and measurement methodologies have been already evaluated in previous sections from a reference palette of 24 colors ad a set of 45 colors with the aim of establishing some guidelines to select appropriate set up depending on the information needed. Here, different colorimetric chemosensors for different analyte concentrations and with different colors have been studied using the aforementioned conditions to obtain their analytical response. PDMS solid sensor doped with NQS for ammonium and urea developed in the section 4.2.1, PDMS doped with Griess reagent as delivery sensor for nitrite[99], paper-based sensor for hydrogen sulfide[31] and nylon supported plasmonic sensors for hydrogen sulfide[63] were selected as different cases of study. The solid sensors allowed the gas or the liquid to penetrate in the material given appropriated color intensity and uniformity. The image of the four selected sensors (with and without being exposed to the analyte) are shown in Figure 62.
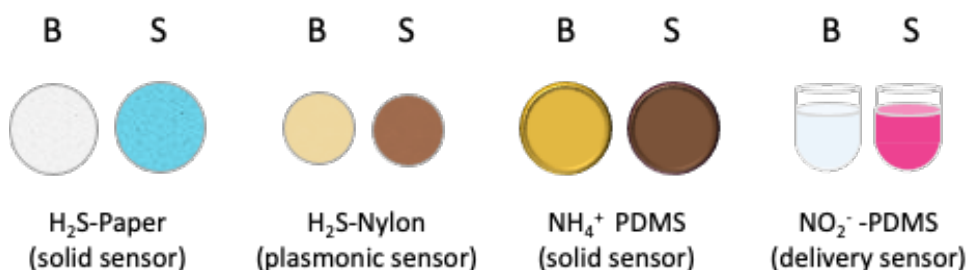
Figure 62 Colorimetric sensors using different supports (paper, nylon, PDMS-solid, PDMS-delivery) exposed to analytes at different concentrations (B: blank and S: Sample).

It is evident that the formed colors of the selected sensor corresponded to different spectral regions with the aim of covering the full wavelength range. Besides, different support materials were chosen to evaluate the versatility of portable instrumentation for measuring colorimetric chemosensors. All of these

materials allowed the light to pass through, so, the analytical signal of some of these sensors was obtained by reflectance. In order to perform the measurements in the transmission mode the sample was introduced at the base of the homemade sample holder and it was placed in between of both pieces (the plastic piece and spectrometer) as it is shown in Figure 39.

Reflectance mode measurements were also performed coupling a fiber optic probe to the smartphone-based spectrometer as described in Figure 40. Spectra analysis as previously established, was obtained by using halogen lamp. In this sense, it was selected as the light source for performing the quantitative analysis. LED light source was selected when performing digital image analysis combined with image processing and RGB parameters. Besides as previously studied a light box to control the influence of ambient light was used to carry out these experiments.

The figures of merit of the different sensors by using the different instruments were also obtained. For all sensors, the analyte quantitation was carried out by external calibration. The limits of detection (LOD) and limits of quantification (LOQ) were calculated as 3 s_a / b_1 and 10 s_a / b_1 respectively where s_a and b_1 are the standard deviation of the blank (n=3) and the slope of the regression. Linear range, sensitivity and precision were also evaluated for all the proposed sensors.

4.2.2.1 Response of the PDMS-based solid sensor for ammonium and urea determinations.

The sensor developed in section 4.2.1 for the determination of ammonium in water and urea in urine after enzymatic hydrolysis was measured in reflectance and transmittance modes in the configuration shown in the Figure 39 and in reflectance mode with a fiber optic probe as in Figure 40. Figure 63 shows the spectra obtained for different approaches when using the smartphone-based spectrometer. Spectra registered using a laboratory spectrometer can also be given as a reference.
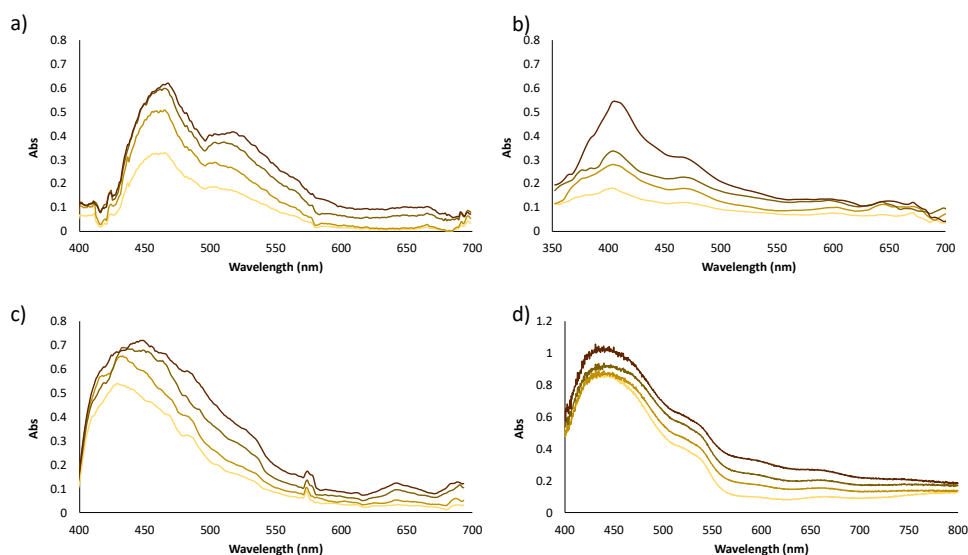
Figure 63 Comparative of the spectra obtained for different concentrations of ammonium in a PDMS solid sensor (0 mg·mL^{-1}, 4 mg·mL^{-1}, 8 mg·mL^{-1} and 12 mg·mL^{-1}) for a) Smartphone spectrometer using transmission mode b) Smartphone spectrometer using reflection mode c) Smartphone spectrometer coupled to a fiber optic probe reflection mode and d) Laboratory spectrometer.

The spectra shape obtained by using the smartphone spectrometer were similar for all the approaches, although the values of absorbance were slightly lower for the smartphone-spectrometer in reflectance mode. Higher values were obtained when coupling the fiber optic probe or by measuring in transmission mode. The figures of merit for all the proposed smartphone-based configurations are summarized in Table 22. For the spectral analysis a maximum of wavelength was stablished at λ=490 nm.

Table 22 Figures of merit of the PDMS sensor for NH$_4^+$ using smartphone-based instrumentation

Data acquisition Mode	Intercept (a±s$_a$)	Slope (b±s$_b$)	R^2	Linearity range (mg·L^{-1})	LODs (mg·L^{-1})
Transmission	0.078 ± 0.004	0.0157 ± 0.0005	0.99	2.24-12	0.67
Reflection	0.119 ± 0.003	0.0128 ± 0.0004	0.99	2.55-12	0.76
Fiber optic probe	0.07 ± 0.03	0.056 ± 0.005	0.97	0.56-8	0.17
RGB image analysis (G)	0.10 ± 0.02	0.104 ± 0.004	0.99	1.91-8	0.58

As can be seen in Table 22, no significant differences were obtained between using reflectance or transmission mode. The sensibility obtained by using the minispectrometer with fiber optic was higher than using the other measurement approaches. Based on these results, the smartphone measuring in reflectance mode fitted with the fiber optic probe was selected for further experiments. Also, suitable values of LODs were observed in all cases. According to the studies carried out above, RGB coordinates analysis also showed good achievements in terms of sensitivity and linearity. Comparing Table 22 with Table 17, it can be derived that better sensitivities were obtained bearing in mind the rules stablished for controlling the incident light, fitting the variables of the smartphone and for image analysis using the procedure proposed for obtaining approximate real colors.

4.2.2.4 Response of the PDMS-based delivery sensor for nitrite

In order to test the suitability of the optimized methodologies for measuring also in solution, measurements have been performed using a PDMS-based delivery sensor for the determination of nitrite in water matrices. The colorimetric response is based on the reaction between the Griess reagents entrapped in the sensor in presence of NO_2^- in solution. This response can be followed by the color change that switches from the clear color samples to a strong pink color. The response measurements were performed using the selected optimized configurations using smartphones. In this sense, the spectral analysis was carried out measuring the colorimetric change in solution at $\lambda=540$ nm using the smartphone spectrometer fitted with the fiber optic probe. On the other hand, as previously established, image analysis was performed processing the images and getting the corresponding RGB parameters. The figures of merits for the two utilised procedures can be seen in Table 23.

Table 23 Figures of merit of the PDMS sensor for nitrite using optimized smartphone instrumentation.

Data acquisition Mode	Intercept $(a \pm s_a)$	Slope(mg·mL^{-1}) $(b \pm s_b)$	R^2	Linearity range (mg·L^{-1})	LODs (mg·L^{-1})
Fiber optic probe	0.148 ± 0.013	0.52 ± 0.02	0.99	0.07-1.30	0.02
RGB image analysis (G)	0.10 ± 0.02	0.64 ± 0.02	0.99	0.02-2.70	0.01

It was observed that similar results were obtained for the two proposed methodologies. Good results were obtained in terms of linearity. According to the World Health Organization (WHO)[384] the limit concentration of NO_2^- in drinking water is 0.5 mg L^{-1}. In this sense, suitable values were also obtained in terms of sensitivity as the achieved LOD values were at least twenty-five times lower than the maximum permitted. These results have shown the adequacy of smartphone-based instrumentation to perform measurements also in solution.

4.2.2.3 Response of the paper-based sensor for hydrogen sulfide

Hydrogen sulfide was determined by the colorimetric analysis of the derivatized sensors. The sensors response was obtained by the formation of the derivatization product methylene blue, which has a characteristic blue color that allow the monitoring of the reaction as it is described in section 3.5.1. The spectra of the paper-based sensor when derivatized in presence of H_2S can be seen in Figure 64. The spectra shape obtained by using the reflection mode was similar for all the instruments, although the values of absorbance were slightly lower for the smartphone-spectrometer. However, by measuring in transmission mode, the values of absorbance were a bit higher than those obtained in reflectance mode.
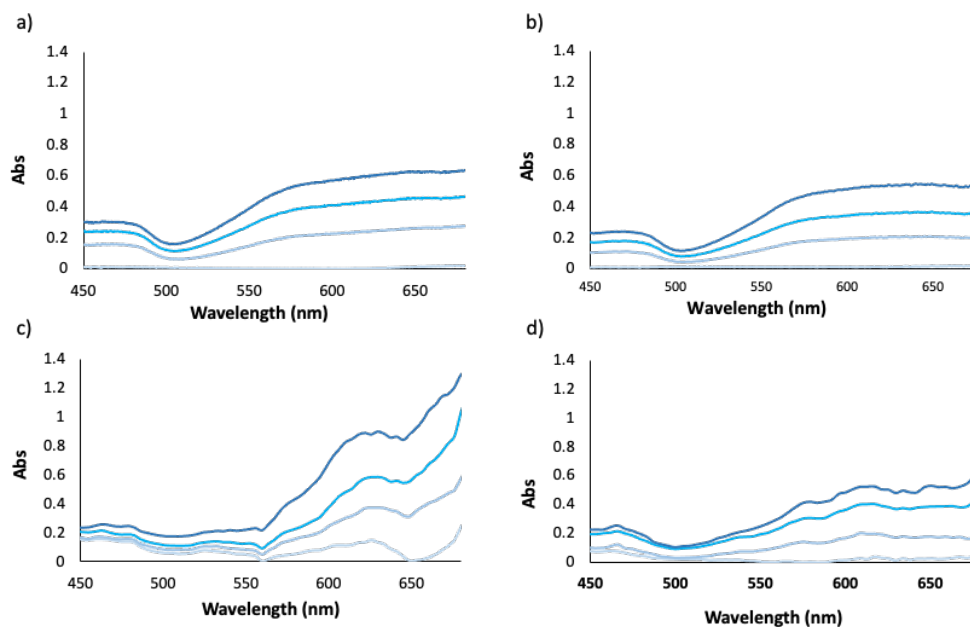
Figure 64 Spectra corresponding to paper-based sensors for the determination of several H$_2$S concentrations (0, 3, 7, 13 mg·L^{-1}) measuring using a) laboratory reflectance spectrometer, b) Portable reflectance spectrometer c) smartphone spectrometer measuring in transmission mode and d) smartphone spectrometer measuring in reflectance mode.

To carry out quantitative analysis λ=670 nm was selected as the measurement wavelength. The precision and the sensitivity of the measurements were improved by using a fiber optic connected to the minispectrometer when measuring in reflectance mode (Figure 40). Thus, this was the chosen method for performing spectral analysis using a smartphone. In order to perform image analysis, sensors were measured placing the sensors inside the light box to control the influence of light and at 5cm of the smartphone camera. Sensor images were analysed with and without image processing in accordance with that stablished in section 4.1.2.
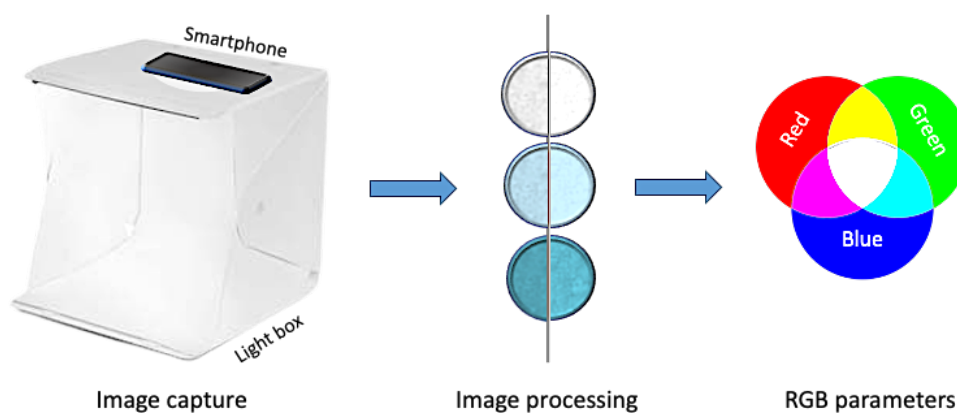
Figure 65 Schematic representation of the procedure followed for digital image analysis.

As can be seen in Figure 65 more real colors were obtained when processing images. The figures of merit for the different applied methods are shown in Table 24. As can be seen comparable results were obtained for all methodologies. Satisfactory values were obtained in terms of LOD and linearity. Besides it has been demonstrated that when using a fiber optic probe coupled to the smartphone-spectrometer very similar results to those obtained with conventional laboratory spectrometer can be achieved. On the other hand, it has been proved that using a smartphone for taking pictures combined with image processing and using the light box to control the influence of ambient light can also provide suitable results for color analysis.

Table 24 Figures of merit of the paper-based sensor for H_2S using different instrumentation

Instrument	Data acquisition	Intercept $(a \pm s_a)$	Slope $(b \pm s_b)$	R^2	Linearity range $(mg \cdot L^{-1})$	LOD $(mg \cdot L^{-1})$
Laboratory spectrometer	Diffuse reflectance	0.018 ± 0.008	0.051 ± 0.004	0.999	0.3-7	0.082
Portable spectrometer	Diffuse reflectance	0.04 ± 0.02	0.068 ± 0.007	0.998	0.55-7	0.17
Smartphone spectrometer	Fiber optic probe	0.008 ± 0.005	0.041 ± 0.002	0.997	0.33-7	0.1
Smartphone	Image analysis RGB (R)	0.054 ± 0.013	0.074 ± 0.002	0.990	1.77-13	0.53

In order to evaluate the accuracy and precision, several samples of known concentration were analyzed. Table 23 shows the concentrations obtained at two different concentration levels and the relative errors corresponding to the use of the different instruments. Moreover, concentration has been also provided by a custom-designed app. As can be seen good results were obtained for all instruments. It is also observed that the concentrations obtained by using the developed app were comparable to those calculated by using the external data treatment. In this sense, it can be concluded that the proposed portable instrumentation can be a suitable tool for in situ analysis, especially smartphone devices, which show an enhanced portability and cost-effectiveness and can provide fast, sensitive and precise results.

Table 25 Concentration of H_2S in solution and relative error obtained using different instruments. [a]Values obtained with an external software. [b] Values obtained with a designed app.

Instrumentation and data acquisition mode	Sample 1 4,5 mg/L	Sample 2 7 mg/L
Lab Difusse Reflectance spectrometer	4.68 ± 0.08 Er = 4.0 % RSD% = 1.7	6.70 ± 0.07 Er = -4.3 % RSD% = 1.0
Portable Spectrometer	4.48 ± 0.08 Er = -0.4 % RSD% = 1.8	6.70 ± 0.04 Er = -4,3 % RSD% = 0.6
Smartphone-Spectrometer [a]	4.32 ± 0.14 Er = -4.0% RSD% = 3.2	6.71 ± 0.05 Er = -4.14 % RSD% = 0.7
Smartphone-Spectrometer [b]	4.64 ± 0.12 Er = 3.2% RSD% = 2.4	6.8 ± 0.3 Er = -2.8 % RSD% = 3.9
Smartphone-Digital imagen (RGB)(R) [a]	4.34 ± 0.09 Er =-3.6 % RSD% = 2.0	7.1 ± 0.2 Er = 1.4% RSD% = 2.8
Smartphone-Digital imagen (RGB)(R) [b]	4.6 ± 0.3 Er = 4.0% RSD% = 4.8	7.3 ± 0.4 Er = 1.2% RSD% = 2.7

4.2.2.4 Response of the nylon-supported plasmonic sensor for hydrogen sulfide

Hydrogen sulfide was also determined using a plasmonic nylon supported sensor. The colorimetric response was obtained by the aggregation of the AgNPs retained on the nylon support, when sensor is in presence of hydrogen sulfide. The nylon membrane suffered a color change from yellow to an orange/brownish color that could be followed by spectral analysis (λ=500nm) and by image analysis. To carry out spectral analysis, portable instrumentations was compared to conventional laboratory spectrometer. On the other hand, image analysis was performed using a smartphone combined with image processing. The figures of merit for the different methodologies are summarized In Table 25.

Table 26 Figures of merit of the nylon-supported sensor for H_2S using different instrumentation

Instrument	Data acquisition	Intercept ($a\pm s_a$)	Slope ($b\pm s_b$)	R^2	Linearity range ($mg \cdot L^{-1}$)	LOD ($mg \cdot L^{-1}$)
Laboratory spectrometer	Diffuse reflectance	0.238 ± 0.002	0.846 ± 0.008	0.999	0.02-0.4	0.006
Portable spectrometer	Diffuse reflectance	0.284 ± 0.012	0.91 ± 0.06	0.990	0.04-0.4	0.012
Smartphone spectrometer	Fiber optic probe	0.169 ± 0.002	0.412 ± 0.012	0.997	0.06-0.4	0.018
Smartphone	Image analysis RGB (G)	0.120 ± 0.002	0.347 ± 0.007	0.999	0.04-0.3	0.012

As can be seen comparable results were obtained for the four proposed methodologies. Satisfactory values were obtained in terms of LOD and linearity detection concentrations at ppb levels. It was observed that spectral analysis can be performed using portable instrumentation obtaining suitable results. Moreover, also adequate results were obtained when images were taken using a smartphone and combined with image processing for color analysis. In conclusion, it was proved that portable instrumentation including smartphones for both, spectral and image analysis, are suitable options to carry out colorimetric and could be used to perform measurements in situ.

4.2.2.5 Conclusions

It is well known that the tested analytes are important in different fields, and in some cases, the concentration levels are legislated. Moreover, the selected sensors formed different colors corresponding to different spectral ranges. Besides measurements have been tested in different support material including in solution. If analytical characteristics of smartphone methodologies are compared to other employed instruments, it can be seen that these options are the cheapest and the easiest for in-situ analysis. They are also the most sustainable. It has been demonstrated that controlling the measurement conditions is of vital importance to perform suitable analysis using portable instrumentation. In this sense, the smartphone spectrometer coupled to a fiber optic probe has been stablished as the better option to carry out colorimetric analysis with smartphone instrumentation using a halogen light source. On the other hand, for image analysis, the use of LED light followed by image processing has proved to provide the best results. Although smartphone instrument requires a strict control of the environmental conditions (light source, mobile position, mobile model, sample size), the operability is very simple. Non specialized personal can carry out it the measurements by following a protocol. The use of smartphone has the advantages of portability, computing power, memory, capability to connect to other IT systems, and the signals registered or captured images can be transmitted. Furthermore, custom-designed apps allow the processing of the information transmitted using an appropriate algorithm, which enables the obtention of the desired concentration. It has been also demonstrated that, although the smartphone is the best selection for analysis in situ, it also can be used as lab instrument if a fast analysis and/or cheap analysis is required. These results have revealed smartphone significant versatility. All these observed qualities, together with its inherent characteristics have made smartphones a remarkable tool for in situ analysis.

4.3 COMBINING HPTLC WITH SMARTPHONE MEASUREMENTS

In this section the combination of high-performance thin layer chromatography with a derivatization reaction and following smartphone based colorimetric detection have been proposed. Two different studies have been performed. On the one hand, a carbohydrates separation was carried out. The aim of this study was the selective detection of lactose in real samples where different sugars are also present. To this end, a separation procedure was developed to

isolate lactose, the main sugar of milk, from other carbohydrates usually present in milk like glucose and galactose and in food samples such as, fructose and sucrose. The chromatographic separation procedure was followed by a colorimetric reaction and further response measurement were performed using the different strategies previously optimized using smartphone-based instrumentation. On the other hand, a chromatographic separation for proteins was also performed for the isolation of gluten. This well-known molecule usually coming from wheat was separated from its constituents gliadin and glutamine and from other proteins present in food samples like albumin from chicken and casein. Similarly, color derivatization was carried out and detection was performed using smartphone for spectral and image analysis.

4.3.1 Lactose quantification in several matrices.

In this study an in place colorimetric method has been proposed for estimation of the quantity of lactose in several matrices (milk, water effluents and surfaces). The produced products and the cleanliness of critical points of the manufacturing process can be controlled analyzing the amount of this carbohydrate, moreover, cross contamination between different products manufactured in food industries can be also avoided. This method combines the use of HPTLC for sugars separation with novel analytical smartphone-based devices. In order to measure the lactose a colorimetric reaction has been used. A solution of thymol was employed to reveal the carbohydrate spots. Spectral analysis of the derivatized spots was carried out using a smartphone-based spectrometer fitted with a fiber optic probe. On the other hand, RGB parameters were obtained by image analysis, processing the pictures of the chromatographic layers. With the aim of obtaining the enhanced separation resolution and higher colorimetric responses the proposed methodology was optimized as described in the following section.

4.3.1.1 Colorimetric reaction optimization in HPTLC plates

In order to obtain a more ecofriendly derivatization method, in this work, the traditionally used phenol was replaced by thymol to produce the colorimetric derivatization. For achieving optimal reaction conditions on solid support (HPTLC phases), several reaction parameters were considered, including the amount of thymol, the sulfuric acid concentration, the addition of reagents and the reaction

time and temperature. Lactose was used as a model compound. As it was expected, the colorimetric response depended on the concentration of lactose and thymol, however too intense coloration hindered the concentrations of lactose to be distinguished. A thymol concentration of 0.033M was chosen for the reaction. On the one hand, 1% H_2SO_4 concentration was too low for the color to be generated, this may occur due to the absence of furfural as reaction product. It was observed that 10% H_2SO_4 concentration produced a colorimetric reaction that evolved in time, this was commonly associated to the degradation of the reaction product. As can be seen in Figure 66, a concentration of 5% H_2SO_4 provided good coloration and the response was stable in time, thus, following the results obtained, 5% H_2SO_4 concentration was selected for the ongoing experiments.
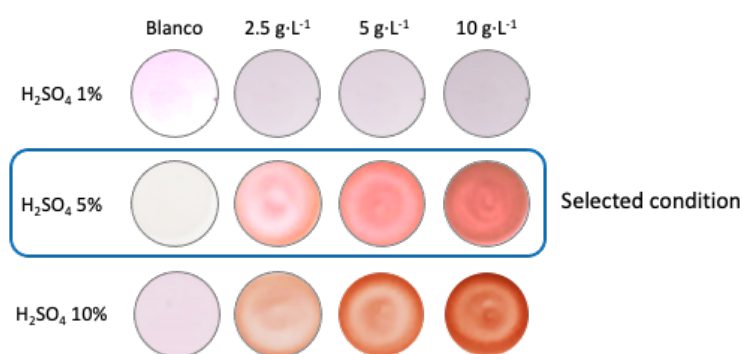
Figure 66 Colorimetric reaction spots at 0, 2.5 ,5 and 10 g·L^{-1}of lactose using different concentrations of sulfuric acid.

The effects of temperature and time were also studied. Temperatures between 70 °C and 150 °C were studied. At assayed higher temperatures (110 °C - 150 °C) colors obtained were typical of the reaction product carbonization. Then, the optimal temperature was stablished around 90 °C. Time of heating was also studied, observing that 3 minutes was the minimum time needed to get a good intensity coloration of the analyte spots. In order to make the procedure as simple as possible and to minimize the response time these were the selected conditions for performing subsequent detection.

The exposure time between the chromatographic layer and the derivatization solution was also evaluated. Different exposure time were studied leaving the reaction solution to stand for 30, 60, 90 and 120 seconds over the HPTLC

plate. Very few responses were obtained when leaving the reaction solution 30 and 60 seconds. However too high exposure times like 120 seconds colored also the thin later surfaces, thus, an exposure time of 90 second was chosen as the optimal time to achieve a suitable color response and clean plates.

The possibility of using plates with the reaction embedded was evaluated, but it was observed that reagent spread when the analyte (lactose) was placed on the plate. The best results were obtained when the plate containing the analyte was immersed in the reagent solution. The color development was performed soaping/immersing the plate in Thymol-sulfuric acid solution to ensure complete derivatization of all spots.

Aluminum HPTLC plates coated with different sorbents (silica gel, nano silica gel, CN modified nano silica gel and NH_2 modified nano silica gel) were tested. In Figure 67 it is shown the responses of different concentrations using lactose as analyte for several stationary phases.
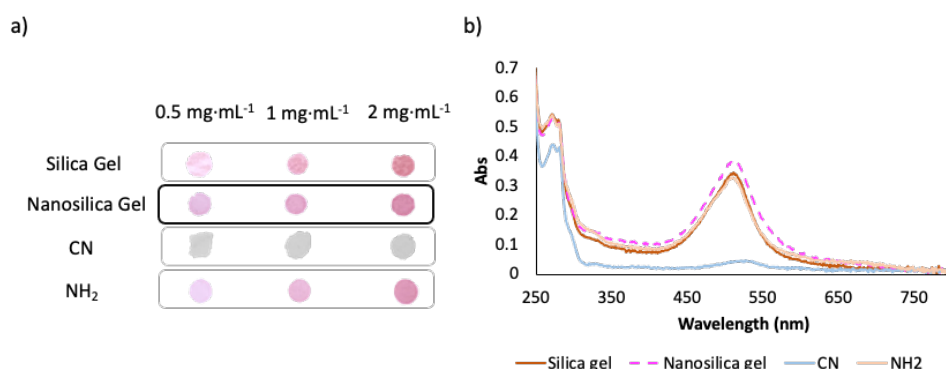
Figure 67 a) Colorimetric reaction spots on different stationary phases at 0.5, 1.0, 2.0 mg·mL^{-1} of Lactose b) Absorbance spectra of the spots on different stationary phases (silica gel, nano silica gel, CN modified nano silica gel and NH2 modified nano silica gel) at 0.5, 1.0, 2.0 mg·mL^{-1} of Lactose.

In all surfaces the reaction product was successfully formed, however, depending on the polarity of the coating different product coloration was obtained. Silica gel, nanosilica gel and NH_2 modified nanosilica gel solid support presented a maximum of absorbance for the reaction product at 510nm and presented a high coloration intensity, while CN modified silica gel support presented a negligible response due to a lower coloration intensity (Figure 67). It was also observed that

when using polar phases, the product had a weaker diffusion on the plate. Best results were obtained using silica gel coating plates, as they showed a lower spot diffusion and a better response. In this sense, they were selected as the surface material for the chromatographic separation.

4.3.1.2 HPTLC separation optimization

As expected regarding previously studies by Rakesh S. Shivatare et al.[385] and Bazila Naseer et al.[130] nano Silica gel plates showed a better separation, providing narrower and cleaner bands than the ones obtained by using TLC plates. Hence, several parallel separations were allowed, resulting in a high output, time saving and rapid low-cost analysis.

Several mobile phases were tested to optimize separation of different sugars using volumes of 1μL at concentrations of 1mg mL^{-1} per each analyte. In order to get an approach into green chemistry, many of the solvents used, as water, acetone, acetonitrile and ethanol, were ecofriendly. Mobile phases composed of acetone or ethanol and water provided poor sugars separation obtaining insufficient retention factors. Previously, Srivastava et al. performed successfully separation of lactose in mammalian milk using n-butanol : glacial acetic acid: water as mobile phase[342]. Likewise, Morlock et al. carried out an streamlined analysis of lactose-free dairy products, separating lactose, glucose and galactose using i-propyl acetate : methanol : water as mobile phase[386]. In addition, Bernardi et al. achieved satisfactory separation of carbohydrates in microbial submerged cultures using as mobile phases different mixes of acetonitrile: water[148]. Following the trends of green analytical chemistry, mobile phases containing acetonitrile: water were tested, showing suitable results and ensuring a promising sugars identification. Furthermore, accordingly to Byrne et al.[387] acetonitrile (ACN) is also considered in some green solvent selection guides a recommended ecofriendly solvent, making ACN:H$_2$O an optimal mobile phase for this case of study. Different compositions of acetonitrile: water were tested to obtain a better separation as it is observed in Figure 68.
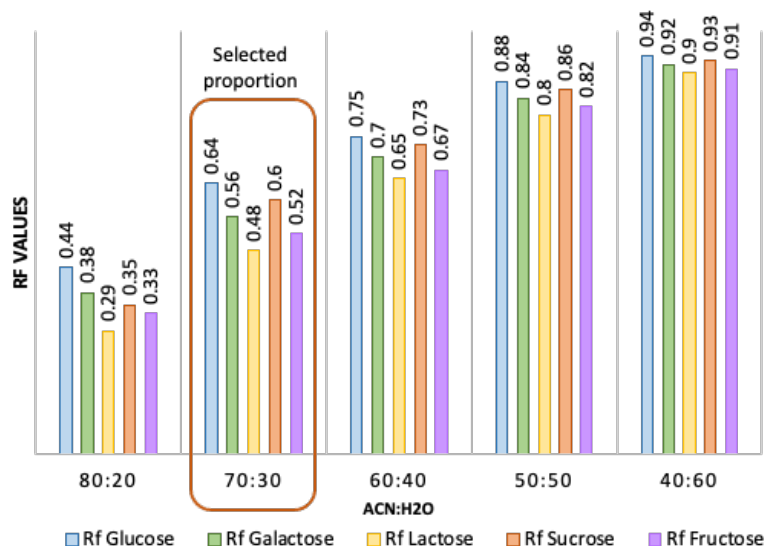
Figure 68 Rf Values for Glucose, Galactose, Lactose, Sucrose and Galactose, using different proportions of ACN:H_2O mobile phase.

As it was expected, a higher proportion of acetonitrile in the mobile phase caused a weakening of the eluting power, allowing the sugars to have a good separation. Similarly, a decrease of the retention factor (Rf) values is observed due to a greater affinity of all sugars to the stationary phase. Considering both, an optimal sugars separation and Rf values, a proportion of 70:30 (ACN : H2O) was chosen to go on this work.

It has been seen before in bibliography that some inorganic acids and bases are commonly used in chromatography as modifiers to get sharper peaks[388]. Applying this concept to HPTLC, acetic acid in different proportion was tested as a modifier to get more defined bands. Acetic acid at 4% was proved to provide the most well-marked bands. According to the results obtained, the working optimized mobile phase was 70:26:4 (ACN : H2O : Acetic Acid).

In Figure 69 is shown the separation of different monosaccharides (glucose, fructose, galactose) and disaccharides (lactose and sucrose) by working at the optimal conditions. Due to the low diffusion on the support a good separation was obtained.
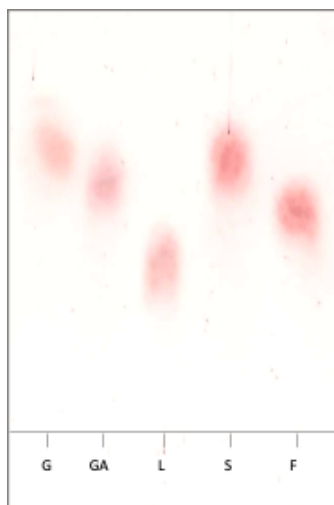
Figure 69 HPTLC plate for different sugars, Glucose (G), Galactose (GA), Lactose (L), Sucrose (S) and Fructose (F), following the optimal conditions for the separation and the derivatization reaction.

4.3.1.3 Lactose determination as a case of study

Lactose concentration in cow milk is about 4,6% ($\approx$46 mg·mL^{-1}) according to Perati et al. Many dairy companies have set a value of 0.01% ($\approx$ 0.1 mg·mL^{-1}) of Lactose as a quality feature for lactose-free products [389]. In order to assess the quantitative capacity of the stablished method, spectra for standard concentrations from 0.25 to 2 mg·L^{-1} were measured using different instrumentation. Measurements were performed using a laboratory spectrometer fitted with a diffuse reflectance accessory as reference at a mean Rf value of 0.48. Measurements were also performed using a portable spectrophotometer equipped with a fiber optic probe coupled to smartphone. The use of the fiber optic probe allows the obtention of very sensitive and accurate measurements, in this sense, lactose at the level of traces could be also determined. The derivatized layers were digitalized taking images by using a smartphone. RGB coordinates were obtained from the colored spots after image processing. Chromatograms were obtained for each color coordinate (Red, Green, Blue) scanning the plate at different Rf values (Figure 70). Good results were obtained for the green and the blue parameters in terms of linearity and sensitivity, however, slightly better results were obtained by using the G component. In this sense it was selected as the parameter for the determination of lactose when using image analysis.
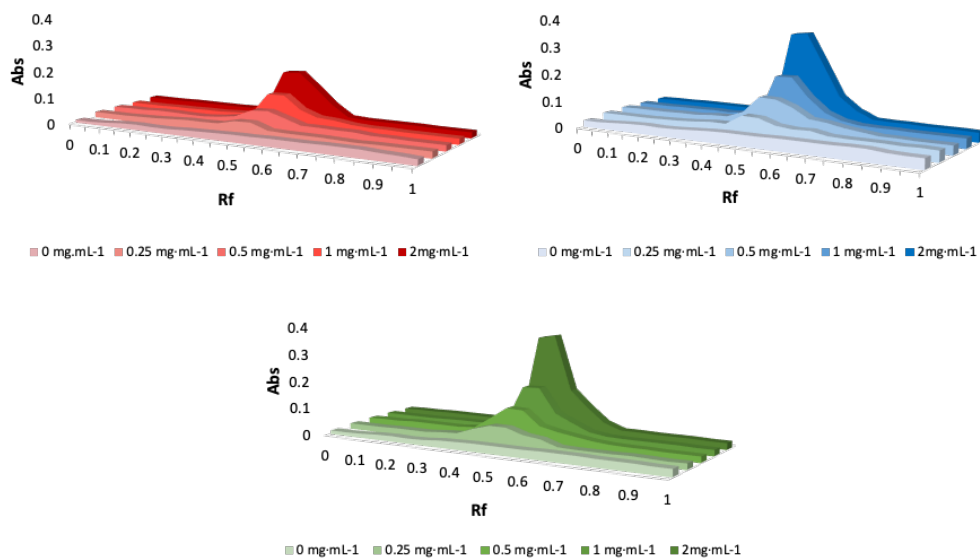
Figure 70 HPTLC chromatogram from RGB coordinates for lactose at different concentrations (0, 0.25, 0.5, 1 and 2 mg·L⁻¹) for a) Red parameter contribution, b) Blue Parameter contribution, c) Green Parameter contribution.

The figures of merits of the lactose determination in HPTLC plates by using different instruments assayed are shown in Table 27. The analyte quantification was carried out following the optimized procedure at a wavelength of 500 nm. The limits of detection (LOD) and limits of quantification (LOQ) were calculated as $3s_{yx}/b_1$ and $10s_{yx}/b_1$, respectively, where s_{yx} and b1 are the standard deviation and the slope of the regression, respectively. Linearity range, sensitivity and precision of the methods were evaluated.

Table 27 Figures of merit by using the different instruments and signals (absorbance or RGB components).

Instrument	Intercept (a±s$_a$)	Slope(mg·L^{-1}) (b±s$_b$)	R^2	Linearity range (mg·L^{-1})	LODs (mg·L^{-1})
Difusse Reflectance spectrometer	0.13 ± 0.02	0.24 ± 0.002	0.98	0.08-2	0.02
Smartphone-Spectrometer probe	0.055 ± 0.008	0.133 ± 0.008	0.99	0.1-2	0.03
Digital image RGB Chromatogram (G component max intensity)	0.030 ± 0.005	0.159 ± 0.005	0.99	0.32-2	0.1
Chromatogram (G compoonent peak área)	0.0001 ± 0.0007	0.0185 ± 0.0007	0.99	0.38-2	0.12
Smartphone-Spectrometer probe (traces level)	0.0273 ± 0.0004	0.254 ± 0.009	0.99	0.01-0.1	0.003

The figures of merit by using portable instrumentation equipped with the fiber optic probe are similar to those obtained by using the traditional lab instrument. Also, good correlations and appropriated detection and quantification limits were obtained. When using the processed images from the smartphone, the RGB parameter selected for the HPTLC plate coloration was G (Green) component. A good correlation was obtained but the analytical parameters (LODs and LQDs) were slightly higher than that obtained with the other instruments. As it is observed, a sensible improvement is achieved using portable instrumentation when fiber optic is equipped. Figure 71 shows the spectra lower concentrations of lactose standard (0.01-0.1 mg·L^{-1}) using a portable spectrophotometer equipped with a fiber optic probe coupled to Smartphone. Structured spectra were obtained taking in consideration the small differences between analyzed concentrations. Amounts of analyte at the level of traces were quantified by standard addition. Measures were also taken at a mean Rf value of 0.48. Results achieved were highly satisfactory as seen in Table 27. A good correlation was obtained and sensitivity expressed as LOD and LOQ values were from 100 to 10 times lower than the maximum of lactose stablished as a quality feature in lactose-free products. As a conclusion, satisfactory results were obtained by using portable instrumentation, especially when fiber optic was used due to the accurate absorbance measurements that can be performed with this accessory.
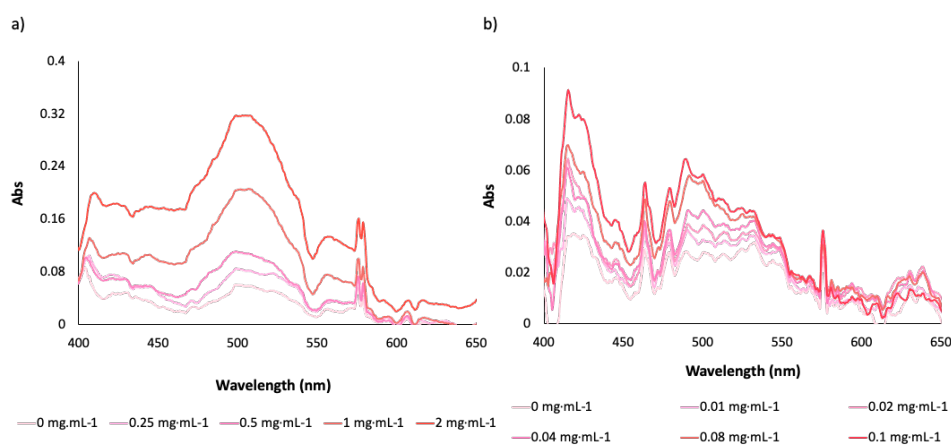
Figure 71 HPTLC smartphone spectrometer measurements for A) Lactose standards (0.25-2 mg·mL-1 per spot) and B) Lactose standards at traces level (0.01-0.1 mg·L-1 per spot).

4.3.1.4 Lactose determination in real samples

The proposed methodology has been applied for the determination of different real samples. Samples of well -known milk brands of whole, semi-skimmed and skimmed milk containing lactose were analyzed. Lactose-free milk samples were also studied in order to evaluate the methods at the level of traces. Effluent samples gathered from dairy companies producing mainly cheese were also analyzed. Samples were collected at different stages of a CIP process used to clean the pasteurizer, tanks and pipes. Finally, analysis was also performed to samples from critical points of food industries.

4.3.1.4.1 Lactose determination from milk samples

In order to evaluate the accuracy and precision, methods were applied to seven samples of whole, semi-skimmed and skimmed milk from known milk brands from different supermarkets. Table 28 shows the concentrations obtained and the relative errors corresponding to the portable spectrometer equipped with a fiber optic probe at mg mL^{-1}, using two different calibration methods, standard addition and external calibration. For the external calibration method, standards of lactose from 0.25 to 2 mg L^{-1} were measured, then, samples were analyzed, and its analytical signal was interpolated in the external calibration. For the standard addition, samples were spiked with known concentration of lactose standard. Lactose free milk samples (S6 and S7) were also spiked with known concentration

150

of lactose standards and analyzed by standard addition to confirm that the treatment with the enzyme lactase actually brakes lactose molecule into its two constituent sugars: glucose and galactose. The concentrations used to calculate the errors were the concentration given by the manufacturer.

Table 28 Found concentrations of lactose in milk sample solutions, relative errors, and standard deviation obtained by using two different methods of quantification. Found concentrations of lactose in effluent samples from CIP processes of dairy industries.

	Commercial milk samples					
	Standard Addition			External Calibration		
Samples	[Lactose] (mg·L^{-1})	E$_r$ (%)	RSD (%)	[Lactose] (mg·L^{-1})	E$_r$ (%)	RSD (%)
S$_1$	47.2 ± 0.2	3	4	49.0 ± 0.07	6	1.4
S$_2$	47.7 ± 0.4	3	8	50.2 ± 0.09	8	1.9
S$_3$	44.4 ± 0.2	7	5	44.7 ± 0.07	7	1.6
S$_4$	46.1 ± 0.3	6	6	45.2 ± 0.03	8	0.7
S$_5$	49.6 ± 0.2	3	3	51.8 ± 0.03	8	0.6
S$_6$	$(3.72 \pm 0.04) \cdot 10^{-5}$	-	1	-	-	-
S$_7$	$(3.62 \pm 0.07) \cdot 10^{-5}$	-	2	-	-	-
	Samples from CIP process of dairy industries					
S$_8$	-	-	-	0.25 , 0.25 [a]	-	-
S$_9$	-	-	-	0.6 , 0.9 [a]	-	-
S$_{10}$	-	-	-	3.9 , 4.2 [a]	-	-
S$_{11}$	-	-	-	7.8 , 8.8 [a]	-	9, 7 [a]
S$_{12}$	-	-	-	6.6 , 7.4 [a]	-	-

[a]Values calculated from RGB parameters

Precision (expressed as relative standard deviation RSD%) was determined from triplicate milk samples for both methods. The values obtained are summarized in Table 28. RSD values were between 3 % and 8 % for Standard Addition and between 0.6 % and 1.9 % for external Calibration method. In terms of accuracy, a recovery assay was carried out, the values were close to 100% in all cases (92-108%) obtaining an average value of Recovery (%) = 101.7. The results obtained indicated that no matrix effect was present in the method and the concentration can be calculated by using external calibration.

4.3.1.4.2 Analysis of effluent samples from CIP processes of dairy industries

The proposed method was used for the analysis of effluent samples collected from dairy companies producing mainly cheese. Samples were collected

at different stages of a CIP process used to clean the pasteurizer, tanks and pipes. Cleaning is accomplished by circulating hot water and solutions of chemicals through the equipment or pipe work in contact with the products. The cleaning system contains four stages: rinse with warm water, rinse with a highly alkaline and acidic solution and chemical disinfection.

Three samples of the first two steps of the cleaning process were collected, and two samples of the last two steps. After the arrival to the laboratory, the samples were stored at 4°C until analysis. Before the analysis each sample was shaken vigorously by hand for 30 s. Each sample was analyzed in triplicate and at room temperature. Lactose values (mg L^{-1}) of the different samples were obtained for two methods of measurement for the colored nano silica gel layer (Diffuse reflectance and RGB parameters). The results are shown in Table 28.

4.3.1.4.3 Carbohydrates determination of samples of food industries

Samples from surface of food industries were also analyzed (Table 29) in order to quantify lactose at usual working content as well as traces level. A cleaning in place surfactant treatment was carried out in many critical points of the factory process, which involves lactose hydrolysis into its constituents namely glucose and galactose. Therefore, glucose and galactose identification were performed in addition to the quantitative analysis.

Table 29 Lactose, Glucose and Galactose detection of samples collected from food industries.

Sample	Description	Lactose	Glucose	Galactose
S1	Formulation tank of gluten-free products	< 0.2 μg	No	No
S2	Dryer tank of gluten-free products	< 0.2 μg	Yes	No
S3	Pipeline to storage silo of gluten-free products	< 0.2 μg	Yes	No
S4	Formulation tank of gluten products	< 0.2 μg	Yes	Yes
S5	Worm screw	> 200 μg	Yes	Yes
S6	Dryer tank of gluten products	< 0.2 μg	Yes	Yes
S7	Loading trolley to dryer	< 0.2 μg	No	No
S8	Sieve line	< 0.2 μg	Yes	Yes

Absence of lactose at traces level was reported for samples presenting a quantity of lactose lower than 0.2μg. Sample 5 showed a presence of lactose higher than 200 μg (maximum amount of analyte quantified), being considered a critical

point during the cleaning in place treatment. Samples S4, S6 and S8 showed no presence of lactose but a positive identification of glucose and galactose in their analysis. This may suggest a possible degradation of lactose into its constituents by the cleaning process. Finally, S2 and S3 only showed presence of Glucose, while S1 and S7 showed no presence of any sugar.

4.3.1.5 Conclusions

In this study it has been developed a new sustainable colorimetric method combined with HPTLC for sugars separation and following in place sugar analysis. The colorimetric response obtained was registered by conventional diffuse reflectance and smartphone-supported spectrometric measurements for quantitative analysis. The figures of merit: linearity, LODs and LQDs, obtained by using the portable smartphone spectrometer coupled to a fiber optic probe were very similar to those obtained with the laboratory spectrometer proving this method to be a promising alternative for in place analysis of lactose. In the present work it has been demonstrated the potential application of the reported method to determine lactose in milk samples and in lactose-free milk samples at traces level. In terms of precision RSD values were in all samples lower than 9% for both Standard Addition and External Calibration method. In terms of accuracy an average recovery of 101.74 % was obtained for standard addition calibration. Samples from surfaces of critical points of food industries and effluent water samples from dairy industries have also been tested obtaining satisfactory results.

4.3.2 Gluten monitoring in food industries

The objective of this study was the development of an analysis platform based on thin layer chromatography combined with colorimetric read-out to make yes/no decisions in gluten cross-contamination. The approach is based on gluten detection by formation of a copper-based complex compound with bicinchoninic acid in basic medium after separation of gluten in nano silica TLC plates. Colorimetric response was measured with a smartphone spectrometer fitted with a fiber optic probe as previously optimized along this Thesis. Image of the chromatographic plates was also taken by the smartphone camera in order to obtain RGB parameters from the digitalized image. Image processing was used in order to enhance the sensitivity and accuracy of the image analysis measurements. Samples from critical points of food industries were analyzed as a practical

application for the evaluation of the proposed approach. Gluten sampling in critical points of the food processing chain was performed with cotton tipped swabs and extraction was carried out with Betelene USP Plus, a commercial surfactant facilitated by a chemical company specialized in cleaning procedures. This study was performed with the aim of developing a strategy to simplify the detection of gluten and hence, help to avoid involuntary transgressions derived from undesirable contaminations.

4.3.2.1 Gluten solubilisation studies

Gluten determination is limited by the low solubility in aqueous media, basically because of the large molecular size and intermolecular aggregation, that results in non-covalent interactions, mainly involving hydrogen bonds and hydrophobic interactions. However, solubility can be improved taking advantage of the ionisable groups at gluten structure by adding different additives, such as salts or surfactant and by pH variations. Since the practical application of the proposed strategy is gluten detection in food processing industries, the solubility performance of NaOH and NaOH: EtOH solution was compared with the solubility of different commercial products used in the cleaning of the processing lines. Figure 72 qualifies the performance of the different solvents as function of solubilisation performance. As can be seen, NaOH and NaOH: EtOH, mainly dispersed gluten and only NaOH provided a stable dispersion. Stable dispersions were also achieved with Ultra SDN, Ultra VF7, Dectocide CDB y TEPHEX CB 34. However, Dectocide CDA and Dectocide A30 resulted in a poor gluten dispersion stability. Only, Betelene USP plus gave rise to a complete dissolution of gluten at percentages lower than 3%. This result indicated the possibility to obtain homogeneous solution that was interesting from two different point of view, to extract gluten from the different critical points in the processing chain and to remove residual gluten to avoid cross-contamination.
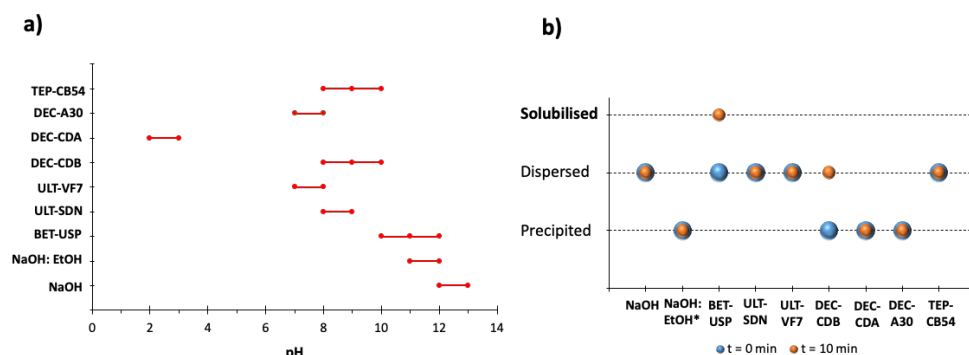
Figure 72 a) Comparison of the pH ranges of the different solvents used in the gluten solubility study b) Plot of the different grades of solubility achieved using the solvents studied for two different agitation times t= 0 min and t= 10 min.

It was observed that gluten solubilisation is related with pH and composition. As can be seen in Figure 72a, basic pH favors solubilisation, however it is necessary the presence of surfactants to achieve a homogeneous solution. The agitation time was also proved to be a key parameter in terms of homogeneity and solubility. Figure 72b shows the variation as a function on the agitation time compared with the initial time. As can be seen, agitation improved gluten solubilisation, in particular when using Betelene as solvent. This solvent, was then employed for further studies. It was observed that gluten solubilisation is then related with pH and composition.

Gluten is a set of proteins mainly composed of gliadins. Gliadins are proteins known as prolamins which are very reach in prolines and glutamines. Under the proposed condition, basic hydrolysis of gluten took place, this process increase the solubility of gluten since protein-protein interactions decrease, reducing aggregation and/or precipitation. This effect can be observed in Figure 73 where the IR spectra of the solubilized gluten was registered. In order, to perform the IR measurements, gluten was dissolved and solution was deposited on a stainless-steel surface, the gluten sample was then left to dry at 40°C. The residues were collected as powder in order to register the IR spectrum.
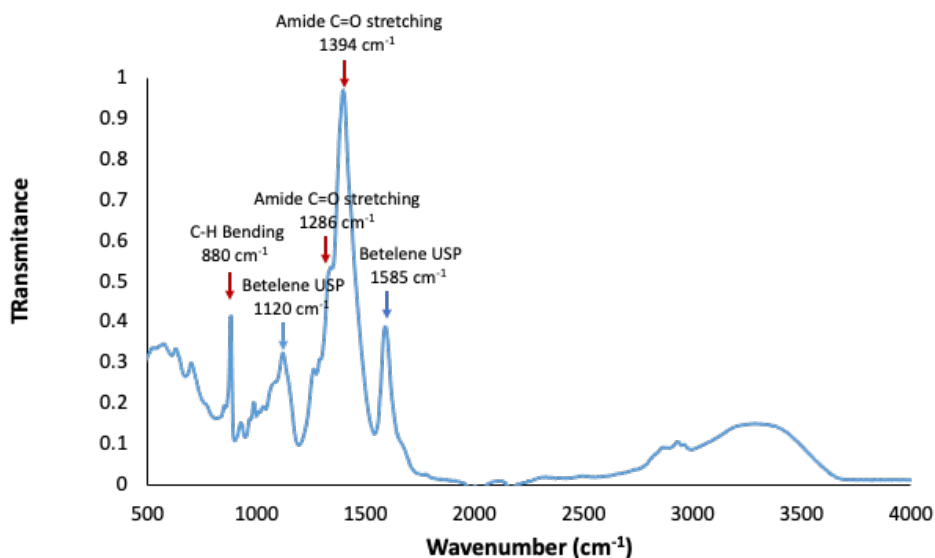
Figure 73 IR spectra of gluten dissolved in Betelene USP Plus.

In order to characterize completely the gluten solubilization, several IR spectra of proteins and amino acids related to gluten were registered. In this sense, the IR spectra of standards from gluten, gliadin, glutenin, proline and glutamine were studied. The IR spectrum of Betelene USP Plus, as well as the spectra for the dissolved species in this solvent were also gathered. As can be seen in Figure 73 characteristic bands from the studied amino acids, proline and glutamine, were present in the IR spectra of Gluten dissolved in Betelene USP Plus. Accordingly, two strong bands, almost overlapped, corresponding to the stretching amide C=O bond were observed at $\nu= 1394$ cm^{-1} and $\nu= 1286$ cm^{-1} respectively. These bands were also seen when proline was dissolved in the selected solvent. It was also observed a quite intense and narrow band at $\nu= 880$ cm^{-1} characteristics of the C-H bending that was also present in the IR spectra of Glutamine dissolved in Betelene. Further characterization was intended, however, most of the bands were overlapped by the strong signals corresponding to the solvent Betelene as can be seen in Figure 73. The results observed by the IR spectra demonstrate the dissolution of Gluten in the studied products.

4.3.2.2 Separation and detection optimization

Gluten solution was spotted onto different thin layers, however, most of the spots could not be added uniformly due to the hydrophobicity of gluten solutions. In this sense CN modified nanosilica plates were chosen as the layer substrates as homogeneous spots were achieved and further separation could be performed satisfactorily. In this sense, different compositions of the mobile phase were studied in order to achieve suitable Rf values. The analytical response for gluten was obtained following the procedure described in the experimental section. Accordingly, gluten spots were visualized by spraying bicinchoninic acid staining solution over the plate. Figure 74 shows the CN modified nanosilica gel plates with the different studied mobile phase compositions after the chromatographic development.
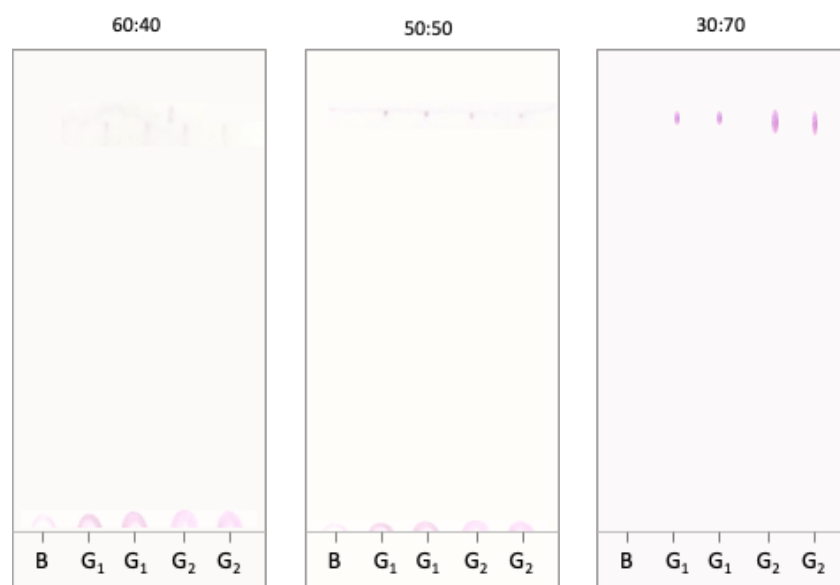
Figure 74 Gluten separation in CN modified nanosilica plates as a function of the mobile phase composition (ACN:H$_2$O).

As can be seen, the elution depended on acetonitrile content, the higher percentage of acetonitrile, the lower Rf value. As it was expected, the interaction between gluten and Nano-silica plates is favored at high percentage of acetonitrile, showing low Rf values. The results indicated that 30:70 ACN:H2O provided satisfactory results in terms of Rf and image analysis.

Taking into account the previous results, the possibility to improve sensitivity was studied by increasing the number of taps per spot. To avoid diffusion of the chromatography layer was dried for 30 seconds between each sample application. Figure 75 depicts the variation of the responses as a function of the number of spots.
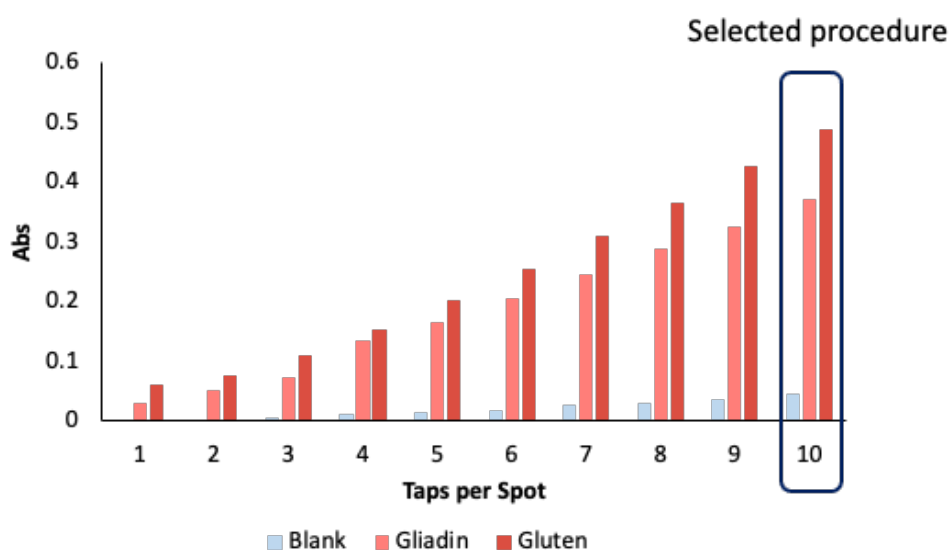
Figure 75 Variation of the analytical response of a blank, gliadin and gluten as a function of the number of taps applied per each spot.

As can be observed with a higher number of taps per spot the signal was increased, as the preconcentration of gluten was being carried out in each spot before the chromatographic development. Moreover, the blank signals remained almost unreacted. In this sense, a number of taps per spot of ten was selected for the ongoing experiments.

With the stablished optimum conditions, the selectivity of the process was also studied since the presence in the processing chain of residues of other proteins is very common. Accordingly, the procedure was applied to a mixture of several proteins composed of gluten, casein and albumin from chicken egg white. The derivatized plate after the chromatographic development using the optimized methodology and the chromatogram obtained, measuring the absorbance at different Rf can be seen in Figure 76.
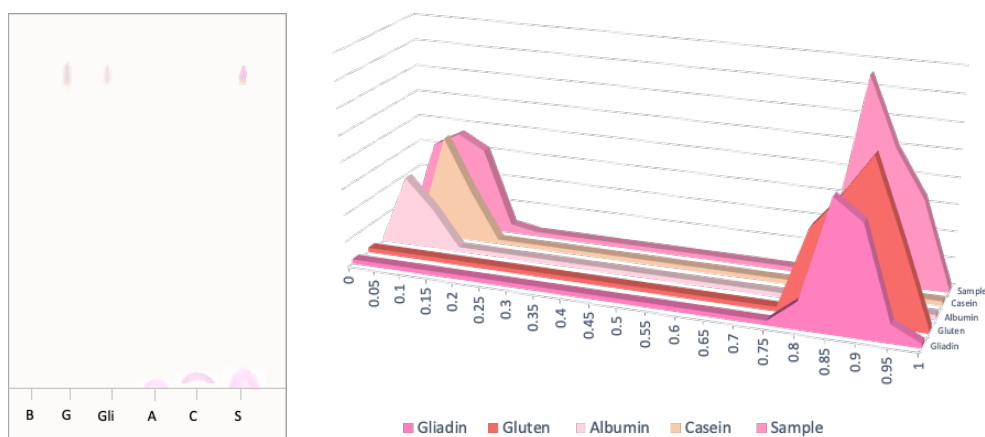
Figure 76 Picture of a HPTLC plate after separation and derivatization of Gluten (G), Gliadin (Gli), Albumin (A) Casein (C) and a Sample or mixture of proteins (S) at a concentration of 1 mg·mL-1 when using optimized conditions and its correspondent chromatogram.

As can be observed a satisfactory separation was achieved, as gluten and gliadins were isolated from casein and albumin. Moreover, suitable separation was obtained when a mixture of proteins was used as sample. In this sense it was concluded that a good separations and detection of gluten and its constituents was achieved using the proposed procedure.

4.3.2.3 Analytical performance

In order to assess the quantitative capacity of the stablished method, spectra for standard concentrations from 2 to 6 mg L^{-1} were measured using different instrumentation. Measurements were performed using a laboratory portable spectrophotometer equipped with a fiber optic probe coupled to smartphone in order to obtain more sensitive and accurate measurements. The derivatized layers were digitalized taking images by using a smartphone. RGB coordinates were obtained from the colored spots after image processing. The registered and the linear curves obtained for the three RGB parameters of the image analysis are shown in Figure 77.
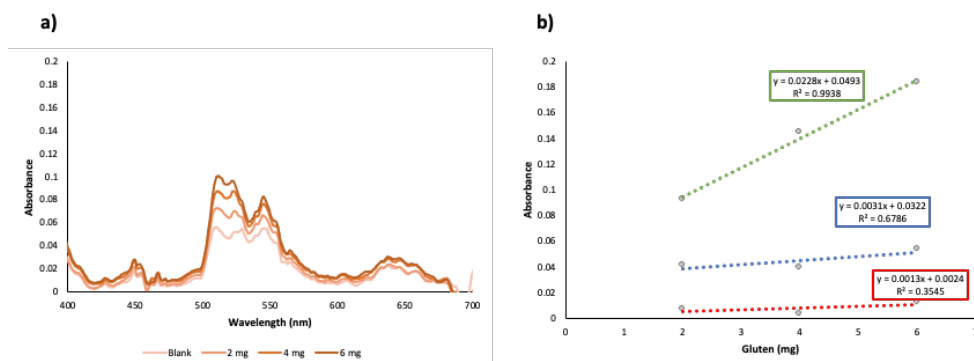
Figure 77 a) Spectra obtained with the smartphone spectrometer coupled to a fiber optic probe for amounts of gluten of 0, 2, 4 and 6 mg. b) Calibration line of the obtained RGB parameters.

Due to the small signals produced on the chromatographic plate, absorbances achieved were relatively low, however, good spectra in terms of shape and suitable sensitivity and linearity were achieved as can be seen in Figure 77. The linear curves for the RGB parameters clearly showed that best results were obtained using the green component. In this sense, the figures of merits of the gluten determination in HPTLC plates by using the tow different approaches are shown in Table 30. The analyte quantification was carried out following the optimized procedure at a wavelength of 510 nm. The limits of detection (LOD) and limits of quantification (LOQ) were calculated as $3s_{yx}/b_1$ and $10s_{yx}/b_1$, respectively, where s_{yx} and b1 are the standard deviation and the slope of the regression, respectively. Linearity range, sensitivity and precision of the methods were evaluated.

Table 30 Figures of merit for the studied method using smartphone spectrometer coupled to a fiber optic probe and smartphone captured image processing.

	Smartphone Spectrometer	RGB
a ± sa	0.0075 ± 0.0003	0.049 ± 0.008
b ± sb (mg^{-1})	0.056 ± 0.0012	0.023 ± 0.002
R^2	0.996	0.994
LOD (mg·mL^{-1})	0.5	0.57
LOQ (mg·mL^{-1})	1.66	1.89
RSD (%)	4.25	4.83

As can be seen in the table 30, good correlations and appropriated detection and quantification limits were obtained when using portable instrumentation equipped with the fiber optic probe. When using the processed images from the smartphone, the G (Green) component also provided a good correlation and the obtained analytical parameters (LODs and LQDs) were suitable for the analysis of gluten in surfaces. The proposed gluten determination strategy can be considered a screening method that provides a binary response using the LOD as cut-off value where positive responses would be indicated by the coloration of the spots at the studied Rf = 0.85.

4.3.2.4 Application to real samples

The application of the proposed test was evaluated to estimate gluten cross contamination at different critical point in food industries. The preliminary studies were performed by comparing differences in gluten residue from gluten-free zones and zones where gluten is present. For this aim, sampling was performed by using swabs and following the procedure described in section 3.6.3. Figure 78 shows the estimation of gluten content in both studied zones. As can be seen, the gluten-free point, were below the cut-off value m = 0.125 (LOD), and then, it can be concluded that theses samples were negative (Samples S1-S4 from Figure 78a). However, zones were, gluten was present showed a value higher than 0.25 mg, it meant two times the LOD and hence positive responses (Samples S6 and S7, Figure 78a).
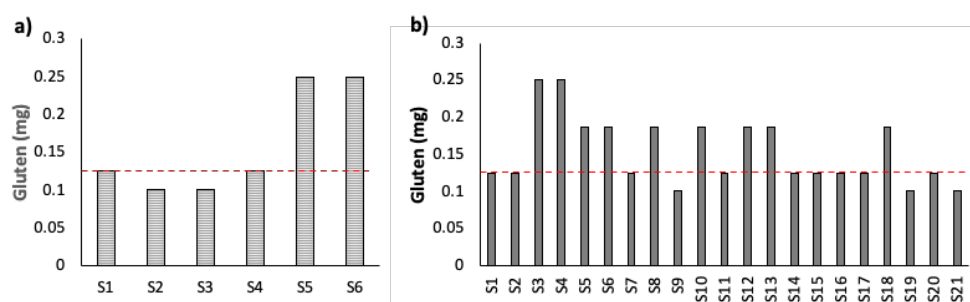
Figure 78 a) Gluten comparison between analyzed simples from a food industry of gluten-free zones (S1-S4) and gluten containing zones (S5-S6) b) Gluten estimation in different samples from critical points at a food industry of different working areas. Cutting and mincing point (S1-S4), filling and extruder machines (S5-S7). Refrigerating and cooling tunnels (S8-S10), conveyor belts (S11-S16) and different devices (S17-S21).

Finally, the propose procedure was used to estimate the presence/absence of gluten at different critical point of the processing chain. Samples from cutting and mincing point (S1-S4), Filling and extruder machines (S5-S7), refrigerating and cooling tunnels (S8-S10), conveyor belts (S11-S16) and different devices (S17-S21) were analysed. As can be seen in Figure 78b, variations in gluten content were obtained as a function of the sampling point. As can be seen, positive responses were estimated in two meat mincers, in two filling machines and in a refrigeration and cooling tunnel. In the case of conveyor belts, positive responses were also obtained in two of the analysed belts. Finally, only in the case of a rough stainless-steel device, gluten was observed above the cut-off limit.

These results demonstrated the potential cross-contamination in the food processing chain by using a simple and cost-effective strategy that allows the estimation by visual inspection and image analysis. Therefore, the making decision process can be performed at real time without the need of laborious analytical procedure and training personal.

4.3.2.5 Conclusions

In this study it has been developed a new sustainable colorimetric method combined with HPTLC for proteins separation and following in place gluten analysis. The colorimetric response obtained was registered by smartphone-supported spectrometric measurements and by digital image obtaining the RGB parameters of processed images for quantitative analysis. The figures of merit: linearity, LODs and LOQs, obtained by using the portable smartphone instrumentation were satisfactory proving this method to be a promising alternative for in place analysis of gluten. In terms of precision RSD values were lower than 5% for both approaches. Furthermore, a screening method that provides a yes/no response using the LOD as cut-off value was proposed to determine glutenin food industries. Samples from surfaces of critical points of food industries have also been tested using the proposed method obtaining satisfactory results.

4.4 ELECTROCHEMICAL SENSING AND PORTABLE VOLTAMMETRY

In this section the development of two electrochemical sensors and the use of different strategies for their fabrication have been studied. First, an electrochemical sensor based on the attachment of a redox active compound as a probe molecule on two different working electrodes was evaluated. In this sense, glassy carbon and boron doped diamond electrode surface were modified via the reduction of a diazonium salt. Further functionalization was carried out using anthraquinone as a probe molecule. The electron transfer kinetics, surface coverage and pK_a of the immobilized anthraquinone for both electrodes were investigated. This investigation is focused on studying the different behaviors of anthraquinone when immobilized on glassy carbon and boron doped diamond in order to build better biosensors. On the other hand, the determination of 2,6-DNT by cyclic voltammetry was also study. In this work a glassy carbon working electrode was modified through the reduction of diazonium salt and subsequent functionalization with 2,6-DNT. Response was measured by cyclic voltammetry using a portable potentiostat. Quantitative analysis was carried out establishing promising limits of detection and quantification and the effect of the pH, electron transfer kinetics and surface coverage were investigated in order to understand the activity of this compound at different concentrations.

4.4.1 Anthraquinone immobilization on carbon-based electrodes

Surface modifications of carbon electrodes are an area of great interest in both fundamental and applied electrochemistry, due to their associated advantages in a variety of applications. In this work it is provided a reliable route for the modification of sp^3 boron-doped diamond through a diazonium reduction and subsequent solid phase synthesis to produce a stable, immobilised layer of surface bound anthraquinone. Immobilization of the anthraquinone on the working electrodes was confirmed by cyclic voltammetry using a portable potentiostat. The electron transfer kinetics, surface coverage, and pK_{a1} of the immobilised anthraquinone was investigated and compared to that for anthraquinone immobilised via an identical synthetic route to sp^2 glassy carbon. The aim of this study was to investigate the influence the underlaying substrate on fundamental chemical and electrochemical properties of immobilized molecules above the substrate surface in order to build better biosensors.

4.4.1.1 Linker attachment and anthraquinone immobilization

The reduction of diazonium is a well-studied method for the functionalisation of many carbon surfaces. The same solid-phase synthetic procedure, in which anthraquinone is tethered to the electrode surface via a diazonium linker, was applied to both the glassy carbon (GC) and boron-doped diamond (BDD) electrodes. When a sufficient negative potential is applied to the electrode surface the diazonium becomes reduced, therefore, a nitrogen radical is formed. This unstable specie leaves in the form N_2 gas, the electrode surface again reduces the aryl radical to promote the formation of a C-C covalent bond between the electrode surface and linker molecule. Accordingly, in the first step, 4-[(N-BOC-aminomethyl) benzene] diazonium tetrafluoroborate was electrochemically reduced at either the GC or BDD electrode surface. The successful reduction of the diazonium salt, and subsequent attachment of the linker was confirmed by cyclic voltammetry (Figure 79). As previously reported by Bartlett and co-workers, it was observed that, on the first scan, GC electrodes displayed a broad peak between -0.25 V and -0.45 V [379], whereas BDD exhibited a sharper reduction peak between potentials -0.2 V and -0.3 V. The irreversible peaks observed on the initial scan for both electrode types correspond to the reduction of the diazonium salt, which leads to its breakdown into gaseous nitrogen and an aryl radical[390,391]. The radical is subsequently reduced onto the electrode surface to form the covalent bond. Subsequent scans are devoid of any comparable reduction, indicating a formation layer that blocks further diazonium reduction at the electrode surface[392].
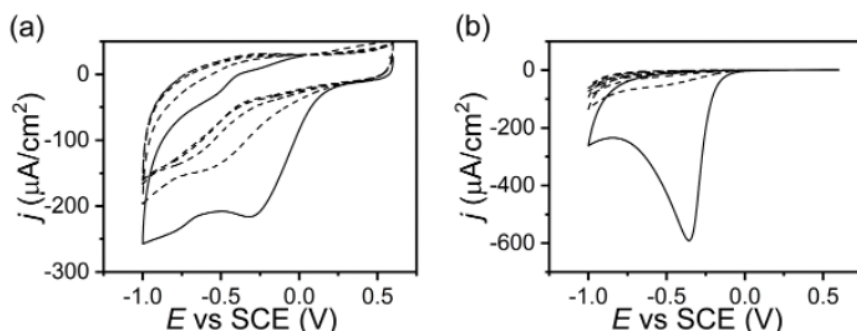
Figure 79 Cyclic voltammogram recorded during the electrografting of 4-[(N-BOC-aminomethyl) benzene] onto (a) GC and (b) BDD electrode surfaces in acetonitrile displaying current density as a function of potential versus SCE at scan rate 0.05 V s^{-1} for 5 scan cycles using a portable potentiostat. The first scan is represented as a solid line and the subsequent scans are dotted lines.

After the electrografting of the BOC protected benzyl amine layer, the BOC protecting group was removed, through the use of hydrochloric acid, and a solid phase synthesis route was employed to attach anthraquinone-2-carboxylic acid to the now deprotected amine, as described in the experimental section. The successful immobilisation of anthraquinone was confirmed by the observation of characteristic oxidation peaks between -0.45 V and -0.55 V for both GC and BDD electrodes (Figure 80). A lower background capacitance is one of the many beneficial properties of BDD when compared to GC[393]. This trend can be significantly observed in Figure 80, where the background current for the BDD modified electrode is substantially lower than the showed by the GC counterpart.
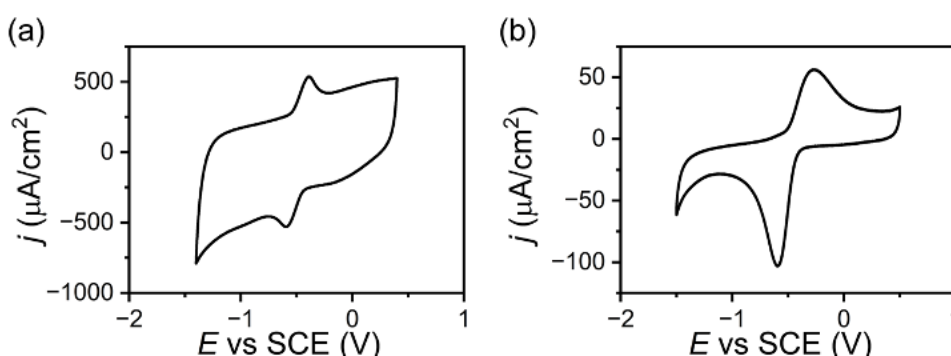
Figure 80 Plot of current density as a function of scan rate of anthraquinone modified (a) GC and (b) BDD electrode in pH 7 PBS versus SCE at 0.5 V s^{-1} using a portable potentiostat.

4.4.1.2 Surface density comparative study for anthraquinone modified electrodes

To determine the surface coverage of the anthraquinone molecule, it was necessary to first determine the electroactive surface area of the electrodes that were used in these experiments. A three-electrode setup was used with the scan rate varied between 0.2 and 2.0 V s^{-1} versus SCE in 0.2 V s^{-1} increments. From a plot of peak current (i_p) versus the square root of scan rate (v), the resulting gradient, along with the Randles–Ševčík Equation (Equation 6), was used to determine the electroactive surface area (A_{sur}) of the electrodes:

$$i_p = 2.69x10^5 n^{\frac{3}{2}} A_{sur} D^{\frac{1}{2}} C v^{\frac{1}{2}}$$

Equation (6)

165

Where i_p is peak current, n is the number of electrons in the process (n=1), A_{sur} is the surface area, D is the diffusion coefficient (7.80 x 10^{-6} cm^2s^{-1}), C is the concentration (C= 0.001 M) and v is the scan rate. In this sense, the average electroactive surface area for GC and BDD were determined to be 0.19 ± 0.05 cm^2 and 0.068 ± 0.003 cm^2 respectively.

The surface coverage of both anthraquinone modified, GC and BDD, electrodes were determined in order to perform a direct comparison. For surface bound redox active molecules of coverage (Γ), the peak current density, of the cathodic peak in this case (j), is known to vary as a function of the scan rate (v) as described by equation 7 [229]:

$$j = \frac{n^2F^2}{4RT}\Gamma v N_A \qquad \textit{(Equation 7)}$$

The surface coverage is determined from the gradient of a plot of j vs v, with the linearity of such a plot confirming the voltammogram peaks arise from surface immobilised redox molecules. Figure 81 shows the relevant plots for GC and BDD, which both show a high degree of linearity, thus confirming the anthraquinone is surface immobilised.
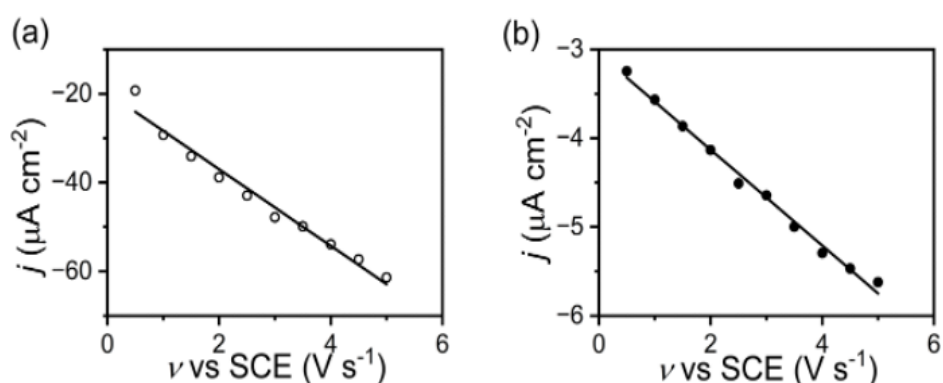
Figure 81 Plot displaying the linear increase of current density as a function of scan rate for anthraquinone modified (a) GC (O) and (b) BDD (●) electrodes in pH 7 PBS buffer versus SCE.

The calculated surface densities of GC modified electrodes ($1.9 \pm 0.7 \times 10^{13}$ molecules·cm^{-2}) was nearly double that of BDD ($0.92 \pm 0.4 \times 10^{13}$ molecules·cm^{-2}), despite an identical synthetic procedure. These differences suggest that either the electrografting step, or the subsequent solid-phase EDC-based coupling reaction, are less efficient on BDD in comparison to GC.

4.4.1.3 Electron transfer comparative study for anthraquinone modified electrodes

The electron transfer kinetics of anthraquinone immobilised at GC and BDD interfaces were determined using the well-known Laviron procedure, in which the overpotential for cathodic and anodic processes are recorded as a function of scan rate[394]. Where the electron transfer is irreversible (i.e., at scan rates > 0.1 V) both α and k_{ET} can be extracted from the anodic branch:

$$E_0 = E_{Ox} - \frac{RT}{\alpha nF}\left(\ln\left(\frac{\alpha nFv}{RTk_{ET}}\right)\right) \qquad \textit{(Equation 8)}$$

And similarly, k_{ET} can be extracted from the cathodic branch using (1-α):

$$E_0 = E_{Red} - \frac{RT}{(1-\alpha)nF}\left(\ln\left(\frac{(1-\alpha)nFv}{RTk_{ET}}\right)\right) \qquad \textit{(Equation9)}$$

Figure 82 shows the Laviron plots for anthraquinone modified GC and BDD electrodes, where the potential shift from the resting potential is measured as the scan rate is varied, from low to high, in order to discern the electron transfer kinetics of these species.
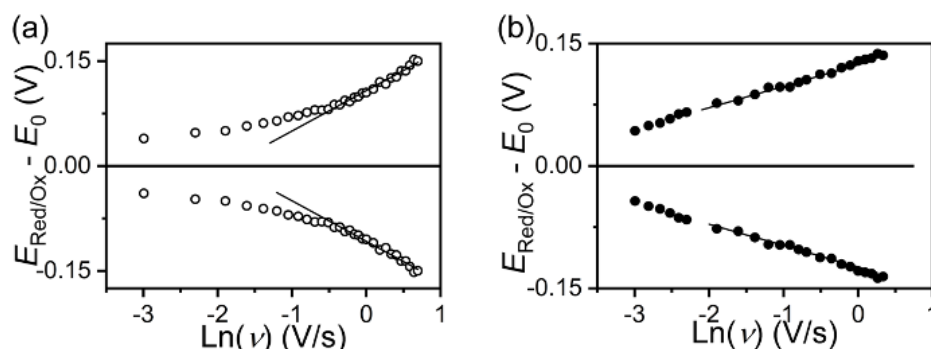
Figure 82 Plot of potential shift from midpoint versus the natural log of scan rate for anthraquinone-modified (a) GC and (b) BDD versus SCE in pH 7 PBS. The upper line represents the anodic peak shift and the lower line represents the cathodic peak shift.

For anthraquinone immobilised on a GC electrode, electron transfer coefficient (α) values of 0.34 and 0.66 were obtained for anodic and cathodic processes respectively, with an average electron transfer rate constant of 0.95 s^{-1}. This value is consistent with similar studies for anthraquinone immobilised GC electrodes, where an electron transfer rate of 1.47 s^{-1} has been reported[379].

For anthraquinone immobilised on a BDD electrode, α values of 0.46 (anodic) and 0.54 (cathodic) were obtained, and the average k_{ET} was determined to be 0.29 s^{-1}. To the best of our knowledge, the electron transfer kinetics for anthraquinone grafted on top of a sp^3 interface has not previously been reported. A reduced rate of electron transfer at BDD relative to other electrode materials has previously been observed for simple one electron transfer processes by Tan et al.[395] and is attributed to the relative lower number of charge carriers in BDD relative to more conductive electrode materials. The reported lower electron transfer kinetics for anthraquinone immobilised at BDD relative to GC are consistent with this observation.

4.4.1.4 Comparative study of pK$_a$ of the immobilised anthraquinone

It was found that the reduction and oxidation peaks of immobilised anthraquinone shift as a function of pH for both electrode types. Distinct profiles for 2e$^-$/2H$^+$ and 2e$^-$/1H$^+$ transfer events are indicated by a shift in peak potential of 59 mV/pH unit and 30 mV/pH unit, respectively.

From previous studies, anthraquinone, and its-closely related aqueous soluble counterpart anthraquinone sulfonate, are known to have two acid dissociation constants (K_a) values[396,397]. Since the second K_a value is very large, the first dissociation constant, K_{a1}, can be determined from a non-linear fitting of midpoint potential of the anthraquinone oxidation and reduction as a function of pH using the following equation[397–399]:

$$E_{mid} = E_0 + \frac{RT}{2F}\ln([H^+]^2 + K_{a1}[H^+])$$

(Equation 10)

This equation can be fitted to a plot of midpoint potential vs. pH, thus Figure 83 shows the plot for the anthraquinone surface modified GC and BDD electrodes.
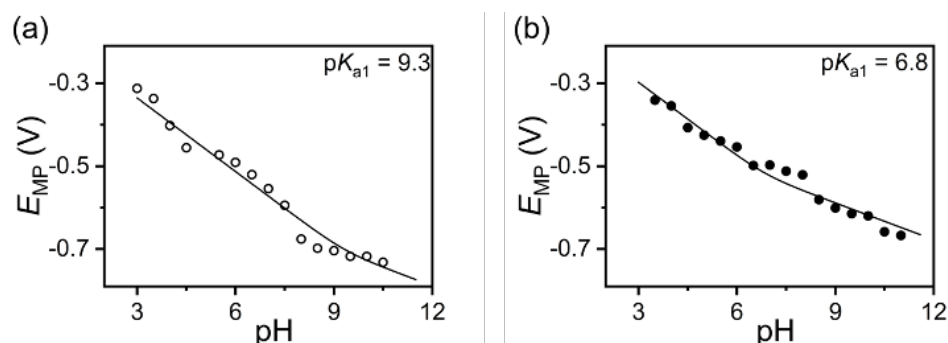
Figure 83 Plot of midpoint peak potential as a function of changing pH for anthraquinone surface modified (a) GC and (b) BDD electrodes versus SCE at 0.05 V s-1, with pKa1 values calculated from Eq. 10 displayed. Data points are from measurement of two separate electrodes.

Anthraquinone modified GC electrodes have been extensively studied and display pK_{a1} values that range from 9.36 to 10.6 depending on the method of immobilisation and linker used[396,397]. The obtained results are consistent with this range, and, immobilising anthraquinone onto GC with the proposed method, an apparent pK_{a1} of 9.3 is observed, while, for anthraquinone immobilised at a BDD electrode the pK_{a1} value was found to be 6.8.

In order to compare the surface immobilised anthraquinone species, with the species in aqueous solution, the pK_{a1} of the aqueous solution based anthraquinone-2-sulfonate (AQ-2-MS) was determined using both the GC and BBD electrodes without surface modification. The plots for the anthraquinone-2-sulfonate in solution for GC and BDD electrodes can be observed in Figure 84.
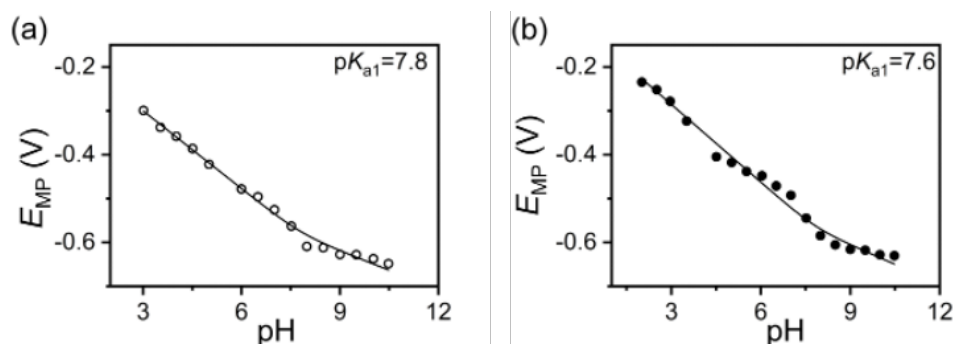
Figure 84 Plot of midpoint peak potential as a function of changing pH for anthraquinone-2-sulfonate in solution (100μM) for unmodified (a) GC and (b) BDD electrodes versus SCE at 0.05 V s-1, with pK^{a1} values calculated from Eq. 10 displayed. Data points are from measurement of two separate electrodes.

Values were found to be 7.8 and 7.6 for GC and BDD, respectively. This can confirm that for diffusing species, the apparent pK_{a1} is independent of the type of carbon substrate used. It was observed that anthraquinone immobilised on GC is reported to exhibit a pK_{a1} substantially more basic than for the analogous anthraquinone sulfonate diffusing freely in solution. In contrast, a shift to more acidic values was observed for the BDD electrode compared to the freely diffusing anthraquinone-sulfonate species. Thus, while anthraquinone becomes a substantially weaker acid when confined to a GC surface, it becomes a slightly stronger acid when confined to BDD, compared to the solution-based species. The reason for such a substantial discrepancy in apparent pK_{a1} values for the same molecule, attached using the same linker when using these two different carbon types, is unclear, but likely arise due to differences in solvent ordering and disordering at glassy carbon and diamond interfaces.

A similar hypothesis was forwarded by Compton and co-workers to explain differences in pK_a for molecules adsorbed at either glassy carbon or graphite interfaces[400] as well as to carbon nanotubes of differing morphologies[401]. In these works, the authors propose that shifts in pK_a upon immobilisation arise from the

differences in the hydrophobicity or hydrophilicity of different interfaces, which either facilitating or impeding the formation of the solvent shell near the surface. In this sense the results here presented can be added to the few examples previously reported describing a shift in pK_a values upon immobilization compared to the solution-based counterpart.

4.4.1.5 Conclusions

A reliable route has been proposed for the consistent surface modification of glassy carbon and boron-doped diamond electrodes through the reduction of an aryl diazonium linker followed by a cross coupled immobilisation of anthraquinone. The immobilisation procedure can be applied identically to both electrode types, permitting an investigation of how the underlying substrate affects the proton coupled electron transfer (PCET) of surface-grafted molecule. Anthraquinone immobilisation on the electrochemical sensors was confirmed by portable cyclic voltammetry. This demonstrates that although portable instrumentation is usually selected for in field analysis it can also be used for laboratory measurements. Additionally, anthraquinone grafted onto glassy carbon and boron-doped diamond interfaces using identical procedures was shown to have different surface densities, apparent pK_{a1} values and electron transfer kinetics. The obtained results highlight the need for caution when immobilising redox molecules to sp^3 surfaces using established surface modification routes for sp^2 interfaces, as it has been proved that the fundamental chemical and electrochemical properties of the attached molecules are highly dependent on the underlying substrate. Thus, the proposed study will provide the means to aid the development of better biosensors, this, together with the implementation of portable devices can involve significant advantages in order to carry out future in situ analysis.

4.4.2 Determination of 2,6-DNT using portable cyclic voltammetry

In this study, the electrochemical detection of the 2,6-Dinitrotoluene (DNT) using glassy carbon electrodes was investigated. Glassy carbon electrode was covalently modified through the electrographting of a diazonium salt, allowing the 2,6-DNT to be immobilized onto the surface of the electrode. The immobilisation of 2,6-DNT without the surface modification was also evaluated. Experiments were

performed to investigate the redox activity of the immobilised 2,6-DNT using a portable potentiostat to perform cyclic voltammetry measurements. Limits of detection for DNT immobilised on GC for both, modified and unmodified electrodes were obtained. The surface density and the pH effect on the potential of the cyclic voltammetry measurements were investigated. Electron transfer kinetics were also determined in order to verify the mechanism of the redox reaction. All these studies will provide the means to aid the development of a novel, rapid, sensitive and cost-effective detection device that can accurately detect the presence of 2,6-DNT.

4.4.2.1 Cyclic voltammetry of 2,6-DNT immobilised glassy carbon electrodes

The immobilisation of 2,6-DNT was evaluated with and without the surface modification via electrochemical reduction of a diazonium salt. Both mechanisms were studied and compared to investigate the redox activity of the 2,6-DNT molecules immobilized on Glassy Carbon surfaces.

4.4.2.1.1 Unmodified glassy carbon electrodes

Initially, the 2,6-DNT was successfully immobilised onto the surface of the clean GC electrode. Since the surface of the GC electrode exhibits almost purely sp^2 hybridized character, the π electrons on the surface form a strong π-π interaction to the delocalised π electrons in the aromatic ring of the DNT molecule[234,402]. The immobilisation on the electrode surface was confirmed by cyclic voltammetry using a portable potentiostat.

Figure 85 shows a cyclic voltammogram performed in aqueous phosphate buffer (10 mM, pH 7), indicating the presence of the compound. One large cathodic peak, at -0.9 V, on the 1st scan and two well-defined anodic and cathodic peaks, at -0.2 V, on all subsequent scans were observed. The reaction which occurs during the 1st scan corresponds to the irreversible reduction of the two nitro groups (NO_2) of the 2,6-DNT to nitroso groups (NO). The redox event which occurs during all subsequent scans indicates the reversible redox reaction of the nitroso groups (NO) to hydroxylamine groups (NHOH) and back to the nitroso group.
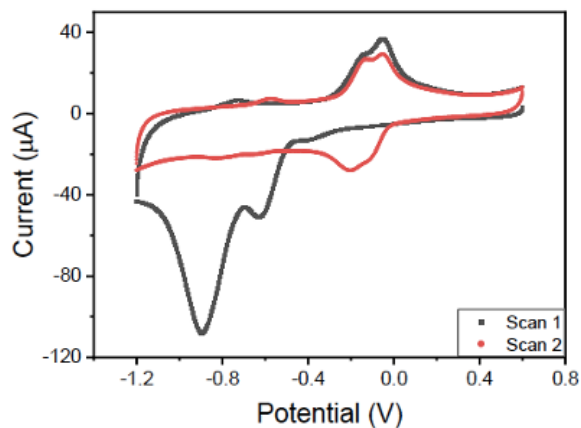
Figure 85 Cyclic voltammogram of the initial irreversible (scan 1) reduction peak and the subsequent reversible (scan 2) redox peaks of the DNT immobilised onto the glassy carbon electrode at a scan rate of 0.05 V/s in 10 mM phosphate buffer (pH 7).

A control cyclic voltammogram of a GC which was manually and electrochemically cleaned was obtained, in aqueous phosphate buffer, to confirm that the peaks present were due to the presence of DNT, and not impurities in solution or on the electrode surface. This was compared with the voltammogram of the 1st scan from the DNT immobilised GC electrode. The control exhibited no new peaks, therefore proving that the presence of the peaks was due to the DNT that had been immobilised onto the surface of the GC electrode (Figure 86).
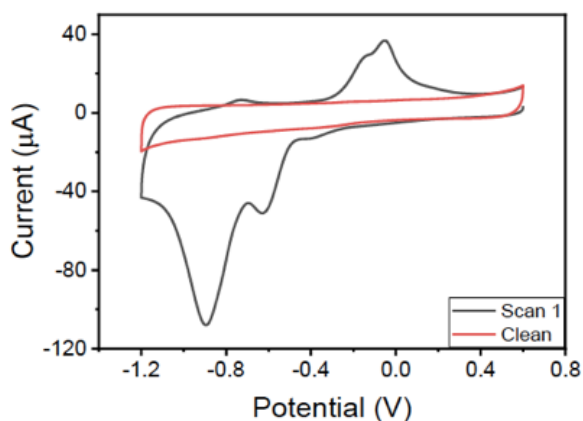
Figure 86 Stacked cyclic voltammograms of the 1st scan of a DNT immobilised GC electrode (black) and a clean GC electrode (red) in aqueous phosphate buffer (10 mM, pH 7)

4.4.2.1.2 Modified glassy carbon electrodes

Further studies involving surface modification in order to improve the detection of DNT on GC surfaces were carried out. Following the mechanisms previously studied in this thesis, the covalent bonding of the 4-[(N-Boc) aminobenzene] diazonium salt via electrochemical reduction procedure was performed. The successful attachment of the linker to the surface of the electrode was observed by the presence of a broad reduction peak in the region of -0.25 V and -0.8 V. (Figure 87).
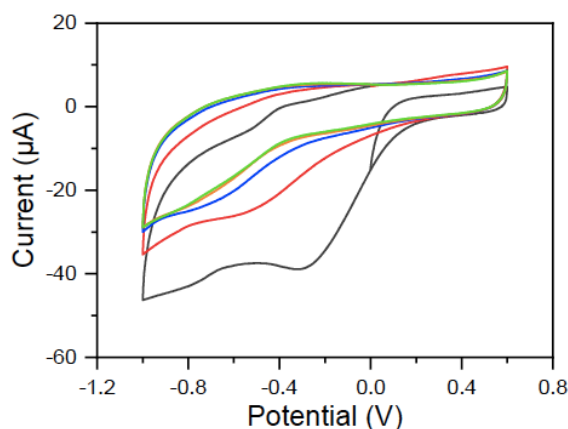
Figure 87 Electrochemical grafting of 4-[(N-Boc) aminobenzene] diazonium on to the surface of a glassy carbon electrode recorded between 0.6 V and -1.0 V versus SCE at 0.05 V/s for 5 cycles.

The presence of the cathodic peak corresponds to the irreversible reduction diazonium salt and formation of the aryl radical, which subsequently reacts with the surface of the electrode to form the covalent bond. Following reduction peaks are significantly decreased indicating that almost all of the electroactive sites at the electrode surface are filled by the linker covalently tethered to the surface.

The Boc protecting group was removed suspending the modified electrode in a HCl (4.0 M) in 1,4-dioxane solution for 4 hours. The deprotection step was required so the DNT could then immobilise onto the surface. Following the suspension of the electrode in the DNT solution overnight, a cyclic voltammogram, performed in aqueous phosphate buffer (10 mM, pH 7), indicated the presenceof the compound. Figure 88 shows voltammograms of the 1st scan of the detection of DNT for the unmodified and the modified electrodes.
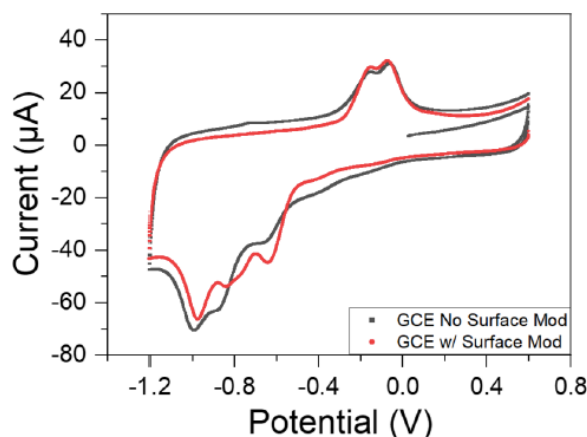
Figure 88 Stacked cyclic voltammograms of the 1st scan of DNT Detection for the unmodified (black) and modified (red) GC electrodes at a scan rate of 0.05 V/s in 10 mM phosphate buffer (pH 7).

The voltammogram observed for the modified electrode are consistent with the voltammogram obtained for the DNT on the unmodified surface, confirming DNT was present. The peak potentials of the irreversible and reversible reactions were similar to unmodified surface, with slight differences in magnitude. This indicates that the initial reduction, and subsequent redox reactions, were not altered by the surface modification, but have possibly been improved in some way.

4.4.2.2 Study of the response with the concentration of 2,6-DNT

In order to assess the quantitative capacity of the proposed glassy carbon electrodes, concentrations from 1 mM to $1\cdot10^{-9}$ mM were measured via cyclic voltammetry. Measurements were performed using a portable potentiostat. The quantitative study was carried out for both, unmodified and surface modified glassy carbon electrodes. The currents for the oxidation peaks of the redox reaction were used to determine the detection of 2,6-DNT. Figure 89 shows the plot of the natural logarithm of the concentration(mM) versus the oxidation peak current (μA) for both electrodes.
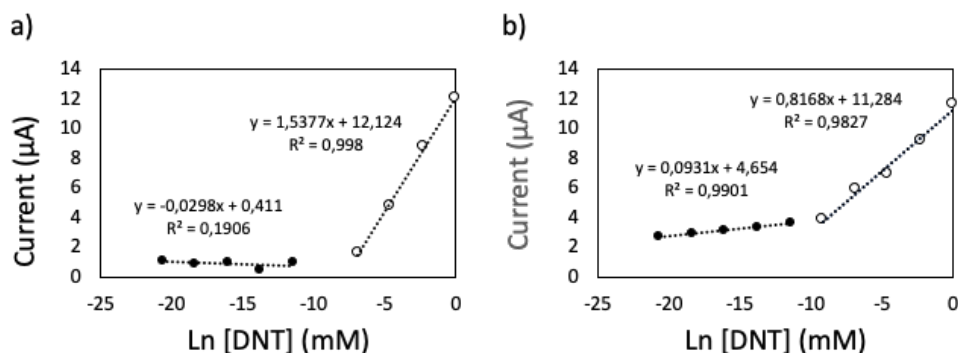
Figure 89 Plot of natural logarithm of concentration (mM) of 2,6-DNT solution vs oxidation peak current (µA) for 2,6-DNT immobilized on a glassy carbon electrode in aqueous phosphate buffer for a) Unmodified surface b) Modified surface.

Comparing both plots, it was observed that unmodified surface electrodes presented a higher sensitivity between 1 mM and $1·10^{-4}$ mM, but no further concentrations of DNT were able to be detected from $1·10^{-5}$ mM. On the other hand, surface modified glassy carbon electrodes presented a lower sensitivity in the first range of concentrations, however lower concentrations were able to be detected between $1·10^{-5}$ mM and $1·10^{-9}$ mM. In this sense, the limit of detection (LOD) was calculated for both electrodes.

As can be seen in Figure 89, peak current shows a linear response with the natural logarithm of the concentrations. The traditional calculation of LOD= $3·s_{xy}/b_1$ could not be used in this case because of the use of the natural logarithms. In this sense, in order to calculate the limit of detection the whole equation needed to be rearranged. Thus, the limit of detection (LOD) was calculated as described in equation 11.

$$LOD = ts_x = \frac{1}{b} e^{\frac{y-a}{b}} \left[s_y^2 + s_a^2 + \left(\frac{y-a}{b}\right)^2 s_b^2 \right]^{1/2} \qquad \textit{(Equation11)}$$

Where *t* is the t of student value dependent of each study, *a* and *b* are the intercept and the slope respectively, s_a and s_b were the standard deviation of the intercept and the slope, *y* is the mean of the lowest concentration of the calibration curve (the blank can also be used) and s_y was the standard deviation of *y*. The figures of merit are shown in Table 31. Linearity range and sensitivity of the methods were evaluated.

Table 31 Figures of merit for the 2,6-DNT determination for modified and unmodified GC electrodes.

Immobilisation	Intercept (a±s$_a$)	Slope (b±s$_b$)	R^2	Linearity range (µM)	LODs (µM)
Unmodified	12.1 ± 0.2	1.54 ± 0.05	0.99	3.1-1000	0.95
Modified	11.3 ± 0.4	0.82 ± 0.06	0.98	1.2-1000	0.35
Modified	4.65 ± 0.09	0.097 ± 0.008	0.99	0.018-10 nM	$5.55 \cdot 10^{-6}$

As can be observed in Table 31, good linearities were observed in all cases. In terms of sensitivities lower limits of detection sensitivities were achieved when modifying the surface of glassy carbon electrodes for the immobilisation of 2,6-DNT. Moreover, it was observed that when working at very low concentrations, outstanding sensitivities were achieved working with the modified glassy carbon surfaces as LOD of 5.55 pM was obtained.

In this sense, it was proved that increased interactions were displayed between the attached 2,6-DNT and the glassy carbon substrate. In light of these results, further experiments were performed in order to investigate the chemical an electrochemical properties of the redox-active species involved in these interactions.

4.4.2.3 Surface density study for 2,6-DNT modified glassy carbon electrodes

The surface coverage for the modified glassy carbon electrode was determined in order to perform a direct comparison between the two different linear ranges. For surface bound redox active molecules of coverage (Γ), the peak current density, of the cathodic peak is known to vary as a function of the scan rate as previously described in previous studies of this Thesis (Equation 7).

The surface coverage was determined from the gradient of a plot of the peak current density versus the scan rate (Figure 90). A linear response in this plot for both working ranges confirmed that the response in the voltammogram peaks was obtained from surface immobilised redox molecules.
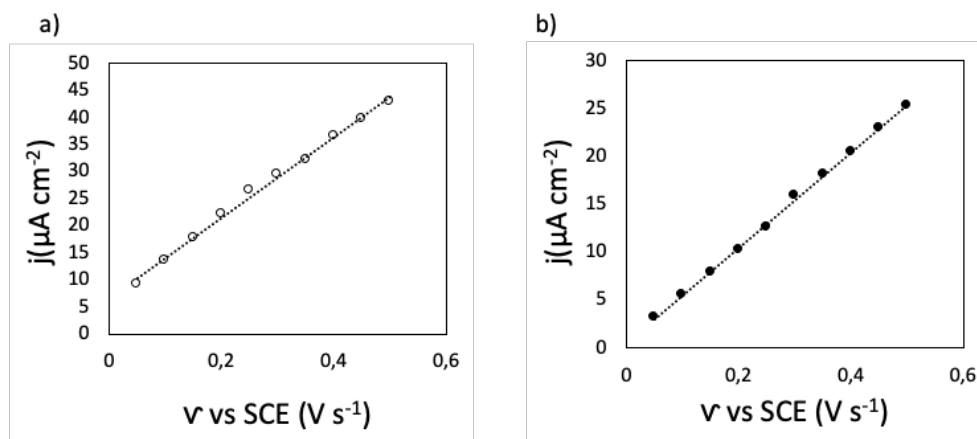
Figure 90 Plot displaying the linear increase of current density as a function of the scan rate for modified GC for two concentrations of both different working range a) 2,6-DNT 0.1 mM b) 2,6-DNT $1 \cdot 10^{-7}$ mM.

The surface coverage was calculated from the slope of the plots of the peak current density versus the scan rate for each concentration. The surface coverage was determined as describes Equation 12:

$$\Gamma = \frac{m4RT}{A_{sur}n^2F^2} N_A \qquad (Equation\ 12)$$

Where m is the slope from the plot, R is the universal gas constant (8.312 J K^{-1} mol^{-1}), T is the room temperature (298K), N_A is the Avogadro's number (6,022 10^{23} mol^{-1}), A_{sur} is the electroactive active surface of the electrode, n is the number of electrons involved in the process (n=4) and F is the Faraday's constant (96485 C mol^{-1}).

In order to understand the behavior of the redox-active species in our system in both working ranges, the plot of the surface coverage as a function of the natural logarithm of the concentration of 2,6-DNT was represented (Figure 91).

178
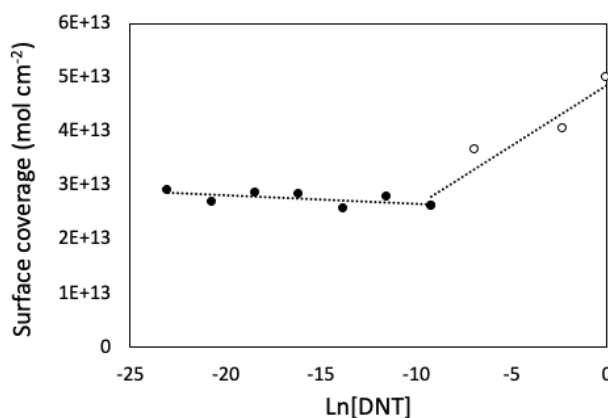
Figure 91 Plot displaying the Surface coverage as a function of the natural logarithm of 2,6-DNT concentration for a surface modified glassy carbon electron.

A linear decrease of the surface coverage was observed in the first working range (from 1 to $1 \cdot 10^{-5}$ mM) as a function of the concentration. On the other hand, in the lower concentration working range (from $1 \cdot 10^{-5}$ to $1 \cdot 10^{-9}$ mM) it was observed that the surface coverage remained constant. This together with the results obtained studying the response of the modified glassy carbon electrode confirm that at higher concentrations the response showed a linear decrease as a function of the reduction of the concentrations, since, the lower the concentration of DNT the lower the molecules attached to the surface and thus, a lower response is obtained. However, as can be seen in Figure 91 at the low concentration range a different behavior is observed, demonstrating that the decrease of the response at these concentrations is not a matter of the number of the molecules attached to the surface. This, may suggest that the signal observed at the low concentration range, although is related to the presence of 2,6-DNT, is not caused directly by the reversible reduction of the NO groups as previously commented.

4.4.2.3 Study of the proton coupled electron transfer events

In order to understand better the mechanism of the reaction when working at lower concentrations, the effect of the pH on the redox reaction of 2,6-DNT was studied. To carry out this investigation, the immobilised DNT on the modified GC electrode was evaluated in a variety of pH values. As previously mentioned, DNT has a four-proton/four-electron reversible redox reaction in which the nitroso groups are reduced to hydroxylamine and oxidized back to nitroso groups[403]. This process is the one observed at the high concentration working range.

The reversible redox reaction was investigated in order to fully understand the redox reaction as function of the concentration of 2,6-DNT. Cyclic voltammograms of the immobilised DNT on the modified GC electrode were ran in aqueous phosphate buffers (10 mM) of pH values ranging from 3 to 12 with increments of 1 pH unit. The midpoint peak potential for each pH value was recorded and analysed to show the change in the potential as a function of pH. The midpoint peak potential was determined as the potential halfway between the oxidation and the reduction peaks. Figure 92 shows the relationship between the midpoint peak potential and the pH.
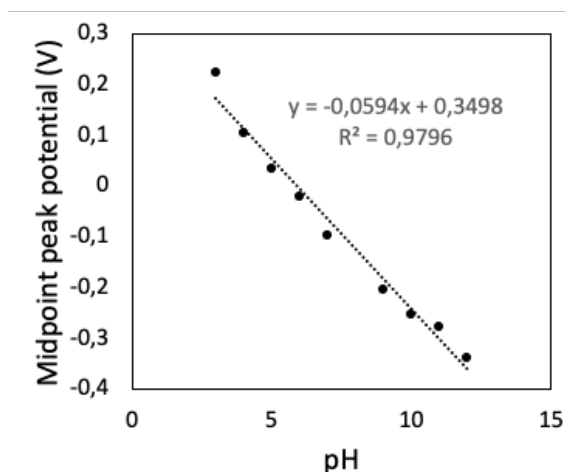
Figure 92 Plot of the midpoint peak potential (E_0) vs pH at 0.05 V s^{-1} vs SCE for 2,6-DNT immobilised modified glassy carbon electrode in aqueous phosphate buffer.

It was observed that when working in the lower concentration range there was a linear response between the midpoint and the pH variations which slope was 59 mV per pH unit.

The Nernst equation predicts how the reaction quotient affects the measured cell potential. It can be derived to utilise the pH to predict the proton coupled electron transfer involved in a redox reaction. In this sense, the slope determined for the low concentration working range, which has a value of 59 mV/pH corresponded to a two-electron/two-proton process. These results are consistent with the obtained in the response and the surface density studies, which

suggest that two different processes were taking place as function of the DNT concentration.

4.4.2.4 Electron transfer kinetics of the modified glassy carbon electrodes

The electron transfer kinetics of 2,6-DNT immobilised on modified glassy carbon were determined using the well-known Laviron procedure, previously described in this Thesis, in which the overpotential for cathodic and anodic processes are recorded as a function of scan rate. Figure 93 shows the Laviron plots for the 2,6-DNT modified GC electrodes, for both working concentration ranges, where the potential shift from the resting potential is measured as the scan rate is varied, from low to high, in order to discern the electron transfer kinetics of these species.
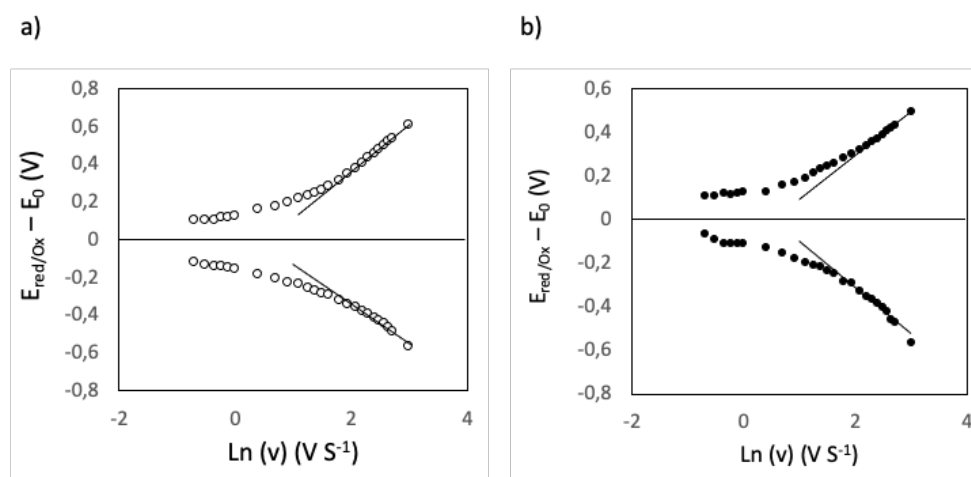
Figure 93 Plot of potential shift from midpoint versus the natural log of scan rate for 2,6-DNT-modified (a) High concentration work range (b) Low concentration working range versus SCE in pH 7 PBS. The upper line represents the anodic peak shift and the lower line represents the cathodic peak shift.

From the analysis of the plot, the k_{ET} values for all the concentrations were calculated as previously described in this thesis (Equations 8 and 9). In light of the results obtained in the proton coupled electron transfer events study, K_{ET} was calculated for n = 4 electrons for the concentrations from the high concentration working range, on the other hand for concentration from the lower concentration range a number of n = 2 electrons was considered. Figure 94 shows the plot of the calculated k_{ET} as a function of the normal logarithm of the concentration of 2,6-DNT.

181
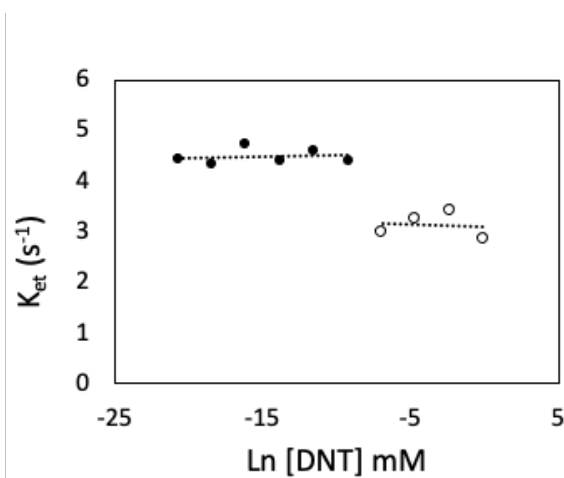
Figure 94 Plot display of the K_{ET} values as function of the normal Log of the 2,6-DNT concentration for the surface modified glassy carbon electrodes.

As can be seen in Figure 94 two different processes can be observed one more time for the two working concentration ranges. This clearly demonstrate that, although the presence of 2,6-DNT produces a linear response that permit the detection of this molecules at very low limits of detection, the reaction involved is not the well-studied reversible reduction of the nitro group into hydroxylamine groups. The redox reaction taking place when 2,6-DNT is immobilised on a surface modified glassy carbon electrode using a diazonium salt as a linker is unclear, but likely arise due some kind of influence of the 2,6-DNT over the aryl diazonium salt which interacts with the glassy carbon substrate.

4.4.2.5 Conclusion

The successful immobilisation of 2,6-DNT onto the surface of a GC electrode was demonstrated for both unmodified and modified glassy carbon surfaces. Both electrodes have shown good linearities and sensitivities, however higher sensitivity has been achieved when using modified glassy carbon electrodes, obtaining outstanding LOD. Besides, it has been proved the presence of two different processes taking place as a function of the concentration of 2,6-DNT. The observed differences have been demonstrated by the study of the surface density, the electron coupled electron transfer events and the transfer kinetics of the 2,6-DNT surface modified glassy carbon electrodes. Moreover, all the sensor preparation processes and the quantitative analysis have been performed by cyclic

voltammetry using a portable potentiostat. Thus, in this study the development of a novel, rapid, ultrasensitive and cost-effective device for the in-situ determination of 2,6-DNT at the level of traces has been satisfactorily demonstrated.

CHAPTER 5. CONCLUSIONS

The present Thesis is focused on the evaluation of several portable devices from different techniques and the development of new strategies in order to enhance the portability, greeness and sustainability in analytical chemistry. The proposed methodologies have been based on the control of experimental and measurement conditions in order to perform more accurate in situ analysis.

In this sense, the analytical methodologies developed in this Thesis, using portable instrumentation, have been aimed at four different research lines:

1. Optimization and measurement validation when using smartphones.
2. Development and measurement of colorimetric sensors.
3. Combination of HPTLC with colorimetric detection.
4. Investigation of electrochemical carbon-based sensors.

The analytical information given by several instruments has been compared from an analytical and a green and sustainable point of view in order to evaluate portable instrumentation including smartphones. One of the most important aspects of working with smartphones is the control of experimental and measurement conditions. To this purpose, measurement conditions such as mobile phone model and sample size and position were optimized and some rules were stablished using a 45-color palette as the validation set. Suitable results were achieved indicating that smartphones are a suitable and a more sustainable alternative for in situ analysis.

Another key aspect when working with smartphones is to control the influence of light. In this sense, several light sources such as halogen, LED and daylight were evaluated in order to improve the results provided by smartphones. Spectral and image color analysis were carried out using a light box to control the incident light, and a set of 45 colors and a color correction palette as the validation set. The color correction palette was also used to perform image processing to obtain more realistic colors when performing image analysis. Results obtained for spectral analysis were slightly better when using a halogen lamp, however, for RGB coordinates analysis better results were obtained with LED light. The choice of a specific RGB color co-ordinate was also studied observing that best results were obtained when the selected RGB parameter was the closer to the complementary color of the tone of the analyzed color. In this sense it was concluded that the adequacy of the light would be evaluated depending on the demanding

information. Furthermore, image processing was also proved to be a remarkable tool to enhance the performance of color analysis.

Another approach studied in this Thesis is the development of colorimetric devices for in situ analysis and their following measurement using the validated strategies. The potential application of NQS-doped PDMS-based sensors to determine both NH4+ in water samples and urea in urine samples has been evaluated. The sensing device showed good precision (RSD < 8%), satisfactory stability, and promising versatility when analyzing different wastewater samples and different human urines. The colorimetric response obtained was registered by conventional diffuse reflectance measurements as a reference and smartphone-supported measurements for quantitative analysis. In both cases, satisfactory results were obtained and showed good concordance. Hence, the results obtained broaden the application of the NQS-based sensor to analyze amino groups present in biological matrices, such as urine, in addition to water matrices demonstrating also the suitability of smartphone devices for performing colorimetric analysis of solid sensors.

The developed strategies were also tested analyzing sensors of multiple colors, covering. different spectral ranges. Solid sensors supported in different materials like PDMS, paper and nylon and a delivery sensor to perform measurements in solution were used to validate the proposed approaches. The smartphone spectrometer coupled to a fiber optic probe was stablished as the better option to carry out colorimetric analysis with smartphone instrumentation using a halogen light source. On the other hand, for image analysis, the use of LED light followed by image processing was proved to provide the best results. Custom-designed apps where also tested showing promising results. These apps enable the obtention of the desired concentration of the target in real time facilitating the decision making in on site measurements. All these observed qualities, together with the inherent characteristics of smartphones such as portability computing power, high memory and good connectivity have proved smartphones as a remarkable tool for in situ analysis.

HPTLC is a very useful technique that can be used to separate analytes in complex matrices. In this sense, a new sustainable colorimetric method combined with HPTLC for sugars separation was developed. The colorimetric response obtained was registered smartphone-supported spectrometric measurements for

quantitative analysis. The figures of merit: linearity, LODs and LQDs, obtained by using the portable smartphone spectrometer coupled to a fiber optic probe were satisfactory achieving LOD at the level of traces. The potential application of the reported method was demonstrated determining lactose in milk samples and in lactose-free milk samples. Good results were obtained in terms of precision and accuracy with RSD values lower than 9% and an average recovery of 101.74 % respectively. Samples from surfaces of critical points of food industries and effluent water samples from dairy industries were also tested obtaining suitable results.

A protein separation method combining HPTLC with smartphone-based colorimetric detection for the in-place analysis of gluten was also developed. The figures of merit: linearity, LODs, LOQs and RSD, obtained by using the portable smartphone instrumentation were satisfactory. Furthermore, a screening method that provides a yes/no response using the LOD as cut-off value was proposed to determine gluten in food industries. Samples from surfaces of critical points of food industries were tested using the proposed method obtaining promising results. These approaches have demonstrated that the combination of HPTLC with smartphone-based colorimetric detection can be a significant option in order to perform in place and in situ analysis of complex matrices.

The use of portable instrumentation in electrochemistry has also been evaluated. Surface modification is an issue of vital importance when performing electrochemical analysis. It has been demonstrated that surface modification of working electrodes can be a remarkable tool to get enhanced selectivity and sensitivity. In this Thesis, a reliable route has been proposed for the consistent surface modification of glassy carbon and boron-doped diamond electrodes through the reduction of an aryl diazonium linker followed by a cross coupled immobilisation of anthraquinone. Surface modification and anthraquinone immobilisation on the electrochemical sensors was confirmed by cyclic voltammetry using a portable potentiostat. This demonstrated that although portable instrumentation can be usually selected for in field analysis, it can also be used for laboratory measurements. Additionally, anthraquinone grafted onto glassy carbon and boron-doped diamond interfaces using identical procedures was shown to have different surface densities, apparent pKa1 values and electron transfer kinetics. The obtained results highlighted that the fundamental chemical and electrochemical properties of the attached molecules are highly dependent on

the underlying substrate, providing the means to aid the development of better biosensors.

The successful immobilisation of 2,6-DNT onto the surface of a glassy carbon electrode was demonstrated for both unmodified and modified glassy carbon surfaces. Both electrodes showed good linearities and sensitivities, however higher sensitivity were achieved when using modified glassy carbon electrodes, obtaining outstanding LOD. Besides, it was proved the presence of two different processes taking place as a function of the concentration of 2,6-DNT. The observed were demonstrated by the study of the surface density, the electron coupled electron transfer events and the transfer kinetics of the 2,6-DNT surface modified glassy carbon electrodes. All the sensor preparation processes and the quantitative analysis were performed by cyclic voltammetry using a portable potentiostat. Thus, the development of a novel, portable, rapid, ultrasensitive and cost-effective device for the in-situ determination of 2,6-DNT at the level of traces was satisfactorily demonstrated.

Future perspectives

The development of new sustainable and greener methodologies is a matter of important concern in the last years in the field of analytical chemistry. Recent technology revolution has led to the implementation of new portable devices that showed a low power consumption, high cost-effectiveness, good connectivity and their ease to perform in situ measurements. Besides, their portability and their capacity to be calibrated in place facilitates the decision making, allowing users to respond in case of obtaining unsatisfied results. In this sense, several methodologies are being developed in different fields of analytical chemistry such as food safety, environmental analysis and health monitoring. In this context, smartphones have emerged as one of the greatest exponents of portability in analytical chemistry. In this Thesis the suitability of portable devices, including smartphones, for performing in situ analysis have been widely demonstrated being combined with different methodologies such as colorimetric sensors, HPTLC and electrochemical procedures.

The study of the applicability of portable devices to perform in situ analysis has been the key point in the present Thesis, as well as the main goal of many future studies.

REFERENCES

(1)   Jornet-Martínez, N.; Moliner-Martínez, Y.; Molins-Legua, C.; Campíns-Falcó, P. Trends for the Development of In Situ Analysis Devices. In *Encyclopedia of Analytical Chemistry*; John Wiley & Sons, Ltd: Chichester, UK, 2017; pp 1–23. https://doi.org/10.1002/9780470027318.a9593.

(2)   Maja; Fowkes, R. Planetary Forecast: The Roots of Sustainability in the Radical Art of the 1970s. *Third Text* **2009**, *23* (5), 669–674. https://doi.org/10.1080/09528820903189277.

(3)   Brundtland, G. Report of the World Commision on Environement and Development: Our Common Future. *Oxford Pap.* **1987**, *Report of*.

(4)   Horváth, I. T. Introduction: Sustainable Chemistry. *Chem. Rev.* **2018**, *118* (2), 369–371. https://doi.org/10.1021/acs.chemrev.7b00721.

(5)   Anastas, P. T.; Warner, J. C. Green Chemistry: Theory and Practice. *Green Chem. Theory Pract. Oxford Univ. Press. New York* **1998**.

(6)   Tobiszewski, M.; Marć, M.; Gałuszka, A.; Namieśnik, J. Green Chemistry Metrics with Special Reference to Green Analytical Chemistry. *Molecules* **2015**, *20* (6), 10928–10946. https://doi.org/10.3390/molecules200610928.

(7)   Gałuszka, A.; Migaszewski, Z.; Namieśnik, J. The 12 Principles of Green Analytical Chemistry and the SIGNIFICANCE Mnemonic of Green Analytical Practices. *TrAC - Trends in Analytical Chemistry*. Elsevier B.V. 2013, pp 78–84. https://doi.org/10.1016/j.trac.2013.04.010.

(8)   Ballester-Caudet, A.; Navarro-Utiel, R.; Campos-Hernández, I.; Campíns-Falcó, P. Evaluation of the Sample Treatment Influence in Green and Sustainable Assessment of Liquid Chromatography Methods by the HEXAGON Tool: Sulfonate-Based Dyes Determination in Meat Samples. *Green Anal. Chem.* **2022**, *3*, 100024. https://doi.org/10.1016/j.greeac.2022.100024.

(9)   Cortés-Bautista, S.; Navarro-Utiel, R.; Ballester-Caudet, A.; Campíns-Falcó, P. Towards in Field Miniaturized Liquid Chromatography: Biocides in Wastewater as a Proof of Concept. *J. Chromatogr. A* **2022**, *1673*, 463119. https://doi.org/10.1016/j.chroma.2022.463119.

(10)   Ballester-Caudet, A.; Campíns-Falcó, P.; Pérez, B.; Sancho, R.; Lorente, M.; Sastre, G.; González, C. A New Tool for Evaluating and/or Selecting Analytical

Methods: Summarizing the Information in a Hexagon. *TrAC Trends Anal. Chem.* **2019**, *118*, 538–547. https://doi.org/10.1016/j.trac.2019.06.015.

(11)   Encyclopedia of Analytical Chemistry: Applications, Theory, and Instrumentation. *Choice Rev. Online* **2001**, *39* (02). https://doi.org/10.5860/choice.39-0662.

(12)   Eren, H. Recent Technological Progress in Portable Instruments. In *2nd ISA/IEEE Sensors for Industry Conference,*; ISA, 2003; pp 78–83. https://doi.org/10.1109/SFICON.2002.1159811.

(13)   Capitán-Vallvey, L. F.; Palma, A. J. Recent Developments in Handheld and Portable Optosensing—A Review. *Anal. Chim. Acta* **2011**, *696* (1–2), 27–46. https://doi.org/10.1016/j.aca.2011.04.005.

(14)   The, F. A PORTABLE S O U R C E O F WOODS L I G H T I N PORPHYRIN ANALYSIS. **1957**, 208–209.

(15)   Kozitsina, A.; Svalova, T.; Malysheva, N.; Okhokhonin, A.; Vidrevich, M.; Brainina, K. Sensors Based on Bio and Biomimetic Receptors in Medical Diagnostic, Environment, and Food Analysis. *Biosensors* **2018**, *8* (2), 35. https://doi.org/10.3390/bios8020035.

(16)   Vashist, S. Point-of-Care Diagnostics: Recent Advances and Trends. *Biosensors* **2017**, *7* (4), 62. https://doi.org/10.3390/bios7040062.

(17)   Jornet-Martinez;Bocanegra-Rodríguez, S; González-Fuenzalida, R.A; Molins-Legua, C; Campíns-Falcó, P, N. *Processing and Sustainability of Beverages*; Elsevier, 2019. https://doi.org/10.1016/C2017-0-02376-5.

(18)   Sharma, S.; Tolley, L. T.; Tolley, H. D.; Plistil, A.; Stearns, S. D.; Lee, M. L. Hand-Portable Liquid Chromatographic Instrumentation. *J. Chromatogr. A* **2015**, *1421*, 38–47. https://doi.org/10.1016/j.chroma.2015.07.119.

(19)   Holmes, J.; Pathirathna, P.; Hashemi, P. Novel Frontiers in Voltammetric Trace Metal Analysis: Towards Real Time, on-Site, in Situ Measurements. *TrAC Trends Anal. Chem.* **2019**, *111*, 206–219. https://doi.org/10.1016/j.trac.2018.11.003.

(20)   Ma, W.; Xu, S.; Liu, H.; Bai, Y. Mass Spectrometry Methods for In Situ Analysis of Clinical Biomolecules. *Small Methods* **2020**, *4* (4), 1900407. https://doi.org/10.1002/smtd.201900407.

(21)   Santana-Jiménez, L. A.; Márquez-Lucero, A.; Osuna, V.; Estrada-Moreno, I.; Dominguez, R. B. Naked-Eye Detection of Glucose in Saliva with Bienzymatic Paper-Based Sensor. *Sensors (Switzerland)* **2018**, *18* (4). https://doi.org/10.3390/S18041071.

(22)   Jornet-Martínez, N.; Moliner-Martínez, Y.; Herráez-Hernández, R.; Molins-Legua, C.; Verdú-Andrés, J.; Campíns-Falcó, P. Designing Solid Optical Sensors for in Situ Passive Discrimination of Volatile Amines Based on a New One-Step Hydrophilic PDMS Preparation. *Sensors Actuators B Chem.* **2016**, *223*, 333–342. https://doi.org/10.1016/j.snb.2015.09.097.

(23)   Prieto-Blanco, M. C.; Jornet-Martínez, N.; Moliner-Martínez, Y.; Molins-Legua, C.; Herráez-Hernández, R.; Verdú Andrés, J.; Campins-Falcó, P. Development of a Polydimethylsiloxane–Thymol/Nitroprusside Composite Based Sensor Involving Thymol Derivatization for Ammonium Monitoring in Water Samples. *Sci. Total Environ.* **2015**, *503–504*, 105–112. https://doi.org/10.1016/j.scitotenv.2014.07.077.

(24)   Mahato, K.; Wang, J. Electrochemical Sensors: From the Bench to the Skin. *Sensors Actuators B Chem.* **2021**, *344*, 130178. https://doi.org/10.1016/j.snb.2021.130178.

(25)   Guo, J. Smartphone-Powered Electrochemical Dongle for Point-of-Care Monitoring of Blood β-Ketone. *Anal. Chem.* **2017**, *89* (17), 8609–8613. https://doi.org/10.1021/acs.analchem.7b02531.

(26)   Fu, Y.; Yan, M.; Yang, H.; Ma, X.; Guo, J. Palm-Sized Uric Acid Test Lab Powered by Smartphone for Proactive Gout Management. *IEEE Trans. Biomed. Circuits Syst.* **2019**, *13* (5). https://doi.org/10.1109/TBCAS.2019.2922674.

(27)   Mu, T.; Wang, S.; Li, T.; Wang, B.; Ma, X.; Huang, B.; Zhu, L.; Guo, J. Detection of Pesticide Residues Using Nano-SERS Chip and a Smartphone-Based Raman Sensor. *IEEE J. Sel. Top. Quantum Electron.* **2018**, *25* (2). https://doi.org/10.1109/JSTQE.2018.2869638.

(28)   Rezazadeh, M.; Seidi, S.; Lid, M.; Pedersen-Bjergaard, S.; Yamini, Y. The Modern Role of Smartphones in Analytical Chemistry. *TrAC - Trends in Analytical Chemistry*. 2019. https://doi.org/10.1016/j.trac.2019.06.019.

(29)   Kılıç, V.; Horzum, N.; Ertugrul Solmaz, M. From Sophisticated Analysis to Colorimetric Determination: Smartphone Spectrometers and Colorimetry. In *Color Detection*; IntechOpen, 2020.

https://doi.org/10.5772/intechopen.82227.

(30)   Martínez-Aviño, A.; Molins-Legua, C.; Pilar, C.-F. Scaling the Analytical Information Given by Several Types of Colorimetric and Spectroscopic Instruments Including Smartphones: Rules for Their Use and Establishing Figures of Merit of Solid Chemosensors. *Anal. Chem.* **2021**, *93* (15), 6043–6052. https://doi.org/10.1021/acs.analchem.0c03994.

(31)   Pla-Tolós, J.; Moliner-Martínez, Y.; Verdú-Andrés, J.; Casanova-Chafer, J.; Molins-Legua, C.; Campíns-Falcó, P. New Optical Paper Sensor for in Situ Measurement of Hydrogen Sulphide in Waters and Atmospheres. *Talanta* **2016**, *156–157*. https://doi.org/10.1016/j.talanta.2016.05.013.

(32)   McCracken, K. E.; Yoon, J.-Y. Recent Approaches for Optical Smartphone Sensing in Resource-Limited Settings: A Brief Review. *Anal. Methods* **2016**, *8* (36), 6591–6601. https://doi.org/10.1039/C6AY01575A.

(33)   Vashist, S. K.; van Oordt, T.; Schneider, E. M.; Zengerle, R.; von Stetten, F.; Luong, J. H. T. A Smartphone-Based Colorimetric Reader for Bioanalytical Applications Using the Screen-Based Bottom Illumination Provided by Gadgets. *Biosens. Bioelectron.* **2015**, *67*, 248–255. https://doi.org/10.1016/j.bios.2014.08.027.

(34)   Sumriddetchkajorn, S.; Chaitavon, K.; Intaravanne, Y. Mobile-Platform Based Colorimeter for Monitoring Chlorine Concentration in Water. *Sensors Actuators B Chem.* **2014**, *191*, 561–566. https://doi.org/10.1016/j.snb.2013.10.024.

(35)   Peregonchaya, O. V.; Korol'kova, N. V; Sokolova, S. A.; D'yakonova, O. V. Possibility of Using Digital Technology in Determining the Color Number of Vegetable Oil. *IOP Conf. Ser. Earth Environ. Sci.* **2020**, *422* (1), 012078. https://doi.org/10.1088/1755-1315/422/1/012078.

(36)   Jia, M.-Y.; Wu, Q.-S.; Li, H.; Zhang, Y.; Guan, Y.-F.; Feng, L. The Calibration of Cellphone Camera-Based Colorimetric Sensor Array and Its Application in the Determination of Glucose in Urine. *Biosens. Bioelectron.* **2015**, *74*, 1029–1037. https://doi.org/10.1016/j.bios.2015.07.072.

(37)   Kim, D.; Kim, S.; Ha, H.-T.; Kim, S. Smartphone-Based Image Analysis Coupled to Paper-Based Colorimetric Devices. *Curr. Appl. Phys.* **2020**, *20* (9), 1013–1018. https://doi.org/10.1016/j.cap.2020.06.021.

(38)   Reda, A.; El-Safty, S. A.; Selim, M. M.; Shenashen, M. A. Optical Glucose

Biosensor Built-in Disposable Strips and Wearable Electronic Devices. *Biosens. Bioelectron.* **2021**, *185*, 113237. https://doi.org/10.1016/j.bios.2021.113237.

(39) Gong, P.; Li, X.; Zhou, X.; Zhang, Y.; Chen, N.; Wang, S.; Zhang, S.; Zhao, Y. Optical Fiber Sensors for Glucose Concentration Measurement: A Review. *Opt. Laser Technol.* **2021**, *139*, 106981. https://doi.org/10.1016/j.optlastec.2021.106981.

(40) Jouyban, A.; Rahimpour, E. Optical Sensors for Determination of Water in the Organic Solvents: A Review. *J. Iran. Chem. Soc.* **2022**, *19* (1), 1–22. https://doi.org/10.1007/s13738-021-02290-0.

(41) Ong, J. J.; Pollard, T. D.; Goyanes, A.; Gaisford, S.; Elbadawi, M.; Basit, A. W. Optical Biosensors - Illuminating the Path to Personalized Drug Dosing. *Biosens. Bioelectron.* **2021**, *188*, 113331. https://doi.org/10.1016/j.bios.2021.113331.

(42) Chen, Y.-T.; Lee, Y.-C.; Lai, Y.-H.; Lim, J.-C.; Huang, N.-T.; Lin, C.-T.; Huang, J.-J. Review of Integrated Optical Biosensors for Point-of-Care Applications. *Biosensors* **2020**, *10* (12), 209. https://doi.org/10.3390/bios10120209.

(43) Pla-Tolós, J.; Serra-Mora, P.; Hakobyan, L.; Molins-Legua, C.; Moliner-Martinez, Y.; Campins-Falcó, P. A Sustainable On-Line CapLC Method for Quantifying Antifouling Agents like Irgarol-1051 and Diuron in Water Samples: Estimation of the Carbon Footprint. *Sci. Total Environ.* **2016**, *569–570*. https://doi.org/10.1016/j.scitotenv.2016.06.181.

(44) Chen, W.; Yao, Y.; Chen, T.; Shen, W.; Tang, S.; Lee, H. K. Application of Smartphone-Based Spectroscopy to Biosample Analysis: A Review. *Biosens. Bioelectron.* **2021**, *172*, 112788. https://doi.org/10.1016/j.bios.2020.112788.

(45) Pebdeni, A. B.; Roshani, A.; Mirsadoughi, E.; Behzadifar, S.; Hosseini, M. Recent Advances in Optical Biosensors for Specific Detection of E. Coli Bacteria in Food and Water. *Food Control* **2022**, *135*, 108822. https://doi.org/10.1016/j.foodcont.2022.108822.

(46) Devi, P.; Singh, J. P. A Highly Sensitive Colorimetric Gas Sensor Based on Indium Oxide Nanostructures for H 2 S Detection at Room Temperature. *IEEE Sens. J.* **2021**, *21* (17), 18512–18518. https://doi.org/10.1109/JSEN.2021.3089290.

(47) Argente-García, A.; Muñoz-Ortuño, M.; Molins-Legua, C.; Moliner-Martínez, Y.; Campíns-Falcó, P. A Solid Device Based on Doped Hybrid Composites for Controlling the Dosage of the Biocide N-(3-Aminopropyl)-N-Dodecyl-1,3-Propanediamine in Industrial Formulations. *Talanta* **2016**, *147*, 147–154. https://doi.org/10.1016/j.talanta.2015.09.051.

(48) Argente-García, A.; Jornet-Martínez, N.; Herráez-Hernández, R.; Campíns-Falcó, P. A Solid Colorimetric Sensor for the Analysis of Amphetamine-like Street Samples. *Anal. Chim. Acta* **2016**, *943*, 123–130. https://doi.org/10.1016/j.aca.2016.09.020.

(49) Beeharry, S.; Sihota, S.; Kelly, C. Profiling Chlorine Residuals Using DPD and Amperometric Field Test Kits in a Chlorinated Small Drinking Water System with Ammonia Present in Source Water. *Environ. Heal. Rev.* **2018**, *61* (2), 39–49. https://doi.org/10.5864/d2018-011.

(50) Kriss, R.; Pieper, K. J.; Parks, J.; Edwards, M. A. Challenges of Detecting Lead in Drinking Water Using At-Home Test Kits. *Environ. Sci. Technol.* **2021**, *55* (3), 1964–1972. https://doi.org/10.1021/acs.est.0c07614.

(51) Schwenke, K. U.; Spiehl, D.; Krauße, M.; Riedler, L.; Ruppenthal, A.; Villforth, K.; Meckel, T.; Biesalski, M.; Rupprecht, D.; Schwall, G. Analysis of Free Chlorine in Aqueous Solution at Very Low Concentration with Lateral Flow Tests. *Sci. Rep.* **2019**, *9* (1), 17212. https://doi.org/10.1038/s41598-019-53687-0.

(52) Chin, C. D.; Linder, V.; Sia, S. K. Lab-on-a-Chip Devices for Global Health: Past Studies and Future Opportunities. *Lab Chip* **2007**, *7* (1), 41–57. https://doi.org/10.1039/B611455E.

(53) Demirkol, D. O.; Dornbusch, K.; Feller, K.-H.; Timur, S. Microfluidic Devices and True-Color Sensor as Platform for Glucose Oxidase and Laccase Assays. *Eng. Life Sci.* **2011**, *11* (2), 182–188. https://doi.org/10.1002/elsc.201000068.

(54) Mark, D.; Haeberle, S.; Roth, G.; von Stetten, F.; Zengerle, R. Microfluidic Lab-on-a-Chip Platforms: Requirements, Characteristics and Applications. *Chem. Soc. Rev.* **2010**, *39* (3), 1153. https://doi.org/10.1039/b820557b.

(55) Coffey, C. C.; Pearce, T. A. Direct-Reading Methods for Workplace Air Monitoring. *J. Chem. Heal. Saf.* **2010**, *17* (3), 10–21. https://doi.org/10.1016/j.jchas.2009.08.003.

(56)   Nash, D. G.; Leith, D. Use of Passive Diffusion Tubes to Monitor Air Pollutants. *J. Air Waste Manage. Assoc.* **2010**, *60* (2), 204–209. https://doi.org/10.3155/1047-3289.60.2.204.

(57)   Fan, J.; Meng, Z.; Dong, X.; Xue, M.; Qiu, L.; Liu, X.; Zhong, F.; He, X. Colorimetric Screening of Nitramine Explosives by Molecularly Imprinted Photonic Crystal Array. *Microchem. J.* **2020**, *158*, 105143. https://doi.org/10.1016/j.microc.2020.105143.

(58)   Kangas, M. J.; Burks, R. M.; Atwater, J.; Lukowicz, R. M.; Williams, P.; Holmes, A. E. Colorimetric Sensor Arrays for the Detection and Identification of Chemical Weapons and Explosives. *Crit. Rev. Anal. Chem.* **2017**, *47* (2), 138–153. https://doi.org/10.1080/10408347.2016.1233805.

(59)   Zhao, M.; Yu, H.; He, Y. A Dynamic Multichannel Colorimetric Sensor Array for Highly Effective Discrimination of Ten Explosives. *Sensors Actuators B Chem.* **2019**, *283*, 329–333. https://doi.org/10.1016/j.snb.2018.12.061.

(60)   Jia, D.; Yang, C.; Zhang, W.; Ding, Y. Dyes Inspired Sensor Arrays for Discrimination of Glycosaminoglycans. *Dye. Pigment.* **2021**, *190*, 109266. https://doi.org/10.1016/j.dyepig.2021.109266.

(61)   Alberti, G.; Zanoni, C.; Magnaghi, L. R.; Biesuz, R. Disposable and Low-Cost Colorimetric Sensors for Environmental Analysis. *Int. J. Environ. Res. Public Health* **2020**, *17* (22), 8331. https://doi.org/10.3390/ijerph17228331.

(62)   Jing, L.; Jianhua, X.; Shuang, X. Volatile Organic Compound Colorimetric Array Based on Zinc Porphyrin and Metalloporphyrin Derivatives. *Energy Procedia* **2011**, *12*, 625–631. https://doi.org/10.1016/j.egypro.2011.10.085.

(63)   Jornet-Martínez, N.; Hakobyan, L.; Argente-García, A. I.; Molins-Legua, C.; Campíns-Falcó, P. Nylon-Supported Plasmonic Assay Based on the Aggregation of Silver Nanoparticles: In Situ Determination of Hydrogen Sulfide-like Compounds in Breath Samples as a Proof of Concept. *ACS Sensors* **2019**, *4* (8), 2164–2172. https://doi.org/10.1021/acssensors.9b01019.

(64)   Masson, J.-F. Surface Plasmon Resonance Clinical Biosensors for Medical Diagnostics. *ACS Sensors* **2017**, *2* (1), 16–30. https://doi.org/10.1021/acssensors.6b00763.

(65)   S, B.; S, B. Plasmonic Sensors for Disease Detection - A Review. *J. Nanomed. Nanotechnol.* **2016**, *7* (3). https://doi.org/10.4172/2157-7439.1000373.

(66)   Balbinot, S.; Srivastav, A. M.; Vidic, J.; Abdulhalim, I.; Manzano, M. Plasmonic Biosensors for Food Control. *Trends Food Sci. Technol.* **2021**, *111*, 128–140. https://doi.org/10.1016/j.tifs.2021.02.057.

(67)   Tseng, S.-Y.; Li, S.-Y.; Yi, S.-Y.; Sun, A. Y.; Gao, D.-Y.; Wan, D. Food Quality Monitor: Paper-Based Plasmonic Sensors Prepared Through Reversal Nanoimprinting for Rapid Detection of Biogenic Amine Odorants. *ACS Appl. Mater. Interfaces* **2017**, *9* (20), 17306–17316. https://doi.org/10.1021/acsami.7b00115.

(68)   Wei, H.; Hossein Abtahi, S. M.; Vikesland, P. J. Plasmonic Colorimetric and SERS Sensors for Environmental Analysis. *Environ. Sci. Nano* **2015**, *2* (2), 120–135. https://doi.org/10.1039/C4EN00211C.

(69)   Xia, Y.; Larock, R. C. Vegetable Oil-Based Polymeric Materials: Synthesis, Properties, and Applications. *Green Chem.* **2010**, *12* (11), 1893. https://doi.org/10.1039/c0gc00264j.

(70)   Chaiyo, S.; Siangproh, W.; Apilux, A.; Chailapakul, O. Highly Selective and Sensitive Paper-Based Colorimetric Sensor Using Thiosulfate Catalytic Etching of Silver Nanoplates for Trace Determination of Copper Ions. *Anal. Chim. Acta* **2015**, *866*, 75–83. https://doi.org/10.1016/j.aca.2015.01.042.

(71)   Ferreira, D. C. M.; Giordano, G. F.; Soares, C. C. D. S. P.; de Oliveira, J. F. A.; Mendes, R. K.; Piazzetta, M. H.; Gobbi, A. L.; Cardoso, M. B. Optical Paper-Based Sensor for Ascorbic Acid Quantification Using Silver Nanoparticles. *Talanta* **2015**, *141*, 188–194. https://doi.org/10.1016/j.talanta.2015.03.067.

(72)   Su, Y.; Ma, S.; Jiang, K.; Han, X. CdTe-Paper-Based Visual Sensor for Detecting Methyl Viologen. *Chinese J. Chem.* **2015**, *33* (4), 446–450. https://doi.org/10.1002/cjoc.201400715.

(73)   Jornet-Martínez, N.; Campíns-Falcó, P.; Hall, E. A. H. Zein as Biodegradable Material for Effective Delivery of Alkaline Phosphatase and Substrates in Biokits and Biosensors. *Biosens. Bioelectron.* **2016**, *86*, 14–19. https://doi.org/10.1016/j.bios.2016.06.016.

(74)   Bocanegra-Rodríguez, S.; Jornet-Martínez, N.; Molins-Legua, C.; Campíns-Falcó, P. Delivering Inorganic and Organic Reagents and Enzymes from Zein and Developing Optical Sensors. *Anal. Chem.* **2018**, *90* (14), 8501–8508. https://doi.org/10.1021/acs.analchem.8b01338.

(75)   Alqahtani, M. S.; Islam, M. S.; Podaralla, S.; Kaushik, R. S.; Reineke, J.; Woyengo, T.; Perumal, O. Food Protein Based Core–Shell Nanocarriers for Oral Drug Delivery: Effect of Shell Composition on in Vitro and in Vivo Functional Performance of Zein Nanocarriers. *Mol. Pharm.* **2017**, *14* (3), 757–769. https://doi.org/10.1021/acs.molpharmaceut.6b01017.

(76)   Jornet-Martínez, N.; Herráez-Hernández, R.; Campíns-Falcó, P. Scopolamine Analysis in Beverages: Bicolorimetric Device vs Portable Nano Liquid Chromatography. *Talanta* **2021**, *232*, 122406. https://doi.org/10.1016/j.talanta.2021.122406.

(77)   Jornet-Martínez, N.; Gómez-Ojea, R.; Tomás-Huercio, O.; Herráez-Hernández, R.; Campíns-Falcó, P. Colorimetric Determination of Alcohols in Spirit Drinks Using a Reversible Solid Sensor. *Food Control* **2018**, *94*, 7–16. https://doi.org/10.1016/j.foodcont.2018.06.020.

(78)   Jornet-Martínez, N.; Samper-Avilés, M.; Herráez-Hernández, R.; Campíns-Falcó, P. Modifying the Reactivity of Copper (II) by Its Encapsulation into Polydimethylsiloxane: A Selective Sensor for Ephedrine-like Compounds. *Talanta* **2019**, *196*, 300–308. https://doi.org/10.1016/j.talanta.2018.12.054.

(79)   Yuan, L.; Zhang, M.; Zhao, T.; Li, T.; Zhang, H.; Chen, L.; Zhang, J. Flexible and Breathable Strain Sensor with High Performance Based on MXene/Nylon Fabric Network. *Sensors Actuators A Phys.* **2020**, *315*, 112192. https://doi.org/10.1016/j.sna.2020.112192.

(80)   Martínez-Aviñó, A.; Hakobyan, L.; Ballester-Caudet, A.; Moliner-Martínez, Y.; Molins-Legua, C.; Campíns-Falcó, P. NQS-Doped PDMS Solid Sensor: From Water Matrix to Urine Enzymatic Application. *Biosensors* **2021**, *11* (6), 186. https://doi.org/10.3390/bios11060186.

(81)   Pastore, A.; Badocco, D.; Bogialli, S.; Cappellin, L.; Pastore, P. Behavior of Sulfonephthalein and Azo Dyes as Effective PH Sensors in Hybrid Materials. *Microchem. J.* **2021**, *160*, 105605. https://doi.org/10.1016/j.microc.2020.105605.

(82)   Tobjörk, D.; Österbacka, R. Paper Electronics. *Adv. Mater.* **2011**, *23* (17), 1935–1961. https://doi.org/10.1002/adma.201004692.

(83)   Cuartero, M.; Crespo, G. A.; Bakker, E. Paper-Based Thin-Layer Coulometric Sensor for Halide Determination. *Anal. Chem.* **2015**, *87* (3), 1981–1990. https://doi.org/10.1021/ac504400w.

(84)   Ali, M. M.; Wolfe, M.; Tram, K.; Gu, J.; Filipe, C. D. M.; Li, Y.; Brennan, J. D. A DNAzyme-Based Colorimetric Paper Sensor for Helicobacter Pylori. *Angew. Chemie Int. Ed.* **2019**, *58* (29), 9907–9911. https://doi.org/10.1002/anie.201901873.

(85)   Dai, G.; Hu, J.; Zhao, X.; Wang, P. A Colorimetric Paper Sensor for Lactate Assay Using a Cellulose-Binding Recombinant Enzyme. *Sensors Actuators B Chem.* **2017**, *238*, 138–144. https://doi.org/10.1016/j.snb.2016.07.008.

(86)   Kim, H. J.; Kim, Y.; Park, S. J.; Kwon, C.; Noh, H. Development of Colorimetric Paper Sensor for Pesticide Detection Using Competitive-Inhibiting Reaction. *BioChip J.* **2018**, *12* (4), 326–331. https://doi.org/10.1007/s13206-018-2404-z.

(87)   Wang, Y.; Yang, L.; Liu, B.; Yu, S.; Jiang, C. A Colorimetric Paper Sensor for Visual Detection of Mercury Ions Constructed with Dual-Emission Carbon Dots. *New J. Chem.* **2018**, *42* (19), 15671–15677. https://doi.org/10.1039/C8NJ03683G.

(88)   Bordbar, M. M.; Tashkhourian, J.; Hemmateenejad, B. Structural Elucidation and Ultrasensitive Analyses of Volatile Organic Compounds by Paper-Based Nano-Optoelectronic Noses. *ACS Sensors* **2019**, *4* (5), 1442–1451. https://doi.org/10.1021/acssensors.9b00680.

(89)   Mata, A.; Fleischman, A. J.; Roy, S. *Characterization of Polydimethylsiloxane (PDMS) Properties for Biomedical Micro/Nanosystems*; Springer Science + Business Media, Inc. Manufactured in The Netherlands, 2005; Vol. 7.

(90)   Löttersby, J. C.; Ithuis, W. O.; Veltink, P. H.; Bergveld, P. *The Mechanical Properties of the Rubber Elastic Polymer Polydimethylsiloxane for Sensor Applications*; 1997; Vol. 7.

(91)   Kumar, P.; Khosla, R.; Soni, M.; Deva, D.; Sharma, S. K. A Highly Sensitive, Flexible SERS Sensor for Malachite Green Detection Based on Ag Decorated Microstructured PDMS Substrate Fabricated from Taro Leaf as Template. *Sensors Actuators B Chem.* **2017**, *246*, 477–486. https://doi.org/10.1016/j.snb.2017.01.202.

(92)   Trantidou, T.; Elani, Y.; Parsons, E.; Ces, O. Hydrophilic Surface Modification of PDMS for Droplet Microfluidics Using a Simple, Quick, and Robust Method via PVA Deposition. *Microsystems Nanoeng.* **2017**, *3* (1), 16091. https://doi.org/10.1038/micronano.2016.91.

(93) Long, H. P.; Lai, C. C.; Chung, C. K. Polyethylene Glycol Coating for Hydrophilicity Enhancement of Polydimethylsiloxane Self-Driven Microfluidic Chip. *Surf. Coatings Technol.* **2017**, *320*, 315–319. https://doi.org/10.1016/j.surfcoat.2016.12.059.

(94) Campins-Falcó, P.; Moliner-Martínez, Y.; Herráez-Hernández, R.; Verdú-Andrés, J.; Jornet-Martínez, N. Passive Sensor for In-Situ Detection of Amines in Chemical Industries.

(95) Ballester-Caudet, A.; Hakobyan, L.; Moliner-Martinez, Y.; Molins-Legua, C.; Campíns-Falcó, P. Ionic-Liquid Doped Polymeric Composite as Passive Colorimetric Sensor for Meat Freshness as a Use Case. *Talanta* **2021**, *223*, 121778. https://doi.org/10.1016/J.TALANTA.2020.121778.

(96) Li, D.; Xu, F.; Liu, Z.; Zhu, J.; Zhang, Q.; Shao, L. The Effect of Adding PDMS-OH and Silica Nanoparticles on Sol–Gel Properties and Effectiveness in Stone Protection. *Appl. Surf. Sci.* **2013**, *266*, 368–374. https://doi.org/10.1016/j.apsusc.2012.12.030.

(97) Argente-García, A.; Jornet-Martínez, N.; Herráez-Hernández, R.; Campíns-Falcó, P. A Passive Solid Sensor for In-Situ Colorimetric Estimation of the Presence of Ketamine in Illicit Drug Samples. *Sensors Actuators B Chem.* **2017**, *253*, 1137–1144. https://doi.org/10.1016/j.snb.2017.07.183.

(98) Hakobyan, L.; Prieto-Blanco, M. C.; Llorens, M. R.; Molins-Legua, C.; Fuster-Garcia, M.; Moliner-Martinez, Y.; Campins-Falcó, P.; Ribes-Koninckx, C. Fast Blue B Functionalized Silica-Polymer Composite to Evaluate 3,5-Dihydroxyhydrocinnamic Acid as Biomarker of Gluten Intake. *Sensors Actuators B Chem.* **2021**, *345*, 130333. https://doi.org/10.1016/j.snb.2021.130333.

(99) Hakobyan, L.; Monforte-Gómez, B.; Moliner-Martínez, Y.; Molins-Legua, C.; Campíns-Falcó, P. Improving Sustainability of the Griess Reaction by Reagent Stabilization on PDMS Membranes and ZnNPs as Reductor of Nitrates: Application to Different Water Samples. *Polymers (Basel).* **2022**, *14* (3). https://doi.org/10.3390/polym14030464.

(100) Mukhopadhyay, S. K. Manufacturing, Properties and Tensile Failure of Nylon Fibres. In *Handbook of Tensile Properties of Textile and Technical Fibres*; Elsevier, 2009; pp 197–222. https://doi.org/10.1533/9781845696801.2.197.

(101) Segatelli, M. G.; Yoshida, I. V. P.; Gonçalves, M. do C. Natural Silica Fiber as

Reinforcing Filler of Nylon 6. *Compos. Part B Eng.* **2010**, *41* (1), 98–105. https://doi.org/10.1016/j.compositesb.2009.05.006.

(102) Nadafpour, N.; Montazeri, M.; Moradi, M.; Ahmadzadeh, S.; Etemadi, A. Bacterial Colonization on Different Suture Materials Used in Oral Implantology: A Randomized Clinical Trial. *Front. Dent.* **2021**, *18*. https://doi.org/10.18502/fid.v18i25.6935.

(103) Farahmand, E.; Ibrahim, F.; Hosseini, S.; Rothan, H. A.; Yusof, R.; Koole, L. H.; Djordjevic, I. A Novel Approach for Application of Nylon Membranes in the Biosensing Domain. *Appl. Surf. Sci.* **2015**, *353*, 1310–1319. https://doi.org/10.1016/j.apsusc.2015.07.004.

(104) Bocanegra-Rodríguez, S.; Jornet-Martínez, N.; Molins-Legua, C.; Campíns-Falcó, P. Portable Solid Sensor Supported in Nylon for Silver Ion Determination: Testing Its Liberation as Biocide. https://doi.org/10.1007/s00216-020-02680-y.

(105) Edwards, P.; Zhang, C.; Zhang, B.; Hong, X.; Nagarajan, V. K.; Yu, B.; Liu, Z. Smartphone Based Optical Spectrometer for Diffusive Reflectance Spectroscopic Measurement of Hemoglobin OPEN. https://doi.org/10.1038/s41598-017-12482-5.

(106) Ding, H.; Chen, C.; Qi, S.; Han, C.; Yue, C. Smartphone-Based Spectrometer with High Spectral Accuracy for MHealth Application. *Sensors Actuators A Phys.* **2018**, *274*, 94–100. https://doi.org/10.1016/J.SNA.2018.03.008.

(107) S McGonigle, A. J.; Wilkes, T. C.; Pering, T. D.; Willmott, J. R.; Cook, J. M.; Mims III, F. M.; Parisi, A. V. Smartphone Spectrometers. https://doi.org/10.3390/s18010223.

(108) Balado Sánchez, C.; Díaz Redondo, R. P.; Fernández Vilas, A.; Sánchez Bermúdez, A. M. Spectrophotometers for Labs: A Cost-Efficient Solution Based on Smartphones. *Comput Appl Eng Educ* **2019**, *27*, 371–379. https://doi.org/10.1002/cae.22081.

(109) Das, A. J.; Wahi, A.; Kothari, I.; Raskar, R. Ultra-Portable, Wireless Smartphone Spectrometer for Rapid, Non-Destructive Testing of Fruit Ripeness OPEN. *Nat. Publ. Gr.* **2016**. https://doi.org/10.1038/srep32504.

(110) Wang, Y.; Liu, X.; Chen, P.; Tran, N. T.; Zhang, J.; Chia, W. S.; Boujday, S.; Liedberg, B. Smartphone Spectrometer for Colorimetric Biosensing †. *Analyst* **2016**, *141*, 3233. https://doi.org/10.1039/c5an02508g.

(111) Scheeline, A. Cell Phone Spectrometry: Science in Your Pocket? *TrAC Trends Anal. Chem.* **2016**, *85*, 20–25. https://doi.org/10.1016/J.TRAC.2016.02.023.

(112) Capitán-Vallvey, L. F.; López-Ruiz, N.; Martínez-Olmos, A.; Erenas, M. M.; Palma, A. J. Recent Developments in Computer Vision-Based Analytical Chemistry: A Tutorial Review. *Anal. Chim. Acta* **2015**, *899*, 23–56. https://doi.org/10.1016/J.ACA.2015.10.009.

(113) Yetisen, A. K.; Martinez-Hurtado, J. L.; Garcia-Melendrez, A.; Da Cruz Vasconcellos, F.; Lowe, C. R. A Smartphone Algorithm with Inter-Phone Repeatability for the Analysis of Colorimetric Tests. *Sensors Actuators B Chem.* **2014**, *196*, 156–160. https://doi.org/10.1016/J.SNB.2014.01.077.

(114) Kim, S. D.; Koo, Y.; Yun, Y. A Smartphone-Based Automatic Measurement Method for Colorimetric PH Detection Using a Color Adaptation Algorithm. **2017**. https://doi.org/10.3390/s17071604.

(115) Saraji, M.; Bagheri, N. Paper-Based Headspace Extraction Combined with Digital Image Analysis for Trace Determination of Cyanide in Water Samples. *Sensors Actuators B Chem.* **2018**, *270*, 28–34. https://doi.org/10.1016/J.SNB.2018.05.021.

(116) Herrero-Latorre, C.; Barciela-García, J.; García-Martín, S.; Peña-Crecente, R. M. Detection and Quantification of Adulterations in Aged Wine Using RGB Digital Images Combined with Multivariate Chemometric Techniques. *Food Chem. X* **2019**, *3*, 100046. https://doi.org/10.1016/j.fochx.2019.100046.

(117) Pla-Tolós, J.; Moliner-Martínez, Y.; Molins-Legua, C.; Campíns-Falcó, P. Solid Glucose Biosensor Integrated in a Multi-Well Microplate Coupled to a Camera-Based Detector: Application to the Multiple Analysis of Human Serum Samples. *Sensors Actuators B Chem.* **2018**, *258*, 331–341. https://doi.org/10.1016/j.snb.2017.11.069.

(118) Venkatesan, V.; Kumar, S. K. A.; Sahoo, S. K. Spectrophotometric and RGB Performances of a New Tetraphenylcyclopenta-Derived Schiff Base for the Quantification of Cyanide Ions. *Anal. Methods* **2019**, *11* (8), 1137–1143. https://doi.org/10.1039/C8AY02401D.

(119) Aguirre, M. Á.; Long, K. D.; Canals, A.; Cunningham, B. T. Point-of-Use Detection of Ascorbic Acid Using a Spectrometric Smartphone-Based System. *Food Chem.* **2019**, *272*, 141–147. https://doi.org/10.1016/J.FOODCHEM.2018.08.002.

(120) Aguirre, M. Á.; Long, K. D.; Cunningham, B. T. Spectrometric Smartphone-Based System for Ibuprofen Quantification in Commercial Dosage Tablets. *J. Pharm. Sci.* **2019**, *108* (8), 2593–2598. https://doi.org/10.1016/j.xphs.2019.03.010.

(121) Liu, W.; Tian, J.; Mao, C.; Wang, Z.; Liu, J.; Dahlgren, R. A.; Zhang, L.; Wang, X. Sulfur Vacancy Promoted Peroxidase-like Activity of Magnetic Greigite (Fe3S4) for Colorimetric Detection of Serum Glucose. *Anal. Chim. Acta* **2020**, *1127*, 246–255. https://doi.org/10.1016/J.ACA.2020.06.056.

(122) Mahato, K.; Chandra, P. Paper-Based Miniaturized Immunosensor for Naked Eye ALP Detection Based on Digital Image Colorimetry Integrated with Smartphone. *Biosens. Bioelectron.* **2019**, *128*, 9–16. https://doi.org/10.1016/J.BIOS.2018.12.006.

(123) Pereira, A. C.; Moreira, F. T. C.; Rodrigues, L. R.; Sales, M. G. F. Paper-Based Aptasensor for Colorimetric Detection of Osteopontin. *Anal. Chim. Acta* **2022**, *1198*, 339557. https://doi.org/10.1016/j.aca.2022.339557.

(124) Böck, F. C.; Gilson, &; Helfer, A.; Da Costa, A. B.; Dessuy, M. B.; Ferrão, M. F. Rapid Determination of Ethanol in Sugarcane Spirit Using Partial Least Squares Regression Embedded in Smartphone. https://doi.org/10.1007/s12161-018-1167-4.

(125) de Oliveira Krambeck Franco, M.; Dias Castro, G. A.; Vilanculo, C.; Fernandes, S. A.; Suarez, W. T. A Color Reaction for the Determination of Cu2+ in Distilled Beverages Employing Digital Imaging. *Anal. Chim. Acta* **2021**, *1177*, 338844. https://doi.org/10.1016/j.aca.2021.338844.

(126) Man, Y.; Li, A.; Li, B.; Liu, J.; Pan, L. A Microfluidic Colorimetric Immunoassay for Sensitive Detection of Altenariol Monomethyl Ether by UV Spectroscopy and Smart Phone Imaging. *Anal. Chim. Acta* **2019**, *1092*, 75–84. https://doi.org/10.1016/j.aca.2019.09.039.

(127) Alam, P.; Salem-Bekhit, M. M.; Al-Joufi, F. A.; Alqarni, M. H.; Shakeel, F. Quantitative Analysis of Cabozantinib in Pharmaceutical Dosage Forms Using Green RP-HPTLC and Green NP-HPTLC Methods: A Comparative Evaluation. *Sustain. Chem. Pharm.* **2021**, *21*, 100413. https://doi.org/10.1016/j.scp.2021.100413.

(128) Jupille, T. H.; Perry, J. A. High-Performance Thin-Layer Chromatography: A Review of Principles, Practice, and Potential. *C R C Crit. Rev. Anal. Chem.* **1977**, *6* (4), 325–359. https://doi.org/10.1080/10408347708542695.

(129)   Reich, E.; Schibli, A. Stationary Phases for Planar Separations - Plates for Modern TLC. *LC-GC North America*. 2005.

(130)   Naseer, B.; Hussain, S. Z.; Maqbool, K.; Kashmir, S.; Kashmir, I. High Performance Thin Layer Chromatography: Principle, Working and Applications. **2019**, *4*, 83–88.

(131)   Ibrahim, R. S.; Khairy, A.; Zaatout, H. H.; Hammoda, H. M.; Metwally, A. M. Digitally-Optimized HPTLC Coupled with Image Analysis for Pursuing Polyphenolic and Antioxidant Profile during Alfalfa Sprouting. *J. Chromatogr. B Anal. Technol. Biomed. Life Sci.* **2018**, *1099*. https://doi.org/10.1016/j.jchromb.2018.09.021.

(132)   Ristivojević, P.; Trifković, J.; Andrić, F.; Milojković-Opsenica, D. Recent Trends in Image Evaluation of HPTLC Chromatograms. *J. Liq. Chromatogr. Relat. Technol.* **2020**, *43* (9–10), 291–299. https://doi.org/10.1080/10826076.2020.1725555.

(133)   Nyiredy, S. Planar Chromatographic Method Development Using the PRISMA Optimization System and Flow Charts. *J. Chromatogr. Sci.* **2002**, *40* (10), 553–563. https://doi.org/10.1093/chromsci/40.10.553.

(134)   Shewiyo, D. H.; Kaale, E.; Risha, P. G.; Dejaegher, B.; Smeyers-Verbeke, J.; Heyden, Y. Vander. HPTLC Methods to Assay Active Ingredients in Pharmaceutical Formulations: A Review of the Method Development and Validation Steps. *J. Pharm. Biomed. Anal.* **2012**, *66*, 11–23. https://doi.org/10.1016/j.jpba.2012.03.034.

(135)   Zarzycki, P. K. Peter E. Wall: Thin-Layer Chromatography. A Modern Practical Approach. *Anal. Bioanal. Chem.* **2006**, *386* (2). https://doi.org/10.1007/s00216-006-0665-1.

(136)   Mohamed, M.; Rizk, S.; Safaa, ·; Toubar, S.; Emad, ·; Abd Almalak Gadallah, R.; Marwa, ·; Helmy, I. M. A Rapid and Reliable Thin-Layer Chromatographic Method for the Simultaneous Estimation of Celecoxib and Diacerein in Their Binary Mixture Using Nanosilica Gel Plate. **2020**, *33*, 511–522. https://doi.org/10.1007/s00764-020-00064-7.

(137)   Rizk, M.; Attia, A. K.; Mohamed, H. Y.; Elshahed, M. S. Development and Validation of Thin-Layer Chromatography and High-Performance Thin-Layer Chromatography Methods for the Simultaneous Determination of Linagliptin and Empagliflozin in Their Co-Formulated Dosage Form. **2020**, *33*, 647–661. https://doi.org/10.1007/s00764-020-00074-5.

(138) Yang, J.; Choi, L.; Li, D.; Yang, F.; Zeng, L.; Zhao, J.; Li, S. Simultaneous Analysis of Hydrophilic and Lipophilic Compounds in Salvia Miltiorrhiza by Double-Development HPTLC and Scanning Densitometry. *J. Planar Chromatogr. – Mod. TLC* **2011**, *24* (3), 257–263. https://doi.org/10.1556/JPC.24.2011.3.16.

(139) Claude, E.; Lafont, R.; Plumb, R. S.; Wilson, I. D. High Performance Reversed-Phase Thin-Layer Chromatography-Desorption Electrospray Ionisation - Time of Flight High Resolution Mass Spectrometric Detection and Imaging (HPTLC/DESI/ToFMS) of Phytoecdysteroids. *J. Chromatogr. B* **2022**, *1200*, 123265. https://doi.org/10.1016/J.JCHROMB.2022.123265.

(140) Chomicki, A.; Dzido, T. H. Pressurized Planar Electrochromatography of DNS Amino Acids Derivatives in Silica Gel and Silanized Silica Gel Systems with Formic Acid Addition to the Water Mobile Phase. *JPC – J. Planar Chromatogr. – Mod. TLC* **2021**, *34* (2), 105–111. https://doi.org/10.1007/s00764-021-00099-4.

(141) Bazylko, A.; Boruc, K.; Borzym, J.; Kiss, A. K. Aqueous and Ethanolic Extracts of Galinsoga Parviflora and Galinsoga Ciliata. Investigations of Caffeic Acid Derivatives and Flavonoids by HPTLC and HPLC-DAD-MS Methods. *Phytochem. Lett.* **2015**, *11*, 394–398. https://doi.org/10.1016/j.phytol.2014.11.005.

(142) Naşcu-Briciu, R. D.; Sârbu, C. A Comparative Study Concerning the Chromatographic Behaviour and Lipophilicity of Certain Natural Toxins. *J. Sep. Sci.* **2012**, *35* (9), 1059–1067. https://doi.org/10.1002/jssc.201200050.

(143) Kuhlmann, C.; Heide, M.; Engelhard, C. Fast Screening and Quantitative Mass Spectral Imaging of Thin-Layer Chromatography Plates with Flowing Atmospheric-Pressure Afterglow High-Resolution Mass Spectrometry. *Anal. Bioanal. Chem.* **2019**, *411* (23), 6213–6225. https://doi.org/10.1007/s00216-019-02013-8.

(144) Heide, M.; Escobar-Carranza, C. C.; Engelhard, C. Quantitative Detection of Caffeine in Beverages Using Flowing Atmospheric-Pressure Afterglow (FAPA) Ionization High-Resolution Mass Spectrometry Imaging and Performance Evaluation of Different Thin-Layer Chromatography Plates as Sample Substrates. *Anal. Bioanal. Chem.* **2022**, *414* (15), 4481–4495. https://doi.org/10.1007/s00216-022-04045-z.

(145) Dołowy, M.; Pyka-Pająk, A.; Jampílek, J. Simple and Accurate HPTLC-Densitometric Method for Assay of Nandrolone Decanoate in Pharmaceutical Formulation. *Molecules* **2019**, *24* (3), 435.

https://doi.org/10.3390/molecules24030435.

(146) Hawryƚ, A.; Hawryƚ, M.; Świeboda, R.; Waksmundzka-Hajnos, M. Thin-Layer Chromatography of Selected Achillea Species on Silica and CN Silica Stationary Phases with Fingerprint and Chemometrics. *JPC - J. Planar Chromatogr. - Mod. TLC* **2017**, *30* (5), 392–400. https://doi.org/10.1556/1006.2017.30.5.8.

(147) Glavnik, V.; Vovk, I. High Performance Thin-Layer Chromatography–Mass Spectrometry Methods on Diol Stationary Phase for the Analyses of Flavan-3-Ols and Proanthocyanidins in Invasive Japanese Knotweed. *J. Chromatogr. A* **2019**, *1598*, 196–208. https://doi.org/10.1016/j.chroma.2019.03.050.

(148) De Lucia, D.; Manfredini, S.; Vertuani, S.; Bernardi, T. New Insights into Sugar Characterization in Complex Plant Matrices by High-Performance Thin-Layer Chromatography. *J. Liq. Chromatogr. Relat. Technol.* **2016**, *39* (13), 607–612. https://doi.org/10.1080/10826076.2016.1217541.

(149) Srivastava, V.; Singh, M.; Malasoni, R.; Shanker, K.; Verma, R. K.; Gupta, M. M.; Gupta, A. K.; Khanuja, S. P. S. Separation and Quantification of Lignans InPhyllanthus Species by a Simple Chiral Densitometric Method. *J. Sep. Sci.* **2008**, *31* (1), 47–55. https://doi.org/10.1002/jssc.200700282.

(150) DoƚOwy, M.; Pyka, A. The Effect of β-Cyclodextrin on the Resolution of Free and Conjugated Forms of Deoxycholic and Chenodeoxycholic Acids by TLC-Densitometry. *Acta Pol. Pharm. - Drug Res.* **2015**, *72* (6).

(151) Remelli, M.; Faccini, S.; Conato, C. Chiral Ligand-Exchange Resolution of Underivatized Amino Acids on a Dynamically Modified Stationary Phase for RP-HPTLC. *Chirality* **2014**, *26* (6), 313–318. https://doi.org/10.1002/chir.22324.

(152) Binert-Kusztal, Ż.; Starek, M.; Żandarek, J.; Dąbrowska, M. Development of TLC Chromatographic-Densitometric Procedure for Qualitative and Quantitative Analysis of Ceftobiprole. *Processes* **2021**, *9* (4), 708. https://doi.org/10.3390/pr9040708.

(153) Jug, U.; Vovk, I.; Glavnik, V.; Makuc, D.; Naumoska, K. Off-Line Multidimensional High Performance Thin-Layer Chromatography for Fractionation of Japanese Knotweed Rhizome Bark Extract and Isolation of Flavan-3-Ols, Proanthocyanidins and Anthraquinones. *J. Chromatogr. A* **2021**, *1637*, 461802. https://doi.org/10.1016/j.chroma.2020.461802.

(154) Moulian, R.; Chacón-Patiño, M.; Lacroix-Andrivet, O.; Mounicou, S.; Mendes Siqueira, A. L.; Afonso, C.; Rodgers, R.; Giust, P.; Bouyssiere, B.; Barrère-Mangote, C. Speciation of Metals in Asphaltenes by High-Performance Thin-Layer Chromatography and Solid–Liquid Extraction Hyphenated with Elemental and Molecular Identification. *Energy & Fuels* **2020**, *34* (10), 12449–12456. https://doi.org/10.1021/acs.energyfuels.0c02525.

(155) Lacroix-Andrivet, O.; Hubert-Roux, M.; Mendes Siqueira, A. L.; Bai, Y.; Afonso, C. Comparison of Silica and Cellulose Stationary Phases to Analyze Bitumen by High-Performance Thin-Layer Chromatography Coupled to Laser Desorption Ionization Fourier Transform Ion Cyclotron Resonance Mass Spectrometry. *Energy & Fuels* **2020**, *34* (8), 9296–9303. https://doi.org/10.1021/acs.energyfuels.0c00709.

(156) Han, X.; Li, L.; Diao, J. Qualitative and Quantitative Analyses of Labiatenic Acid, Apigenin and Buddleoside in Hyssopus Officinalis by High-Performance Thin-Layer Chromatography. *JPC – J. Planar Chromatogr. – Mod. TLC* **2021**, *34* (1), 45–53. https://doi.org/10.1007/s00764-021-00087-8.

(157) Jiang, M.; Liu, J.; Tian, S. Qualitative and Quantitative Analyses of Gallic Acid and Orientin and Orientin-2"-O-β-l-Galactoside in Chinese Medicine Compound Antibacterial Gel by High-Performance Thin-Layer Chromatography. *JPC – J. Planar Chromatogr. – Mod. TLC* **2021**, *34* (4), 307–313. https://doi.org/10.1007/s00764-021-00118-4.

(158) Zeng, Y.; Liu, J.; Tian, S. Qualitative and Quantitative Analyses of Gallic Acid and Methyl Gallate in Guyinye Residue Extracts and Turkish Gall Cream by High-Performance Thin-Layer Chromatography. *JPC - J. Planar Chromatogr. - Mod. TLC* **2019**, *32* (5), 365–370. https://doi.org/10.1556/1006.2019.32.5.3.

(159) Sherma, J. Planar Chromatography. *Anal. Chem.* **2008**, *80* (12), 4253–4267. https://doi.org/10.1021/ac7023415.

(160) Snyder, L. R. Classification off the Solvent Properties of Common Liquids. *J. Chromatogr. Sci.* **1978**, *16* (6), 223–234. https://doi.org/10.1093/chromsci/16.6.223.

(161) Rashmin, P.; Mrunali, P.; Nitin, D.; Nidhi, D.; Bharat, P. HPTLC Method Development and Validation: Strategy to Minimize Methodological Failures. *Journal of Food and Drug Analysis*. 2012. https://doi.org/10.6227/jfda.2012200408.

(162) Byrne, F. P.; Jin, S.; Paggiola, G.; Petchey, T. H. M.; Clark, J. H.; Farmer, T. J.; Hunt, A. J.; Robert McElroy, C.; Sherwood, J. Tools and Techniques for Solvent Selection: Green Solvent Selection Guides. *Sustain. Chem. Process.* **2016**, *4* (1), 7. https://doi.org/10.1186/s40508-016-0051-z.

(163) Jaenchen, D. E.; Reich, E. CHROMATOGRAPHY: THIN-LAYER (PLANAR) | Instrumentation. In *Encyclopedia of Separation Science*; Elsevier, 2000; pp 839–847. https://doi.org/10.1016/B0-12-226770-2/00421-X.

(164) Sherma, J. Review of HPTLC in Drug Analysis: 1996-2009. *J. AOAC Int.* **2010**, *93* (3), 754–764. https://doi.org/10.1093/jaoac/93.3.754.

(165) Kaźmierczak, D.; Ciesielski, W.; Zakrzewski, R. Application of the Iodine-Azide Procedure for Detection of Biogenic Amines in TLC. *J. Liq. Chromatogr. Relat. Technol.* **2006**, *29* (16), 2425–2436. https://doi.org/10.1080/10826070600864908.

(166) Hosu, A.; Cimpoiu, C. A Simple TLC Method for Evaluation of Nicotine in Cigarettes. *Stud. Univ. Babes-Bolyai Chem.* **2015**, *60* (4), 107–114.

(167) Mohammad, A.; Ullah, Q.; Khan, M.; Aziz, S. S.; Rahman, P. F.; Mohammad, F. Detection Reagents Used in On-Plate Identification of Amino Acids by Thin Layer Chromatography: A Review. *J. Liq. Chromatogr. Relat. Technol.* **2018**, *41* (10), 595–603. https://doi.org/10.1080/10826076.2018.1485035.

(168) Rasouli, M.; Ostovar-Ravari, A.; Shokri-Afra, H. Characterization and Improvement of Phenol-Sulfuric Acid Microassay for Glucose-Based Glycogen. *Eur. Rev. Med. Pharmacol. Sci.* **2014**, *18* (14).

(169) Agatonovic-Kustrin, S.; Kustrin, E.; Gegechkori, V.; Morton, D. High-Performance Thin-Layer Chromatography Hyphenated with Microchemical and Biochemical Derivatizations in Bioactivity Profiling of Marine Species. *Mar. Drugs* **2019**, *17* (3), 148. https://doi.org/10.3390/md17030148.

(170) Dey, A.; Pandey, D. K. HPTLC Detection of Altitudinal Variation of the Potential Antivenin Stigmasterol in Different Populations of the Tropical Ethnic Antidote Rauvolfia Serpentina. *Asian Pac. J. Trop. Med.* **2014**, *7* (S1), S540–S545. https://doi.org/10.1016/S1995-7645(14)60287-X.

(171) Ristivojević, P.; Morlock, G. E. High-Performance Thin-Layer Chromatography Combined with Pattern Recognition Techniques as Tool to Distinguish Thickening Agents. *Food Hydrocoll.* **2017**, *64*, 78–84. https://doi.org/10.1016/j.foodhyd.2016.10.005.

(172) Zarzycki, P.; Bartoszuk, M. Improved TLC Detection of Prostaglandins by Post-Run Derivatization with Phosphomolybdic Acid. *J. Planar Chromatogr. – Mod. TLC* **2008**, *21* (5), 387–390. https://doi.org/10.1556/JPC.21.2008.5.12.

(173) Sagi, S.; Avula, B.; Wang, Y.-H.; Zhao, J.; Khan, I. A. Quantitative Determination of Seven Chemical Constituents and Chemo-Type Differentiation of Chamomiles Using High-Performance Thin-Layer Chromatography. *J. Sep. Sci.* **2014**, *37* (19), 2797–2804. https://doi.org/10.1002/jssc.201400646.

(174) Huber,C.N.; Scobell, H; Tai,H. Determination of Saccharide Distribution of Corn Syrup by Direct Densitometry of Thin-Layer Chromatography. *Cereal Chem.* **1966**, *43*, 342–346.

(175) Petrović, M.; Babić, S.; Kaštelan-Macan, M. Quantitative Determination of Pesticides in Soil by Thin-Layer Chromatography and Video Densitometry. *Croat. Chem. Acta* **2000**, *73* (1).

(176) Sajewicz, M.; Gontarska, M.; Dąbrowa, A.; Kowalska, T. Use of Video Densitometry and Scanning Densitometry to Study an Impact of Silica Gel and <scp>L</Scp> -Arginine on the Retention of Ibuprofen and Naproxen in TLC Systems. *J. Liq. Chromatogr. Relat. Technol.* **2007**, *30* (16), 2369–2383. https://doi.org/10.1080/10826070701465548.

(177) Alam, P.; Ezzeldin, E.; Iqbal, M.; Mostafa, G. A. E.; Anwer, M. K.; Alqarni, M. H.; Foudah, A. I.; Shakeel, F. Determination of Delafloxacin in Pharmaceutical Formulations Using a Green RP-HPTLC and NP-HPTLC Methods: A Comparative Study. *Antibiotics* **2020**, *9* (6), 359. https://doi.org/10.3390/antibiotics9060359.

(178) Neamţu, A. S.; Biţă, A.; Scorei, I. R.; Ră999u, G.; Bejenaru, L. E.; Bejenaru, C.; Rogoveanu, O.-C.; Oancea, C. N.; Radu, A.; Pisoschi, C. G.; Neamţu, J.; Mogoşanu, G. D. Simultaneous Quantitation of Nicotinamide Riboside and Nicotinamide in Dietary Supplements via HPTLC–UV with Confirmation by Online HPTLC–ESI–MS. *Acta Chromatogr.* **2020**, *32* (2), 128–133. https://doi.org/10.1556/1326.2019.00600.

(179) Jana, S. N.; Sing, D.; Banerjee, S.; Haldar, P. K.; Dasgupta, B.; Kar, A.; Sharma, N.; Bandyopadhayay, R.; Mukherjee, P. K. Quantification of Piperine in Different Varieties of Piper Nigrum by a Validated High-Performance Thin-Layer Chromatography–densitometry Method. *JPC – J. Planar Chromatogr. – Mod. TLC* **2021**, *34* (6), 521–530. https://doi.org/10.1007/s00764-021-

00149-x.

(180) Nyiredy, S. Chapter 6 Planar Chromatography. In *Journal of Chromatography Library*; Elsevier, 2004; Vol. 69, pp 253–296. https://doi.org/10.1016/S0301-4770(04)80012-5.

(181) Mehl, J. T.; Hercules, D. M. Direct TLC-MALDI Coupling Using a Hybrid Plate. *Anal. Chem.* **2000**, *72* (1), 68–73. https://doi.org/10.1021/ac990003y.

(182) Jautz, U.; Morlock, G. Efficacy of Planar Chromatography Coupled to (Tandem) Mass Spectrometry for Employment in Trace Analysis. *J. Chromatogr. A* **2006**, *1128* (1–2), 244–250. https://doi.org/10.1016/j.chroma.2006.06.070.

(183) Luftmann, H.; Aranda, M.; Morlock, G. E. Automated Interface for Hyphenation of Planar Chromatography with Mass Spectrometry. *Rapid Commun. Mass Spectrom.* **2007**, *21* (23), 3772–3776. https://doi.org/10.1002/rcm.3276.

(184) Kochin, V.; Imanishi, S. Y.; Eriksson, J. E. Fast Track to a Phosphoprotein Sketch – MALDI-TOF Characterization of TLC-Based Tryptic Phosphopeptide Maps at Femtomolar Detection Sensitivity. *Proteomics* **2006**, *6* (21), 5676–5682. https://doi.org/10.1002/pmic.200600457.

(185) Dreisewerd, K.; Kölbl, S.; Peter-Katalinić, J.; Berkenkamp, S.; Pohlentz, G. Analysis of Native Milk Oligosaccharides Directly from Thin-Layer Chromatography Plates by Matrix-Assisted Laser Desorption/Ionization Orthogonal-Time-of-Flight Mass Spectrometry with a Glycerol Matrix. *J. Am. Soc. Mass Spectrom.* **2006**, *17* (2), 139–150. https://doi.org/10.1016/j.jasms.2005.10.003.

(186) Salo, P. K.; Salomies, H.; Harju, K.; Ketola, R. A.; Kotiaho, T.; Yli-Kauhaluoma, J.; Kostiainen, R. Analysis of Small Molecules by Ultra Thin-Layer Chromatography-Atmospheric Pressure Matrix-Assisted Laser Desorption/Ionization Mass Spectrometry. *J. Am. Soc. Mass Spectrom.* **2005**, *16* (6), 906–915. https://doi.org/10.1016/j.jasms.2005.02.025.

(187) Agatonovic-Kustrin, S.; Morton, D. W. The Power of HPTLC-ATR-FTIR Hyphenation in Bioactivity Analysis of Plant Extracts. *Appl. Sci.* **2020**, *10* (22), 8232. https://doi.org/10.3390/app10228232.

(188) Agatonovic-Kustrin, S.; Balyklova, K. S.; Gegechkori, V.; Morton, D. W. HPTLC and ATR/FTIR Characterization of Antioxidants in Different Rosemary

Extracts. *Molecules* **2021**, *26* (19), 6064. https://doi.org/10.3390/molecules26196064.

(189) Li, H.; Zhao, Y.; Yang, W.; Zhang, Z. Characterization of Astragaloside I-IV Based on the Separation of HPTLC from Pleurotus Ostreatus Cultivated with Astragalus. *J. Food Sci.* **2020**, *85* (10), 3183–3190. https://doi.org/10.1111/1750-3841.15398.

(190) Koglin, E. Combining Surface Enhanced Raman Scattering (SERS) and High-Performance Thin-Layer Chromatography (HPTLC). *J. Mol. Struct.* **1988**, *173* (C), 369–376. https://doi.org/10.1016/0022-2860(88)80068-1.

(191) Yao, H.; Dong, X.; Xiong, H.; Liu, J.; Zhou, J.; Ye, Y. Functional Cotton Fabric-Based TLC-SERS Matrix for Rapid and Sensitive Detection of Mixed Dyes. *Spectrochim. Acta Part A Mol. Biomol. Spectrosc.* **2022**, *280*, 121464. https://doi.org/10.1016/j.saa.2022.121464.

(192) Chen, Y.; Chen, Q.; Wei, X. Separable Surface Enhanced Raman Spectroscopy Sensor Platformed by HPTLC for Facile Screening of Malachite Green in Fish. *Microchem. J.* **2021**, *170*, 106694. https://doi.org/10.1016/j.microc.2021.106694.

(193) Zhu, Q.; Cao, Y.; Cao, Y.; Chai, Y.; Lu, F. Rapid On-Site TLC–SERS Detection of Four Antidiabetes Drugs Used as Adulterants in Botanical Dietary Supplements. *Anal. Bioanal. Chem.* **2014**, *406* (7), 1877–1884. https://doi.org/10.1007/s00216-013-7605-7.

(194) Chen, Y.; Huang, C.; Jin, Z.; Xu, X.; Cai, Y.; Bai, Y. HPTLC-Bioautography/SERS Screening Nifedipine Adulteration in Food Supplement Based on Ginkgo Biloba. *Microchem. J.* **2020**, *154*, 104647. https://doi.org/10.1016/j.microc.2020.104647.

(195) Ţebrencu, C. E.; Creţu, R. M.; Mitroi, G. R.; Iacob, E.; Ionescu, E. Phytochemical Evaluation and HPTLC Investigation of Bark and Extracts of Rhamnus Frangula Linn. *Phytochem. Rev.* **2015**, *14* (4), 613–621. https://doi.org/10.1007/s11101-015-9410-8.

(196) Ferreira, M. A.; Fernandes, M. M.; da Silva, W. V.; Bezerra, I. F.; de Souza, T.; Pimentel, M.; Soares, L. L. Chromatographic and Spectrophotometric Analysis of Phenolic Compounds from Fruits of Libidibia Ferrea Martius. *Pharmacogn. Mag.* **2016**, *12* (46), 285. https://doi.org/10.4103/0973-1296.182165.

(197) Morlock, G. E.; Sabir, G. Reagent Sequence for Planar Chromatographic Analysis of Eight Sweeteners in Food Products Approved in the European Union. *JPC − J. Planar Chromatogr. − Mod. TLC* **2022**, *35* (3), 273–279. https://doi.org/10.1007/s00764-022-00178-0.

(198) Fichou, D.; Morlock, G. E. QuanTLC, an Online Open-Source Solution for Videodensitometric Quantification. *J. Chromatogr. A* **2018**, *1560*, 78–81. https://doi.org/10.1016/j.chroma.2018.05.027.

(199) Báez, E.; Quiñones, J.; Santiesteban, C.; Torres, J. Sistema de Análisis de Imágenes de Placas de HPTLC Analysis System of HPTLC Plate Images. *Rev. Cuba. Ciencias Informáticas* **2017**, *11* (3).

(200) Ristivojević, P.; Andrić, F. L.; Trifković, J. Đ.; Vovk, I.; Stanisavljević, L. Ž.; Tešić, Ž. L.; Milojković-Opsenica, D. M. Pattern Recognition Methods and Multivariate Image Analysis in HPTLC Fingerprinting of Propolis Extracts. *J. Chemom.* **2014**, *28* (4), 301–310. https://doi.org/10.1002/cem.2592.

(201) Agatonovic-Kustrin, S.; Milojković-Opsenica, D.; Morton, D. W.; Ristivojević, P. Chemometric Characterization of Wines According to Their HPTLC Fingerprints. *Eur. Food Res. Technol.* **2017**, *243* (4), 659–667. https://doi.org/10.1007/s00217-016-2779-9.

(202) Simion, I. M.; Casoni, D.; Sârbu, C. Classification of Romanian Medicinal Plant Extracts According to the Therapeutic Effects Using Thin Layer Chromatography and Robust Chemometrics. *J. Pharm. Biomed. Anal.* **2019**, *163*, 137–143. https://doi.org/10.1016/j.jpba.2018.09.047.

(203) Simion, I. M.; Casoni, D.; Sârbu, C. Multivariate Color Scale Image Analysis – Thin Layer Chromatography for Comprehensive Evaluation of Complex Samples Fingerprint. *J. Chromatogr. B* **2021**, *1170*, 122590. https://doi.org/10.1016/j.jchromb.2021.122590.

(204) Li, T.; Tian, R.; Yu, X.; Sun, L.; He, Y.; Xie, P.; Ma, S. Application of Chemometric Algorithms in the High-Performance Thin-Layer Chromatography Fingerprint of Traditional Chinese Medicines. *J. AOAC Int.* **2019**, *102* (3), 720–725. https://doi.org/10.5740/jaoacint.18-0306.

(205) Qu, L.-L.; Jia, Q.; Liu, C.; Wang, W.; Duan, L.; Yang, G.; Han, C.-Q.; Li, H. Thin Layer Chromatography Combined with Surface-Enhanced Raman Spectroscopy for Rapid Sensing Aflatoxins. *J. Chromatogr. A* **2018**, *1579*, 115–120. https://doi.org/10.1016/j.chroma.2018.10.024.

(206) Fang, F.; Qi, Y.; Lu, F.; Yang, L. Highly Sensitive On-Site Detection of Drugs Adulterated in Botanical Dietary Supplements Using Thin Layer Chromatography Combined with Dynamic Surface Enhanced Raman Spectroscopy. *Talanta* **2016**, *146*, 351–357. https://doi.org/10.1016/j.talanta.2015.08.067.

(207) Li, D.; Qu, L.; Zhai, W.; Xue, J.; Fossey, J. S.; Long, Y. Facile On-Site Detection of Substituted Aromatic Pollutants in Water Using Thin Layer Chromatography Combined with Surface-Enhanced Raman Spectroscopy. *Environ. Sci. Technol.* **2011**, *45* (9), 4046–4052. https://doi.org/10.1021/es104155r.

(208) Zhang, S.; Fan, Q.; Guo, J.; Jiao, X.; Kong, X.; Yu, Q. Surface-Enhanced Raman Spectroscopy Tandem with Derivatized Thin-Layer Chromatography for Ultra-Sensitive on-Site Detection of Histamine from Fish. *Food Control* **2022**, *138*, 108987. https://doi.org/10.1016/j.foodcont.2022.108987.

(209) Shen, Z.; Fan, Q.; Yu, Q.; Wang, R.; Wang, H.; Kong, X. Facile Detection of Carbendazim in Food Using TLC-SERS on Diatomite Thin Layer Chromatography. *Spectrochim. Acta Part A Mol. Biomol. Spectrosc.* **2021**, *247*, 119037. https://doi.org/10.1016/J.SAA.2020.119037.

(210) Yu, H.; Zhuang, D.; Hu, X.; Zhang, S.; He, Z.; Zeng, M.; Fang, X.; Chen, J.; Chen, X. Rapid Determination of Histamine in Fish by Thin-Layer Chromatography-Image Analysis Method Using Diazotized Visualization Reagent Prepared with: P -Nitroaniline. *Anal. Methods* **2018**, *10* (27). https://doi.org/10.1039/c8ay00336j.

(211) Sowers, M. E.; Ambrose, R.; Bethea, E.; Harmon, C.; Jenkins, D. Quantitative Thin Layer Chromatography for the Determination of Medroxyprogesterone Acetate Using a Smartphone and Open-Source Image Analysis. *J. Chromatogr. A* **2022**, *1669*, 462942. https://doi.org/10.1016/j.chroma.2022.462942.

(212) Ibrahim, M. M.; Kelani, K. M.; Ramadan, N. K.; Elzanfaly, E. S. Smartphone as a Portable Detector for Thin-Layer Chromatographic Determination of Some Gastrointestinal Tract Drugs. *ACS Omega* **2022**, *7* (27), 23815–23820. https://doi.org/10.1021/acsomega.2c02482.

(213) Wang, J. Portable Electrochemical Systems. *TrAC Trends Anal. Chem.* **2002**, *21* (4), 226–232. https://doi.org/10.1016/S0165-9936(02)00402-8.

(214) Nemiroski, A.; Christodouleas, D. C.; Hennek, J. W.; Kumar, A. A.; Maxwell,

E. J.; Fernández-Abedul, M. T.; Whitesides, G. M. Universal Mobile Electrochemical Detector Designed for Use in Resource-Limited Applications. *Proc. Natl. Acad. Sci.* **2014**, *111* (33), 11984–11989. https://doi.org/10.1073/pnas.1405679111.

(215) Majdinasab, M.; Daneshi, M.; Louis Marty, J. Recent Developments in Non-Enzymatic (Bio)Sensors for Detection of Pesticide Residues: Focusing on Antibody, Aptamer and Molecularly Imprinted Polymer. *Talanta* **2021**, *232*, 122397. https://doi.org/10.1016/j.talanta.2021.122397.

(216) Waheed, A.; Mansha, M.; Ullah, N. Nanomaterials-Based Electrochemical Detection of Heavy Metals in Water: Current Status, Challenges and Future Direction. *TrAC Trends Anal. Chem.* **2018**, *105*, 37–51. https://doi.org/10.1016/j.trac.2018.04.012.

(217) Kim, H.; Jang, G.; Yoon, Y. Specific Heavy Metal/Metalloid Sensors: Current State and Perspectives. *Appl. Microbiol. Biotechnol.* **2020**, *104* (3), 907–914. https://doi.org/10.1007/s00253-019-10261-y.

(218) Raghavan, V. S.; O'Driscoll, B.; Bloor, J. M.; Li, B.; Katare, P.; Sethi, J.; Gorthi, S. S.; Jenkins, D. Emerging Graphene-Based Sensors for the Detection of Food Adulterants and Toxicants – A Review. *Food Chem.* **2021**, *355*, 129547. https://doi.org/10.1016/j.foodchem.2021.129547.

(219) Balogun, S. A.; Fayemi, O. E. Electrochemical Sensors for Determination of Bromate in Water and Food Samples—Review. *Biosensors* **2021**, *11* (6), 172. https://doi.org/10.3390/bios11060172.

(220) Akbari, A.; Divband, B.; Dehghan, P.; Moradi, A. H. Application of Nanocomposites Based on Graphene and Metal Materials in Measurement of Nitrate/Nitrite in Food Samples. *Biointerface Res. Appl. Chem.* **2021**, *11* (5), 12769–12783. https://doi.org/10.33263/BRIAC115.1276912783.

(221) Li, Z.; Zhou, J.; Dong, T.; Xu, Y.; Shang, Y. Application of Electrochemical Methods for the Detection of Abiotic Stress Biomarkers in Plants. *Biosens. Bioelectron.* **2021**, *182*, 113105. https://doi.org/10.1016/j.bios.2021.113105.

(222) Meenakshi, S.; Rama, R.; Pandian, K.; Gopinath, S. C. B. Modified Electrodes for Electrochemical Determination of Metronidazole in Drug Formulations and Biological Samples: An Overview. *Microchem. J.* **2021**, *165*, 106151. https://doi.org/10.1016/j.microc.2021.106151.

(223) Choi, H. K.; Lee, M.-J.; Lee, S. N.; Kim, T.-H.; Oh, B.-K. Noble Metal Nanomaterial-Based Biosensors for Electrochemical and Optical Detection of Viruses Causing Respiratory Illnesses. *Front. Chem.* **2021**, *9*, 672739. https://doi.org/10.3389/fchem.2021.672739.

(224) Goud, K. Y.; Reddy, K. K.; Khorshed, A.; Kumar, V. S.; Mishra, R. K.; Oraby, M.; Ibrahim, A. H.; Kim, H.; Gobi, K. V. Electrochemical Diagnostics of Infectious Viral Diseases: Trends and Challenges. *Biosens. Bioelectron.* **2021**, *180*, 113112. https://doi.org/10.1016/j.bios.2021.113112.

(225) Lee, I.; Probst, D.; Klonoff, D.; Sode, K. Continuous Glucose Monitoring Systems - Current Status and Future Perspectives of the Flagship Technologies in Biosensor Research -. *Biosens. Bioelectron.* **2021**, *181*, 113054. https://doi.org/10.1016/j.bios.2021.113054.

(226) Grieshaber, D.; Mackenzie, R.; Vörös, J.; Reimhult, E. Electrochemical Biosensors-Sensor Principles and Architectures. *Sensors* **2008**, *8*, 1400–1458.

(227) Ekrami, E.; Pouresmaieli, M.; Shariati, P.; Mahmoudifard, M. A Review on Designing Biosensors for the Detection of Trace Metals. *Appl. Geochemistry* **2021**, *127*, 104902. https://doi.org/10.1016/j.apgeochem.2021.104902.

(228) Khadka, R.; Aydemir, N.; Carraher, C.; Hamiaux, C.; Baek, P.; Cheema, J.; Kralicek, A.; Travas-Sejdic, J. Investigating Electrochemical Stability and Reliability of Gold Electrode-electrolyte Systems to Develop Bioelectronic Nose Using Insect Olfactory Receptor. *Electroanalysis* **2019**, *31* (4), 726–738. https://doi.org/10.1002/elan.201800733.

(229) Allen J. Bard, L. R. F. Electrochemical Methods: Fundamentals and Applications, 2nd Edition. *John Wiley Sons, New York* **2020**.

(230) Taleat, Z.; Khoshroo, A.; Mazloum-Ardakani, M. Screen-Printed Electrodes for Biosensing: A Review (2008–2013). *Microchim. Acta* **2014**, *181* (9–10), 865–891. https://doi.org/10.1007/s00604-014-1181-1.

(231) Zittel, H. E.; Miller, F. J. A Glassy-Carbon Electrode for Voltammetry. *Anal. Chem.* **1965**, *37* (2), 200–203. https://doi.org/10.1021/ac60221a006.

(232) Yang, N.; Yu, S.; Macpherson, J. V.; Einaga, Y.; Zhao, H.; Zhao, G.; Swain, G. M.; Jiang, X. Conductive Diamond: Synthesis, Properties, and Electrochemical Applications. *Chem. Soc. Rev.* **2019**, *48* (1), 157–204. https://doi.org/10.1039/C7CS00757D.

(233) GOTO, T.; YASUKAWA, T.; KANDA, K.; MATSUI, S.; MIZUTANI, F. Inhibition of Electrochemical Fouling against Biomolecules on a Diamond-Like Carbon Electrode. *Anal. Sci.* **2011**, *27* (1), 91–94. https://doi.org/10.2116/analsci.27.91.

(234) Uskoković, V. A Historical Review of Glassy Carbon: Synthesis, Structure, Properties and Applications. *Carbon Trends* **2021**, *5*, 100116. https://doi.org/10.1016/j.cartre.2021.100116.

(235) Unnikrishnan, B.; Palanisamy, S.; Chen, S.-M. A Simple Electrochemical Approach to Fabricate a Glucose Biosensor Based on Graphene–Glucose Oxidase Biocomposite. *Biosens. Bioelectron.* **2013**, *39* (1), 70–75. https://doi.org/10.1016/j.bios.2012.06.045.

(236) Ravenna, Y.; Xia, L.; Gun, J.; Mikhaylov, A. A.; Medvedev, A. G.; Lev, O.; Alfonta, L. Biocomposite Based on Reduced Graphene Oxide Film Modified with Phenothiazone and Flavin Adenine Dinucleotide-Dependent Glucose Dehydrogenase for Glucose Sensing and Biofuel Cell Applications. *Anal. Chem.* **2015**, *87* (19), 9567–9571. https://doi.org/10.1021/acs.analchem.5b02949.

(237) Härtl, A.; Schmich, E.; Garrido, J. A.; Hernando, J.; Catharino, S. C. R.; Walter, S.; Feulner, P.; Kromka, A.; Steinmüller, D.; Stutzmann, M. Protein-Modified Nanocrystalline Diamond Thin Films for Biosensor Applications. *Nat. Mater.* **2004**, *3* (10), 736–742. https://doi.org/10.1038/nmat1204.

(238) Chaubey, A.; Malhotra, B. D. Mediated Biosensors. *Biosens. Bioelectron.* **2002**, *17* (6–7), 441–456. https://doi.org/10.1016/S0956-5663(01)00313-X.

(239) Zhang, L.; Zhang, J.; Zhang, C. Electrochemical Synthesis of Polyaniline Nano-Network on α-Alanine Functionalized Glassy Carbon Electrode and Its Application for the Direct Electrochemistry of Horse Heart Cytochrome C. *Biosens. Bioelectron.* **2009**, *24* (7), 2085–2090. https://doi.org/10.1016/j.bios.2008.10.025.

(240) Zhang, L.; Jiang, X. Attachment of Gold Nanoparticles to Glassy Carbon Electrode and Its Application for the Voltammetric Resolution of Ascorbic Acid and Dopamine. *J. Electroanal. Chem.* **2005**, *583* (2), 292–299. https://doi.org/10.1016/j.jelechem.2005.06.014.

(241) Sivanesan, A.; John, S. A. Highly Sensitive Electrochemical Sensor for Nitric Oxide Using the Self-Assembled Monolayer of 1,8,15,22-Tetraaminophthalocyanatocobalt(II) on Glassy Carbon Electrode.

Electroanalysis **2010**, *22* (6), 639–644. https://doi.org/10.1002/elan.200900443.

(242) Wang, C.; Li, C.; Wang, F.; Wang, C. Covalent Modification of Glassy Carbon Electrode with L-Cysteine for the Determination of Acetaminophen. *Microchim. Acta* **2006**, *155* (3–4), 365–371. https://doi.org/10.1007/s00604-006-0616-8.

(243) Arotiba, O.; Owino, J.; Songa, E.; Hendricks, N.; Waryo, T.; Jahed, N.; Baker, P.; Iwuoha, E. An Electrochemical DNA Biosensor Developed on a Nanocomposite Platform of Gold and Poly(Propyleneimine) Dendrimer. *Sensors* **2008**, *8* (11), 6791–6809. https://doi.org/10.3390/s8116791.

(244) Downard, A. J.; Jackson, S. L.; Tan, E. S. Q. Fluorescence Microscopy Study of Protein Adsorption at Modified Glassy Carbon Surfaces. *Aust. J. Chem.* **2005**, *58* (4), 275. https://doi.org/10.1071/CH04259.

(245) Tsujimura, S.; Katayama, A.; Kano, K. Osmium Complex Grafted on a Carbon Electrode Surface as a Mediator for a Bioelectrocatalytic Reaction. *Chem. Lett.* **2006**, *35* (11), 1244–1245. https://doi.org/10.1246/cl.2006.1244.

(246) Ameur, S.; Bureau, C.; Charlier, J.; Palacin, S. Immobilization of Biomolecules on Electrodes Modified by Electrografted Films. **2004**. https://doi.org/10.1021/jp0482262.

(247) Barba, F.; Batanero, B.; Tissaoui, K.; Raouafi, N.; Boujlel, K. Cathodic Reduction of Diazonium Salts in Aprotic Medium. *Electrochem. commun.* **2010**, *12* (7), 973–976. https://doi.org/10.1016/j.elecom.2010.05.004.

(248) Pazo-Llorente, R.; Bravo-Diaz, C.; Gonzalez-Romero, E. PH Effects on Ethanolysis of Some Arenediazonium Ions: Evidence for Homolytic Dediazoniation Proceeding through Formation of Transient Diazo Ethers. *European J. Org. Chem.* **2004**, *2004* (15), 3221–3226. https://doi.org/10.1002/ejoc.200400170.

(249) Elofson, R. M.; Gadallah, F. F. Pschorr Reaction by Electrochemical Generation of Free Radicals. I. Phenanthrene Synthesis. *J. Org. Chem.* **1971**, *36* (13), 1769–1771. https://doi.org/10.1021/jo00812a010.

(250) Betelu, S.; Vautrin-Ul, C.; Chaussé, A. Novel 4-Carboxyphenyl-Grafted Screen-Printed Electrode for Trace Cu(II) Determination. *Electrochem. commun.* **2009**, *11* (2), 383–386. https://doi.org/10.1016/j.elecom.2008.11.035.

(251) Mahouche Chergui, S.; Abbas, N.; Matrab, T.; Turmine, M.; Bon Nguyen, E.; Losno, R.; Pinson, J.; Chehimi, M. M. Uptake of Copper Ions by Carbon Fiber/Polymer Hybrids Prepared by Tandem Diazonium Salt Chemistry and in Situ Atom Transfer Radical Polymerization. *Carbon N. Y.* **2010**, *48* (7), 2106–2111. https://doi.org/10.1016/j.carbon.2010.01.050.

(252) Fan, L.; Chen, J.; Zhu, S.; Wang, M.; Xu, G. Determination of Cd2+ and Pb2+ on Glassy Carbon Electrode Modified by Electrochemical Reduction of Aromatic Diazonium Salts. *Electrochem. commun.* **2009**, *11* (9), 1823–1825. https://doi.org/10.1016/j.elecom.2009.07.026.

(253) Üstündağ, Z.; Solak, A. O. EDTA Modified Glassy Carbon Electrode: Preparation and Characterization. *Electrochim. Acta* **2009**, *54* (26), 6426–6432. https://doi.org/10.1016/j.electacta.2009.06.015.

(254) Betelu, S.; Vautrin-Ul, C.; Ly, J.; Chaussé, A. Screen-Printed Electrografted Electrode for Trace Uranium Analysis. *Talanta* **2009**, *80* (1), 372–376. https://doi.org/10.1016/j.talanta.2009.06.076.

(255) Alonso-Lomillo, M. A.; Domínguez-Renedo, O.; Hernández-Martín, A.; Arcos-Martínez, M. J. Horseradish Peroxidase Covalent Grafting onto Screen-Printed Carbon Electrodes for Levetiracetam Chronoamperometric Determination. *Anal. Biochem.* **2009**, *395* (1), 86–90. https://doi.org/10.1016/j.ab.2009.08.004.

(256) Flavel, B. S.; Garrett, D. J.; Lehr, J.; Shapter, J. G.; Downard, A. J. Chemically Immobilised Carbon Nanotubes on Silicon: Stable Surfaces for Aqueous Electrochemistry. *Electrochim. Acta* **2010**, *55* (12), 3995–4001. https://doi.org/10.1016/j.electacta.2010.02.046.

(257) Hansen, M. N.; Farjami, E.; Kristiansen, M.; Clima, L.; Pedersen, S. U.; Daasbjerg, K.; Ferapontova, E. E.; Gothelf, K. V. Synthesis and Application of a Triazene–Ferrocene Modifier for Immobilization and Characterization of Oligonucleotides at Electrodes. *J. Org. Chem.* **2010**, *75* (8), 2474–2481. https://doi.org/10.1021/jo9024368.

(258) Yang, N.; Uetsuka, H.; Nebel, C. E. DNA-Sensing with Nano-Textured Diamond Electrodes. *Diam. Relat. Mater.* **2009**, *18* (2–3), 592–595. https://doi.org/10.1016/j.diamond.2008.08.007.

(259) Shabani, A.; Mak, A. W. H.; Gerges, I.; Cuccia, L. A.; Lawrence, M. F. DNA Immobilization onto Electrochemically Functionalized Si(100) Surfaces. *Talanta* **2006**, *70* (3), 615–623.

https://doi.org/10.1016/j.talanta.2006.01.033.

(260) Guiseppi-Elie, A.; Lingerfelt, L. Impedimetric Detection of DNA Hybridization: Towards Near-Patient DNA Diagnostics. In *Immobilisation of DNA on Chips I*; Springer-Verlag: Berlin/Heidelberg, 2005; Vol. 260, pp 161–186. https://doi.org/10.1007/128_006.

(261) Thévenot, D. R.; Toth, K.; Durst, R. A.; Wilson, G. S. Electrochemical Biosensors: Recommended Definitions and Classification1International Union of Pure and Applied Chemistry: Physical Chemistry Division, Commission I.7 (Biophysical Chemistry); Analytical Chemistry Division, Commission V.5 (Electroanalytical. *Biosens. Bioelectron.* **2001**, *16* (1–2), 121–131. https://doi.org/10.1016/S0956-5663(01)00115-4.

(262) Yunus, S.; Attout, A.; Vanlancker, G.; Bertrand, P.; Ruth, N.; Galleni, M. A Method to Probe Electrochemically Active Material State in Portable Sensor Applications. *Sensors Actuators B Chem.* **2011**, *156* (1), 35–42. https://doi.org/10.1016/j.snb.2011.03.070.

(263) Bembnowicz, P.; Yang, G.-Z.; Anastasova, S.; Spehar-Deleze, A.-M.; Vadgama, P. Wearable Electronic Sensor for Potentiometric and Amperometric Measurements. In *2013 IEEE International Conference on Body Sensor Networks*; IEEE, 2013; pp 1–5. https://doi.org/10.1109/BSN.2013.6575531.

(264) Jeanneret, S.; Crespo, G. A.; Ghahraman Afshar, M.; Bakker, E. GalvaPot, a Custom-Made Combination Galvanostat/Potentiostat and High Impedance Potentiometer for Decentralized Measurements of Ionophore-Based Electrodes. *Sensors Actuators B Chem.* **2015**, *207* (PartA), 631–639. https://doi.org/10.1016/j.snb.2014.10.084.

(265) Wongkittisuksa, B.; Limsakul, C.; Kanatharana, P.; Limbut, W.; Asawatreratanakul, P.; Dawan, S.; Loyprasert, S.; Thavarungkul, P. Development and Application of a Real-Time Capacitive Sensor. *Biosens. Bioelectron.* **2011**, *26* (5), 2466–2472. https://doi.org/10.1016/j.bios.2010.10.033.

(266) Williams, N. X.; Carroll, B.; Noyce, S. G.; Hobbie, H. A.; Joh, D. Y.; Rogers, J. G.; Franklin, A. D. Fully Printed Prothrombin Time Sensor for Point-of-Care Testing. *Biosens. Bioelectron.* **2021**, *172*, 112770. https://doi.org/10.1016/j.bios.2020.112770.

(267) Huang, C.-Y.; Huang, H.-T.; Yuan, R.-T. Design of a Portable Mini Potentiostat

for Electrochemical Biosensors. In *2017 IEEE 2nd Advanced Information Technology, Electronic and Automation Control Conference (IAEAC)*; IEEE, 2017; pp 200–203. https://doi.org/10.1109/IAEAC.2017.8054006.

(268)   Huang, C.-Y.; Lee, M.-H.; Wu, Z.-H.; Tseng, H.-Y.; Huang, Y.-C.; Liu, B.-D.; Lin, H.-Y. A Portable Potentiostat with Molecularly Imprinted Polymeric Electrode for Dopamine Sensing. In *2009 IEEE Circuits and Systems International Conference on Testing and Diagnosis*; IEEE, 2009; pp 1–4. https://doi.org/10.1109/CAS-ICTD.2009.4960767.

(269)   Huang, C.-Y.; Syu, M.-J.; Chang, Y.-S.; Chang, C.-H.; Chou, T.-C.; Liu, B.-D. A Portable Potentiostat for the Bilirubin-Specific Sensor Prepared from Molecular Imprinting. *Biosens. Bioelectron.* **2007**, *22* (8), 1694–1699. https://doi.org/10.1016/j.bios.2006.07.036.

(270)   Bezuidenhout, P.; Smith, S.; Joubert, T.-H. A Low-Cost Inkjet-Printed Paper-Based Potentiostat †. *Appl. Sci.* **2018**, *8* (6), 968. https://doi.org/10.3390/app8060968.

(271)   Xu, Y.; Dai, Y.; Li, C.; Zhang, H.; Guo, M.; Yang, Y. PC Software-Based Portable Cyclic Voltammetry System with PB-MCNT-GNPs-Modified Electrodes for E. Coli Detection. *Rev. Sci. Instrum.* **2020**, *91* (1), 014103. https://doi.org/10.1063/1.5113655.

(272)   Nagabooshanam, S.; Roy, S.; Mathur, A.; Mukherjee, I.; Krishnamurthy, S.; Bharadwaj, L. M. Electrochemical Micro Analytical Device Interfaced with Portable Potentiostat for Rapid Detection of Chlorpyrifos Using Acetylcholinesterase Conjugated Metal Organic Framework Using Internet of Things. *Sci. Rep.* **2019**, *9* (1), 19862. https://doi.org/10.1038/s41598-019-56510-y.

(273)   Patolsky, F.; Zheng, G.; Lieber, C. M. Nanowire-Based Biosensors. *Anal. Chem.* **2006**, *78* (13), 4260–4269.

(274)   Mahato, J.; Raj, C. R.; Biswas, K. Low-Noise Potentiostat Circuit for Electrochemical Detection of Heavy Metals or Metalloids. *IEEE Trans. Instrum. Meas.* **2022**, *71*, 1–9. https://doi.org/10.1109/TIM.2022.3169560.

(275)   Hwang, S.; Sonkusale, S. CMOS VLSI Potentiostat for Portable Environmental Sensing Applications. *IEEE Sens. J.* **2010**, *10* (4), 820–821. https://doi.org/10.1109/JSEN.2009.2035098.

(276)   Janyasupab, M.; Asavakijthananont, N. Development of Wireless Based

Potentiostat in Biomedical Applications. In *2019 7th International Electrical Engineering Congress (iEECON)*; IEEE, 2019; pp 1–4. https://doi.org/10.1109/iEECON45304.2019.8938828.

(277) Huang, C.-Y.; Huang, Y.-C.; Lin, T.-Y.; Chang, C.-H.; Li, X.-F. An SOC-Based Portable Cyclic Voltammetry Potentiostat for Micro-Albumin Biosensors. In *2007 2nd IEEE Conference on Industrial Electronics and Applications*; IEEE, 2007; pp 604–609. https://doi.org/10.1109/ICIEA.2007.4318478.

(278) Li, J.; Si, Y.; Nde, D. T.; Lee, H. J. Development of Voltammetric Nanobio-Incorporated Analytical Method for Protein Biomarker Specific to Early Diagnosis of Lung Cancer. *Appl. Chem. Eng.* **2021**, *32* (4). https://doi.org/10.14478/ace.2021.1057.

(279) Findik, M.; Bingol, H.; Erdem, A. Electrochemical Detection of Interaction between Daunorubicin and DNA by Hybrid Nanoflowers Modified Graphite Electrodes. *Sensors Actuators B Chem.* **2021**, *329*, 129120. https://doi.org/10.1016/j.snb.2020.129120.

(280) Lee, H. S.; Han, J. H.; Pak, J. Development of a Portable Potentiostat with Wireless Communications for Measuring Dissolved Oxygen. *Trans. Korean Inst. Electr. Eng.* **2018**, *67* (12). https://doi.org/10.5370/KIEE.2018.67.12.1641.

(281) Fan, L.; Huang, J. J.; Liao, J. Competitive Smartphone-Based Portable Electrochemical Aptasensor System Based on an MXene/CDNA-MB Probe for the Determination of Microcystin-LR. *Sensors Actuators B Chem.* **2022**, *369*, 132164. https://doi.org/10.1016/j.snb.2022.132164.

(282) Peng, S.; Wang, A.; Lian, Y.; Zhang, X.; Zeng, B.; Chen, Q.; Yang, H.; Li, J.; Li, L.; Dan, J.; Liao, J.; Zhou, S. Smartphone-Based Molecularly Imprinted Sensors for Rapid Detection of Thiamethoxam Residues and Applications. *PLoS One* **2021**, *16* (11), e0258508. https://doi.org/10.1371/journal.pone.0258508.

(283) Chien, M.-N.; Fan, S.-H.; Huang, C.-H.; Wu, C.-C.; Huang, J.-T. Continuous Lactate Monitoring System Based on Percutaneous Microneedle Array. *Sensors* **2022**, *22* (4), 1468. https://doi.org/10.3390/s22041468.

(284) Zhang, X.; Wei, Y.; Wu, H.; Yan, H.; Liu, Y.; Lučev Vasić, Ž.; Pan, H.; Cifrek, M.; Du, M.; Gao, Y. Smartphone-based Electrochemical On-site Quantitative Detection Device for Nonenzyme Lactate Detection. *Electroanalysis* **2022**, *34* (9), 1411–1421. https://doi.org/10.1002/elan.202100674.

(285) Joe, C.; Lee, B. H.; Kim, S. H.; Ko, Y.; Gu, M. B. Aptamer Duo-Based Portable Electrochemical Biosensors for Early Diagnosis of Periodontal Disease. *Biosens. Bioelectron.* **2022**, *199*, 113884. https://doi.org/10.1016/j.bios.2021.113884.

(286) Zimmerman, J. B.; Mihelcic, J. R.; Smith, and J. Global Stressors on Water Quality and Quantity. *Environ. Sci. Technol.* **2008**, *42* (12), 4247–4254. https://doi.org/10.1021/es0871457.

(287) Jørgensen, N. O. G. Organic Nitrogen. In *Encyclopedia of Inland Waters*; Elsevier, 2009; pp 832–851. https://doi.org/10.1016/B978-012370626-3.00119-8.

(288) Zhu, A.; Chen, B.; Zhang, L.; Westerhoff, P. Improved Analysis of Dissolved Organic Nitrogen in Water via Electrodialysis Pretreatment. *Anal. Chem.* **2015**, *87* (4), 2353–2359. https://doi.org/10.1021/ac504224r.

(289) Šraj, L. O. C.; Almeida, M. I. G. S.; Swearer, S. E.; Kolev, S. D.; McKelvie, I. D. Analytical Challenges and Advantages of Using Flow-Based Methodologies for Ammonia Determination in Estuarine and Marine Waters. *TrAC Trends Anal. Chem.* **2014**, *59*, 83–92. https://doi.org/10.1016/j.trac.2014.03.012.

(290) Jeong, H.; Park, J.; Kim, H. Determination of NH 4 + in Environmental Water with Interfering Substances Using the Modified Nessler Method. *J. Chem.* **2013**, *2013*, 1–9. https://doi.org/10.1155/2013/359217.

(291) Schindler, D. W.; Dillon, P. J.; Schreier, H. A Review of Anthropogenic Sources of Nitrogen and Their Effects on Canadian Aquatic Ecosystems. *Biogeochemistry* **2006**, *79* (1–2), 25–44. https://doi.org/10.1007/s10533-006-9001-2.

(292) Udvardi, M.; Brodie, E. L.; Riley, W.; Kaeppler, S.; Lynch, J. Impacts of Agricultural Nitrogen on the Environment and Strategies to Reduce These Impacts. *Procedia Environ. Sci.* **2015**, *29*, 303. https://doi.org/10.1016/j.proenv.2015.07.275.

(293) Li, D.; Watson, C. J.; Yan, M. J.; Lalor, S.; Rafique, R.; Hyde, B.; Lanigan, G.; Richards, K. G.; Holden, N. M.; Humphreys, J. A Review of Nitrous Oxide Mitigation by Farm Nitrogen Management in Temperate Grassland-Based Agriculture. *J. Environ. Manage.* **2013**, *128*, 893–903. https://doi.org/10.1016/j.jenvman.2013.06.026.

(294) Mahmud, M. A. P.; Ejeian, F.; Azadi, S.; Myers, M.; Pejcic, B.; Abbassi, R.;

Razmjou, A.; Asadnia, M. Recent Progress in Sensing Nitrate, Nitrite, Phosphate, and Ammonium in Aquatic Environment. *Chemosphere* **2020**, *259*, 127492. https://doi.org/10.1016/j.chemosphere.2020.127492.

(295) Capitán-Vallvey, L. F.; Arroyo-Guerrero, E.; Fernández-Ramos, M. D.; Santoyo-Gonzalez, F. Disposable Receptor-Based Optical Sensor for Nitrate. *Anal. Chem.* **2005**, *77* (14), 4459–4466. https://doi.org/10.1021/ac050117b.

(296) Khongpet, W.; Pencharee, S.; Puangpila, C.; Hartwell, S. K.; Lapanantnoppakhun, S.; Jakmunee, J. A Compact Hydrodynamic Sequential Injection System for Consecutive On-Line Determination of Phosphate and Ammonium. *Microchem. J.* **2019**, *147*, 403–410. https://doi.org/10.1016/j.microc.2019.03.040.

(297) Yang, L.; Wang, J.; Wang, S.; Liao, Y.; Li, Y. A New Method to Improve the Sensitivity of Nitrate Concentration Measurement in Seawater Based on Dispersion Turning Point. *Optik (Stuttg).* **2020**, *205*, 164202. https://doi.org/10.1016/j.ijleo.2020.164202.

(298) Murray, E.; Roche, P.; Briet, M.; Moore, B.; Morrin, A.; Diamond, D.; Paull, B. Fully Automated, Low-Cost Ion Chromatography System for in-Situ Analysis of Nitrite and Nitrate in Natural Waters. *Talanta* **2020**, *216*, 120955. https://doi.org/10.1016/j.talanta.2020.120955.

(299) Hakobyan, L.; Monforte-Gómez, B.; Moliner-Martínez, Y.; Molins-Legua, C.; Campíns-Falcó, P. Improving Sustainability of the Griess Reaction by Reagent Stabilization on PDMS Membranes and ZnNPs as Reductor of Nitrates: Application to Different Water Samples. *Polymers (Basel).* **2022**, *14* (3), 464. https://doi.org/10.3390/polym14030464.

(300) Li, Z.; Li, M.; Wang, C.; Zhou, X.; Li, J.; Li, D. Highly Sensitive and Selective Method for Detection of Trace Amounts of Nitrite in Aquaculture Water by SERRS Coupled with Diazo Reaction. *Sensors Actuators B Chem.* **2019**, *297*, 126757. https://doi.org/10.1016/j.snb.2019.126757.

(301) Sargazi, M.; Kaykhaii, M. Application of a Smartphone Based Spectrophotometer for Rapid In-Field Determination of Nitrite and Chlorine in Environmental Water Samples. *Spectrochim. Acta Part A Mol. Biomol. Spectrosc.* **2020**, *227*, 117672. https://doi.org/10.1016/j.saa.2019.117672.

(302) Prieto-Blanco, M. C.; Ballester-Caudet, A.; Souto-Varela, F. J.; López-Mahía, P.; Campíns-Falcó, P. Rapid Evaluation of Ammonium in Different Rain Events Minimizing Needed Volume by a Cost-Effective and Sustainable

PDMS Supported Solid Sensor. *Environ. Pollut.* **2020**, *265*, 114911. https://doi.org/10.1016/j.envpol.2020.114911.

(303) Peters, J. J.; Almeida, M. I. G. S.; O'Connor Šraj, L.; McKelvie, I. D.; Kolev, S. D. Development of a Micro-Distillation Microfluidic Paper-Based Analytical Device as a Screening Tool for Total Ammonia Monitoring in Freshwaters. *Anal. Chim. Acta* **2019**, *1079*, 120–128. https://doi.org/10.1016/j.aca.2019.05.050.

(304) Kan, Y. An All-Solid-State Ammonium Ion-Selective Electrode Based on Polyaniline as Transducer and Poly (o-Phenylenediamine) as Sensitive Membrane. *Int. J. Electrochem. Sci.* **2016**, *11* (12), 9928–9940. https://doi.org/10.20964/2016.12.03.

(305) Lambert, D. F.; Sherwood, J. E.; Francis, P. S. The Determination of Urea in Soil Extracts and Related Samples—a Review. *Soil Res.* **2004**, *42* (7), 709. https://doi.org/10.1071/SR04028.

(306) Safitri, E.; Heng, L. Y.; Ahmad, M.; Ling, T. L. Fluorescence Bioanalytical Method for Urea Determination Based on Water Soluble ZnS Quantum Dots. *Sensors Actuators B Chem.* **2017**, *240*, 763–769. https://doi.org/10.1016/j.snb.2016.08.129.

(307) Alizadeh, T.; Ganjali, M. R.; Rafiei, F. Trace Level and Highly Selective Determination of Urea in Various Real Samples Based upon Voltammetric Analysis of Diacetylmonoxime-Urea Reaction Product on the Carbon Nanotube/Carbon Paste Electrode. *Anal. Chim. Acta* **2017**, *974*, 54–62. https://doi.org/10.1016/j.aca.2017.04.039.

(308) Tůma, P.; Samcová, E.; Duška, F. Determination of Ammonia, Creatinine and Inorganic Cations in Urine Using CE with Contactless Conductivity Detection. *J. Sep. Sci.* **2008**, *31* (12), 2260–2264. https://doi.org/10.1002/jssc.200700655.

(309) Mizobuchi, M.; Tamase, K.; Kitada, Y.; Sasaki, M.; Tanigawa, K. High-Performance Liquid Chromatographic Analysis of Ammonium in Human Urine. *Anal. Biochem.* **1984**, *137* (1). https://doi.org/10.1016/0003-2697(84)90351-8.

(310) Raphael, K. L.; Carroll, D. J.; Murray, J.; Greene, T.; Beddhu, S. Urine Ammonium Predicts Clinical Outcomes in Hypertensive Kidney Disease. *J. Am. Soc. Nephrol.* **2017**, *28* (8), 2483–2490. https://doi.org/10.1681/ASN.2016101151.

(311) Ali, S. M. U.; Ibupoto, Z. H.; Salman, S.; Nur, O.; Willander, M.; Danielsson, B. Selective Determination of Urea Using Urease Immobilized on ZnO Nanowires. *Sensors Actuators B Chem.* **2011**, *160* (1), 637–643. https://doi.org/10.1016/j.snb.2011.08.041.

(312) Prats-Alfonso, E.; Abad, L.; Casañ-Pastor, N.; Gonzalo-Ruiz, J.; Baldrich, E. Iridium Oxide PH Sensor for Biomedical Applications. Case Urea–Urease in Real Urine Samples. *Biosens. Bioelectron.* **2013**, *39* (1), 163–169. https://doi.org/10.1016/j.bios.2012.07.022.

(313) Velychko, T. P.; Soldatkin, O. O.; Melnyk, V. G.; Marchenko, S. V.; Kirdeciler, S. K.; Akata, B.; Soldatkin, A. P.; El'skaya, A. V.; Dzyadevych, S. V. A Novel Conductometric Urea Biosensor with Improved Analytical Characteristic Based on Recombinant Urease Adsorbed on Nanoparticle of Silicalite. *Nanoscale Res. Lett.* **2016**, *11* (1), 106. https://doi.org/10.1186/s11671-016-1310-3.

(314) Yang, Z.; Zhang, C. Single-Enzyme Nanoparticles Based Urea Biosensor. *Sensors Actuators B Chem.* **2013**, *188*, 313–317. https://doi.org/10.1016/j.snb.2013.07.004.

(315) Kuralay, F.; Özyörük, H.; Yıldız, A. Amperometric Enzyme Electrode for Urea Determination Using Immobilized Urease in Poly(Vinylferrocenium) Film. *Sensors Actuators B Chem.* **2006**, *114* (1), 500–506. https://doi.org/10.1016/j.snb.2005.05.026.

(316) Danial, E. N.; Hamza, A. H.; Mahmoud, R. H. Characteristics of Immobilized Urease on Grafted Alginate Bead Systems. *Brazilian Arch. Biol. Technol.* **2015**, *58* (2), 147–153. https://doi.org/10.1590/S1516-8913201400204.

(317) Sassolas, A.; Blum, L. J.; Leca-Bouvier, B. D. Immobilization Strategies to Develop Enzymatic Biosensors. *Biotechnol. Adv.* **2012**, *30* (3), 489–511. https://doi.org/10.1016/j.biotechadv.2011.09.003.

(318) Zucca, P.; Sanjust, E. Inorganic Materials as Supports for Covalent Enzyme Immobilization: Methods and Mechanisms. *Molecules* **2014**, *19* (9), 14139–14194. https://doi.org/10.3390/molecules190914139.

(319) Zhang, Z.; Chen, Z.; Wang, S.; Qu, C.; Chen, L. On-Site Visual Detection of Hydrogen Sulfide in Air Based on Enhancing the Stability of Gold Nanoparticles. *ACS Appl. Mater. Interfaces* **2014**, *6* (9), 6300–6307. https://doi.org/10.1021/am500564w.

(320) Petruci, J. F. D. S.; Cardoso, A. A. Sensitive Luminescent Paper-Based Sensor for the Determination of Gaseous Hydrogen Sulfide. *Anal. Methods* **2015**, *7* (6), 2687–2692. https://doi.org/10.1039/C4AY02952F.

(321) SEN, A.; ALBARELLA, J.; CAREY, J.; KIM, P.; MCNAMARAIII, W. Low-Cost Colorimetric Sensor for the Quantitative Detection of Gaseous Hydrogen Sulfide. *Sensors Actuators B Chem.* **2008**, *134* (1), 234–237. https://doi.org/10.1016/j.snb.2008.04.046.

(322) Sarfraz, J.; Tobjork, D.; Osterbacka, R.; Linden, M. Low-Cost Hydrogen Sulfide Gas Sensor on Paper Substrates: Fabrication and Demonstration. *IEEE Sens. J.* **2012**, *12* (6), 1973–1978. https://doi.org/10.1109/JSEN.2011.2181498.

(323) Choi, M. M. F.; Hawkins, P. Development of an Optical Hydrogen Sulphide Sensor. *Sensors Actuators B Chem.* **2003**, *90* (1–3), 211–215. https://doi.org/10.1016/S0925-4005(03)00030-3.

(324) Hughes, M. N.; Centelles, M. N.; Moore, K. P. Making and Working with Hydrogen Sulfide. *Free Radic. Biol. Med.* **2009**, *47* (10), 1346–1353. https://doi.org/10.1016/j.freeradbiomed.2009.09.018.

(325) Lawrence, N. Analytical Strategies for the Detection of Sulfide: A Review. *Talanta* **2000**, *52* (5), 771–784. https://doi.org/10.1016/S0039-9140(00)00421-5.

(326) Arsawiset, S.; Teepoo, S. Ready-to-Use, Functionalized Paper Test Strip Used with a Smartphone for the Simultaneous on-Site Detection of Free Chlorine, Hydrogen Sulfide and Formaldehyde in Wastewater. *Anal. Chim. Acta* **2020**, *1118*, 63–72. https://doi.org/10.1016/J.ACA.2020.04.041.

(327) Leal, V. G.; Batista, A. D.; Petruci, J. F. da S. 3D-Printed and Fully Portable Fluorescent-Based Platform for Sulfide Determination in Waters Combining Vapor Generation Extraction and Digital Images Treatment. *Talanta* **2021**, *222*, 121558. https://doi.org/10.1016/J.TALANTA.2020.121558.

(328) Feng, Y.; Hu, S.; Wang, Y.; Song, X.; Cao, C.; Wang, K.; Jing, C.; Zhang, G.; Liu, W. A Multifunctional Fluorescent Probe for Visualizing H2S in Wastewater with Portable Smartphone via Fluorescent Paper Strip and Sensing GSH in Vivo. *J. Hazard. Mater.* **2021**, *406*, 124523. https://doi.org/10.1016/J.JHAZMAT.2020.124523.

(329) Pla-Tolós, J.; Moliner-Martínez, Y.; Verdú-Andrés, J.; Casanova-Chafer, J.;

Molins-Legua, C.; Campíns-Falcó, P. New Optical Paper Sensor for in Situ Measurement of Hydrogen Sulphide in Waters and Atmospheres. *Talanta* **2016**, *156–157*, 79–86. https://doi.org/10.1016/J.TALANTA.2016.05.013.

(330) Senapati, M.; Sahu, P. P. Onsite Fish Quality Monitoring Using Ultra-Sensitive Patch Electrode Capacitive Sensor at Room Temperature. *Biosens. Bioelectron.* **2020**, *168*. https://doi.org/10.1016/j.bios.2020.112570.

(331) Sicherer, S. H.; Sampson, H. A. Food Allergy: Epidemiology, Pathogenesis, Diagnosis, and Treatment. *J. Allergy Clin. Immunol.* **2014**, *133* (2), 291-307.e5. https://doi.org/10.1016/j.jaci.2013.11.020.

(332) Hefle, S. L.; Nordlee, J. A.; Taylor, S. L. Allergenic Foods. *Crit. Rev. Food Sci. Nutr.* **1996**, *36* (sup001), 69–89. https://doi.org/10.1080/10408399609527760.

(333) Dominguez-Salas, P.; Galiè, A.; Omore, A.; Omosa, E.; Ouma, E. Contributions of Milk Production to Food and Nutrition Security. In *Encyclopedia of Food Security and Sustainability*; Elsevier, 2018; pp 278–291. https://doi.org/10.1016/B978-0-08-100596-5.21526-6.

(334) Mahoney, R. R. Galactosyl-Oligosaccharide Formation during Lactose Hydrolysis: A Review. *Food Chem.* **1998**, *63* (2), 147–154. https://doi.org/10.1016/S0308-8146(98)00020-X.

(335) Silanikove, N.; Leitner, G.; Merin, U. The Interrelationships between Lactose Intolerance and the Modern Dairy Industry: Global Perspectives in Evolutional and Historical Backgrounds. *Nutrients* **2015**, *7* (9), 7312–7331. https://doi.org/10.3390/nu7095340.

(336) Naglova, Z.; Boberova, B.; Horakova, T.; Smutka, L. Statistical Analysis of Factors Influencing the Results of Enterprises in Dairy Industry. *Agric. Econ. (Czech Republic)* **2017**, *63* (6), 259–270. https://doi.org/10.17221/353/2015-AGRICECON.

(337) Bórawski, P.; Dunn, J.; Harper, J.; Pawlewicz, A. THE INTRA-EUROPEAN UNION TRADE OF MILK AND DAIRY PRODUCTS. *Acta Sci. Pol. Oeconomia* **2019**, *18* (2), 13–23. https://doi.org/10.22630/ASPE.2019.18.2.15.

(338) Suri, S.; Kumar, V.; Prasad, R.; Tanwar, B.; Goyal, A.; Kaur, S.; Gat, Y.; Kumar, A.; Kaur, J.; Singh, D. Considerations for Development of Lactose-Free Food. *J. Nutr. Intermed. Metab.* **2019**, *15*, 27–34. https://doi.org/10.1016/j.jnim.2018.11.003.

(339) Maria C. Perotti; Wolf I. Veronica; Venica C. Ines; Bergamini C. Viviana. Dairy Products Modified in Their Lactose Content. *Curr. Nutr. Food Sci.* **2012**, *8* (1), 8–18. https://doi.org/10.2174/157340112800269597.

(340) Garballo-Rubio, A.; Soto-Chinchilla, J.; Moreno, A.; Zafra-Gómez, A. Determination of Residual Lactose in Lactose-Free Cow Milk by Hydrophilic Interaction Liquid Chromatography (HILIC) Coupled to Tandem Mass Spectrometry. *J. Food Compos. Anal.* **2018**, *66*, 39–45. https://doi.org/10.1016/j.jfca.2017.11.006.

(341) Li, Y.; Zhang, Q.; Pang, X.; Luo, Y.; Huang, K.; He, X.; Yao, Z.; Li, J. C.; Cheng, N. Fe-N-C Nanozyme Mediated Bioactive Paper-3D Printing Integration Technology Enables Portable Detection of Lactose in Milk. *Sensors Actuators B Chem.* **2022**, *368*, 132111. https://doi.org/10.1016/J.SNB.2022.132111.

(342) Srivastava, A.; Tripathi, R.; Verma, S.; Srivastava, N.; Rawat, A. K. S.; Deepak, D. A Novel Method for Quantification of Lactose in Mammalian Milk through HPTLC and Determination by a Mass Spectrometric Technique. *Anal. Methods* **2014**, *6* (18), 7268–7276. https://doi.org/10.1039/c4ay00625a.

(343) Gursoy, O.; Sen Gursoy, S.; Cogal, S.; Celik Cogal, G. Development of a New Two-Enzyme Biosensor Based on Poly(Pyrrole-Co-3,4-Ethylenedioxythiophene) for Lactose Determination in Milk. *Polym. Eng. Sci.* **2018**, *58* (6), 839–848. https://doi.org/10.1002/pen.24632.

(344) Conzuelo, F.; Gamella, M.; Campuzano, S.; Ruiz, M. A.; Reviejo, A. J.; Pingarrón, J. M. An Integrated Amperometric Biosensor for the Determination of Lactose in Milk and Dairy Products. *J. Agric. Food Chem.* **2010**, *58* (12). https://doi.org/10.1021/jf101173e.

(345) Ivory, R.; Delaney, E.; Mangan, D.; McCleary, B. V. Determination of Lactose Concentration in Low-Lactose and Lactose-Free Milk, Milk Products, and Products Containing Dairy Ingredients, Enzymatic Method: Single-Laboratory Validation First Action Method 2020.08. *J. AOAC Int.* **2021**, *104* (5), 1308–1322. https://doi.org/10.1093/jaoacint/qsab032.

(346) Scherf, K. A.; Catassi, C.; Chirdo, F.; Ciclitira, P. J.; Feighery, C.; Gianfrani, C.; Koning, F.; Lundin, K. E. A.; Schuppan, D.; Smulders, M. J. M.; Tranquet, O.; Troncone, R.; Koehler, P. Recent Progress and Recommendations on Celiac Disease From the Working Group on Prolamin Analysis and Toxicity. *Front. Nutr.* **2020**, *7*. https://doi.org/10.3389/fnut.2020.00029.

(347) Falcomer, A. L.; Santos Araújo, L.; Farage, P.; Santos Monteiro, J.; Yoshio

Nakano, E.; Puppin Zandonadi, R. Gluten Contamination in Food Services and Industry: A Systematic Review. *Crit. Rev. Food Sci. Nutr.* **2020**, *60* (3), 479–493. https://doi.org/10.1080/10408398.2018.1541864.

(348) Parsons, K.; Brown, L.; Clark, H.; Allen, E.; McCammon, E.; Clark, G.; Oblad, R.; Kenealey, J. Gluten Cross-Contact from Common Food Practices and Preparations. *Clin. Nutr.* **2021**, *40* (5), 3279–3287. https://doi.org/10.1016/j.clnu.2020.10.053.

(349) Atasoy, G.; Ulutas, B.; Turhan, M. Potential Ways for Gluten Contamination of Gluten-Free Grain and Gluten-Free Foods: The Buckwheat Case. *Food Addit. Contam. Part A* **2020**, *37* (10), 1591–1600. https://doi.org/10.1080/19440049.2020.1787529.

(350) Fuciños, C.; Estévez, N.; Míguez, M.; Fajardo, P.; Chapela, M. J.; Gondar, D.; Rúa, M. L. Effectiveness of Proteolytic Enzymes to Remove Gluten Residues and Feasibility of Incorporating Them into Cleaning Products for Industrial Purposes. *Food Res. Int.* **2019**, *120*, 167–177. https://doi.org/10.1016/j.foodres.2019.02.037.

(351) Zhang, J.; Portela, S. B.; Horrell, J. B.; Leung, A.; Weitmann, D. R.; Artiuch, J. B.; Wilson, S. M.; Cipriani, M.; Slakey, L. K.; Burt, A. M.; Dias Lourenco, F. J.; Spinali, M. S.; Ward, J. R.; Seit-Nebi, A.; Sundvor, S. E.; Yates, S. N. An Integrated, Accurate, Rapid, and Economical Handheld Consumer Gluten Detector. *Food Chem.* **2019**, *275*, 446–456. https://doi.org/10.1016/J.FOODCHEM.2018.08.117.

(352) Chiriacò, M. S.; De Feo, F.; Primiceri, E.; Monteduro, A. G.; De Benedetto, G. E.; Pennetta, A.; Rinaldi, R.; Maruccio, G. Portable Gliadin-Immunochip for Contamination Control on the Food Production Chain. *Talanta* **2015**, *142*, 57–63. https://doi.org/10.1016/J.TALANTA.2015.04.040.

(353) Mousavizadeh, F. S.; Sarlak, N. Encapsulation of Gold Nanoparticles into Functionalized Silica Nanoparticles Stabilized on Triacetyl Cellulose for Gluten Determination. *J. Nanostructures* **2022**, *12* (3), 474–490. https://doi.org/10.22052/JNS.2022.03.001.

(354) Sarver, R. W.; Almy, D. J.; Bergeron, E. R.; Strong, B. F.; Steiner, B. A.; Donofrio, R.; Lupo, A. J.; Gray, R. L.; Sperry, A. K. Overview of Portable Assays for the Detection of Mycotoxins, Allergens, and Sanitation Monitoring. *Journal of AOAC International*. 2021. https://doi.org/10.1093/jaoacint/qsaa113.

(355) Lin, H.-Y.; Huang, C.-H.; Park, J.; Pathania, D.; Castro, C. M.; Fasano, A.; Weissleder, R.; Lee, H. Integrated Magneto-Chemical Sensor For On-Site Food Allergen Detection. **2017**. https://doi.org/10.1021/acsnano.7b04318.

(356) Manfredi, A.; Giannetto, M.; Mattarozzi, M.; Costantini, M.; Mucchino, C.; Careri, M. Competitive Immunosensor Based on Gliadin Immobilization on Disposable Carbon-Nanogold Screen-Printed Electrodes for Rapid Determination of Celiotoxic Prolamins. *Anal. Bioanal. Chem.* **2016**, *408* (26). https://doi.org/10.1007/s00216-016-9494-z.

(357) Nishino, S. F.; Spain, J. C.; He, Z. Strategies for Aerobic Degradation of Nitroaromatic Compounds by Bacteria: Process Discovery to Field Application. In *Biodegradation of Nitroaromatic Compounds and Explosives*; 2000.

(358) Wexler, P. *Encyclopedia of Toxicology*; 2005. https://doi.org/10.1093/jat/bku065.

(359) Honeychurch, K. C.; Hart, J. P.; Pritchard, P. R. J.; Hawkins, S. J.; Ratcliffe, N. M. Development of an Electrochemical Assay for 2,6-Dinitrotoluene, Based on a Screen-Printed Carbon Electrode, and Its Potential Application in Bioanalysis, Occupational and Public Health. In *Biosensors and Bioelectronics*; 2003; Vol. 19. https://doi.org/10.1016/S0956-5663(03)00208-2.

(360) Ishaque, A. B.; Timmons, C.; Ballard, F. V.; Hupke, C.; Dulal, K.; Johnson, L. R.; Gerald, T. M.; Boucaud, D.; Tchounwou, P. B. Cytotoxicity of Dinitrotoluenes (2,4-DNT, 2,6-DNT) to MCF-7 and MRC-5 Cells. *Int. J. Environ. Res. Public Health* **2005**, *2* (2). https://doi.org/10.3390/ijerph2005020015.

(361) Sağlam, Ş.; Üzer, A.; Erçağ, E.; Apak, R. Electrochemical Determination of TNT, DNT, RDX, and HMX with Gold Nanoparticles/Poly(Carbazole-Aniline) Film-Modified Glassy Carbon Sensor Electrodes Imprinted for Molecular Recognition of Nitroaromatics and Nitramines. *Anal. Chem.* **2018**, *90* (12). https://doi.org/10.1021/acs.analchem.8b00715.

(362) Clausen, J. L.; Scott, C.; Osgerby, I. Fate of Nitroglycerin and Dinitrotoluene in Soil at Small Arms Training Ranges. *Soil Sediment Contam.* **2011**, *20* (6). https://doi.org/10.1080/15320383.2011.594108.

(363) (EPA), U. S. E. P. A. Drinking Water Health Advisory for 2,4-Dinitrotoluene and 2,6-Dinitrotoluene. **2008**, 76.

(364) Senesac, L.; Thundat, T. G. Nanosensors for Trace Explosive Detection. *Materials Today*. 2008. https://doi.org/10.1016/S1369-7021(08)70017-8.

(365) Wang, J. Electrochemical Sensing of Explosives. *Electroanalysis*. 2007. https://doi.org/10.1002/elan.200603748.

(366) Amaral, H. I. F.; Fernandes, J.; Berg, M.; Schwarzenbach, R. P.; Kipfer, R. Assessing TNT and DNT Groundwater Contamination by Compound-Specific Isotope Analysis and 3H-3He Groundwater Dating: A Case Study in Portugal. *Chemosphere* **2009**, *77* (6). https://doi.org/10.1016/j.chemosphere.2009.08.011.

(367) Amaral, H. I. F.; Gama, A. C.; Gonçalves, C.; Fernandes, J.; Batista, M. J.; Abreu, M. Long-Term TNT and DNT Contamination: 1-D Modeling of Natural Attenuation in the Vadose Zone: Case Study, Portugal. *Environ. Earth Sci.* **2016**, *75* (1). https://doi.org/10.1007/s12665-015-4937-y.

(368) Caygill, J. S.; Collyer, S. D.; Holmes, J. L.; Davis, F.; Higson, S. P. J. Disposable Screen-Printed Sensors for the Electrochemical Detection of TNT and DNT. *Analyst* **2013**, *138* (1), 346–352. https://doi.org/10.1039/C2AN36351H.

(369) Banga, I.; Paul, A.; Muthukumar, S.; Prasad, S. Characterization of Room-Temperature Ionic Liquids to Study the Electrochemical Activity of Nitro Compounds. *Sensors* **2020**, *20* (4), 1124. https://doi.org/10.3390/s20041124.

(370) Perr, J. M.; Furton, K. G.; Almirall, J. R. Solid Phase Microextraction Ion Mobility Spectrometer Interface for Explosive and Taggant Detection. *J. Sep. Sci.* **2005**, *28* (2), 177–183. https://doi.org/10.1002/jssc.200401893.

(371) Zhang, H.-X.; Cao, A.-M.; Hu, J.-S.; Wan, L.-J.; Lee, S.-T. Electrochemical Sensor for Detecting Ultratrace Nitroaromatic Compounds Using Mesoporous SiO 2 -Modified Electrode. *Anal. Chem.* **2006**, *78* (6), 1967–1971. https://doi.org/10.1021/ac051826s.

(372) Chen, T.; Sheng, Z.; Wang, K.; Wang, F.; Xia, X. Determination of Explosives Using Electrochemically Reduced Graphene. *Chem. – An Asian J.* **2011**, *6* (5), 1210–1216. https://doi.org/10.1002/asia.201000836.

(373) Ahmad, K.; Mohammad, A.; Mathur, P.; Mobin, S. M. Preparation of SrTiO 3 Perovskite Decorated RGO and Electrochemical Detection of Nitroaromatics. *Electrochim. Acta* **2016**, *215*, 435–446. https://doi.org/10.1016/j.electacta.2016.08.123.

(374) Ibarlucea, B.; Fernández-Sánchez, C.; Demming, S.; Büttgenbach, S.; Llobera, A. Selective Functionalisation of PDMS-Based Photonic Lab on a Chip for Biosensing. *Analyst* **2011**, *136* (17), 3496. https://doi.org/10.1039/c0an00941e.

(375) Kreider, A.; Richter, K.; Sell, S.; Fenske, M.; Tornow, C.; Stenzel, V.; Grunwald, I. Functionalization of PDMS Modified and Plasma Activated Two-Component Polyurethane Coatings by Surface Attachment of Enzymes. *Appl. Surf. Sci.* **2013**, *273*, 562–569. https://doi.org/10.1016/j.apsusc.2013.02.080.

(376) Vianello, F.; Zennaro, L.; Rigo, A. A Coulometric Biosensor to Determine Hydrogen Peroxide Using a Monomolecular Layer of Horseradish Peroxidase Immobilized on a Glass Surface. *Biosens. Bioelectron.* **2007**, *22* (11), 2694–2699. https://doi.org/10.1016/j.bios.2006.11.007.

(377) Jornet-Martínez, N.; Moliner-Martínez, Y.; Herráez-Hernández, R.; Molins-Legua, C.; Verdú-Andrés, J.; Campíns-Falcó, P. Designing Solid Optical Sensors for in Situ Passive Discrimination of Volatile Amines Based on a New One-Step Hydrophilic PDMS Preparation. *Sensors Actuators B Chem.* **2016**, *223*, 333–342. https://doi.org/10.1016/j.snb.2015.09.097.

(378) Lee, J.; Lee, J.; Kang, M.; Shin, M.; Kim, J.-M.; Kang, S.-U.; Lim, J.-O.; Choi, H.-K.; Suh, Y.-G.; Park, H.-G.; Oh, U.; Kim, H.-D.; Park, Y.-H.; Ha, H.-J.; Kim, Y.-H.; Toth, A.; Wang, Y.; Tran, R.; Pearce, L. V.; Lundberg, D. J.; Blumberg, P. M. N-(3-Acyloxy-2-Benzylpropyl)-N '-[4-(Methylsulfonylamino)Benzyl]Thiourea Analogues: Novel Potent and High Affinity Antagonists and Partial Antagonists of the Vanilloid Receptor. *J. Med. Chem.* **2003**, *46* (14), 3116–3126. https://doi.org/10.1021/jm030089u.

(379) Chrétien, J.-M.; Ghanem, M. A.; Bartlett, P. N.; Kilburn, J. D. Covalent Tethering of Organic Functionality to the Surface of Glassy Carbon Electrodes by Using Electrochemical and Solid-Phase Synthesis Methodologies. *Chem. - A Eur. J.* **2008**, *14* (8), 2548–2556. https://doi.org/10.1002/chem.200701559.

(380) Love, J. C.; Estroff, L. A.; Kriebel, J. K.; Nuzzo, R. G.; Whitesides, G. M. Self-Assembled Monolayers of Thiolates on Metals as a Form of Nanotechnology. *Chem. Rev.* **2005**, *105* (4), 1103–1170. https://doi.org/10.1021/cr0300789.

(381) Pla-Tolós, J.; Serra-Mora, P.; Hakobyan, L.; Molins-Legua, C.; Moliner-Martinez, Y.; Campins-Falcó, P. A Sustainable On-Line CapLC Method for

Quantifying Antifouling Agents like Irgarol-1051 and Diuron in Water Samples: Estimation of the Carbon Footprint. *Sci. Total Environ.* **2016**, *569–570*, 611–618. https://doi.org/10.1016/j.scitotenv.2016.06.181.

(382) Vashist, S. K.; van Oordt, T.; Schneider, E. M.; Zengerle, R.; von Stetten, F.; Luong, J. H. T. A Smartphone-Based Colorimetric Reader for Bioanalytical Applications Using the Screen-Based Bottom Illumination Provided by Gadgets. *Biosens. Bioelectron.* **2015**, *67*, 248–255. https://doi.org/10.1016/j.bios.2014.08.027.

(383) Argente-García, A.; Muñoz-Ortuño, M.; Molins-Legua, C.; Moliner-Martínez, Y.; Campíns-Falcó, P. A Solid Device Based on Doped Hybrid Composites for Controlling the Dosage of the Biocide N-(3-Aminopropyl)-N-Dodecyl-1,3-Propanediamine in Industrial Formulations. *Talanta* **2016**, *147*, 147–154. https://doi.org/10.1016/j.talanta.2015.09.051.

(384) WHO. Nitrate and Nitrite in Drinking Water: Background Document for Development of WHO Guidelines for Drinking Water Quality. *Geneva World Heal. Organ.* **2016**.

(385) Shivatare, R.; Hanumansingh Nagore, D. "HPTLC" an Important Tool in Standardization of Herbal Medical Product: A Review. **2013**.

(386) Morlock, G. E.; Morlock, L. P.; Lemo, C. Streamlined Analysis of Lactose-Free Dairy Products. *J. Chromatogr. A* **2014**, *1324*, 215–223. https://doi.org/10.1016/j.chroma.2013.11.038.

(387) Byrne, F. P.; Jin, S.; Paggiola, G.; Petchey, T. H. M.; Clark, J. H.; Farmer, T. J.; Hunt, A. J.; Mcelroy, C. R.; Sherwood, J. Tools and Techniques for Solvent Selection: Green Solvent Selection Guides. *Sustain Chem Process* **2016**, *4*, 7. https://doi.org/10.1186/s40508-016-0051-z.

(388) Trani, A.; Gambacorta, G.; Loizzo, P.; Cassone, A.; Fasciano, C.; Zambrini, A. V.; Faccia, M. Comparison of HPLC-RI, LC/MS-MS and Enzymatic Assays for the Analysis of Residual Lactose in Lactose-Free Milk. *Food Chem.* **2017**, *233*, 385–390. https://doi.org/10.1016/j.foodchem.2017.04.134.

(389) Perati, P.; Borba, B. De; Rohrer, J. Determination of Lactose in Lactose-Free Milk Products by High-Performance Anion-Exchange Chromatography with Pulsed Amperometric Detection. *Thermo Fish. Sci.* **2016**, *248*, 1–8.

(390) Delamar, M.; Hitmi, R.; Pinson, J.; Saveant, J. M. Covalent Modification of Carbon Surfaces by Grafting of Functionalized Aryl Radicals Produced from

Electrochemical Reduction of Diazonium Salts. *J. Am. Chem. Soc.* **1992**, *114* (14), 5883–5884. https://doi.org/10.1021/ja00040a074.

(391) Allongue, P.; Delamar, M.; Desbat, B.; Fagebaume, O.; Hitmi, R.; Pinson, J.; Savéant, J.-M. Covalent Modification of Carbon Surfaces by Aryl Radicals Generated from the Electrochemical Reduction of Diazonium Salts. *J. Am. Chem. Soc.* **1997**, *119* (1), 201–207. https://doi.org/10.1021/ja963354s.

(392) de Villeneuve, C. H.; Pinson, J.; Bernard, M. C.; Allongue, P. Electrochemical Formation of Close-Packed Phenyl Layers on Si(111). *J. Phys. Chem. B* **1997**, *101* (14), 2415–2420. https://doi.org/10.1021/jp962581d.

(393) Ivandini, T. A.; Rao, T. N.; Fujishima, A.; Einaga, Y. Electrochemical Oxidation of Oxalic Acid at Highly Boron-Doped Diamond Electrodes. *Anal. Chem.* **2006**, *78* (10), 3467–3471. https://doi.org/10.1021/ac052029x.

(394) Laviron, E. General Expression of the Linear Potential Sweep Voltammogram in the Case of Diffusionless Electrochemical Systems. *J. Electroanal. Chem. Interfacial Electrochem.* **1979**, *101* (1), 19–28. https://doi.org/10.1016/S0022-0728(79)80075-3.

(395) Tan, S.; Lazenby, R. A.; Bano, K.; Zhang, J.; Bond, A. M.; Macpherson, J. V.; Unwin, P. R. Comparison of Fast Electron Transfer Kinetics at Platinum, Gold, Glassy Carbon and Diamond Electrodes Using Fourier-Transformed AC Voltammetry and Scanning Electrochemical Microscopy. *Phys. Chem. Chem. Phys.* **2017**, *19* (13), 8726–8734. https://doi.org/10.1039/C7CP00968B.

(396) Forster, R. J.; O'Kelly, J. P. Protonation Reactions of Anthraquinone-2,7-Disulphonic Acid in Solution and within Monolayers. *J. Electroanal. Chem.* **2001**, *498* (1–2). https://doi.org/10.1016/S0022-0728(00)00331-4.

(397) Hamzah, H. H.; Chein, W. C.; Rahiman, S. S. F.; Shafiee, S. A. Investigating the Effects of Primary Amine Linkers with Different Carbon Chain Lengths on the Acid Dissociation Constant (p K a) for Covalently Immobilized Anthraquinone at the Electrode Surface Using Linear and Non-Linear Fittings. *J. Electrochem. Soc.* **2019**, *166* (16), H877–H887. https://doi.org/10.1149/2.0301916jes.

(398) Wardman, P. Reduction Potentials of One-Electron Couples Involving Free Radicals in Aqueous Solution. *J. Phys. Chem. Ref. Data* **1989**, *18* (4), 1637–1755. https://doi.org/10.1063/1.555843.

(399) Jovanovic, S. V.; Steenken, S.; Hara, Y.; Simic, M. G. Reduction Potentials of

Flavonoid and Model Phenoxyl Radicals. Which Ring in Flavonoids Is Responsible for Antioxidant Activity? *J. Chem. Soc. Perkin Trans. 2* **1996**, No. 11, 2497. https://doi.org/10.1039/p29960002497.

(400) Abiman, P.; Crossley, A.; Wildgoose, G. G.; Jones, J. H.; Compton, R. G. Investigating the Thermodynamic Causes Behind the Anomalously Large Shifts in p K a Values of Benzoic Acid-Modified Graphite and Glassy Carbon Surfaces. *Langmuir* **2007**, *23* (14), 7847–7852. https://doi.org/10.1021/la7005277.

(401) Masheter, A. T.; Abiman, P.; Wildgoose, G. G.; Wong, E.; Xiao, L.; Rees, N. V.; Taylor, R.; Attard, G. A.; Baron, R.; Crossley, A.; Jones, J. H.; Compton, R. G. Investigating the Reactive Sites and the Anomalously Large Changes in Surface PKa Values of Chemically Modified Carbon Nanotubes of Different Morphologies. *J. Mater. Chem.* **2007**, *17* (25), 2616. https://doi.org/10.1039/b702492d.

(402) Wei, H. Z.; van de Ven, T. G. M.; Omanovic, S.; Zeng, Y. W. Adsorption Behavior of Dinucleotides on Bare and Ru-Modified Glassy Carbon Electrode Surfaces. *Langmuir* **2008**, *24* (21), 12375–12384. https://doi.org/10.1021/la801926t.

(403) Olson, E. J.; Isley, W. C.; Brennan, J. E.; Cramer, C. J.; Bühlmann, P. Electrochemical Reduction of 2,4-Dinitrotoluene in Aprotic and PH-Buffered Media. *J. Phys. Chem. C* **2015**, *119* (23), 13088–13097. https://doi.org/10.1021/acs.jpcc.5b02840.

ANNEX

A.1. ABBREVIATIONS

2,4-DNT	2,4 dinitrotoluene
2,6-DNT	2,6-dinitrotoluene
3,5-DHCA	3,5-dihydroxyhydrocinnamic acid
AgNPs	Silver nanoparticles
ALP	Alkaline phosphatase
AME	Alternariol monomethyl ether
APTMS	Aminopropyltrimethoxysilane
AQ	Anthraquinone-2-carboxylic acid
AQ-2-MS	Anthraquinone-2-sulfonate
ATR	Attenuated total reflectance
AuNPs	Gold nanoparticles
BCIP	5-Bromo-4-Chloro-3-Indolyl phosphate
BDDE	Boron doped diamond electrodes
CIELAB	Iluminance-color change from red
CMOS	Conductive metal-oxide semiconductor
CMYK	Cyan magenta yelllow black
CRI	Color rendering index
CV	Cyclic Voltammetry
DESI	Desorption electrospray ionization
DIN	Dissolved inorganic nitrogen
DNT	Dinitrotoluene
DON	Dissolved organic nitrogen
DR	Diffuse reflectance
EDC	N-(-3-dimethylaminoprpyl)-N'-ethylcarbodiimide hydrochloride
EU	European union
FAB	Fast atom bormbardement
FTIR	Fourier transform infrared
GC	Gas chromatography
GCE	Glassy carbon electrode
GIMP	GNU image manipulation program
HMF	5-hydroxymethylfurfural
HPTLC	High performance thin layer chromatography
HSV	Hue saturation value
IR	Infrared

ISO	Sensitivity to light
LC	Liquid chromatography
LED	Light emitting diode
LOD	Limit od detection
LOQ	Limit of quantification
MALDI	Matrix-assisted laser desorption/ionization
MNPs	Metallic nanoparticles
MS	Mass spectrometry
NanoSiO$_2$	Nano silica
NEDD	N-1-Naphthyl ethylendiamine dihydrochloride
NHS	N-hydroxysuccinimide
NP	Normal phase
NPs	Nanoparticles
NQS	1,2-naphtoquinone-4-sulfonate
OMIM PF6	1-methyl-3-octylimidazolium
OPN	Osteopontin
PBS	Phosphate buffer solution
PCA	Principal component analysis
PCET	Proton coupled electron transfer
PDMS	Polydimethylsiloxane
PEG	Polyethylene glycol
PMS	Pantone matching system
PVA	Polyvinyl alchohol
Rf	Retention factor
RGB	Red Green Blue
RP	Reverse phase
Rs	Resolution
RSD	Relative standard deviation
S/N	Signal-to-noise ratio
SA	Sulfanilamide
SCE	Saturated calomelans electrode
SEM	Scanning electron microscopy
SERS	Surface enhanced raman spectroscopy
SIMCA	Soft independent modeling of class analysis
SIMS	Secondary-ion mass spectroscopy

SiONPs	Silica nanoparticles
TDN	Total dissolved nitrogen
TEOS	Tetraethylortosilicate
TLC	Thin layer chromatography
TNT	Trinitrotoluene
UV	Ultraviolet
Vis	Visible
WHO	World health organisation
WOS	Web of science

A2. FIGURE LIST

A3. TABLE LIST

A4. PhD CONTRIBUTIONS TO PUBLICATIONS

- **Martínez-Aviño, A**; Molins-Legua, C; Campíns-Falcó, P; Scaling the Analytical Information Given by Several Types of Colorimetric and Spectroscopic Instruments Including Smartphones: Rules for Their Use and Establishing Figures of Merit of Solid Chemosensors. Anal Chem, 2021, 93, 6043-6052. Doi: 10.1021/acs.analchem.0c03994. **Contribution (100%).**

- **Adrià Martínez-Aviñó**, Lusine Hakobyan, Ana Ballester-Caudet, Yolanda Moliner-Martínez, Carmen Molins-Legua and Pilar Campíns-Falcó; NQS-Doped PDMS Solid Sensor: From Water Matrix to Urine Enzymatic Application. Biosensors 2021, 11, 186. Doi: 10.3390/bios11060186. **Contribution (100%).**

- **Martínez-Aviñó A**, Molins-Legua C, Campíns-Falcó P. Combining high performance thin layer chromatography with minispectrometer-fiber optic probe-coupled to smartphone for in place analysis: Lactose quantification in several matrices. J Chromatogr A. 2022, 1661:462694. Doi: 10.1016/j.chroma.2021.462694. **Contribution (100%).**

- **Martínez-Aviñó A**, De Diego-Llorente-Luque M, Molins-Legua C, Campíns-Falcó P. Advances in the measurement of polymeric colorimetric sensors using portable instrumentation: Testing the light influence. Polymers 2022, 14,4285. Doi: 10.3390/polym14204285. **Contribution (100%).**

- **Martínez-Aviñó A**, Moliner-Martínez Y, Molins-Legua C, Campíns-Falcó P. Colorimetric analysis platform based on thin layer chromatography for monitoring gluten cross-contamination in food industries. **Contribution (100%).**

- Shane P. O Neill, **Adria Martinez**, Charlie Keane, Sammi Hassan, Catriona Houston, Shekemi Denuga, Emer Farrell, Guzman G. Ramirez, Robert P. Johnson; Comparative Proton Coupled Electron Transfer at Glassy Carbon and Boron-Doped Diamond Electrodes. **Contribution (50%).**

- **Martínez-Aviñó A**, O Neill SP, Grealish R, Johnson R.P. Surface modification of glassy carbon electrode for ultrasensitive 2,6-DNT detection. **Contribution (100%).**